

STUDIES ON CORROSION INHIBITION OF 18% Ni M 250 GRADE MARAGING STEEL UNDER WELDED CONDITION IN ACIDIC MEDIA

Thesis

Submitted in partial fulfillment of the requirements for the degree of

DOCTOR OF PHILOSOPHY

by

PRADEEP KUMAR



DEPARTMENT OF CHEMISTRY

NATIONAL INSTITUTE OF TECHNOLOGY KARNATAKA

SURATHKAL, MANGALORE -575 025

JULY, 2014

DECLARATION

I hereby *declare* that the Research Thesis entitled “**Studies on corrosion inhibition of 18% Ni M 250 grade maraging steel under welded condition in acidic media**” which is being submitted to the **National Institute of Technology Karnataka Surathkal**, in partial fulfillment of the requirements for the award of the Degree of **Doctor of Philosophy in Chemistry** is a *bonafide report of the research work carried out by me*. The material contained in this Research Thesis has not been submitted to any University or Institution for the award of any degree.

(Signature of the Research Scholar)

Name: **PRADEEP KUMAR**

Reg. No: **CY10F07**

Department: **CHEMISTRY**

Place: **NITK, SURATHKAL**

Date: **11th JULY, 2014**

CERTIFICATE

This is to *certify* that the Research Thesis entitled “**Studies on corrosion inhibition of 18% Ni M 250 grade maraging steel under welded condition in acidic media**” submitted by **Pradeep Kumar** (Register Number: **CY10F07**) as the record of the research work carried out by him, is accepted as the Research Thesis submission in partial fulfillment of the requirements for the award of degree of **Doctor of Philosophy**.

Dr. A. Nityananda shetty

Research Guide

Chairman – DRPC

*I dedicate this thesis to my family members, research guide and friends to say thank you
for everything.*

ACKNOWLEDGEMENT

I wish to express my gratitude to my research supervisor Dr. A. Nityananda Shetty, Professor Department of Chemistry, National Institute of Technology Karnataka, Surathkal, for giving me an opportunity to carry out research in corrosion studies under his able guidance. It has been an honour to be his research student. I appreciate all his contributions of time and ideas to make my research experience productive and stimulating. I remain ever grateful to my supervisor who has made this thesis possible.

I would like to thank the members of RPAC, Dr. Jagannath Nayak, Professor, Department of Metallurgical and Materials Engineering, National Institute of Technology Karnataka, Surathkal, and Dr. D. Krishna Bhat, Professor, Department of Chemistry, National Institute of Technology Karnataka, Surathkal, for their valuable suggestions throughout this work.

I am grateful to Dr. A. C. Hegde, Head, Department of Chemistry, National Institute of Technology Karnataka, Surathkal for providing me the required experimental facilities of the department. I am thankful to faculty of the Department of Chemistry, National Institute of Technology Karnataka, Surathkal, Dr. A. V. Adhikari, Dr. B. Ramachandra Bhat, Dr. Arun M. Isloor, Dr. Uday Kumar D and Dr. Darshak R. Trivedi for their suggestions and support. I am ever grateful to the Department of Chemistry, NITK for all the laboratory facility and Department of Metallurgical and Materials Engineering, NITK for SEM facility.

I am indebted to the nonteaching staff, Department of Chemistry NITK, Mrs. Kasturi Rohidas for her help in official work, Mr. Pradeep Crasta, Mr. Prashanth, Mr. Ashoka and Mr. Harish for their assistance in the laboratory.

It is a pleasure to thank my fellow research scholars, Dr. Poornima, Dr. Reena Kiran, Dr. Sanat Kumar, Mr. Vijayaganapathi Karanth, Mr. Yathish Ullal, Mr. Sudarshan Shetty, Mr. Subramanya. B., Mrs. Nandini, Mr. Vasant Kumar, Miss. Kshama Shetty and Mr. Kishor. K. S. and all others for making my stay at NITK during research a memorable one.

I gratefully acknowledge the cooperation and encouragement given by the Principal and lectures of Government Pre University College, Shankaranarayana, Kundapur.

At this point of time I must acknowledge my chemistry teacher, Prof. Joseph Peter Fernades, Milagres College Kallianpur, Udupi, who inspired me to take up chemistry as my career.

Lastly and most importantly, I wish to thank my parents, all my family members and friends for their cooperation, care and love. To them I dedicate this thesis.

PRADEEP KUMAR

ABSTRACT

The corrosion behaviour of 18% Ni M250 grade maraging steel under welded conditions in two different acid media, namely, hydrochloric acid and sulphuric acid in various concentrations and temperatures have been studied by potentiodynamic polarization and electrochemical impedance spectroscopy techniques. The corrosion rate in the sulphuric acid medium was higher than in the hydrochloric acid medium.

The effect of corrosion inhibition on welded maraging steel was carried out by using five inhibitors, namely, 2,5-Bis (3,4,5-trimethoxy phenyl)-1,3,4-oxadiazole (BTPO), 1-Phenyl-4-(4-nitrophenyl) thiosemicarbazide (PNPT), 3,4,5-Trimethoxy benzoic acid(3,4,5-trimethoxy-benzylidene) hydrazide (TBTBH), 2-(5-Chloro-1H-benzoimidazol-2-yl) phenol (CBP), 2-(4-Methoxy-phenyl)-benzo[d]imidazo[2,1-b]thiazole (MPBIT). The results pertaining to the corrosion inhibition studies of five inhibitors in two different acid media at different temperatures in the presence of varying concentrations of inhibitors are reported in the thesis. Activation parameters for the corrosion of the alloy and thermodynamic parameters for the adsorption of the inhibitors have been calculated and the results have been analysed.

The adsorption of all five inhibitors on the alloy was through both physisorption and chemisorption, with predominant physisorption in both the media. The adsorption of all the five inhibitors on alloy surfaces follows Langmuir adsorption isotherm. The inhibition efficiencies of all five inhibitors decrease with the increase in temperature and increase in concentration of acidic media.

Key Words: Maraging steel, Corrosion, Inhibitor, Adsorption.

| CONTENTS | | Page No |
|-------------------------------|--|----------------|
| CHAPTER 1 INTRODUCTION | | |
| 1.1 | IMPORTANCE OF CORROSION STUDIES | 2 |
| 1.2 | NEED FOR CORROSION STUDY | 2 |
| 1.3 | ELECTROCHEMICAL THEORY OF CORROSION | 3 |
| 1.4 | CLASSIFICATION OF CORROSION | 5 |
| 1.4.1 | Forms of Corrosion | 5 |
| 1.4.1.1 | Uniform corrosion | 5 |
| 1.4.1.2 | Galvanic corrosion | 5 |
| 1.4.1.3 | Crevice corrosion | 6 |
| 1.4.1.4 | Pitting corrosion | 6 |
| 1.4.1.5 | Intergranular corrosion | 6 |
| 1.4.1.6 | Selective leaching | 6 |
| 1.4.1.7 | Erosion corrosion | 7 |
| 1.4.1.8 | Stress corrosion | 7 |
| 1.5 | FACTORS AFFECTING THE CORROSION RATE | 7 |
| 1.5.1 | Nature of the metal | 7 |
| 1.5.2 | Difference in potential between anodic and cathodic region | 7 |
| 1.5.3 | Nature of the corrosion product | 8 |
| 1.5.4 | Ratio of anodic to cathodic area | 8 |
| 1.5.5 | Hydrogen overvoltage | 8 |
| 1.5.6 | Temperature | 8 |
| 1.5.7 | pH | 8 |
| 1.5.8 | Presence of oxidising agents | 9 |
| 1.5.9 | Polarization at anodic and cathodic region | 9 |
| 1.5.10 | Effect of dissolved oxygen | 9 |
| 1.5.11 | Effect of velocity of the medium | 9 |
| 1.5.12 | Effect of other ions present in the solution | 9 |
| 1.6 | THERMODYNAMICS OF CORROSION | 10 |
| 1.7 | ELECTROCHEMICAL POLARISATION | 12 |
| 1.8 | MIXED POTENTIAL THEORY | 13 |
| 1.9 | DETERMINATION OF CORROSION RATE | 15 |
| 1.9.1 | DC Electrochemical monitoring techniques | 16 |
| 1.9.1.1 | Potentiodynamic polarization method | 16 |

| | | |
|--|--|----|
| 1.9.1.2 | Linear polarization method | 18 |
| 1.9.2 | Electrochemical impedance spectroscopy (EIS) | 20 |
| 1.9.2.1 | Equivalent electric circuit models | 22 |
| 1.9.2.2 | EIS modeling parameters | 23 |
| 1.10 | CORROSION CONTROL BY INHIBITORS | 24 |
| 1.11 | TYPES OF INHIBITORS | 25 |
| 1.11.1 | Anodic (passivating) inhibitors | 25 |
| 1.11.2 | Cathodic inhibitors | 26 |
| 1.11.3 | Mixed inhibitors | 26 |
| 1.11.3.1 | Physical adsorption | 27 |
| 1.11.3.2 | Chemical adsorption | 27 |
| 1.11.3.3 | Film formation | 27 |
| 1.11.4 | Ohmic inhibitors | 28 |
| 1.11.5 | Precipitation inhibitors | 28 |
| 1.11.6 | Vapor-phase inhibitors | 28 |
| 1.11.7 | Some examples of corrosion inhibitors | 28 |
| 1.12 | MECHANISM OF CORROSION INHIBITION | 29 |
| 1.13 | MARAGING STEELS | 30 |
| 1.13.1 | Welded maraging steel | 31 |
| 1.13.2 | Uses of maraging steel | 32 |
| 1.13.3 | Role of alloying elements in maraging steel | 33 |
| 1.14 | LITERATURE REVIEW | 33 |
| 1.14.1 | Corrosion of maraging steels | 33 |
| 1.14.2 | Organic inhibitors for the corrosion inhibition of iron and iron alloys in aqueous media | 35 |
| 1.15 | SCOPE | 37 |
| 1.16 | OBJECTIVES | 38 |
| CHAPTER 2 MATERIALS AND METHODS | | |
| 2.1 | MATERIALS | 41 |
| 2.1.1 | 18% Ni M250 grade maraging steel | 41 |
| 2.1.2 | Material conditions | 41 |
| 2.1.3 | Preparation of test coupons | 42 |
| 2.2 | MEDIA | 42 |
| 2.2.1 | Preparation of standard hydrochloric acid solution | 42 |
| 2.2.2 | Preparation of standard sulphuric acid solution | 42 |

| | | |
|--|--|----|
| 2.3 | INHIBITORS | 42 |
| 2.3.1 | Synthesis of 1-Phenyl-4-(4-nitrophenyl) thiosemicarbazide (PNPT) | 42 |
| 2.3.2 | Synthesis of 2,5-Bis (3,4,5-trimethoxy phenyl)-1,3,4-oxadiazole (BTPO) | 43 |
| 2.3.3 | Synthesis of 3,4,5-Trimethoxy-benzoic acid(3,4,5-trimethoxy-benzylidene) hydrazide (TBTBH) | 44 |
| 2.3.4 | Synthesis of 2-(4-Methoxy-phenyl)-benzo[d]imidazo[2,1-b]thiazole (MPBIT) | 44 |
| 2.3.5 | Synthesis of 2-(5-Chloro-1H-benzoimidazol-2-yl) phenol (CBP) | 45 |
| 2.4 | METHODS | 45 |
| 2.4.1 | Electrochemical measurements | 45 |
| 2.4.1.1 | Potentiodynamic polarisation studies | 46 |
| 2.4.1.2 | Electrochemical impedance spectroscopy studies (EIS) | 47 |
| 2.4.2 | Scanning electron microscopy (SEM)/ EDX analysis | 47 |
| 2.5 | ACTIVATION PARAMETERS | 48 |
| 2.6 | ADSORPTION ISOTHERMS | 49 |
| 2.7 | THERMODYNAMIC PARAMETERS | 50 |
| CHAPTER 3 RESULTS AND DISCUSSIONS | | |
| 3.1 | CORROSION BEHAVIOUR OF 18% Ni M250 GRADE MARAGING STEEL UNDER WELDED CONDITION IN HYDROCHLORIC ACID MEDIUM | |
| 3.1.1 | Potentiodynamic polarization studies | 52 |
| 3.1.2 | Electrochemical impedance spectroscopy (EIS) studies | 54 |
| 3.1.3 | Effect of temperature | 57 |
| 3.1.4 | Effect of concentration | 60 |
| 3.1.5 | Scanning electron microscope (SEM)/EDX studies | 60 |
| 3.2 | CORROSION BEHAVIOR OF 18% Ni M250 GRADE MARAGING STEEL UNDER WELDED CONDITION IN SULPHURIC ACID MEDIUM | |
| 3.2.1 | Potentiodynamic polarization studies | 66 |
| 3.2.2 | Electrochemical impedance spectroscopy (EIS) studies | 66 |
| 3.2.3 | Effect of temperature | 67 |
| 3.2.4 | Scanning electron microscope studies (SEM)/EDX studies | 70 |
| 3.3 | 2,5-BIS(3,4,5-TRIMETHOXY PHENYL)-1,3,4-OXADIAZOLE (BTPO) AS INHIBITOR FOR THE CORROSION OF WELDED MARAGING STEEL IN HYDROCHLORIC ACID MEDIUM | |
| 3.3.1 | Potentiodynamic polarization measurements | 75 |
| 3.3.2 | Electrochemical impedance spectroscopy (EIS) studies | 77 |
| 3.3.3 | Effect of temperature | 80 |
| 3.3.4 | Effect of hydrochloric acid concentration | 83 |
| 3.3.5 | Adsorption isotherm | 83 |

| | | |
|-------|--|-----|
| 3.3.6 | Mechanism of corrosion inhibition | 86 |
| 3.3.7 | SEM/EDX studies | 88 |
| 3.4 | 2,5-BIS(3,4,5-TRIMETHOXY PHENYL)-1,3,4-OXADIAZOLE (BTPO) AS INHIBITOR FOR THE CORROSION OF WELDED MARAGING STEEL IN SULPHURIC ACID MEDIUM | |
| 3.4.1 | Potentiodynamic polarization measurements | 103 |
| 3.4.2 | Electrochemical impedance spectroscopy (EIS) studies | 104 |
| 3.4.3 | Effect of temperature | 106 |
| 3.4.4 | Effect of acid concentration | 108 |
| 3.4.5 | Adsorption isotherm | 108 |
| 3.4.6 | Mechanism of corrosion inhibition | 109 |
| 3.4.7 | SEM/EDX studies | 109 |
| 3.5 | 1-PHENYL-4-(4-NITROPHENYL)THIOSEMICARBAZIDE (PNPT) AS INHIBITOR FOR THE CORROSION OF WELDED MARAGING STEEL IN HYDROCHLORIC ACID MEDIUM | |
| 3.5.1 | Potentiodynamic polarization measurements | 125 |
| 3.5.2 | Electrochemical impedance spectroscopy (EIS) studies | 126 |
| 3.5.3 | Effect of temperature | 128 |
| 3.5.4 | Effect of hydrochloric acid concentration | 130 |
| 3.5.5 | Adsorption isotherm | 130 |
| 3.5.6 | Mechanism of corrosion inhibition | 131 |
| 3.5.7 | SEM/EDX studies | 132 |
| 3.6 | 1-PHENYL-4-(4-NITROPHENYL)THIOSEMICARBAZIDE (PNPT) AS INHIBITOR FOR THE CORROSION OF WELDED MARAGING STEEL IN SULPHURIC ACID MEDIUM | |
| 3.6.1 | Potentiodynamic polarization measurements | 147 |
| 3.6.2 | Electrochemical impedance spectroscopy (EIS) studies | 148 |
| 3.6.3 | Effect of temperature | 150 |
| 3.6.4 | Effect of acid concentration | 151 |
| 3.6.5 | Adsorption isotherm | 151 |
| 3.6.6 | Mechanism of corrosion inhibition | 152 |
| 3.6.7 | SEM/EDX studies | 153 |
| 3.7 | 3,4,5-TRIMETHOXY-BENZOICACID(3,4,5-TRIMETHOXY- BENZYLIDENE) HYDRAZIDE (TBTBH) AS INHIBITOR FOR THE CORROSION OF WELDED MARAGING STEEL IN HYDROCHLORIC ACID MEDIUM | |
| 3.7.1 | Potentiodynamic polarization measurements | 168 |
| 3.7.2 | Electrochemical impedance spectroscopy (EIS) studies | 169 |
| 3.7.3 | Effect of temperature | 170 |
| 3.7.4 | Effect of acid concentration | 172 |
| 3.7.5 | Adsorption isotherm | 172 |

| | | |
|--------|---|-----|
| 3.7.6 | Mechanism of corrosion inhibition | 173 |
| 3.7.7 | SEM/EDX studies | 173 |
| 3.8 | 3,4,5-TRIMETHOXY-BENZOICACID(3,4,5-TRIMETHOXY-BENZYLIDENE) HYDRAZIDE (TBTBH) AS INHIBITOR FOR THE CORROSION OF WELDED MARAGING STEEL IN SULPHURIC ACID MEDIUM | |
| 3.8.1 | Potentiodynamic polarization measurements | 188 |
| 3.8.2 | Electrochemical impedance spectroscopy (EIS) studies | 189 |
| 3.8.3 | Effect of temperature | 190 |
| 3.8.4 | Effect of acid concentration | 192 |
| 3.8.5 | Adsorption isotherm | 192 |
| 3.8.6 | Mechanism of corrosion inhibition | 193 |
| 3.8.7 | SEM/EDX studies | 194 |
| 3.9 | 2-(5-CHLORO-1H-BENZOIMIDAZOL-2-YL) PHENOL (CBP) AS INHIBITOR FOR THE CORROSION OF WELDED MARAGING STEEL IN HYDROCHLORIC ACID MEDIUM | |
| 3.9.1 | Potentiodynamic polarization measurements | 209 |
| 3.9.2 | Electrochemical impedance spectroscopy (EIS) studies | 209 |
| 3.9.3 | Effect of temperature | 211 |
| 3.9.4 | Effect of hydrochloric acid concentration | 213 |
| 3.9.5 | Adsorption isotherm | 213 |
| 3.9.6 | Mechanism of corrosion inhibition | 214 |
| 3.9.7 | SEM/EDX studies | 214 |
| 3.10 | 2-(5-CHLORO-1H-BENZOIMIDAZOL-2-YL) PHENOL (CBP) AS INHIBITOR FOR THE CORROSION OF WELDED MARAGING STEEL IN SULPHURIC ACID MEDIUM | |
| 3.10.1 | Potentiodynamic polarization measurements | 229 |
| 3.10.2 | Electrochemical impedance spectroscopy (EIS) studies | 230 |
| 3.10.3 | Effect of temperature | 231 |
| 3.10.4 | Effect of hydrochloric acid concentration | 233 |
| 3.10.5 | Adsorption isotherm | 233 |
| 3.10.6 | Mechanism of corrosion inhibition | 234 |
| 3.10.7 | SEM/EDX studies | 234 |
| 3.11 | 2-(4-METHOXY-PHENYL)-BENZO[d]IMIDAZO[2,1-b]THIAZOLE (MPBIT) AS INHIBITOR FOR THE CORROSION OF WELDED MARAGING STEEL IN HYDROCHLORIC ACID MEDIUM | |
| 3.11.1 | Potentiodynamic polarization measurements | 250 |
| 3.11.2 | Electrochemical impedance spectroscopy (EIS) studies | 251 |
| 3.11.3 | Effect of temperature | 252 |
| 3.11.4 | Effect of acid concentration | 254 |
| 3.11.5 | Adsorption isotherm | 254 |

| | | |
|--|--|-----|
| 3.11.6 | Mechanism of corrosion inhibition | 255 |
| 3.11.7 | SEM/EDX studies | 255 |
| 3.12 | 2-(4-METHOXY-PHENYL)-BENZO[d]IMIDAZO[2,1-b]THIAZOLE (MPBIT) AS INHIBITOR FOR THE CORROSION OF WELDED MARAGING STEEL IN SULPHURIC ACID MEDIUM | |
| 3.12.1 | Potentiodynamic polarization measurements | 271 |
| 3.12.2 | Electrochemical impedance spectroscopy (EIS) studies | 272 |
| 3.12.3 | Effect of temperature | 273 |
| 3.12.4 | Effect of acid concentration | 275 |
| 3.12.5 | Adsorption isotherm | 275 |
| 3.12.6 | Mechanism of corrosion inhibition | 276 |
| 3.12.7 | SEM/EDX studies | 276 |
| 3.13 | COMPARISON OF INHIBITION EFFICIENCIES OF THE FIVE INHIBITORS | 292 |
| CHAPTER 4 SUMMARY AND CONCLUSIONS | | |
| 4.1 | SUMMARY | 296 |
| 4.2 | CONCLUSIONS | 296 |
| 4.3 | SCOPE FOR FUTURE WORK | 297 |
| | REFERENCES | 298 |
| | LIST OF PUBLICATIONS | 309 |
| | BIO DATA | 310 |

LIST OF FIGURES

| Fig. No. | Caption | Page No. |
|----------|--|----------|
| 1.1 | The electrochemical cell set up between anodic and cathodic sites on a metal surface undergoing corrosion. | 4 |
| 1.2 | Pourbaix diagram for iron/water/dissolved oxygen system. | 11 |
| 1.3 | Electrode kinetic behavior of pure iron in acid solution (schematic). | 15 |
| 1.4 | Tafel plot | 17 |
| 1.5 | Linear Polarization Curve | 19 |
| 1.6 | Nyquist plot | 21 |
| 1.7 | Bode plot | 21 |
| 1.8 | Evans diagrams showing the effect of addition of a) anodic inhibitor, b) cathodic inhibitor, c) mixed inhibitor. | 26 |
| 3.1 | Potentiodynamic polarization curves for the corrosion of welded maraging steel in different concentrations of HCl at 35 °C. | 52 |
| 3.2 | Nyquist plots for the corrosion of welded maraging steel in different concentrations of HCl at 35 °C. | 55 |
| 3.3 | The equivalent circuit model used to fit the experimental data for the corrosion of the welded maraging steel in 0.5 M HCl solution at 30 °C. | 56 |
| 3.4 | Potentiodynamic polarization curves for the corrosion of welded maraging steel in 1.5 M HCl at different temperatures. | 57 |
| 3.5 | Nyquist plots for the corrosion of welded maraging steel in 1.5 M HCl at different temperatures. | 58 |
| 3.6 | Arrhenius plots for the corrosion of welded maraging steel in HCl. | 59 |
| 3.7 | Plots of $\ln(\nu_{corr}/T)$ versus $1/T$ for the corrosion of welded maraging steel in HCl. | 59 |
| 3.8 | SEM images of (a) freshly polished surface (b) corroded surface. | 61 |
| 3.9 (a) | EDX spectra of the freshly polished surface of welded maraging steel. | 61 |
| 3.9 (b) | EDX spectra of the welded maraging steel after immersion in 2.0 M hydrochloric acid. | 62 |
| 3.10 | Potentiodynamic polarisation curves for the corrosion of welded maraging steel in different concentrations of H ₂ SO ₄ at 50 °C. | 66 |
| 3.11 | Nyquist plots for the corrosion of welded maraging steel in different concentrations of H ₂ SO ₄ at 50 °C. | 67 |
| 3.12 | Potentiodynamic polarization curves for the corrosion of welded maraging steel in 1.0 M H ₂ SO ₄ at different temperatures. | 68 |
| 3.13 | Nyquist plots for the corrosion of welded maraging steel in | 69 |

| | | |
|------|---|-----|
| | 1.0 M H ₂ SO ₄ at different temperatures. | |
| 3.14 | Arrhenius plots for the corrosion of welded sample of maraging steel in H ₂ SO ₄ . | 69 |
| 3.15 | Plots of $\ln (U_{corr}/ T)$ versus 1/T for the corrosion of welded sample of maraging steel in H ₂ SO ₄ . | 70 |
| 3.16 | SEM images of (a) freshly polished surface (b) corroded surface. | 71 |
| 3.17 | EDX spectra of the welded maraging steel after immersion in 2.0 M sulphuric acid. | 71 |
| 3.18 | Potentiodynamic polarization curves for the corrosion of welded maraging steel in 1.0 M hydrochloric acid containing different concentrations of BTPO at 30 °C. | 75 |
| 3.19 | Nyquist plots for the corrosion of welded maraging steel in 1.0 M hydrochloric acid containing different concentrations of BTPO at 30 °C. | 77 |
| 3.20 | Equivalent circuit used to fit the experimental EIS data for the corrosion of welded maraging steel in 1.0 M HCl at 30 °C in the presence of BTPO. | 78 |
| 3.21 | Bode (a) phase angle plots and (b) amplitude plots for the corrosion of welded maraging steel in 1.0 M HCl containing different concentrations of BTPO at 30 °C. | 80 |
| 3.22 | Arrhenius Plots for the corrosion of welded maraging steel in 1.0 M hydrochloric acid containing different concentrations of BTPO. | 81 |
| 3.23 | Plots of $\ln(v_{corr}/T)$ versus 1/T for the corrosion of welded maraging steel in 1.0 M hydrochloric acid containing different concentrations of BTPO. | 82 |
| 3.24 | Langmuir adsorption isotherms for the adsorption of BTPO on welded maraging steel in 1.0 M HCl at different temperatures. | 85 |
| 3.25 | SEM images of the welded maraging steel after immersion in 1.0 M HCl (a) in the absence and (b) in the presence of BTPO. | 89 |
| 3.26 | EDX spectra of the welded maraging steel after immersion in 1.0 M HCl in the presence of BTPO. | 89 |
| 3.27 | Potentiodynamic polarization curves for the corrosion of welded maraging steel in 1.0 M sulphuric acid containing different concentrations of BTPO at 30 °C. | 103 |
| 3.28 | Nyquist plots for the corrosion of welded maraging steel in 1.0 M H ₂ SO ₄ containing different concentrations of BTPO at 30 °C. | 104 |
| 3.29 | Equivalent circuit used to fit the experimental EIS data for the corrosion of welded maraging steel in 1.0 M H ₂ SO ₄ at 30 °C in presence of BTPO. | 105 |
| 3.30 | Bode (a) phase angle plots and (b) amplitude plots for the | 106 |

| | | |
|------|--|-----|
| | corrosion of welded maraging steel in 1.0 M H ₂ SO ₄ containing different concentrations of BTPO at 30 °C. | |
| 3.31 | Arrhenius plots for the corrosion of welded maraging steel in 1.0 M H ₂ SO ₄ containing different concentrations of BTPO. | 107 |
| 3.32 | Plots of $\ln(v_{corr}/T)$ versus 1/T for the corrosion of welded maraging steel in 1.0 M H ₂ SO ₄ containing different concentrations of BTPO. | 107 |
| 3.33 | Langmuir adsorption isotherms for the adsorption of BTPO on welded maraging steel in 1.0 M H ₂ SO ₄ at different temperatures. | 109 |
| 3.34 | SEM images of the welded maraging steel after immersion in 1.0 M H ₂ SO ₄ (a) in the absence and (b) in the presence of BTPO. | 110 |
| 3.35 | EDX spectra of the welded maraging steel after immersion in 1.0 M H ₂ SO ₄ in the presence of BTPO. | 110 |
| 3.36 | Potentiodynamic polarization curves for the corrosion of welded maraging steel in 1.0 M hydrochloric acid containing different concentrations of PNPT at 30 °C. | 125 |
| 3.37 | Nyquist plots for the corrosion of welded maraging steel in 1.0 M hydrochloric acid containing different concentrations of PNPT at 30 °C. | 126 |
| 3.38 | Bode (a) phase angle plots and (b) amplitude plots for the corrosion of welded maraging steel in 1.0 M HCl containing different concentrations of PNPT at 30 °C. | 127 |
| 3.39 | Arrhenius Plots for the corrosion of welded maraging steel in 1.0 M hydrochloric acid containing different concentrations of PNPT. | 128 |
| 3.40 | Plots of $\ln(v_{corr}/T)$ versus 1/T for the corrosion of welded maraging steel in 1.0 M hydrochloric acid containing different concentrations of PNPT. | 129 |
| 3.41 | Langmuir adsorption isotherms for the adsorption of PNPT on the welded maraging steel in 1.0 M HCl at different temperatures. | 131 |
| 3.42 | SEM image of the welded maraging steel after immersion in 1.0 M HCl in the presence of PNPT. | 132 |
| 3.43 | EDX spectra of the welded maraging steel after immersion in 1.0 M HCl in the presence of PNPT. | 132 |
| 3.44 | Potentiodynamic polarization curves for the corrosion of welded maraging steel in 1.0 M H ₂ SO ₄ containing different concentrations of PNPT at 30 °C. | 147 |
| 3.45 | Nyquist plots for the corrosion of welded maraging steel in 1.0 M H ₂ SO ₄ containing different concentrations of PNPT at 30 °C. | 149 |
| 3.46 | Bode (a) phase angle plots and (b) amplitude plots for the corrosion of welded maraging steel in 1.0 M H ₂ SO ₄ | 149 |

| | | |
|------|--|-----|
| | containing different concentrations of PNPT at 30 °C. | |
| 3.47 | Arrhenius plots for the corrosion of welded maraging steel in 1.0 M H ₂ SO ₄ containing different concentrations of PNPT. | 150 |
| 3.48 | Plots of $\ln(v_{corr}/T)$ versus $1/T$ for the corrosion of welded maraging steel in 1.0 M H ₂ SO ₄ containing different concentrations of PNPT. | 151 |
| 3.49 | Langmuir adsorption isotherms for the adsorption of PNPT on welded maraging steel in 1.0 M H ₂ SO ₄ at different temperatures. | 152 |
| 3.50 | SEM image of the welded maraging steel after immersion in 1.0 M H ₂ SO ₄ in the presence of PNPT. | 153 |
| 3.51 | EDX spectra of the welded maraging steel after immersion in 1.0 M H ₂ SO ₄ in the presence of PNPT. | 153 |
| 3.52 | Potentiodynamic polarization curves for the corrosion of welded maraging steel in 1.0 M hydrochloric acid containing different concentrations of TBTBH at 30 °C. | 168 |
| 3.53 | Nyquist plots for the corrosion of welded maraging steel in 1.0 M hydrochloric acid containing different concentrations of TBTBH at 30 °C. | 169 |
| 3.54 | Bode (a) phase angle plots and (b) amplitude plots for the corrosion of welded maraging steel in 1.0 M HCl containing different concentrations of TBTBH at 30 °C. | 170 |
| 3.55 | Arrhenius Plots for the corrosion of welded maraging steel in 1.0 M hydrochloric acid containing different concentrations of TBTBH. | 171 |
| 3.56 | Plots of $\ln(v_{corr}/T)$ versus $1/T$ for the corrosion of welded maraging steel in 1.0 M hydrochloric acid containing different concentrations of TBTBH. | 171 |
| 3.57 | Langmuir adsorption isotherms for the adsorption of TBTBH on welded maraging steel in 1.0 M HCl at different temperatures. | 173 |
| 3.58 | SEM image of the welded maraging steel after immersion in 1.0 M HCl in the presence of TBTBH. | 174 |
| 3.59 | EDX spectra of the welded maraging steel after immersion in 1.0 M HCl in the presence of TBTBH. | 174 |
| 3.60 | Potentiodynamic polarization curves for the corrosion of welded maraging steel in 1.0 M H ₂ SO ₄ containing different concentrations of TBTBH at 30 °C. | 188 |
| 3.61 | Nyquist plots for the corrosion of welded maraging steel in 1.0 M H ₂ SO ₄ containing different concentrations of TBTBH at 30 °C. | 190 |
| 3.62 | Bode (a) phase angle plots and (b) amplitude plots for the corrosion of welded maraging steel in 1.0 M H ₂ SO ₄ containing different concentrations of TBTBH at 30 °C. | 190 |
| 3.63 | Arrhenius plots for the corrosion of welded maraging steel in 1.0 M H ₂ SO ₄ containing different concentrations of TBTBH. | 191 |

| | | |
|------|---|-----|
| 3.64 | Plots of $\ln(v_{corr}/T)$ versus $1/T$ for the corrosion of welded maraging steel in 1.0 M H_2SO_4 containing different concentrations of TBTBH. | 192 |
| 3.65 | Langmuir adsorption isotherms for the adsorption of TBTBH on welded maraging steel in 1.0 M H_2SO_4 at different temperatures. | 193 |
| 3.66 | SEM image of the welded maraging steel after immersion in 1.0 M H_2SO_4 in the presence of TBTBH. | 194 |
| 3.67 | EDX spectra of the welded maraging steel after immersion in 1.0 M H_2SO_4 in the presence of TBTBH. | 194 |
| 3.68 | Potentiodynamic polarization curves for the corrosion of welded maraging steel in 1.0 M hydrochloric acid containing different concentrations of CBP at 30 °C. | 209 |
| 3.69 | Nyquist plots for the corrosion of welded maraging steel in 1.0 M hydrochloric acid containing different concentrations of CBP at 30 °C. | 210 |
| 3.70 | Bode (a) phase angle plots and (b) amplitude plots for the corrosion of welded maraging steel in 1.0 M HCl containing different concentrations of CBP at 30 °C. | 211 |
| 3.71 | Arrhenius Plots for the corrosion of welded maraging steel in 1.0 M hydrochloric acid containing different concentrations of CBP. | 212 |
| 3.72 | Plots of $\ln(v_{corr}/T)$ versus $1/T$ for the corrosion of welded maraging steel in 1.0 M hydrochloric acid containing different concentrations of CBP. | 212 |
| 3.73 | Langmuir adsorption isotherms for the adsorption of CBP on welded maraging steel in 1.0 M HCl at different temperatures. | 214 |
| 3.74 | SEM image of the welded maraging steel after immersion in 1.0 M HCl in the presence of CBP. | 215 |
| 3.75 | EDX spectra of the welded maraging steel after immersion in 1.0 M HCl in the presence of CBP. | 215 |
| 3.76 | Potentiodynamic polarization curves for the corrosion of welded maraging steel in 1.0 M H_2SO_4 containing different concentrations of CBP at 30 °C. | 229 |
| 3.77 | Nyquist plots for the corrosion of welded maraging steel in 1.0 M H_2SO_4 containing different concentrations of CBP at 30 °C. | 230 |
| 3.78 | Bode (a) phase angle plots and (b) amplitude plots for the corrosion of welded maraging steel in 1.0 M H_2SO_4 containing different concentrations of CBP at 30 °C. | 231 |
| 3.79 | Arrhenius plots for the corrosion of welded maraging steel in 1.0 M H_2SO_4 containing different concentrations of CBP. | 232 |
| 3.80 | Plots of $\ln(v_{corr}/T)$ versus $1/T$ for the corrosion of welded maraging steel in 1.0 M H_2SO_4 containing different concentrations of CBP. | 232 |

| | | |
|------|--|-----|
| 3.81 | Langmuir adsorption isotherms for the adsorption of CBP on welded maraging steel in 1.0 M H ₂ SO ₄ at different temperatures. | 234 |
| 3.82 | SEM image of the welded maraging steel after immersion in 1.0 M H ₂ SO ₄ in the presence of CBP. | 235 |
| 3.83 | EDX analysis of the welded maraging steel after immersion in 1.0 M H ₂ SO ₄ in the presence of CBP. | 235 |
| 3.84 | Potentiodynamic polarization curves for the corrosion of welded maraging steel in 1.0 M hydrochloric acid containing different concentrations of MPBIT at 30 °C. | 250 |
| 3.85 | Nyquist plots for the corrosion of welded maraging steel in 1.0 M hydrochloric acid containing different concentrations of MPBIT at 30 °C. | 251 |
| 3.86 | Bode (a) phase angle plots and (b) amplitude plots for the corrosion of welded maraging steel in 1.0 M HCl containing different concentrations of MPBIT at 30 °C. | 252 |
| 3.87 | Arrhenius plots for the corrosion of welded maraging steel in 1.0 M hydrochloric acid containing different concentrations of MPBIT. | 253 |
| 3.88 | Plots of $\ln(v_{corr}/T)$ versus $1/T$ for the corrosion of welded maraging steel in 1.0 M hydrochloric acid containing different concentrations of MPBIT. | 253 |
| 3.89 | Langmuir adsorption isotherms for the adsorption of MPBIT on welded maraging steel in 1.0 M HCl at different temperatures. | 255 |
| 3.90 | SEM images of the welded maraging steel after immersion in 1.0 M HCl in the presence of MPBIT. | 256 |
| 3.91 | EDX spectra of the welded maraging steel after immersion in 1.0 M HCl in the presence of MPBIT. | 256 |
| 3.92 | Potentiodynamic polarization curves for the corrosion of welded maraging steel in 1.0 M H ₂ SO ₄ containing different concentrations of MPBIT at 30 °C. | 271 |
| 3.93 | Nyquist plots for the corrosion of welded maraging steel in 1.0 M H ₂ SO ₄ containing different concentrations of MPBIT at 30 °C. | 272 |
| 3.94 | Bode (a) phase angle plots and (b) amplitude plots for the corrosion of welded maraging steel in 1.0 M H ₂ SO ₄ containing different concentrations of MPBIT at 30 °C. | 273 |
| 3.95 | Arrhenius plots for the corrosion of welded maraging steel in 1.0 M H ₂ SO ₄ containing different concentrations of MPBIT. | 274 |
| 3.96 | Plots of $\ln(v_{corr}/T)$ versus $1/T$ for the corrosion of welded maraging steel in 1.0 M H ₂ SO ₄ containing different concentrations of MPBIT. | 274 |
| 3.97 | Langmuir adsorption isotherms for the adsorption of MPBIT on welded maraging steel in 1.0 M H ₂ SO ₄ at different temperatures. | 276 |

| | | |
|------|---|-----|
| 3.98 | SEM image of the welded maraging steel after immersion in 1.0 M H ₂ SO ₄ in the presence of MPBIT. | 277 |
| 3.99 | EDX analysis of the welded maraging steel after immersion in 1.0 M H ₂ SO ₄ in the presence of MPBIT. | 277 |

LIST OF TABLES

| Table No. | Captions | Page No. |
|-----------|---|----------|
| 1.1 | Common anchoring organic groups. | 29 |
| 1.2 | Important inhibitors used for iron and iron alloys. | 35 |
| 2.1 | Composition of the specimen (% by weight). | 41 |
| 2.2 | Composition of the filler material used for welding (% by weight). | 41 |
| 2.3 | Adsorption isotherms to characterise the adsorption of inhibitors on the metal surface. | 49 |
| 3.1 | Results of potentiodynamic polarization studies for the corrosion of welded maraging steel in different concentrations of HCl at different temperatures. | 63 |
| 3.2 | EIS data for the corrosion of welded maraging steel in different concentrations of HCl at different temperatures. | 64 |
| 3.3 | Activation parameters for the corrosion of welded maraging steel in hydrochloric acid. | 65 |
| 3.4 | Results of potentiodynamic polarization studies for the corrosion of welded maraging steel in different concentrations of H ₂ SO ₄ at different temperatures. | 72 |
| 3.5 | EIS data for the corrosion of welded maraging steel in different concentrations of H ₂ SO ₄ at different temperatures. | 73 |
| 3.6 | Activation parameters for the corrosion of welded maraging steel in H ₂ SO ₄ medium. | 74 |
| 3.7 | Results of potentiodynamic polarization studies for the corrosion of welded maraging steel in 0.1 M hydrochloric acid containing different concentrations of BTPO. | 90 |
| 3.8 | Results of potentiodynamic polarization studies for the corrosion of welded maraging steel in 0.5 M hydrochloric acid containing different concentrations of BTPO. | 91 |
| 3.9 | Results of potentiodynamic polarization studies for the corrosion of welded maraging steel in 1.0 M hydrochloric acid containing different concentrations of BTPO. | 92 |
| 3.10 | Results of potentiodynamic polarization studies for the corrosion of welded maraging steel in 1.5 M hydrochloric acid containing different concentrations of BTPO. | 93 |
| 3.11 | Results of potentiodynamic polarization studies for the corrosion of welded maraging steel in 2.0 M hydrochloric acid containing different concentrations of BTPO. | 94 |
| 3.12 | EIS data for the corrosion of welded maraging steel in 0.1 M hydrochloric acid containing different concentrations of BTPO. | 95 |
| 3.13 | EIS data for the corrosion of welded maraging steel in 0.5 M hydrochloric acid containing different concentrations of BTPO. | 96 |
| 3.14 | EIS data for the corrosion of welded maraging steel in 1.0 M | 97 |

| | | |
|------|---|-----|
| | hydrochloric acid containing different concentrations of BTPO. | |
| 3.15 | EIS data for the corrosion of welded maraging steel in 1.5 M hydrochloric acid containing different concentrations of BTPO. | 98 |
| 3.16 | EIS data for the corrosion of welded maraging steel in 2.0 M hydrochloric acid containing different concentrations of BTPO. | 99 |
| 3.17 | Activation parameters for the corrosion of welded maraging steel in hydrochloric acid containing different concentrations of BTPO. | 100 |
| 3.18 | Maximum inhibition efficiency attained in different concentrations of hydrochloric acid at different temperatures for BTPO. | 101 |
| 3.19 | Thermodynamic parameters for the adsorption of BTPO on welded maraging steel surface in hydrochloric acid at different temperatures. | 102 |
| 3.20 | Results of potentiodynamic polarization studies for the corrosion of welded maraging steel in 0.1 M sulphuric acid containing different concentrations of BTPO. | 112 |
| 3.21 | Results of potentiodynamic polarization studies for the corrosion of welded maraging steel in 0.5 M sulphuric acid containing different concentrations of BTPO. | 113 |
| 3.22 | Results of potentiodynamic polarization studies for the corrosion of welded maraging steel in 1.0 M sulphuric acid containing different concentrations of BTPO. | 114 |
| 3.23 | Results of potentiodynamic polarization studies for the corrosion of welded maraging steel in 1.5 M sulphuric acid containing different concentrations of BTPO. | 115 |
| 3.24 | Results of potentiodynamic polarization studies for the corrosion of welded maraging steel in 2.0 M sulphuric acid containing different concentrations of BTPO. | 116 |
| 3.25 | EIS data for the corrosion of welded maraging steel in 0.1 M sulphuric acid containing different concentrations of BTPO. | 117 |
| 3.26 | EIS data for the corrosion of welded maraging steel in 0.5 M sulphuric acid containing different concentrations of BTPO. | 118 |
| 3.27 | EIS data for the corrosion of welded maraging steel in 1.0 M sulphuric acid containing different concentrations of BTPO. | 119 |
| 3.28 | EIS data for the corrosion of welded maraging steel in 1.5 M sulphuric acid containing different concentrations of BTPO. | 120 |
| 3.29 | EIS data for the corrosion of welded maraging steel in 2.0 M sulphuric acid containing different concentrations of BTPO. | 121 |
| 3.30 | Activation parameters for the corrosion of welded maraging steel in sulphuric acid containing different concentrations of BTPO. | 122 |
| 3.31 | Maximum inhibition efficiency attained in different | 123 |

| | | |
|------|--|-----|
| | concentrations of sulphuric acid at different temperatures for BTPO. | |
| 3.32 | Thermodynamic parameters for the adsorption of BTPO on welded maraging steel surface in sulphuric acid at different temperatures. | 124 |
| 3.33 | Results of potentiodynamic polarization studies for the corrosion of welded maraging steel in 0.1 M hydrochloric acid containing different concentrations of PNPT. | 134 |
| 3.34 | Results of potentiodynamic polarization studies for the corrosion of welded maraging steel in 0.5 M hydrochloric acid containing different concentrations of PNPT. | 135 |
| 3.35 | Results of potentiodynamic polarization studies for the corrosion of welded maraging steel in 1.0 M hydrochloric acid containing different concentrations of PNPT. | 136 |
| 3.36 | Results of potentiodynamic polarization studies for the corrosion of welded maraging steel in 1.5 M hydrochloric acid containing different concentrations of PNPT. | 137 |
| 3.37 | Results of potentiodynamic polarization studies for the corrosion of welded maraging steel in 2.0 M hydrochloric acid containing different concentrations of PNPT. | 138 |
| 3.38 | EIS data for the corrosion of welded maraging steel in 0.1 M hydrochloric acid containing different concentrations of PNPT. | 139 |
| 3.39 | EIS data for the corrosion of welded maraging steel in 0.5 M hydrochloric acid containing different concentrations of PNPT. | 140 |
| 3.40 | EIS data for the corrosion of welded maraging steel in 1.0 M hydrochloric acid containing different concentrations of PNPT. | 141 |
| 3.41 | EIS data for the corrosion of welded maraging steel in 1.5 M hydrochloric acid containing different concentrations of PNPT. | 142 |
| 3.42 | EIS data for the corrosion of welded maraging steel in 2.0 M hydrochloric acid containing different concentrations of PNPT. | 143 |
| 3.43 | Activation parameters for the corrosion of welded maraging steel in hydrochloric acid containing different concentrations of PNPT. | 144 |
| 3.44 | Maximum inhibition efficiency attained in different concentrations of hydrochloric acid at different temperatures for PNPT. | 145 |
| 3.45 | Thermodynamic parameters for the adsorption of PNPT on welded maraging steel surface in hydrochloric acid at different temperatures. | 146 |
| 3.46 | Results of potentiodynamic polarization studies for the corrosion of welded maraging steel in 0.1 M sulphuric acid | 155 |

| | | |
|------|---|-----|
| | containing different concentrations of PNPT. | |
| 3.47 | Results of potentiodynamic polarization studies for the corrosion of welded maraging steel in 0.5 M sulphuric acid containing different concentrations of PNPT. | 156 |
| 3.48 | Results of potentiodynamic polarization studies for the corrosion of welded maraging steel in 1.0 M sulphuric acid containing different concentrations of PNPT. | 157 |
| 3.49 | Results of potentiodynamic polarization studies for the corrosion of welded maraging steel in 1.5 M sulphuric acid containing different concentrations of PNPT. | 158 |
| 3.50 | Results of potentiodynamic polarization studies for the corrosion of welded maraging steel in 2.0 M sulphuric acid containing different concentrations of PNPT. | 159 |
| 3.51 | EIS data for the corrosion of welded maraging steel in 0.1 M sulphuric acid containing different concentrations of PNPT. | 160 |
| 3.52 | EIS data for the corrosion of welded maraging steel in 0.5 M sulphuric acid containing different concentrations of PNPT. | 161 |
| 3.53 | EIS data for the corrosion of welded maraging steel in 1.0 M sulphuric acid containing different concentrations of PNPT. | 162 |
| 3.54 | EIS data for the corrosion of welded maraging steel in 1.5 M sulphuric acid containing different concentrations of PNPT. | 163 |
| 3.55 | EIS data for the corrosion of welded maraging steel in 2.0 M sulphuric acid containing different concentrations of PNPT. | 164 |
| 3.56 | Activation parameters for the corrosion of welded maraging steel in sulphuric acid containing different concentrations of PNPT. | 165 |
| 3.57 | Maximum inhibition efficiency attained in different concentrations of sulphuric acid at different temperatures for PNPT. | 166 |
| 3.58 | Thermodynamic parameters for the adsorption of PNPT on welded maraging steel surface in sulphuric acid at different temperatures. | 167 |
| 3.59 | Results of potentiodynamic polarization studies for the corrosion of welded maraging steel in 0.1 M hydrochloric acid containing different concentrations of TBTBH. | 175 |
| 3.60 | Results of potentiodynamic polarization studies for the corrosion of welded maraging steel in 0.5 M hydrochloric acid containing different concentrations of TBTBH. | 176 |
| 3.61 | Results of potentiodynamic polarization studies for the corrosion of welded maraging steel in 1.0 M hydrochloric acid containing different concentrations of TBTBH. | 177 |
| 3.62 | Results of potentiodynamic polarization studies for the corrosion of welded maraging steel in 1.5 M hydrochloric acid containing different concentrations of TBTBH. | 178 |
| 3.63 | Results of potentiodynamic polarization studies for the corrosion of welded maraging steel in 2.0 M hydrochloric | 179 |

| | | |
|------|--|-----|
| | acid containing different concentrations of TBTBH. | |
| 3.64 | EIS data for the corrosion of welded maraging steel in 0.1 M hydrochloric acid containing different concentrations of TBTBH. | 180 |
| 3.65 | EIS data for the corrosion of welded maraging steel in 0.5 M hydrochloric acid containing different concentrations of TBTBH. | 181 |
| 3.66 | EIS data for the corrosion of welded maraging steel in 1.0 M hydrochloric acid containing different concentrations of TBTBH. | 182 |
| 3.67 | EIS data for the corrosion of welded maraging steel in 1.5 M hydrochloric acid containing different concentrations of TBTBH. | 183 |
| 3.68 | EIS data for the corrosion of welded maraging steel in 2.0 M hydrochloric acid containing different concentrations of TBTBH. | 184 |
| 3.69 | Activation parameters for the corrosion of welded maraging steel in hydrochloric acid containing different concentrations of TBTBH. | 185 |
| 3.70 | Maximum inhibition efficiency attained in different concentrations of hydrochloric acid at different temperatures for TBTBH. | 186 |
| 3.71 | Thermodynamic parameters for the adsorption of TBTBH on welded maraging steel surface in hydrochloric acid at different temperatures. | 187 |
| 3.72 | Results of potentiodynamic polarization studies for the corrosion of welded maraging steel in 0.1 M sulphuric acid containing different concentrations of TBTBH. | 196 |
| 3.73 | Results of potentiodynamic polarization studies for the corrosion of welded maraging steel in 0.5 M sulphuric acid containing different concentrations of TBTBH. | 197 |
| 3.74 | Results of potentiodynamic polarization studies for the corrosion of welded maraging steel in 1.0 M sulphuric acid containing different concentrations of TBTBH. | 198 |
| 3.75 | Results of potentiodynamic polarization studies for the corrosion of welded maraging steel in 1.5 M sulphuric acid containing different concentrations of TBTBH. | 199 |
| 3.76 | Results of potentiodynamic polarization studies for the corrosion of welded maraging steel in 2.0 M sulphuric acid containing different concentrations of TBTBH. | 200 |
| 3.77 | EIS data for the corrosion of welded maraging steel in 0.1 M sulphuric acid containing different concentrations of TBTBH. | 201 |
| 3.78 | EIS data for the corrosion of welded maraging steel in 0.5 M sulphuric acid containing different concentrations of TBTBH. | 202 |

| | | |
|------|---|-----|
| 3.79 | EIS data for the corrosion of welded maraging steel in 1.0 M sulphuric acid containing different concentrations of TBTBH. | 203 |
| 3.80 | EIS data for the corrosion of welded maraging steel in 1.5 M sulphuric acid containing different concentrations of TBTBH. | 204 |
| 3.81 | EIS data for the corrosion of welded maraging steel in 2.0 M sulphuric acid containing different concentrations of TBTBH. | 205 |
| 3.82 | Activation parameters for the corrosion of welded maraging steel in sulphuric acid containing different concentrations of TBTBH. | 206 |
| 3.83 | Maximum inhibition efficiency attained in different concentrations of sulphuric acid at different temperatures for TBTBH. | 207 |
| 3.84 | Thermodynamic parameters for the adsorption of TBTBH on welded maraging steel surface in sulphuric acid at different temperatures. | 208 |
| 3.85 | Results of potentiodynamic polarization studies for the corrosion of welded maraging steel in 0.1 M hydrochloric acid containing different concentrations of CBP. | 216 |
| 3.86 | Results of potentiodynamic polarization studies for the corrosion of welded maraging steel in 0.5 M hydrochloric acid containing different concentrations of CBP. | 217 |
| 3.87 | Results of potentiodynamic polarization studies for the corrosion of welded maraging steel in 1.0 M hydrochloric acid containing different concentrations of CBP. | 218 |
| 3.88 | Results of potentiodynamic polarization studies for the corrosion of welded maraging steel in 1.5 M hydrochloric acid containing different concentrations of CBP. | 219 |
| 3.89 | Results of potentiodynamic polarization studies for the corrosion of welded maraging steel in 2.0 M hydrochloric acid containing different concentrations of CBP. | 220 |
| 3.90 | EIS data for the corrosion of welded maraging steel in 0.1 M hydrochloric acid containing different concentrations of CBP. | 221 |
| 3.91 | EIS data for the corrosion of welded maraging steel in 0.5 M hydrochloric acid containing different concentrations of CBP. | 222 |
| 3.92 | EIS data for the corrosion of welded maraging steel in 1.0 M hydrochloric acid containing different concentrations of CBP. | 223 |
| 3.93 | EIS data for the corrosion of welded maraging steel in 1.5 M hydrochloric acid containing different concentrations of CBP. | 224 |
| 3.94 | EIS data for the corrosion of welded maraging steel in 2.0 M | 225 |

| | | |
|-------|--|-----|
| | hydrochloric acid containing different concentrations of CBP. | |
| 3.95 | Activation parameters for the corrosion of welded maraging steel in hydrochloric acid containing different concentrations of CBP. | 226 |
| 3.96 | Maximum inhibition efficiency attained in different concentrations of hydrochloric acid at different temperatures for CBP. | 227 |
| 3.97 | Thermodynamic parameters for the adsorption of CBP on welded maraging steel surface in hydrochloric acid at different temperatures. | 228 |
| 3.98 | Results of potentiodynamic polarization studies for the corrosion of welded maraging steel in 0.1 M sulphuric acid containing different concentrations of CBP. | 237 |
| 3.99 | Results of potentiodynamic polarization studies for the corrosion of welded maraging steel in 0.5 M sulphuric acid containing different concentrations of CBP. | 238 |
| 3.100 | Results of potentiodynamic polarization studies for the corrosion of welded maraging steel in 1.0 M sulphuric acid containing different concentrations of CBP. | 239 |
| 3.101 | Results of potentiodynamic polarization studies for the corrosion of welded maraging steel in 1.5 M sulphuric acid containing different concentrations of CBP. | 240 |
| 3.102 | Results of potentiodynamic polarization studies for the corrosion of welded maraging steel in 2.0 M sulphuric acid containing different concentrations of CBP. | 241 |
| 3.103 | EIS data for the corrosion of welded maraging steel in 0.1 M sulphuric acid containing different concentrations of CBP. | 242 |
| 3.104 | EIS data for the corrosion of welded maraging steel in 0.5 M sulphuric acid containing different concentrations of CBP. | 243 |
| 3.105 | EIS data for the corrosion of welded maraging steel in 1.0 M sulphuric acid containing different concentrations of CBP. | 244 |
| 3.106 | EIS data for the corrosion of welded maraging steel in 1.5 M sulphuric acid containing different concentrations of CBP. | 245 |
| 3.107 | EIS data for the corrosion of welded maraging steel in 2.0 M sulphuric acid containing different concentrations of CBP. | 246 |
| 3.108 | Activation parameters for the corrosion of welded maraging steel in sulphuric acid containing different concentrations of CBP. | 247 |
| 3.109 | Maximum inhibition efficiency attained in different concentrations of sulphuric acid at different temperatures for CBP. | 248 |
| 3.110 | Thermodynamic parameters for the adsorption of CBP on welded maraging steel surface in sulphuric acid at different temperatures. | 249 |
| 3.111 | Results of potentiodynamic polarization studies for the | 258 |

| | | |
|-------|---|-----|
| | corrosion of welded maraging steel in 0.1 M hydrochloric acid containing different concentrations of MPBIT. | |
| 3.112 | Results of potentiodynamic polarization studies for the corrosion of welded maraging steel in 0.5 M hydrochloric acid containing different concentrations of MPBIT. | 259 |
| 3.113 | Results of potentiodynamic polarization studies for the corrosion of welded maraging steel in 1.0 M hydrochloric acid containing different concentrations of MPBIT. | 260 |
| 3.114 | Results of potentiodynamic polarization studies for the corrosion of welded maraging steel in 1.5 M hydrochloric acid containing different concentrations of MPBIT. | 261 |
| 3.115 | Results of potentiodynamic polarization studies for the corrosion of welded maraging steel in 2.0 M hydrochloric acid containing different concentrations of MPBIT. | 262 |
| 3.116 | EIS data for the corrosion of welded maraging steel in 0.1 M hydrochloric acid containing different concentrations of MPBIT. | 263 |
| 3.117 | EIS data for the corrosion of welded maraging steel in 0.5 M hydrochloric acid containing different concentrations of MPBIT. | 264 |
| 3.118 | EIS data for the corrosion of welded maraging steel in 1.0 M hydrochloric acid containing different concentrations of MPBIT. | 265 |
| 3.119 | EIS data for the corrosion of welded maraging steel in 1.5 M hydrochloric acid containing different concentrations of MPBIT. | 266 |
| 3.120 | EIS data for the corrosion of welded maraging steel in 2.0 M hydrochloric acid containing different concentrations of MPBIT. | 267 |
| 3.121 | Activation parameters for the corrosion of welded maraging steel in hydrochloric acid containing different concentrations of MPBIT. | 268 |
| 3.122 | Maximum inhibition efficiency attained in different concentrations of hydrochloric acid at different temperatures for MPBIT. | 269 |
| 3.123 | Thermodynamic parameters for the adsorption of MPBIT on welded maraging steel surface in hydrochloric acid at different temperatures. | 270 |
| 3.124 | Results of potentiodynamic polarization studies for the corrosion of welded maraging steel in 0.1 M sulphuric acid containing different concentrations of MPBIT. | 279 |
| 3.125 | Results of potentiodynamic polarization studies for the corrosion of welded maraging steel in 0.5 M sulphuric acid containing different concentrations of MPBIT. | 280 |
| 3.126 | Results of potentiodynamic polarization studies for the corrosion of welded maraging steel in 1.0 M sulphuric acid | 281 |

| | | |
|-------|--|-----|
| | containing different concentrations of MPBIT. | |
| 3.127 | Results of potentiodynamic polarization studies for the corrosion of welded maraging steel in 1.5 M sulphuric acid containing different concentrations of MPBIT. | 282 |
| 3.128 | Results of potentiodynamic polarization studies for the corrosion of welded maraging steel in 2.0 M sulphuric acid containing different concentrations of MPBIT. | 283 |
| 3.129 | EIS data for the corrosion of welded maraging steel in 0.1 M sulphuric acid containing different concentrations of MPBIT. | 284 |
| 3.130 | EIS data for the corrosion of welded maraging steel in 0.5 M sulphuric acid containing different concentrations of MPBIT. | 285 |
| 3.131 | EIS data for the corrosion of welded maraging steel in 1.0 M sulphuric acid containing different concentrations of MPBIT. | 286 |
| 3.132 | EIS data for the corrosion of welded maraging steel in 1.5 M sulphuric acid containing different concentrations of MPBIT. | 287 |
| 3.133 | EIS data for the corrosion of welded maraging steel in 2.0 M sulphuric acid containing different concentrations of MPBIT. | 288 |
| 3.134 | Activation parameters for the corrosion of welded maraging steel in sulphuric acid containing different concentrations of MPBIT. | 289 |
| 3.135 | Maximum inhibition efficiency attained in different concentrations of sulphuric acid at different temperatures for MPBIT. | 290 |
| 3.136 | Thermodynamic parameters for the adsorption of MPBIT on welded maraging steel surface in hydrochloric acid at different temperatures. | 291 |
| 3.137 | Comparison of inhibition efficiencies of BTPO, PNPT, TBTBH, CBP and MPBIT for the corrosion of welded maraging steel in 0.1 M hydrochloric acid medium at different temperatures, obtained by Tafel polarization and EIS techniques. | 293 |
| 3.138 | Comparison of inhibition efficiencies of BTPO, PNPT, TBTBH, CBP and MPBIT for the corrosion of welded maraging steel in 0.1 M sulphuric acid medium at different temperatures, obtained by Tafel polarization and EIS techniques. | 294 |

LIST OF ABBREVIATIONS

| Abbreviations | Nomenclature |
|----------------------|--|
| BTPO | 2,5-Bis (3,4,5-trimethoxy phenyl)-1,3,4-oxadiazole |
| PNPT | 1-Phenyl-4-(4-nitrophenyl) thiosemicarbazide |
| TBTBH | 3,4,5-Trimethoxy benzoicacid(3,4,5-trimethoxy-benzylidene) hydrazide |
| CBP | 2-(5-Chloro-1H-benzimidazol-2-yl) phenol |
| MPBIT | 2-(4-Methoxy-phenyl)-benzo[d]imidazo[2,1-b] thiazole |
| bcc | Body centred cubic structure |
| EIS | Electrochemical impedance spectroscopy |
| e.m.f | Electromotive force |
| Fig. | Figure |
| HF | High frequency |
| LF | Low frequency |
| M250 | Maraging steel 250 grade |
| OCP | Open circuit potential |
| SCE | Saturated calomel electrode |
| SEM | Scanning electron microscopic |
| SCC | Stress Corrosion Cracking |
| VPI | Vapour phase inhibitor |
| ZCP | Zero charge potential |

LIST OF SYMBOLS

| Symbol | Definition |
|-----------------|--|
| T | Absolute temperature |
| E_a | Activation energy |
| η_{act} | Activation overpotential |
| E_0 | Amplitude of the signal |
| ω | Angular frequency |
| $Z(\omega)$ | Angular frequency (ω) dependent impedance |
| b_a | Anodic Tafel slope |
| W_i | Atomic weight of the i^{th} element in the alloy |
| C_f | Capacitance of the inhibitor film |
| b_c | Cathodic Tafel slope |
| E | Cell potential |
| R_{ct} | Charge transfer resistance |
| C_{inh} | Concentration of the inhibitor |
| η_{conc} | Concentration overpotential |
| B | Constant |
| K | Constant |
| Q | Constant phase element |
| R^2 | Correlation coefficient |
| i_{corr} | Corrosion current density |
| $i_{corr(inh)}$ | Corrosion current density in the presence of inhibitor |
| E_{corr} | Corrosion potential |
| v_{corr} | Corrosion rate |
| C_{dl} | Double layer capacitance |
| EDX | Energy dispersive X-ray spectroscopy |
| EW | Equivalent weight |
| F | Faraday constant |
| R_f | Film resistance |
| R | Gas constant |
| Z'' | Imaginary part impedance |
| Inh | Inhibitor |
| η | inhibition efficiency |
| l | Length |
| ϵ | Local dielectric constant |
| f_i | Mass fraction of the i^{th} element in the alloy |
| IR | Ohmic drop |
| a_{ox} | Oxidized species |
| ϵ^o | Permittivity of the air |
| Z' | Real part of impedance |

| | |
|---------------------------|---|
| a_{red} | Reduced species |
| ρ | Resistivity of the solution |
| SEM | Scanning electron microscope |
| χ | Size ratio |
| R_s | Solution resistance |
| E^0 | Standard cell potential |
| ΔH_{ads}^0 | Standard enthalpy of adsorption |
| ΔS_{ads}^0 | Standard entropy of adsorption |
| ΔG_{ads}^0 | Standard free energy of adsorption |
| θ | Surface coverage |
| S | Surface of the electrode |
| d | Thickness of the film |
| t | Time |
| n_i | Valence of the i^{th} element of the alloy |
| $\psi_{\text{z.ch}}$ | Zero charge potential |

CHAPTER 1

INTRODUCTION

1.1 IMPORTANCE OF CORROSION STUDIES

Corrosion is a natural process and a universal phenomenon. It can be defined as “the destruction or deterioration of a material because of the reaction with its environment”. Generally it is applicable mainly to metals and where a metal undergoes corrosion, its properties are changed due to the unintentional but destructive reaction with the environment. The corrosion process is continuous and irreversible. The life of a metal gets shortened by the corrosion process (Einar Bardal 2003). The corrosion can be a fast or a slow process depending upon the metal and the environment in which it is undergoing corrosion. Corrosion is a complex phenomenon influenced by so many environmental factors such as atmospheric constituents, underground/soil waste, acidic/alkaline solutions and combinations of these. Many of the corrosion problems generated in the industries involve the surroundings associated with acids and in certain cases alkalies and solvents.

It occurs with all metals except the least active noble metals such as gold and platinum (Banerjee 1985). Most of the metals occur in combined state except the noble metals. Pure metal is extracted from their ores by metallurgical process, energy being supplied in the form of heat or electrical energy (Pierre 2008). The obtained pure metals are relatively at higher energy state compared to their corresponding ores, and they have a natural tendency to revert back to their combined state. Thus corrosion of metals can be considered as extractive metallurgy in reverse (Fontana 1987).

1.2 NEED FOR CORROSION STUDY

Corrosion is a complex phenomenon influenced by so many environmental factors such as atmospheric constituents, underground/soil wastes, acidic/alkaline solutions and combinations of these. Many of the corrosion problems generated in the industries involve the surroundings associated with acids and in certain cases alkalies and solvents. The rapid growth in different sectors and the increasing pollution of the environment produces a more corrosive atmosphere. Thus the contamination of the industrial and other environmental factors is unavoidable. This leads to the destruction of

materials. The concerning of economic factor is a very important motivation for much of the current research in corrosion. The scientist studies corrosion mechanism to improve

- the understanding of the causes of corrosion,
- the ways to protect or minimize damage caused by corrosion,
- the understanding of mechanism of corrosion and the possible methods and mechanism of control.

Some of the economic and social consequences of corrosion are:

- Poor appearance,
- Contamination of a product,
- Loss of efficiency,
- Loss of valuable product,
- Effects on safety and reliability in handling hazardous materials,
- Health, example: pollution due to escaping of product from corroded equipment or corrosion product itself,
- Depletion of natural resources including metals and fuels used to manufacture them.

1.3 ELECTROCHEMICAL THEORY OF CORROSION

Corrosion of metals takes place due to the formation of anodic and cathodic regions on the same metal surface or when two different metals are in contact with each other in the presence of a conducting medium. At the anodic region oxidation reaction takes place and the metal gets converted into its ions, liberating electrons. Consequently, metal undergoes corrosion at the anodic region. At the cathodic region, reduction reaction takes place. Since the metal cannot be reduced further, metal atoms at the cathodic region are unaffected by the cathodic reaction. The electrons liberated at the anodic region migrate to the cathodic region constituting corrosion current. The metal ions liberated at the anode and some anions formed at the cathode diffuse towards each other through the conducting medium and form a corrosion product somewhere between the anode and cathode.

Corrosion reactions:

At the anodic region: Anodic reaction is a simple oxidation reaction in which the metal atoms are converted into their ions liberating electrons.

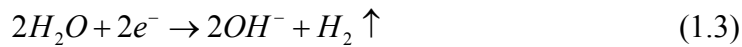


At the cathodic region: the following four reactions are possible

i) In acidic medium and in the absence of oxygen,



ii) In neutral or alkaline medium and in the absence of oxygen,



iii) In acidic medium and in the presence of oxygen,



iv) In neutral or alkaline medium and in the presence of oxygen,

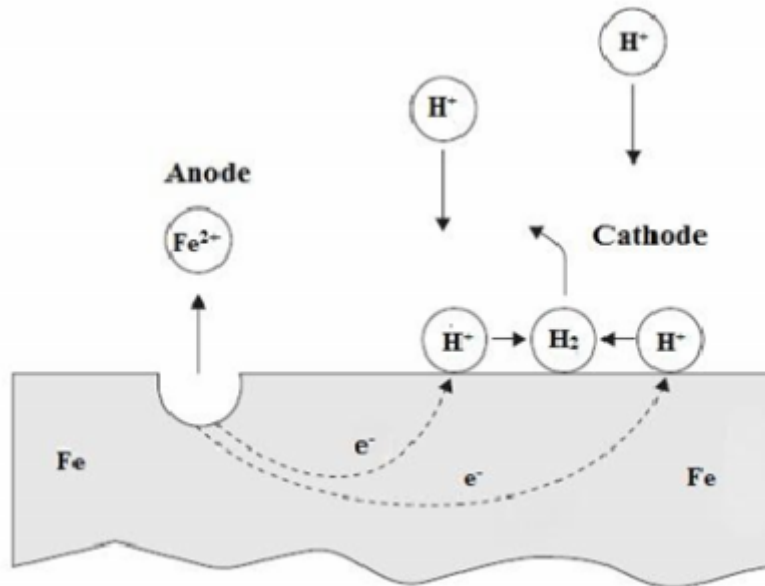


Fig. 1.1: The electrochemical cell set up between anodic and cathodic sites on a metal surface undergoing corrosion.

1.4 CLASSIFICATION OF CORROSION

Corrosion has been classified in many different ways. Classification is usually based on one of three factors.

- Nature of the corrodent: Corrosion can be classified as “wet corrosion” or “dry corrosion.” A liquid or moisture is necessary for the former, and dry corrosion usually involves reaction with high-temperature gases.
- Mechanism of corrosion: This involves either electrochemical or chemical reactions.
- Appearance of the corroded metal: Corrosion is either uniform or the localized metal areas are affected (Davis 2000).

1.4.1 Forms of corrosion

On the basis of the appearance of the corroded metal or mechanism of attack, corrosion is divided into eight categories as follows:

1.4.1.1 Uniform corrosion

Uniform or general corrosion, as the name implies results in a fairly uniform penetration (or thinning) over the entire exposed metal surface. The general attack results from local corrosion cell action; that is, multiple anodes and cathodes are operating on the metal surface at any given time. Uniform corrosion represents the greatest destruction of metal on a tonnage basis. This form of corrosion however, is not of too great concern from a technical standpoint because the life of equipment can be accurately estimated on the basis of comparatively simple immersion tests.

1.4.1.2 Galvanic corrosion

Galvanic corrosion occurs when a metal or alloy is electrically coupled to another metal or conducting nonmetal in the same electrolyte.

The three essential components are the following:

- Materials possessing different surface potential
- A common electrolyte
- A common electrical path

During galvanic coupling, the less corrosion-resistant metal becomes anodic, while the more corrosion-resistant metal becomes cathodic. The driving force for corrosion or

current flow is the potential developed between the dissimilar metals. Example: Steel in contact with copper.

1.4.1.3 Crevice corrosion

Crevice corrosion is a form of localized attack that occurs at narrow openings or spaces between metal-to-metal or nonmetal-to-metal components. This type of attack results from a concentration cell formed between the electrolyte within the crevice, which is oxygen starved, and the electrolyte outside the crevice, where oxygen is more plentiful. The material within the crevice acts as the anode, and the exterior material becomes the cathode. Example: corrosion of steel in an industrial environment resulting from wetted area within crevice.

1.4.1.4 Pitting corrosion

Pitting is a highly localized form of corrosion that produces sharply defined holes. These holes may be small or large in diameter, but in most cases, they are relatively small. Pits may be isolated from each other on the surface or so close together that they resemble a roughened surface. Pitting occurs when one area of a metal becomes anodic with respect to the rest of the surface or when highly localized changes in the corrodent in contact with the metal, as in crevices, cause accelerated localized attack. Example: stainless steel exposed to chloride containing water.

1.4.1.5 Intergranular corrosion

Intergranular corrosion is defined as the selective dissolution of grain boundaries, or closely adjacent regions, without appreciable attack of the grains themselves. This dissolution is caused by potential differences between the grain-boundary region and any precipitates, intermetallic phases, or impurities that form at the grain boundaries. Example: Depletion of chromium in the grain boundary regions results in intergranular corrosion of stainless steels.

1.4.1.6 Selective leaching

It is the removal of one specific element from a solid alloy due to an electrochemical interaction with the environment. It is the preferential dissolution of one element from an alloy. The result of this corrosion is that of leaving a porous and usually

brittle shadow of the original component. Example: Dezincification is a type of attack occurring with brass alloys, leaving a porous residue of copper.

1.4.1.7 Erosion corrosion

Erosion-corrosion is the corrosion on a metal because of the mechanical wear or abrasive contributions in the presence of a corrosion medium. The combination of a wear or abrasive and corrosion results in more severe attack than would be realized with either mechanical or chemical corrosive action alone. Metals that depend on a relatively thick protective coating of corrosion product for corrosion resistance are frequently subject to erosion-corrosion. Example: propellers, impellers exposed to moving fluids.

1.4.1.8 Stress corrosion

Stress corrosion cracking refers to cracking caused by the simultaneous presence of tensile stress and a specific corrosive medium. During stress corrosion, the metal or alloy is virtually unattacked over most of its surface, while fine cracks progress through it normal to the direction of tensile stress. Example: season cracking of brass in the presence of ammonia.

1.5 FACTORS AFFECTING THE CORROSION RATE

Some of the important factors which influence the rate of corrosion are discussed below (Speller 1951, West 1965, Jones 1996, Gadag and Shetty 2006).

1.5.1 Nature of the metal

The tendency of a metal to undergo corrosion in aqueous solution depends upon its electrode potential, which is variable, subject to other conditions such as temperature, pressure and concentration. In general, the metals with lower electrode potentials are more susceptible for corrosion than the ones with higher electrode potentials. However there are exceptions to this general trend as some metals show passivity.

1.5.2 Difference in potential between anodic and cathodic region

Larger the potential difference between the anodic region and the cathodic region of the corrosion cell, higher is the corrosion rate.

1.5.3 Nature of the corrosion product

The corrosion product formed on the surface of the metal may or may not act as a protective film. If the corrosion product deposited is insoluble, stable, uniform, nonporous and adherent it acts as a protective film. A thin, invisible, impervious, continuous film formed on the surface acts as a barrier between the fresh metal surface and the corrosion environment, and thereby prevents further corrosion.

1.5.4 Ratio of anodic to cathodic area

The rate of corrosion is greatly influenced by the relative sizes of anodic and cathodic areas. If a metal has a small anodic area and large cathodic area, then the corrosion is more intensive at the anodic region because electrons released at the anode are rapidly consumed at the cathode. If cathode is smaller than anode, the consumption of electrons at the cathode will be slower and lower will be the corrosion rate.

1.5.5 Hydrogen overvoltage

Hydrogen over potential is an important factor of corrosion where hydrogen evolution is the cathodic reaction. Under the given environmental conditions of temperature, pressure and flow rate of medium, each metal exhibits its own characteristic resistance (hydrogen over potential) to hydrogen evolution reaction. Higher the hydrogen overvoltage, more difficult is the liberation of hydrogen on the metal surface. Hence any factor, which increases hydrogen over potential, will considerably retard the corrosion rate.

1.5.6 Temperature

In general, corrosion rate increases with the increase in temperature, probably due to the increase in conductance of the medium, decrease in polarization effects, solubility of corrosion products, breakdown of protective film, etc.

1.5.7 pH

Depending on the pH of the medium and the nature of the metal, either hydrogen evolution or oxygen reduction reaction predominates. In general, lower the

pH of the corrosion medium, higher is the corrosion rate. However, some metals like Al, Zn, etc., undergo fast corrosion in highly alkaline solutions.

1.5.8 Presence of oxidizing agents

The presence of oxidizing agents increases the corrosion rate of the metal. Even noble metals undergo corrosion in the presence of oxidizing agents.

1.5.9 Polarization at anodic and cathodic region

During the process of corrosion, the polarization of the anode and the cathode decreases the corrosion rate substantially. Polarization at the electrodes is due to: (i) change in concentration at the vicinity of the electrode (ii) overvoltage or (iii) presence of surface films on the electrodes.

1.5.10 Effect of dissolved oxygen

Amount of dissolved oxygen in the corrosion medium plays a significant role in cathodic reaction of the corrosion. Differential aeration or oxygen concentration cell is formed on the metal surface, when the metal is exposed to the environment having different oxygen concentrations. Oxygen rich area becomes cathodic whereas oxygen deficient area becomes anodic. In some cases the metal oxide formed acts as a passive barrier between metal and the environment.

1.5.11 Effect of velocity of the medium

If the corrosion is due to the presence of stagnant zone of corrosive fluid or due to the formation of shielded area, increase in velocity will decrease the corrosion rate. If the corrosive ions are supplied because of velocity, the corrosion rate will increase. Increase in velocity can also increase the corrosion rate where the corrosion resistance is due to formation of weak surface film.

1.5.12 Effect of other ions present in the solution

The rate of corrosion process is affected by the presence of certain ions like Cl^- , SO_4^{2-} , NO_3^- , etc. For instance in the formation of protective film on the metals such as aluminium, iron, copper, etc., chloride ions will interfere and can cause extensive damage. Similar effects with less severity were also observed in the presence of sulphate ions. Sometimes the intermediate corrosion products

become predominant in controlling the rate of corrosion process.

1.6 THERMODYNAMICS OF CORROSION (Fontana1987, Davis 2003, Philip 2007, Revie and Uhlig 2008).

Thermodynamic approach of energy changes involved in the electrochemical reactions of corrosion provides the information about the driving force and the spontaneous direction of the reaction. The change in free energy ΔG is a direct measure of the work capacity or maximum electric energy available from a system. If the change in free energy accompanying the transition of a system from one state to another state is negative, this indicates a loss in free energy and also the spontaneous reaction of the system. It is not possible to predict accurately the velocity of a reaction from change in free energy. This parameter reflects only the direction of reaction by its sign, and any predictions of velocity based on the magnitude of the change in free energy may be erroneous. The free energy change accompanying an electrochemical reaction can be calculated by the following equation.

$$\Delta G = - nFE \quad (1.6)$$

where, ΔG is the free energy change, n is the number of electrons involved in the reaction, F is the Faraday constant and E is the cell potential.

To determine the potential of a system in which the reactants are not at unit activity, the Nernst equation can be employed, that is

$$E = E^0 + 2.303 \frac{RT}{nF} \log \frac{a_{ox}}{a_{red}} \quad (1.7)$$

where, E is the cell potential, E^0 the standard cell potential, R is the gas constant, T is absolute temperature, n is the number of electrons transferred, F is the Faraday constant, a_{ox} and a_{red} are the activities of oxidized and reduced species. Thus, there is a definite relation between the free energy change and the cell potential of an electrochemical reaction. In any electrochemical reaction, the most negative or active half-cell tends to be oxidized, and most positive or noble half-cell tends to be reduced.

Electrode potentials are very useful in predicting corrosion behaviour. All metals with reversible potentials more active than hydrogen will tend to be corroded by acid solutions. Hence, electrode potentials can be used to state a criterion for corrosion.

Potential/pH diagrams (Pourbaix diagrams) graphically represent the stability of a metal and its corrosion products as a function of the potential and pH of an aqueous solution. The pH is shown on the horizontal axis and the potential on the vertical axis. The main uses of these diagrams are, i) predicting the spontaneous direction of reactions, ii) estimating the composition of corrosion products, iii) predicting the environmental changes that will prevent or reduce corrosive attack.

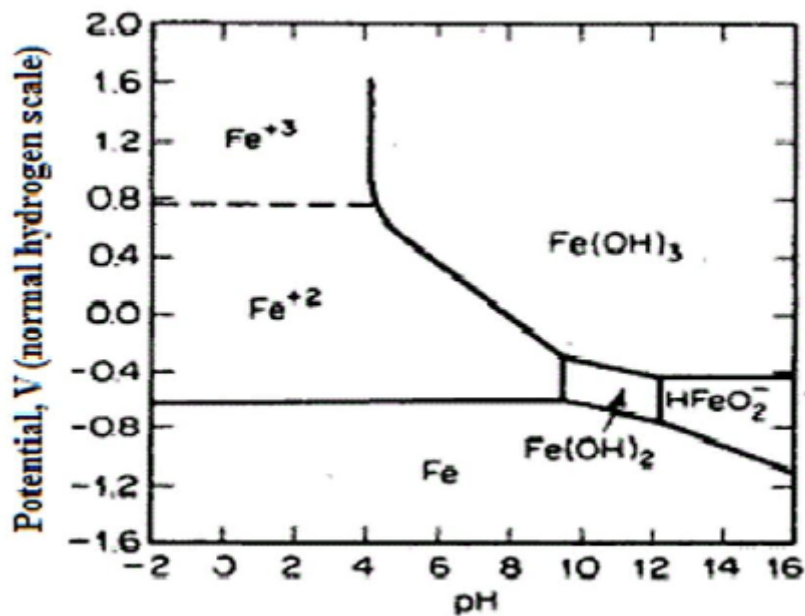


Fig. 1.2: Pourbaix diagram for iron/water/dissolved oxygen system.

From a corrosion engineering perspective, the value of Pourbaix diagrams is their usefulness in identifying potential – pH domains where corrosion does not occur - that is, where the metal itself is the stable phase. By controlling potential (e.g., by cathodic protection) and/or by adjusting the pH in specific domains identified using Pourbaix diagrams, it may be possible to prevent corrosion from taking place.

A typical Pourbaix diagram for iron is shown in Fig. 1.2. As shown, it is

possible to delineate areas in which iron, iron hydroxide, ferrous iron, etc., are thermodynamically stable. That is these forms represent states of lowest free energy. Thermodynamics does not predict how fast the corrosion reaction will occur. To understand the kinetics of corrosion, examination of a number of electrochemical principles for example, mixed potential behaviour, polarization behaviour, and the concept of exchange currents, are required. Some useful terms used to explain electrochemical kinetics of corrosion are explained in the following sections.

1.7 ELECTROCHEMICAL POLARIZATION

During electrochemical corrosion the anode and cathode are not at their equilibrium potential. This deviation from equilibrium potential is called polarization. For cathodic polarization, η_c , electrons are supplied to the surface, and a buildup in the metal due to the slow reaction rate causes the surface potential to become negative and hence η_c is negative. For anodic polarization, η_a , electrons are removed from the metal, a deficiency results in a positive potential change due to the slow liberation of electrons by the surface reaction, and η_a must be positive.

Electrochemical polarizations are divided into three main types.

a) Activation polarization

Activation polarization is usually the controlling factor during corrosion in strong acids since both the concentration overpotential and the ohmic drop are relatively small. Activation polarization is caused by the resistance against the reaction itself at the metal-electrolyte interface. In other words activation polarization is caused by a slow electrode reaction because the reaction at the electrode requires activation energy. Both anodic and cathodic reactions can be under activation polarization. A reaction for which activation polarization dominates is referred to as activation controlled.

b) Concentration polarization

Concentration polarization is observed when the reaction rates are controlled by the diffusion of the specific species in the bulk electrolyte to the metal electrolyte interface. When a chemical species participating in a corrosion process is in short supply, the mass transport of that species to the corroding surface can

become rate controlling. Concentration polarization usually predominates when the concentration of the active species is low; for example, in dilute acids or in aerated waters where the active component, dissolved oxygen, is only present at very low levels.

c) Ohmic polarization

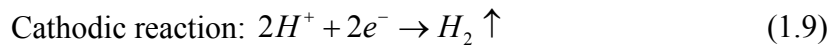
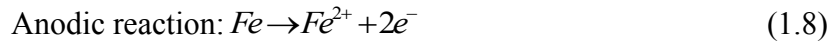
Solutions of electrolytes have rather poor conductivity compared to metals, particularly in dilute solutions. In corrosion systems, if the metal surface is covered by paints or other films of insulating material or if the electrolyte surrounding the electrode has high resistance, it will give rise to a potential drop through either a portion of electrolyte or through the film on the metal surface or both, which is known as resistance polarization. If resistance polarization dominates a reaction, it is referred as resistance or the ohmic drop controlled.

1.8 MIXED POTENTIAL THEORY

According to this theory (Wagner and Truad 1938), any electrochemical reaction can be divided into two or more oxidation and reduction reactions, and there can be no accumulation of electrical charge during the reaction. There are two basic premises underlie mixed-potential theory. First, the anodic current in an electrochemical cell must equal the cathodic current. This is a requirement of the conservation of electrical charge. The number of electrons generated by the total of all oxidation reactions must be exactly equal to the number of electrons consumed by the total of all reduction reactions. Second, for the purpose of examination and definition of the electrochemical cell, the anodic (oxidation) and cathodic (reduction) reactions can be defined, written, and treated independently. Oxidation reaction occurring at the anode liberates electrons as given by equation (1.1). The mixed potential theory proposes that all the electrons generated by anodic reactions are consumed by corresponding reduction reactions. The more common cathodic reactions encountered in aqueous corrosion are given in equations (1.2) to (1.5).

During corrosion more than one anodic and more than one cathodic reaction may be operative. The mixed potential itself, which is commonly referred to as the corrosion potential (E_{corr}), is the potential at which the total rates of all the anodic

reactions are equal to the total rates of all the cathodic reactions. The current density at E_{corr} is called the corrosion current density, i_{corr} , and is a measure of the corrosion rate. When a metal such as iron is corroding in an acid solution, both the half-cell reactions occur simultaneously on the surface.



The corrosion behavior of iron in dilute mineral acid solution (HCl) can be taken to illustrate the importance of kinetic factor in determining the rate of corrosion. The electrochemical characteristics of the system can be represented by the modified Evan's diagram schematically shown in Fig.1.3. Each electrode has its own half-cell electrode potential and exchange current density, as shown in Fig. 1.3. However, the two half-cell electrode potentials $E_{\text{Fe}^{2+}/\text{Fe}}$ and $E_{\text{H}^{+}/\text{H}_2}$ cannot coexist separately on an electrically conductive surface. Each must polarise or change potential to a common intermediate value, E_{corr} , (corrosion potential) which is also referred to as a mixed potential since it is a combination or mixture of the half-cell electrode potentials for reaction (1.14) and (1.15) (Jones 1996, Fontana 1987).

If an iron piece is dipped in HCl containing some ferrous ions, the electrode cannot remain at either of these two reversible potentials but must lie at some other potential. Iron is metallic and a good conductor of electricity and therefore the entire surface must be at a constant potential. The total rates of oxidation and reduction reactions are equal at the intersection of polarization curves for the two processes represented by E_{corr} . The rate of hydrogen evolution and the rate of iron dissolution will be equal and this is expressed in terms of i_{corr} , corrosion current density. For most of the metals the corrosion current density of $1\mu\text{A cm}^{-2}$ will be equal to the corrosion rate of 1 mpy (mills per year).

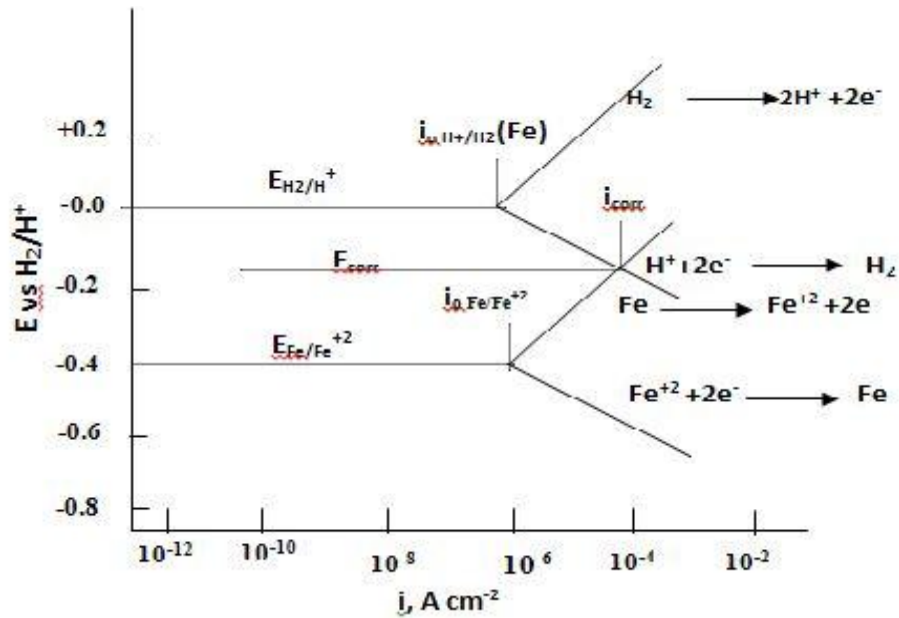


Fig. 1.3: Electrode kinetic behavior of pure iron in acid solution (schematic).

1.9 DETERMINATION OF CORROSION RATE

The rate of electrochemical reaction is limited by various physical and chemical factors. Corrosion of metal occurs through electrochemical reactions at the metal-solution interface. Understanding the electrochemical phenomenon of a corrosion process will help to monitor and reduce corrosion reaction. By using electrochemical methods, it is possible to monitor as well as understand the actual electrochemical process taking place on the metal surface. Mixed potential theory forms the basis for two electrochemical methods used to determine the corrosion rate. These are Tafel extrapolation and linear polarization techniques (Metals Handbook 1992). According to mixed potential theory any electrochemical reactions can be divided into two or more partial oxidation and reduction reactions. Electrochemical techniques can be used to measure the kinetics of electrochemical process, in specific environment and also to measure the oxidizing power of the environment.

Polarization experiments involve measuring the relationship between the electrochemical potential and the corrosion current. The potential current response of

electrochemical cell is determined over a desired potential range. The experiments can be determined in two ways,

- Potentiostatically, where potential is controlled and resulting current is measured.
- Galvanostatically, where the current is controlled and the resulting potential is measured.

The corrosion measurement techniques are classified in two types

- a) DC Electrochemical monitoring techniques.
- b) AC Electrochemical monitoring techniques.

1.9.1 DC Electrochemical monitoring techniques

Usually electrochemical technique has been employed to both speed data development and to better understand the corrosion mechanisms. DC polarization test is a potentiodynamic corrosion testing technique, where the potential of the electrode is varied at a selected rate by the application of a current through the electrolyte. When an electrode is polarized, it can cause current to flow via electrochemical reactions that occur at the electrode surface. The amount of current generated is controlled by the kinetics of the reactions and the diffusion of reactants both towards and away from the electrode. In a cell where an electrode undergoes uniform corrosion at open circuit, the open circuit potential is controlled by the equilibrium between two different electrochemical reactions.

1.9.1.1 Potentiodynamic polarization method

The Tafel plots are generated by applying a potential of 250 mV in both the positive and negative directions from the open circuit potential against a reference electrode. The current density is measured and usually plotted on a logarithmic scale. The corrosion potential (E_{corr}) and the corrosion current density (i_{corr}) are obtained from the Tafel plots as shown in Fig. 1.4. The corrosion potential (E_{corr}) or the open-circuit potential is the potential a metal will assume when placed in contact with a conductive medium. The value of the corrosion potential is determined by half-reactions of the corrosion process. E_{corr} is a characteristic of the corroding system and is unrelated with the electrochemical instrumentation. The Tafel plot provides a direct measure of

corrosion current, which can be used to calculate the corrosion rate. The corrosion plot consists of an anodic and a cathodic branch, the intersection of these branches can be projected on the X and Y axes to give the i_{corr} and the E_{corr} values, respectively. Tangents are drawn to the anodic and cathodic regions of the Tafel curve, the intersection of these provide the values of E_{corr} and i_{corr} when projected on the corresponding axes. The slopes of the linear portions of this plot are called the Tafel constants, which are used to calculate the polarization resistance (R_p) using the Stern-Geary equation (El- Sayed, 1997).

$$R_p = \frac{B}{i_{\text{corr}}} \quad (1.10)$$

$$B = \frac{b_a b_c}{2.303(b_a + b_c)} \quad (1.11)$$

where, b_a & b_c are the Tafel proportionality constants for the anodic and the cathodic reactions, respectively.

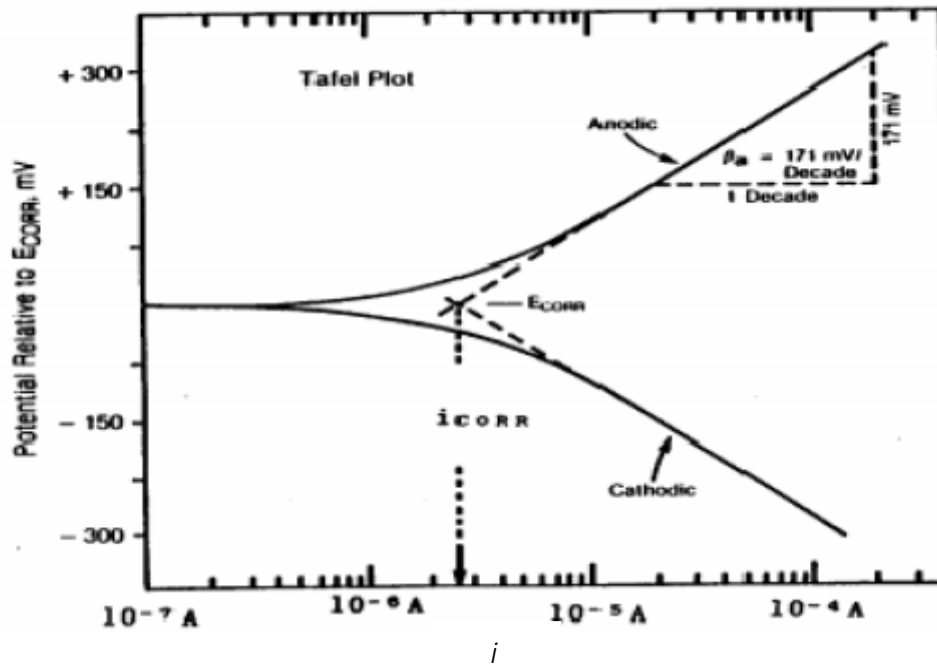


Fig. 1.4: Tafel plot

The corrosion rate (v_{corr}) is calculated using the Faraday's laws

$$v_{\text{corr}}(\text{mmy}^{-1}) = \frac{0.00327(E.W)i_{\text{corr}}}{\rho} \quad (1.12)$$

where, i_{corr} = corrosion current density in $\mu\text{A cm}^{-2}$

ρ = density of corroding material in g cm^{-3}

$E.W$ = equivalent weight of corroding material (atomic weight/oxidation number)

Advantages of Tafel methods

- It is possible to continuously measure very low corrosion rates.
- Monitoring the corrosion rate of a system, continuously.
- This method is very rapid than the conventional weight loss methods.
- The Tafel constants b_a and b_c can be used with linear polarization data.

Disadvantages of Tafel methods

- It can be applied only to systems containing one reduction process since Tafel region is distorted if more than one reduction process occurs.
- The system gets disturbed due to polarization of material under test by several hundred mV from corrosion potential.

1.9.1.2 Linear polarization method

Linear polarization technique is another method that utilizes polarization behavior to determine the corrosion rate of metals. The disadvantages of the Tafel extrapolation can be largely overcome by using a linear polarization analysis. Within ± 10 mV of the corrosion potential, the plot of the applied potential versus measured current is often linear. In this method the metal is polarized within ± 20 mV from the rest potential and the polarization plot is obtained. The usefulness of this measurement is that the slope of potential versus current plot, i.e., $\Delta E/\Delta i_{\text{app}}$. The relationship of the slope of the linear polarization curve to the corrosion current, the anodic and the cathodic Tafel slopes are,

$$\frac{\Delta E}{\Delta i_{\text{app}}} = \frac{b_a b_c}{2.3 i_{\text{corr}} (b_a + b_c)} \quad (1.13)$$

where, $\Delta E/\Delta i_{app}$ is the slope of the linear portion of the curve, b_a and b_c are the anodic and cathodic Tafel slopes and i_{corr} is the corrosion current.

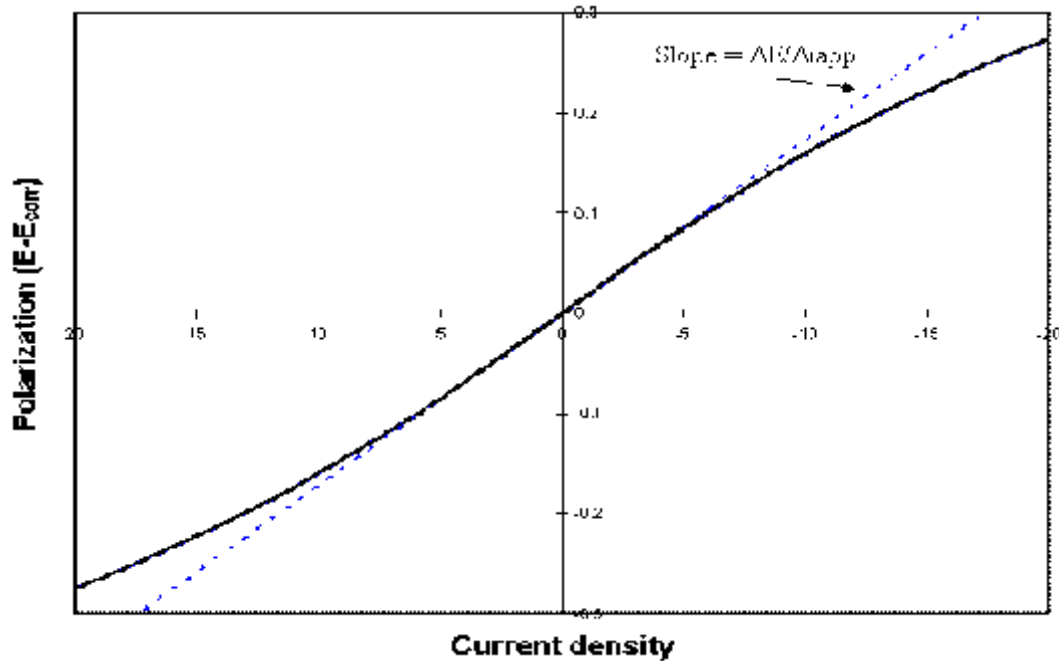


Fig. 1.5: Linear Polarization Curve

The slope of the linear polarization curves is determined experimentally, and the values of the anodic and cathodic Tafel slopes are determined either experimentally or estimated. After these values are obtained, the corrosion rate can be calculated from the calculated value of the corrosion current density i_{corr} . For example for system where anodic and cathodic slopes are equal to 0.12V per decade, the relationship between the slope of linear polarization curve and corrosion rate is

$$\frac{\Delta E}{\Delta i_{app}} = \frac{0.026}{i_{corr}} \quad (1.14)$$

Advantages of linear polarization technique

- It can be used for measuring very low corrosion rates in nuclear, pharmaceutical and food processing industries.

- They permit rapid corrosion rate measurement and can be used to monitor corrosion rate in various process streams.
- Electrochemical corrosion rate measurements may be used to measure the corrosion rate of structures that cannot be visually inspected or subjected to weight loss tests, like underground pipes tanks and large chemical plant components.

1.9.2 Electrochemical impedance spectroscopy (EIS)

Electrochemical impedance spectroscopy (EIS) measurement is a technique that has been used for a long time to study electrochemical processes at electrode surfaces. In electrochemical impedance experiments, a small AC voltage perturbation is applied to an electrode/solution interface, the resulting alternate current intensity is measured, and corresponding electrical impedance, is obtained. Electrochemical impedance is usually measured by applying an AC potential to an electrochemical cell and measuring the current through the cell. EIS can be used appropriately in the following areas of corrosion measurement:

- Rapid estimation of corrosion rates,
- Estimation of extremely low corrosion rate and metal contamination rate,
- Estimation of corrosion rates in low conductivity media,
- Rapid assessment of corrosion inhibitor performance in aqueous and nonaqueous media,
- Rapid evaluation of coatings.

The time dependent current response $I(t)$ of an electrode surface to a sinusoidal alternating potential signal $V(t)$ has been expressed as an angular frequency(ω) dependent impedance $Z(\omega)$,

$$Z(\omega) = V(t)/I(t) \quad (1.15)$$

where, 't' is the time, $V(t) = V_0 \sin \omega t$, $I(t) = I_0 \sin (\omega t + \theta)$ and θ = phase angle between $V(t)$ and $I(t)$.

Various processes at the surface absorb electrical energy at discrete frequencies, causing a time lag and a measurable phase angle θ , between the time dependent excitation

and response signals. These processes have been simulated by resistive capacitive electrical networks.

The impedance, $Z(\omega)$ may be expressed in terms of real $Z^I(\omega)$ and imaginary $Z^{II}(\omega)$ components.

$$Z(\omega) = Z^I(\omega) + Z^{II}(\omega) \quad (1.16)$$

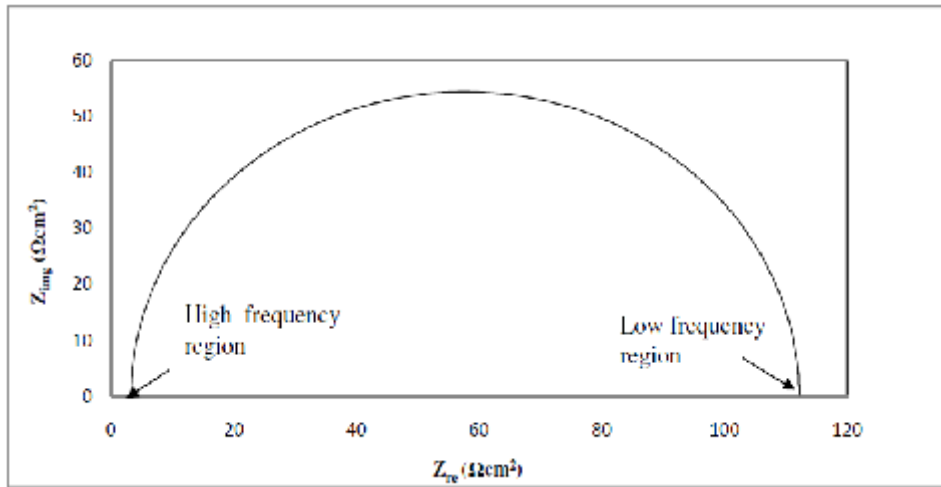


Fig. 1.6: Nyquist plot

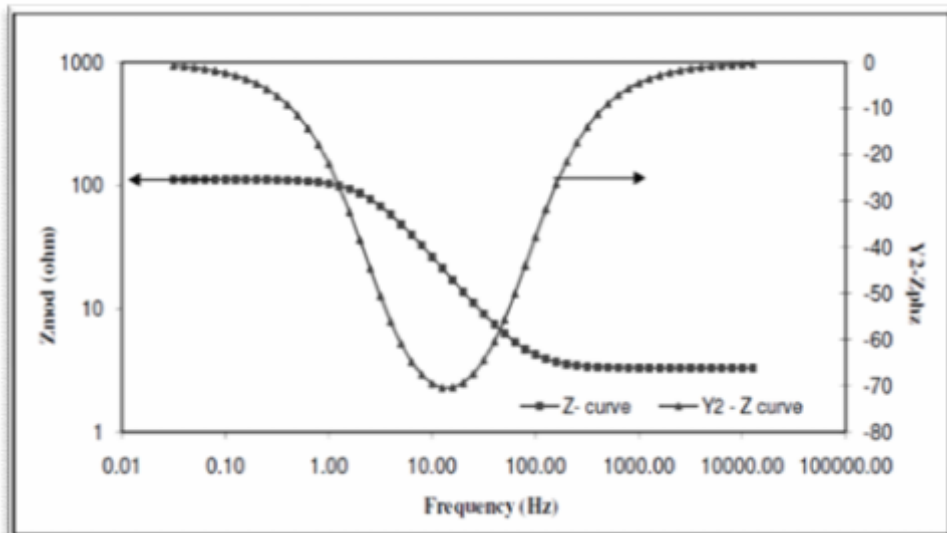


Fig. 1.7: Bode plot

The impedance behavior of an electrode may be expressed in Nyquist plots of $Z^{\text{II}}(\omega)$ as a function of $Z^{\text{I}}(\omega)$ (Fig. 1.6) or in Bode plot of $\log |Z|$ and $\log \theta$ versus frequency f in cycles per second (Hz) (Fig. 1.7), where $\omega=2\pi f$. An important part of the EIS analysis is to create an "equivalent circuit" of the system using resistors and capacitors in series and in parallel. The physical behavior of the corrosion system can be simulated and quantified with this circuit to gain insight into the important processes in the corrosion system. The impedance spectra are modeled by assuming a circuit made up of resistors, capacitors and inductors and then fitting that circuit to the spectra to extract values of circuit elements. The values may then related to physical phenomena to try to verify that the circuit model is a reasonable representation of the corrosion process.

The Nyquist plot shows a semicircle, with increasing frequency in counterclockwise direction as shown in the Fig. 1.6. At very high frequency, the imaginary component Z^{II} disappears, leaving only the solution resistance, R_s . At very low frequency, Z^{II} again disappears, leaving a sum of R_s and the Faradaic reaction resistance or polarization resistance R_p . The Faradiac reaction resistance or polarisation resistance R_p is inversely proportional to the corrosion rate. R_s measured at high frequency can be subtracted from the sum of $R_p + R_s$ at low frequency to give a compensated value of R_p free of ohmic interferences. The corrosion rates are calculated by using the Stern-Geary equation

$$i_{corr} = \frac{B}{R_p} \quad (1.17)$$

$$\text{where, } B = \frac{b_a b_c}{2.303(b_a + b_c)} \quad (1.18)$$

In this EIS technique a small amplitude AC signal of 10mV and frequency spectrum from 100 kHz to 0.01 mHz is impressed and impedance data are analysed.

1.9.2.1 Equivalent electric circuit models

The analysis of Nyquist and Bode plots from experimental data is done by fitting the experimental curves to an equivalent electrical circuit consisting of common

electrical circuit elements such as resistors, capacitors, and inductors. These circuit elements should have some physical relationship to the electrochemical parameters of the reaction. For example a resistor can be used in places where there are possible conductive paths in the electrochemical reaction. Therefore electrochemical parameters such as solution resistance (between the reference electrode and the working electrode) and polarization resistance are represented by an equivalent resistor in the model circuit. Capacitors and inductors are used where there are possible space charge polarization region in the electrochemical process. The impedance of a capacitor has inverse relationship with frequency and the current through a capacitor leads the voltage across the capacitor by 90 degrees. These electric circuit elements are connected in a fashion that represents the actual electrochemical process taking place. Since electrical circuit models can be made in different configurations with different elements to give the same output, there could be more than one possible circuit model for a particular electrochemical reaction (Deepika 2003, Venkatasubramaniyan 2009).

1.9.2.2 EIS modeling parameters (Stansbury 2000, Deepika 2003, Robert 2003, Nestor 2004)

While fitting the EIS data to electrical circuits, some important parameters need to be considered.

Electrolyte Resistance (R_s)

Electrolyte resistance or solution resistance is often a significant factor in the impedance of an electrochemical cell. Solution resistance is a resistance of the solution enclosed between the working electrode and the counter electrode. However any solution resistance between the reference electrode and the working electrode must be considered when the system is modeled. The resistance of an ionic solution depends on the ionic concentration, type of ions, temperature and the geometry of the area in which current is carried.

Double Layer Capacitance (C_{dl})

An electrical double layer exists at the interface between an electrode and its surrounding electrolyte. This double layer is formed as ions from the solution stick on

to the electrode surface. Charges in the electrode are separated from the charges of these ions. The separation is very small, of the order of angstroms. The value of the double layer capacitance depends on many variables including electrode potential, temperature, ionic concentrations, types of ions, oxide layers, electrode roughness, impurity adsorption, etc.

Charge Transfer Resistance (R_{ct})

The charge transfer resistance is formed by a single kinetically controlled electrochemical reaction. In this case, there is a single reaction at equilibrium. Consider a metal substrate in contact with an electrolyte. This charge transfer reaction has a certain speed, which is dependent on the kind of reaction, the temperature, the concentration of the reaction products and the potential.

1.10 CORROSION CONTROL BY INHIBITORS

Inhibitors are defined as substances which slow down either anodic, cathodic or both the electrochemical processes when added at a suitable concentration to the corrosive medium. A good inhibitor must fulfill the following requirements.

- It should be chemically inert and a small amount of it should be able to effectively inhibit the dissolution of metal.
- It should not decompose during service condition.
- It should be cost effective and should not cause environmental pollution.
- It should also inhibit the diffusion of hydrogen into metal.

Usually the corrosion inhibitor is rated in terms of inhibition efficiency (η) and is given by the relationship:

$$\eta(\%) = \frac{i_{corr} - i_{corr(inh)}}{i_{corr}} \times 100 \quad (1.19)$$

where, i_{corr} and $i_{corr(inh)}$ signify the corrosion current densities in the absence and presence of inhibitors, respectively. A corrosion inhibitor can function in two ways. In some situations the added inhibitors can alter the corrosive environment into a noncorrosive or less corrosive environment through its interaction with the corrosive species. In other

cases the corrosion inhibitor interacts with the metal surface and as a consequence inhibits the corrosion of the metal. Thus, based on the mode of interaction, there are two broad classes of inhibitors.

- Environment modifiers

In the case of environment modifiers the action and mechanism of inhibition is a simple interaction with the aggressive species in the environment, and thus reduce the attack of the metal by the aggressive species.

- Adsorption inhibitors

In the case of inhibitors which adsorb on the metal surface and inhibit the corrosion, there are two steps, namely: (i) transport of inhibitor to the metal surface; and (ii) metal–inhibitor interactions.

1.11 TYPES OF INHIBITORS

Various types of inhibitors commonly used include the following:

- Cathodic
- Anodic
- Mixed
- Ohmic
- Precipitation
- Vapour phase

1.11.1 Anodic (passivating) inhibitors

Anodic inhibitors are the substances which inhibit the anodic reactions and thereby reduce the corrosion rate. Basically, oxyanions such as chromates, molybdates, tungstates and also sodium nitrite are very effective anodic inhibitors. The anodic inhibitors combine with metal ions formed at the anodic region, forming the sparingly soluble respective salts. These compounds formed are deposited on the anodic sites forming the protective films, which acts as barrier between fresh metal surface and corrosive medium, thereby preventing further anodic reaction. Anodic inhibitors are found to be effective only when sufficient amount of the inhibitor is added into the corrosion medium. When concentration of an anodic inhibitor is not sufficient, corrosion

may be accelerated rather than inhibited. The effect of anodic inhibitors on polarization curves is shown in Fig1.7 (a).

1.11.2 Cathodic inhibitors

Cathodic inhibitors are the substances which inhibit the cathodic reactions and thereby reduce the corrosion rate of the metal. Cathodic inhibitors may be divided into three categories viz., (i) those that absorb oxygen (deaerators or oxygen scavengers), (ii) those that reduce the area of cathode, and (iii) those that increase the hydrogen over potential of cathodic process. The effect of cathodic inhibitors on polarization curves is shown in Fig1.8 (b).

1.11.3 Mixed inhibitors

These are substances which affect both the cathodic and anodic reactions. Corrosion potential change in such a case is smaller. Mixed types of inhibitors are generally organic compounds which adsorbed on metal surface and suppress the metal dissolution and reduction reactions (Papavinasam 2000). The effect of mixed inhibitors on polarization curves is shown in Fig1.8 (c).

The choice of effective inhibitors has been mostly done by using the empirical knowledge based on their macroscopically physico-chemical properties, mechanism of action and electron donating ability. The most significant criteria involved in the selection of an inhibitor are its hydrophobicity, molecular structure, electron density at their donor atoms, solubility and dispersibility.

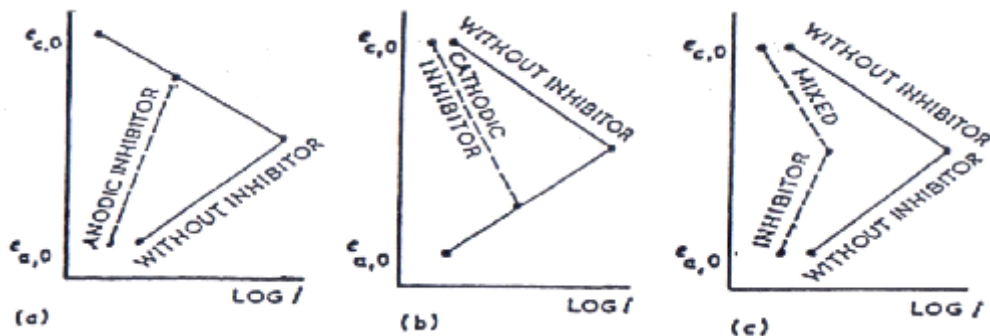


Fig. 1.8: Evans diagrams showing the effect of addition of a) anodic inhibitor, b) cathodic inhibitor, c) mixed inhibitor.

Mixed inhibitors protect the metal in three possible ways:

- a) Physical adsorption.
- b) Chemisorption.
- c) Film formation.

1.11.3.1 Physical adsorption

Physical adsorption is the result of the electrostatic attractive forces between inhibiting organic ions or dipoles and electrically charged surface of the metal. Inhibiting species that undergo physical adsorption interact rapidly with the surface; however they can also be removed easily from the surface. It depends on:

- Structural parameters, such as hydrocarbon chain length and the nature and position of substituent in aromatic ring.
- Electrical characteristics of inhibitors, i.e., charge of the hydrophilic group.
- Type of ions present in the solution.
- Potential of the metal.

1.11.3.2 Chemical adsorption

Chemisorption of inhibitor molecules on metals is slow and involves interaction forces stronger than the forces in physisorption. A coordinate type of bond between the metal and the inhibitor is thought to be present with charge transfer from the inhibitor to the metal. An opposing view is that a chemical bond is not necessarily present in chemisorption of an inhibitor on the metal surface. The most effective inhibitors are those that chemically adsorb (chemisorb), a process that involves charge sharing or charge transfer between the inhibitor molecules and the metal surface.

1.11.3.3 Film formation

During the chemical adsorption adsorbed inhibitor molecules may undergo surface reactions producing films. The properties of films are dependent upon its thickness, composition, solubility, temperature and other physical forces. Some adsorbed inhibitor molecules produce polymeric films. Corrosion protection increases markedly as the films grow from nearly two-dimensional adsorbed layers to three-dimension films up to several hundred angstroms thick. Inhibition is effective only when the films are

adherent, insoluble and prevent access of the solution to the metal.

1.11.4 Ohmic inhibitors

Ohmic inhibitors increase the ohmic resistance of the electrolyte circuit and belong to the anodic and cathodic film forming inhibitors. Because it is usually impractical to increase resistance of the bulk electrolyte, increased resistance is practically achieved by the formation of a film on the metal surface. Example: amines, sulphonates, etc.

1.11.5 Precipitation inhibitors

Precipitation inhibitors are compounds that cause formation of precipitates on the surface of metals, blocking both anodic and cathodic sites indirectly. Inhibitors promote the formation of bulky precipitation film over the entire surface. Example: silicates, phosphates, etc.

1.11.6 Vapour-phase inhibitors

These are very similar to the organic adsorption type inhibitors and possess a very high vapour pressure. As a consequence, these materials can be used to inhibit atmospheric corrosion of metals without being placed in direct contact with the metal surface. In use, such inhibitors are placed in the vicinity of the metal to be protected, and they are transferred by sublimation and condensation to the metal surface. The vapour-phase inhibitors are usually only effective if used in closed spaces such as inside packages or on the interior of machinery during shipment (Fontana 1987). On contact with metal surface, vapours of these inhibitors condense on the metal surface forming the protective film.

1.11.7 Some examples of corrosion inhibitors

Organic substances have been used extensively as corrosion inhibitors. The efficiency of an inhibitor does not only depend on its structure, but also on the characteristics of the environment in which it acts, the nature of the metal and other experimental conditions. Commercial inhibitor packages contain, in addition to active inhibitor other chemicals like surfactants, demulsifiers, carriers and biocides. The active ingredient of organic inhibitors invariably contain one or more functional groups

containing one or more heteroatoms, N, O, S, P or Se through which the inhibitors anchor to the metal surface. Some of the common anchoring groups are given in the Table 1.1.

Table 1.1: Common anchoring organic groups.

| Structure | Name | Structure | Name |
|------------------|----------|--------------------|-------------|
| –OH | Hydroxyl | –CONH ₂ | Amide |
| –C≡C– | -yne | –SH | Thiol |
| –C–O–C– | Epoxy | –S– | Sulphide |
| –COOH | Carboxy | –S=O– | Sulphoxide |
| –C–N–C– | Amine | –C=S– | Thio |
| –NH ₂ | Amino | –P=O | Phosphonium |
| =NH | Imino | –P– | Phospho |
| –NO ₂ | Nitro | –As– | Arsano |
| –N=N–N– | Triazole | –Se– | Seleno |

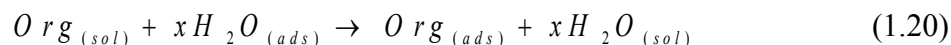
These groups are attached to a parent chain (backbone), which increases the ability of the inhibitor molecule to cover a large surface area. The backbone may contain additional molecules, or substituent groups, to enhance the electronic bonding strength of the anchoring group on the metal and/or to enhance the surface coverage.

1.12 MECHANISM OF CORROSION INHIBITION

When inhibitor is added to the corrosion medium, it retards the cathodic, anodic or both the reactions. This action occurs by following mechanisms (Quraishi 2003):

1) By adsorption mechanism

According to the well accepted model, the adsorption of organic inhibitor molecules on the metal surface is a displacement of adsorbed water molecules by organic molecule in the solution.



where, $Org_{(sol)}$ and $Org_{(ads)}$ are the organic molecules in the aqueous solution and adsorbed on the metal surface, respectively; $H_2O_{(ads)}$ is the water molecules adsorbed on

the metal surface; x is the size ratio representing the number of water molecules displaced by one molecule of organic adsorbate. The adsorption is influenced by the following factors:

- a) Surface charge on the metal,
- b) The structure of inhibitor,
- c) Interaction of adsorbed inhibitor species with metal,
- d) Reaction of adsorbed inhibitors (stability of the inhibitor).

The adsorbed inhibitor molecules may retard either anodic or cathodic or both reaction(s) depending upon where they are adsorbed.

2) By diffusion barrier film

The inhibitor may form a surface film on the metal surface which prevents interaction of corrosive species with the metal surface. Organic compounds of high molecular weight such as protein and polysaccharides usually form physical barrier on the metal surface. Acetylenic alcohols also form multimolecular film.

3) By blocking of reaction sites

The adsorbed inhibitors can also inhibit the corrosion by blocking the active sites of the metals. This effect is exhibited by aliphatic sulphides or quinoline during corrosion of iron in H_2SO_4 .

4) By participation in the electrode reactions

The adsorbed inhibitors can also retard the corrosion reaction by participating in electrode reactions thereby affecting the mechanism of inhibition.

1.13 MARAGING STEELS

The development and production of martensitic hardenable steels (maraging steels) started in the early 1960s in the USA with steels containing 18% Ni, 8–9% Co and Mo together with small additions of Ti. Their name, “maraging,” is derived from the heat treatment which involves the age hardening of low carbon martensite. Maraging steel is essentially low carbon, which distinguishes it from most other types of steel. Nickel maraging steels have been extensively used in a variety of applications due to their attractive combination of high strength, moderate toughness and good weldability.

They have higher modulus of elasticity and lower thermal expansion coefficient. Another important property is their better thermal conductivity, which reduces surface temperature during thermal loading and lowers thermal stresses. Maraging steels are iron alloys which are known for possessing superior strength and toughness without losing malleability, although they cannot hold a good cutting edge. These steels are a special class of low-carbon ultra-high-strength steels which derive their strength not from carbon, but from precipitation of inter-metallic compounds. For the optimum strength and toughness such elements as carbon, silicon, manganese, sulphur and phosphorus are restricted to low levels.

The strength of Fe-Ni alloys can be increased by the addition of cobalt and molybdenum, whereas alloying with aluminium and titanium forms intermetallics with other elements, in particular with Mo and Ni. Maraging steels generally contain less than 0.03% carbon, 5-25% Ni, 7-9% Co, 4.5-5% Mo, 0.1-1.4% Ti, 0.1-0.3% Al, 0.1-0.4% Nb, 0.1% Be, 0.1-0.2% Cu and W and V up to 6 % in special cases. They can be finely polished and easily fabricated. Maraging steels work well in electro-mechanical components where ultra-high strength is required, along with good dimensional stability during heat treatment.

1.13.1 Welded maraging steel

The welding is the important means of fabrication. In order to obtain the best properties it is advisable during welding to:

- a) avoid prolonged times at elevated temperature
- b) use minimum weld energy inputs
- c) avoid conditions causing slow cooling rates

From the weldability point of view, the most important feature of maraging steel is the fact that they are relatively soft after cooling from the austenitizing temperatures. This means that the heat-affected zones are softened by the heat of welding with the result that, the residual stresses are lowered and there are fewer tendencies for hydrogen cold cracking. The unique property of being weldable in solutionised condition followed by a low temperature (480 °C), post - weld maraging treatment makes these steel attractive for

fabrication of large structures (Klobcar et al. 2008). Several welding processes have been recommended for steels. Through with low heat input processes, like electron beam welding, high joint efficiencies can be achieved, in common practice, gas tungsten - arc welding [GTAW] is widely employed in view of the consistency of weld quality and overall economy. During welding the metal will be in liquid state (fusion zone) which will be subsequently cooled to room temperature. Hence the principal microstructure change in the weld fusion zone is transformation of austenite to martensite on cooling. It was reported that the use of filler material similar in composition to the maraging steel base material results in segregation of alloying elements, particularly molybdenum and titanium, at the substrate boundaries in the weld fusion zone (Ronald Schnitzer et al. 2010). An important practical benefit is that martensite is formed at all cooling rates and therefore in all section sizes. The common concepts of hardenability do not apply to maraging steels.

1.13.2 Uses of maraging steel

1. Maraging steel (250 grade) has been widely used in the aerospace industry because of its high strength and malleability.
2. They are suited to engine component applications such as crankshafts and gears that work at 'warm' temperatures and the firing pins of automatic weapons that cycle from hot to cool repeatedly while under substantial loads and impacts.
3. Their uniform expansion and easy machinability, carried out before aging makes maraging steel useful in high wear portions of assembly lines, as well as in the manufacture of dies.
4. It is used in creating gas centrifuges for uranium enrichment, nuclear bomb casing due to its extremely high strength and balance. Nations importing maraging steel often find themselves receiving a great deal of attention (Hossein Nedjad et al. 2008).
5. In surgical components and hypodermic syringes.

1.13.3 Role of alloying elements in maraging steel

Nickel maraging steels have been extensively used in a variety of applications due to their attractive combination of high strength, moderate toughness and good weldability. Although Fe-Ni system, particularly at Fe-18 % Ni level, offered a number of technological advantages including moderately strong and very tough martensite on solution annealing, the negligible dimensional changes, insensitivity of the transformation product to cooling rate, etc., there was a need to strengthen the Fe-Ni martensite with various alloying elements to a level of engineering interests without affecting the toughness. The important alloying elements in the Fe based maraging steel are nickel, molybdenum, cobalt, titanium and aluminium. The residual elements should be kept as low as possible as they adversely affect the properties of maraging steels. Common residual elements present are carbon, sulphur, silicon, manganese, aluminium, hydrogen, oxygen and nitrogen (Avadhani 2001, Nayak 2004).

1.14 LITERATURE REVIEW

1.14.1 Corrosion of maraging steels

The corrosion of maraging steel is of fundamental, academic and industrial concern that has received a considerable amount of attention. In most of the industries like fertilizers and chemicals, oil refineries, nuclear power plants, etc., the maraging steel is used for making containers, steam generators, liquid carrying pipes and so on. In steel and ferrous alloy industries, the hydrochloric acid is used as a pickling agent. Moisture, micro dust particles, acids and bases and other agents of the environment influence the extent of corrosion taking place in these industries. It is inevitable to expose the surface of the maraging steel to different industrial environments while in use. A search of the literature reveals only a few reports on the corrosion studies of 18 Ni 250 grade maraging steel, which is entirely in martensitic phase (Nayak 2004, Poornima et al. 2010).

According to the available literature, 18 Ni maraging steel, when exposed to the atmosphere, is subjected to more or less uniform corrosion and is completely covered with rust (Kirk et al. 1968). Pit depths tend to be shallower than in high strength steels

(Dean and Copson 1965). Bellanger et al. (1996) have studied the effect of slightly acid pH with or without chloride in radioactive water on the corrosion of maraging steel and have reported that corrosion behaviour of maraging steel at the corrosion potential depends on pH and intermediates remaining on maraging steel surface in the active region, favoring the passivity. The effect of carbonate ions in slightly alkaline medium on the corrosion of maraging steel was studied by Bellanger (1994). Maraging steels are found to be less susceptible to hydrogen embrittlement than common high strength steels owing to significantly low diffusion of hydrogen in them (Rezek et al. 1997). The critical and passive current densities increase as the structure is varied from fully annealed to fully aged. Stress corrosion of maraging steel may also occur in acid environments (Dautovich 1976). Poornima et al. (2010) have studied the corrosion behaviour of 18 Ni M 250 grade maraging steel in a phosphoric acid medium and reported that the corrosion rate of the annealed sample is less than that of the aged sample. Similar observations also have been reported for the corrosion of 18 Ni 250 grade maraging steel in sulphuric acid medium (Poornima et al. 2011).

The corrosion rate of maraging steel in acid solutions such as sulphuric acid, hydrochloric acid formic acid and stearic acid are substantial. Heat treatment affects corrosion rate. Critical and passive current densities increase as the structure is varied from fully annealed to fully aged (Data bulletin on 18%Ni maraging steel 1964). Investigations on electrochemical corrosion behaviour of 350 grade maraging steel in 1.0 N H₂SO₄, 1.0 N HCl and in artificial sea water showed passive behaviour in 1N H₂SO₄ but not in 1N HCl and in artificial sea water (Iqbal et al. 1993)

Nayak (2004) has studied corrosion behaviour of 18Ni 250 grade maraging steel in aqueous medium and reported that, the rate of corrosion decreases as pH increases and near neutral region corrosion rate is independent of pH, corrosion rate increases with increase in temperature, aged samples show higher rate of corrosion than annealed samples and mechanism of corrosion was found to be due to anodic dissolution at the grain boundary and pitting corrosion was also

observed.

Literature is saturated with corrosion inhibitors for different metals and alloys. But very less work seems to be available regarding the corrosion inhibition of maraging steel.

Application of corrosion inhibitors is the most economical and practical method to mitigate electrochemical corrosion. Organic substances such as heterocyclic compounds containing nitrogen, oxygen and sulphur atoms, multiple bonds in the molecule, can adsorb on the metallic surface and can act as inhibitors by blocking the active sites or by generating a physical barrier to reduce the transport of corrosive species to the metal surface (Bentiss et al. 2005). The extent of adsorption of an inhibitor depends on many factors such as the nature and the surface charge of the metal; the mode of adsorption of the inhibitor; the chemical structure of the inhibitor molecule; and the type of the aggressive solution (Schmitt 1984).

1.14.2 Organic compounds for the corrosion inhibition of iron and iron alloys in aqueous media.

A large number of investigations were carried out using organic compounds as corrosion inhibitors for pure iron and iron alloys in various aqueous media. Organic inhibitors play a major role as they cover the maximum surface area of the metal. Hence small amount of the inhibitor is sufficient to cover the large surface area. However, limited literatures reported the corrosion inhibition of maraging steel. Some of the important inhibitors used for iron and iron alloys are given in Table 1.2.

Table 1.2: Important inhibitors used for iron and iron alloys.

| Inhibitor | Medium | Remarks | References |
|--------------------------------------|--|------------------------------|------------------------|
| 2-Amino-5-mercapto-1,3,4-thiadiazole | Mild steel corrosion in 1.0 M H ₂ SO ₄ | Langmuir adsorption isotherm | (Ali Döner et al.2011) |
| 2-Ethylamine thiophene | Steel in 0.5 M H ₂ SO ₄ | Frumkin isotherm model | (Bouklah et al. 2004) |

| Inhibitor | Medium | Remarks | References |
|---|--|---|--------------------------------|
| 2,5-Bis(4-methoxyphenyl)-1,3,4-oxadiazole | Mild steel corrosion in 0.5 M H ₂ SO ₄ | Langmuir adsorption isotherm | (Bouklah et al. 2005) |
| 2,3-Diphenylbenzoquinoline | Mild steel corrosion in 0.5 M H ₂ SO ₄ | Langmuir adsorption isotherm | (Obot et al. 2010) |
| 1,2,3-Benzotriazole | Stainless steel in H ₂ SO ₄ | Physical interaction, Langmuir isotherm. | Satpati and Ravindran 2008 |
| Hexamethylpararosaniline chloride | Mild steel in H ₂ SO ₄ | Adsorption of protonated inhibitor, Langmuir isotherm | Oguzie et al. 2008 |
| 1-Methyl-3-pyridin-2-yl-thiourea | Mild steel in H ₂ SO ₄ | Mixed inhibitor, Langmuir adsorption isotherm | Hosseini et al. 2009 |
| 3,4-Dimethoxybenzaldehyde thiosemicarbazone | Aged maraging steel in 0.5 M H ₂ SO ₄ medium | Mixed inhibitor, Langmuir isotherm | Poornima et al. (2011) |
| 2-(4-Chlorophenyl)-2-oxoethyl benzoate | Weld aged maraging steel in 1.0 M sulphuric acid medium | Mixed inhibitor, Langmuir isotherm | Sanatkumar et al. (2012) |
| 6-Benzylaminopurine | Cold Rolled steel in H ₂ SO ₄ | Mixed inhibitor, Temkin isotherm | Xianghog et al. 2009 |
| 6-Amino-m-cresol | Mild steel in 0.5 M HCl medium | Langmuir adsorption isotherm | (Dehri and Ozcan 2006) |
| Quinol-2-thione | Mild steel in 1 M HCl | Langmuir adsorption isotherm | (Prabhu et al. 2008) |
| 3H-Phenothiazin-3-one and 7-dimethylamine | Mild steel in 1 M HCl | Langmuir adsorption isotherm | (Ashassi-Sorkhabi et al. 2000) |

| Inhibitor | Medium | Remarks | References |
|--|--|------------------------------|--------------------------|
| 1(2E)-1-(4-Aminophenyl)-3-(2-thienyl) prop-2-en- 1-one | maraging steel under weld aged condition in 1.5 M HCl medium | Langmuir adsorption isotherm | Sanatkumar et al. (2011) |
| Piperazine derivatives | Mild steel in HCl | Langmuir adsorption model | Ousslim et al. 2009 |
| Thiourea | Mild steel in HCl | Langmuir adsorption model | Benali et al. 2009 |
| 3-Anilino-5-imino-4-phenyl-1,2,4-thiadiazoline | Mild steel in HCl | Mixed inhibitors | Quraishi and Sardar 2003 |
| Hydrazide derivatives | Mild Steel in 1.0 M HCl | Langmuir adsorption isotherm | (Prabhu et al. 2008) |

Poornima et al. (2011) have also studied the corrosion inhibition efficiency of 3, 4-dimethoxybenzaldehydethiosemicarbazone on maraging steel corrosion in 0.5 M sulphuric acid. Sanathkumar et al. (2012) studied that influence of 2-(4-chlorophenyl)-2-oxoethyl benzoate on the hydrogen evolution and corrosion inhibition of 18 Ni 250 grade weld aged maraging steel in 1.0 M sulphuric acid media at different temperatures. Poornima et al. (2011) studied that the effect of 4-(N, N- diethylamino) benzaldehyde thiosemicarbazone on the corrosion of aged 18 Ni 250 grade maraging steel in phosphoric acid solution. Sanathkumar et al. (2012) studied that the corrosion inhibition of maraging steel under weld aged condition by 1(2E)-1-(4-aminophenyl)-3-(2-thienyl) prop-2-en-1-one in 1.5 M hydrochloric acid medium. Sanathkumar et al. (2012) studied the adsorption and corrosion inhibitive effect of 1(2E)-1-(4 amino phenyl)-3- (2-thienyl) prop-2-en-1-one on corrosion of weld aged maraging steel in 0.5 M sulphuric acid media.

1.15 SCOPE

Maraging steels have been extensively used in a variety of applications due to their attractive combination of properties such as high strength, moderate toughness and

good weldability. Due to low carbon content, maraging steels have good machinability. Its strength and malleability allow it to be used in the preparation of rocket and missile skins in aerospace industries, engine components like crankshafts and gears, bearings, submarine hulls, surgical components, nuclear and gas turbine applications. Due to the variety of applications, maraging steels frequently come in contact with acid during cleaning, pickling, descaling, acidizing, etc. Hence studying their corrosion behaviour in acid medium and finding out a suitable corrosion inhibitor is of prime importance. A review of literature has revealed large number of corrosion inhibitors for various metals and alloys. But very less study appears to be done in the area of corrosion behaviour and corrosion inhibition of welded maraging steel. So it is planned specifically to study the corrosion behaviour of welded maraging steel in a medium of sulphuric acid and hydrochloric acid and then synthesize and use suitable inhibitors having necessary structural requirements of a good inhibitor. It is intended to study their inhibition behaviour in acid medium at different temperatures by suitable electrochemical techniques.

1.16 OBJECTIVES

1. To study the corrosion behaviour of welded maraging steel in a medium of hydrochloric acid of different concentrations at different temperatures.
2. To study the corrosion behaviour of welded maraging steel in a medium of sulphuric acid of different concentrations at different temperatures.
3. To investigate the corrosion inhibition performance of the given organic compounds on the corrosion of the welded maraging steel in a medium of hydrochloric acid and sulphuric acid of different concentrations at different temperatures.
4. To evaluate the activation parameters for the corrosion of welded maraging steel in the absence and presence of the inhibitors.
5. To study the adsorption behaviour of the inhibitors, to calculate the thermodynamic parameters for the adsorption of the inhibitor molecules on the alloy surface and to propose the mechanism of inhibition.

OUTLINE OF THE THESIS

The present investigation has been documented in the thesis under 4 different chapters. **Chapter 1** includes the introduction to corrosion problem, theoretical concepts of electrochemistry of corrosion, corrosion rate measurement techniques, corrosion inhibitors, maraging steels and the literature survey on the corrosion and corrosion inhibition of maraging steel. The chapter also explains the scope and objectives of the study.

In **Chapter 2**, the materials, medium, inhibitors, methods and calculation of various corrosion parameters, used for the present investigation have been discussed.

Chapter 3 presents the results and discussion on the work carried out. The results of investigations on the corrosion behaviour of welded maraging steel in hydrochloric acid medium and sulphuric acid medium have been discussed in section 3.1 and 3.2, respectively. The sections 3.3, 3.5, 3.7, 3.9 and 3.11 describes the inhibition effect of the five compounds, BTPO, TBTBH, PNPT, CBP and MPBIT on the corrosion of welded maraging steel in the hydrochloric acid medium and the sections 3.4, 3.6, 3.8, 3.10 and 3.12 in the sulphuric acid medium, respectively. The effect of temperature, concentration of the medium, and concentration of the inhibitor on the inhibition efficiency is discussed in the chapter. The type of adsorption and mechanism of inhibition in each case is explained in the chapter.

Chapter 4 summarises the work included in the thesis and also lists the conclusions drawn on the basis of experimental evidences and discussions.

CHAPTER 2

MATERIALS AND METHODS

2.1 MATERIALS

2.1.1 18% Ni M250 grade maraging steel

The 18% Ni M250 grade maraging steel samples were obtained from National Institute of Interdisciplinary Science and Technology (NIIST) Thiruvananthapuram. The composition of the maraging steel used in the present investigation is given in Table 2.1.

Table 2.1: Composition of the specimen (% by weight).

| Element | Composition | Element | Composition |
|---------|-------------|---------|-------------|
| C | 0.015% | Ti | 0.3% |
| Ni | 18% | Al | 0.15% |
| Mo | 4.8% | Mn | 0.1% |
| Co | 7.5% | P | 0.01% |
| Si | 0.1% | S | 0.01% |
| O | 30 ppm | N | 30 ppm |
| H | 2.0 ppm | Fe | Balance |

2.1.2 Material conditions

Investigations were carried out on 18% Ni M250 grade maraging steel specimen under welded condition. The maraging steel plates of composition as given in Table 2.1 were welded by GTAW-DCSP (Gas tungsten arc welding - Direct-current straight polarity), with 5 passes using filler material of composition as given in Table 2.2. The weld specimens were taken from the all weld regions. The specimen was taken from plates.

Table 2.2: Composition of the filler material used for welding (% by weight).

| Element | Composition | Element | Composition |
|---------|-------------|---------|-------------|
| C | 0.015% | Ti | 0.015% |
| Ni | 17% | Al | 0.4% |
| Mo | 2.55% | Mn | 0.1% |
| Co | 12% | Si | 0.1% |
| Fe | Balance | | |

2.1.3 Preparation of test coupons

Cylindrical test coupons were cut from the plate and sealed with epoxy resin in such a way that, the area exposed to the medium was 0.65 cm². These coupons were polished as per standard metallographic practice, belt grinding followed by polishing on emery papers of 180, 400, 600, 800, 1000, 1200, 1500 and 2000 grit sizes, finally on polishing wheel using levigated alumina to obtain a mirror finish, degreased with acetone, washed with double distilled water and dried before immersing in the corrosion medium.

2.2 MEDIA

The media used for the investigation were standard hydrochloric acid and sulphuric acid at five different concentrations. Experiments were carried out at temperatures 30 °C, 35 °C, 40 °C, 45 °C and 50 °C (± 0.5 °C) using calibrated thermostat.

2.2.1 Preparation of standard hydrochloric acid solution

A stock solution of hydrochloric acid was prepared by diluting a known volume of 37% analytical grade hydrochloric acid to an approximate volume. The solution was standardised by titrimetry. Solutions of different concentrations (0.1 M, 0.5 M, 1.0 M, 1.5 M and 2.0 M) were prepared by diluting the stock solution with distilled water.

2.2.2 Preparation of standard sulphuric acid solution

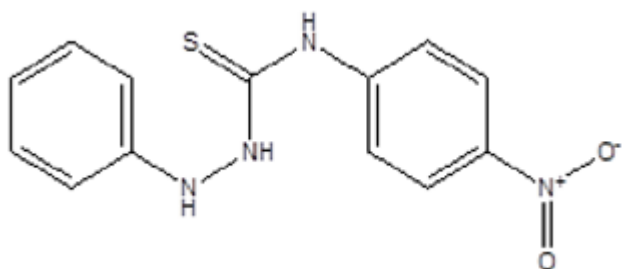
A stock solution of sulphuric acid was prepared by diluting a known volume of 98% analytical grade sulphuric acid to an approximate volume. The solution was standardised by titrimetry. Solutions of different concentrations (0.1 M, 0.5 M, 1.0 M, 1.5 M and 2.0 M) were prepared by diluting the stock solution with distilled water.

2.3 INHIBITORS

2.3.1 Synthesis of 1-Phenyl-4-(4-nitrophenyl) thiosemicarbazide (PNPT)

The inhibitor PNPT was synthesized as per the reported procedure (Britto et al. 2006). A solution of phenyl hydrazine in toluene and phenylisothiocyanate was added to round bottom flask. Then this mixture was heated under reflux for 30 min, and a white

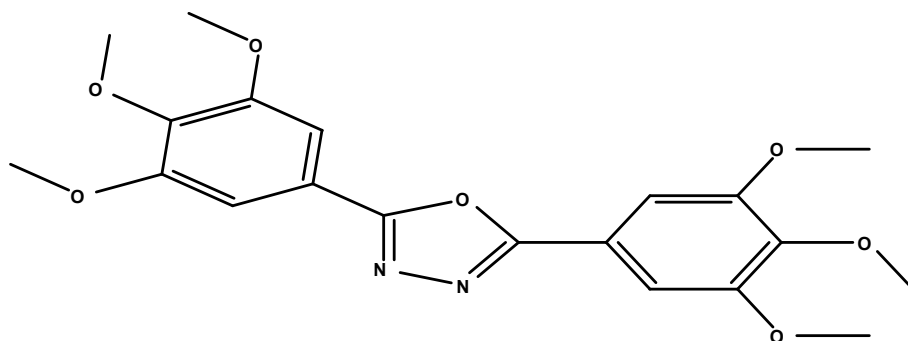
solid precipitated. After cooling, the precipitate was filtered and washed with diethyl ether and recrystallized with ethanol to get pure 1-phenyl-4-(4-nitrophenyl) thiosemicarbazide (PNPT). The product was characterized by elemental analysis [Theoretical (found); C: 59.01% (58.91%), N: 22.95% (21.95%) and H: 5.01% (5.12%)], melting point (234-236 °C) and infrared spectra.



1-Phenyl-4-(4-nitrophenyl) thiosemicarbazide (PNPT)

2.3.2 Preparation of 2,5-Bis (3,4,5-trimethoxy phenyl)-1,3,4-oxadiazole (BTPO)

To a mixture of 3,4,5-trimethoxy benzoic acid (0.05 mol) and 3,4,5-trimethoxy benzoic acid hydrazide (0.05 mol) phosphorous oxychloride was added dropwise. The mixture was refluxed on a water bath for 5 h. Then the reaction mixture was allowed to cool at room temperature and poured into crushed ice. The solid precipitated was filtered, dried and recrystallized from ethanol (Mazzone et al. 1984).

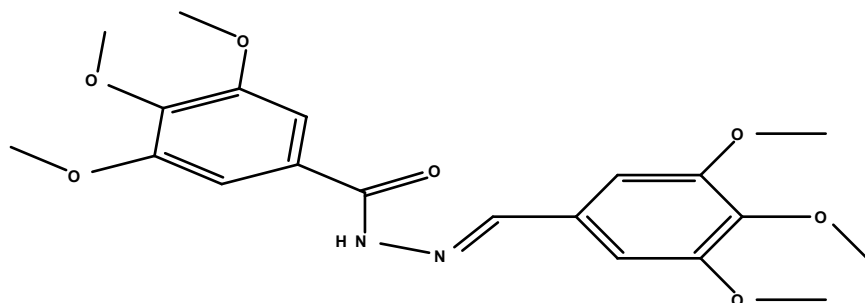


2,5-Bis (3,4,5-trimethoxy phenyl)-1,3,4-oxadiazole (BTPO)

The product was characterized by elemental analysis [Theoretical (found); C: 58.46% (58.37%), N: 7.05% (6.93%) and H: 5.60% (5.48%)], melting point (207-208 °C) and infrared spectra.

2.3.3 Synthesis of 3,4,5-Trimethoxy-benzoicacid(3,4,5-trimethoxy-benzylidene) hydrazide (TBTBH)

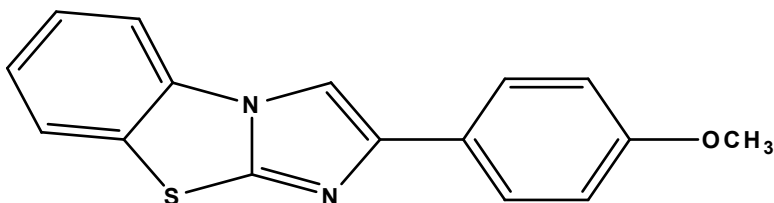
A solution of 3,4,5-trimethoxy benzaldehyde (0.05 mol) in ethanol was added to a solution of substituted 3,4,5-trimethoxy benzoic acid hydrazides (0.05 mol) in 50 ml ethanol. The mixture was refluxed on a water bath for 3 h. Then the reaction mixture was allowed to cool at room temperature and the precipitate obtained was filtered, dried and recrystallized from ethanol (Mazzone et al. 1984). The product was characterized by elemental analysis [Theoretical (found); C: 58.16% (58.11%), N: 7.10% (7.06%) and H: 6.10% (6.03%)], melting point (192-194 °C) and infrared spectra.



3,4,5-Trimethoxy-benzoicacid(3,4,5-trimethoxy-benzylidene) hydrazide (TBTBH)

2.3.4 Synthesis of 2-(4-Methoxy-phenyl)-benzo[d]imidazo [2,1-b]thiazole (MPBIT)

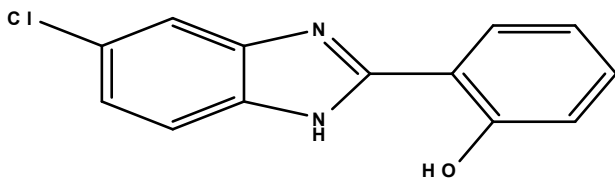
A mixture of p-methoxyphenacyl bromide (20 mmol) and 2-aminobenzothiazole (40 mmol) in ethanol (15 mL) was refluxed for 1-2 h. To the reaction mixture was cooled and the precipitated solid was collected by filtration and recrystallized from ethanol (Kumbhare et al. 2011). The product was characterized by elemental analysis [Theoretical (found); C: 57.97% (57.91%), N: 13.52% (13.41%), S: 15.46% (15.27%) and H: 5.31% (5.28%)], melting point (214-216 °C) and infrared spectra.



2-(4-Methoxy-phenyl)-benzo[d]imidazo[2,1-b]thiazole (MPBIT)

2.3.5 Synthesis of 2-(5-Chloro-1H-benzimidazol-2-yl) phenol (CBP)

To a mixture of (2-hydroxyphenyl) methane sulfonate salt (0.01 mol) and *o*-phenylenediamine (0.01 mol) in 30 mL of dimethyl formamide (DMF) were refluxed for 2 h at 150 °C in an oil bath and the mixture was poured in an ice bath. 2-(2-Hydroxyphenyl)-1H-benzimidazole was filtered and recrystallized from methanol/ water (Coban et al. 2009). The product was characterized by elemental analysis [Theoretical (found); C: 63.93% (63.41%), N: 11.48% (11.65%) and H: 3.68% (3.63%)], melting point (203-205°C) and infrared spectra.



2-(5-Chloro-1H-benzimidazol-2-yl) phenol (CBP)

2.4 METHODS

2.4.1 Electrochemical measurements

Electrochemical measurements were carried out using an electrochemical workstation, Gill AC having ACM instrument Version 5 software. Three electrode system was used for the electrochemical measurements. The working electrode was made of welded maraging steel. A saturated calomel electrode (SCE) and a platinum electrode were used as the reference and the counter electrodes respectively. Electrode potentials were measured with respect to the saturated calomel electrode (SCE). The polarization studies

were done immediately after the EIS studies on the same electrode without any further surface treatment.

2.4.1.1 Potentiodynamic polarisation studies

Finely polished maraging steel specimens were exposed to the corrosion media of hydrochloric acid and sulphuric acid in the presence and absence of studied inhibitors at temperatures 30 °C, 35 °C, 40 °C, 45 °C, 50 °C and allowed to establish steady state open circuit potentials. The potentiodynamic current-potential curves were recorded by polarizing the specimen to -250 mV cathodically and +250 mV anodically with respect to the open circuit potential (OCP) at a scan rate of 1 mV s⁻¹.

The corrosion rate (v_{corr}), in mm y⁻¹, is calculated from the following equation (Dean 1999):

$$\text{Corrosion rate } (v_{corr}) = K \frac{i_{corr}}{\rho} EW \quad (2.1)$$

where, K is 3.27×10^{-3} , a constant that defines the unit for the corrosion rate, i_{corr} is the current density in A cm⁻², ρ is the density in g cm⁻³ and EW is equivalent weight of the alloy. Equivalent weight for the alloy was calculated from the following equation (Dean 1999).

$$EW = \frac{1}{\sum \frac{n_i f_i}{W_i}} \quad (2.2)$$

where, f_i is the mass fraction of the i^{th} element in the alloy, W_i is the atomic weight of the i^{th} element in the alloy and n_i is the valence of the i^{th} element of the alloy. It is usually assumed that the process of oxidation is uniform and does not occur selectively to any component of the alloy.

The inhibition efficiency was calculated from following equation:

$$\eta(\%) = \frac{i_{corr} - i_{corr(inh)}}{i_{corr}} \times 100 \quad (2.3)$$

where, i_{corr} and $i_{corr(inh)}$ signify the corrosion current densities in the absence and presence of inhibitors, respectively.

The surface coverage (θ) was calculated from potentiodynamic polarization data using the equation:

$$\theta = \frac{\eta(\%)}{100} \quad (2.4)$$

where, η (%) is the percentage inhibition efficiency.

2.4.1.2 Electrochemical impedance spectroscopy studies (EIS)

In EIS technique, a small amplitude ac signal of 10 mV was applied to the electrochemical system over a wide range of frequencies (10 kHz to 0.01 Hz) at OCP and the response to the input signal was measured. These measurements were carried out for the welded maraging steel specimen in hydrochloric acid as well as in sulphuric acid medium in the absence and presence of all the studied inhibitors at temperatures 30 °C, 35 °C, 40 °C, 45 °C and 50 °C. The impedance data were analysed using an equivalent circuit (EC) that tentatively models the physical processes occurring at the metal-electrolyte interface (Machnikova et al. 2008). The polarisation resistance R_p was obtained from the diameter of the capacitive semicircle. The inhibition efficiency (η %) of the studied inhibitors was evaluated from R_p by using the equation (2.5).

$$\eta(\%) = \frac{R_{p(inh)} - R_p}{R_{p(inh)}} \times 100 \quad (2.5)$$

where, $R_{p(inh)}$ and R_p are the polarisation resistances obtained in inhibited and uninhibited solutions, respectively.

In all the above measurements, at least three similar results were considered and their average values are reported.

2.4.2 Scanning electron microscopy (SEM)/ EDX analysis

The surface morphology of the welded maraging steel specimen immersed in hydrochloric acid as well as in sulphuric acid solution in the presence and absence of

inhibitor were compared by recording the SEM images of the samples using JEOL JSM - 6380LA analytical scanning electron microscopy. Energy dispersive X-ray spectroscopy (EDX) investigations were carried out in order to identify the elemental composition of the species formed on the metal surface after its immersion in acid in the presence and absence of inhibitor.

2.5 ACTIVATION PARAMETERS

The apparent activation energy (E_a) for the corrosion process in the presence and absence of the inhibitor was calculated using Arrhenius rate equation (Bouklah et al. 2004)

$$\ln(v_{\text{corr}}) = B - \frac{E_a}{RT} \quad (2.6)$$

where, B is a constant which depends on the metal type and R is the universal gas constant, v_{corr} is the corrosion rate, E_a is the activation energy, T is absolute temperature. The plot of $\ln(v_{\text{corr}})$ versus reciprocal of absolute temperature ($1/T$) gives a straight line with slope = $-E_a / R$, from which, the activation energy values for the corrosion process were calculated (Atta et al. 2011).

The entropy of activation (ΔH^\ddagger) and enthalpy of activation (ΔS^\ddagger) for the corrosion of alloy were calculated from the transition state theory equation (Abd EL-Rehim et al. 1999).

$$v_{\text{corr}} = \frac{RT}{Nh} \exp\left(\frac{\Delta S^\ddagger}{R}\right) \exp\left(\frac{-\Delta H^\ddagger}{R}\right) \quad (2.7)$$

where, h is Plank's constant, N is Avagadro's number. A plot of $\ln(v_{\text{corr}}/T)$ vs $1/T$ gives straight line with the slope being given by equation (2.8) and intercept given by equation (2.9).

$$\text{Slope} = \frac{-\Delta H^\ddagger}{R} \quad (2.8)$$

$$\text{Intercept} = \ln\left(\frac{R}{N_h}\right) + \frac{\Delta S^\#}{R} \quad (2.9)$$

2.6 ADSORPTION ISOTHERMS

To evaluate the nature and strength of adsorption of the inhibitor on the alloy surface, the experimental data were fitted to the isotherm, and from the best fit, the thermodynamic data for adsorption were evaluated. In the present study attempts were made to fit the degree of surface coverage (θ) values obtained for the welded maraging steel specimen in different concentrations of hydrochloric acid and sulphuric acid in the presence of different concentrations of inhibitor to various isotherms including Langmuir, Temkin, Frumkin, Freundlich and Flory- Huggins isotherms, etc. Various adsorption isotherms, the mathematical expressions and the verification plots are shown in Table 2.3

Table 2.3: Adsorption isotherms to characterise the adsorption of inhibitors on the metal surface.

| Name | Isotherm | Verification Plot |
|------------------|--|---|
| Langmuir | $\theta/(1-\theta) = \beta.c$ | $\theta/(1-\theta)$ vs c modified: c/θ vs c |
| Frumkin | $[\theta/(1-\theta)]e^{f\theta} = \beta.c$ | θ vs $\log c$ |
| Bockris-Swinkels | $\theta/(1-\theta)^n \cdot [\theta + n(1-\theta)]^{n-1}/n^n = c \cdot e^{-\beta/55.4}$ | $\theta/(1-\theta)$ vs $\log c$ |
| Temkin | $\theta = (1/f)\ln K.c$ | θ vs $\log c$ |
| Virial Parson | $\theta \cdot e^{2f\theta} = \beta.c$ | θ vs $\log(\theta/c)$ |
| Flory Huggins | $\log(\theta/c) = \log nK + n \log(1-\theta)$ | $\log(\theta/c)$ vs $\log(1-\theta)$ |
| El – Awady | $\log[\theta/(1-\theta)] = \log K + y \log c$ | $\log[\theta/(1-\theta)]$ vs $\log c$. |

where, $\theta = \eta/100$, surface coverage; $\beta = \Delta G/2.303RT$, ΔG is free energy of adsorption; R is gas constant; T is temperature; c is bulk inhibitor concentration; n is number of water molecules; f is inhibitor interaction parameter (0, no interaction; +, attraction; -, repulsion); K is constant; and η is percentage inhibition efficiency.

2.7 THERMODYNAMIC PARAMETERS

The standard free energy of adsorption of the inhibitor molecules on the alloy surface, ΔG_{ads}^0 was calculated using the relation:

$$K_{ads} = \frac{1}{55.5} \exp\left(\frac{-\Delta G_{ads}^0}{RT}\right) \quad (2.10)$$

where, the value 55.5 is the concentration of water in solution in mol dm^{-3} , R is the universal gas constant and T is absolute temperature in K.

Standard enthalpy of adsorption (ΔH_{ads}^0) and standard entropy of adsorption (ΔS_{ads}^0) were calculated from Gibbs–Helmholtz equation:

$$\Delta G_{ads}^0 = \Delta H_{ads}^0 - T\Delta S_{ads}^0 \quad (2.11)$$

The variation of ΔG_{ads}^0 with T gives a straight line with slope equals to ΔS_{ads}^0 and an intercept equals to ΔH_{ads}^0 .

CHAPTER 3

RESULTS AND DISCUSSION

3.1 CORROSION BEHAVIOUR OF 18% Ni M250 GRADE MARAGING STEEL UNDER WELDED CONDITION IN HYDROCHLORIC ACID MEDIUM

3.1.1 Potentiodynamic polarization studies

The effect of hydrochloric acid concentration and solution temperature on the corrosion rate of welded samples of maraging steel was studied by potentiodynamic polarization technique. Fig. 3.1 represents the potentiodynamic polarization curves for the corrosion of welded maraging steel in hydrochloric acid medium of different concentrations at 35 °C. Similar plots were obtained at other temperatures also. The potentiodynamic polarization parameters like corrosion potential (E_{corr}), corrosion current density (i_{corr}), anodic and cathodic Tafel slopes (b_a and b_c) and corrosion rate (v_{corr}) were calculated from the Tafel plots and tabulated in Table 3.1.

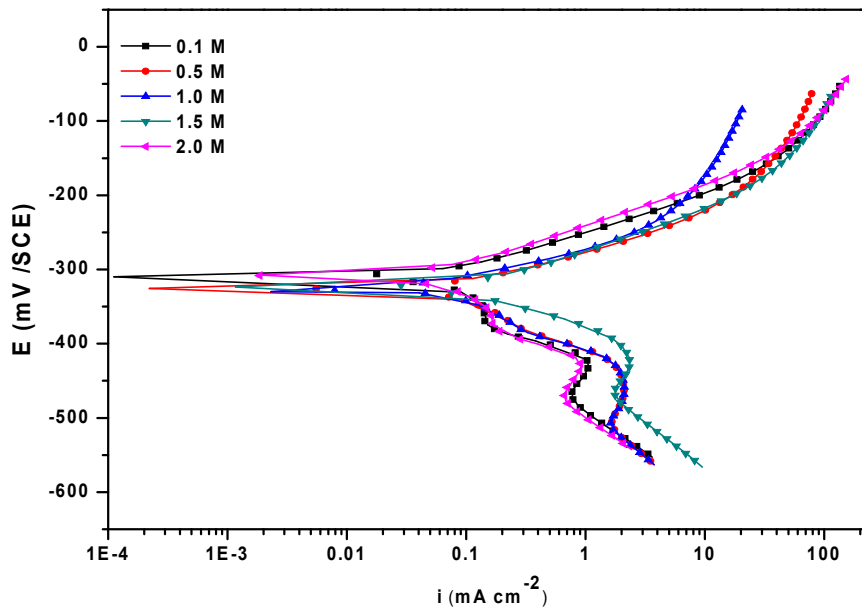


Fig. 3.1: Potentiodynamic polarization curves for the corrosion of welded maraging steel in different concentrations of HCl at 35 °C.

It is clear from the data presented in Table 3.1 that the corrosion rate of welded maraging steel increases with the increase in the concentration of hydrochloric acid in the solution. There is no definite trend observed for the corrosion potential (E_{corr}) values with

the varying HCl concentrations. The corrosion of steel in acid medium normally proceeds via two partial reactions in acid solutions. The partial anodic reaction involves the oxidation of metal and formation of soluble Fe^{2+} ions, while the partial cathodic reaction involves the evolution of hydrogen gas (Kriaa et al. 2009).

The chemical reaction can be expressed as follows (Amin et al. 2010).



The overall chemical reaction is the sum of these two half-cell reactions



In HCl solution, the following mechanism is proposed for the corrosion of iron and steel. The corrosion reaction is a sum of two reactions, the anodic reaction and the cathodic reaction (Morad et al. 1995).

The anodic reaction involving the metal dissolution is as follows:



The nickel present in the maraging steel also undergoes anodic dissolution as follows:





The cathodic reaction, hydrogen evolution takes place as follows:



3.1.2 Electrochemical impedance spectroscopy (EIS) studies

Fig. 3.2 represents the Nyquist plots for the corrosion of welded maraging steel in different concentrations of HCl at 35 °C. Similar plots were obtained at other temperatures also. The point where the semi-circle of the Nyquist plot intersects the real axis at high frequency (close to the origin) yields solution resistance (R_s). The intercept on real axis at the other end of the semicircle (low frequency) gives the sum of solution resistance and the charge transfer resistance (R_{ct}). Hence the charge transfer resistance value is simply the diameter of the semicircle (Prabhu et al. 2008). The diagonal region in between the high frequency and low frequency region has a negative slope due to the capacitive behaviour of the electrochemical double layer. R_{ct} is inversely proportional to the corrosion current and was used to calculate the corrosion rate.

From Fig. 3.2 it is clear that the diameter of the semicircle decreases with the increase in the concentration of HCl, indicating the decrease in R_{ct} value and increase in corrosion rate. The fact that impedance diagrams have semicircular appearance shows that the corrosion of welded maraging steel is controlled by a charge transfer process and the mechanism of dissolution of metal in HCl is not altered with the change in the HCl concentration (Larabi et al. 2005). As seen from the figure, the Nyquist plots are not perfect semicircles. The deviation has been attributed to the frequency dispersion. The

“depressed” semicircles have a center under the real axis, and can be seen as depressed capacitive loops. Such phenomena often correspond to surface heterogeneity which may be the result of surface roughness, dislocations, distribution of the active sites or adsorption of molecules/ions (Li et al. 2008).

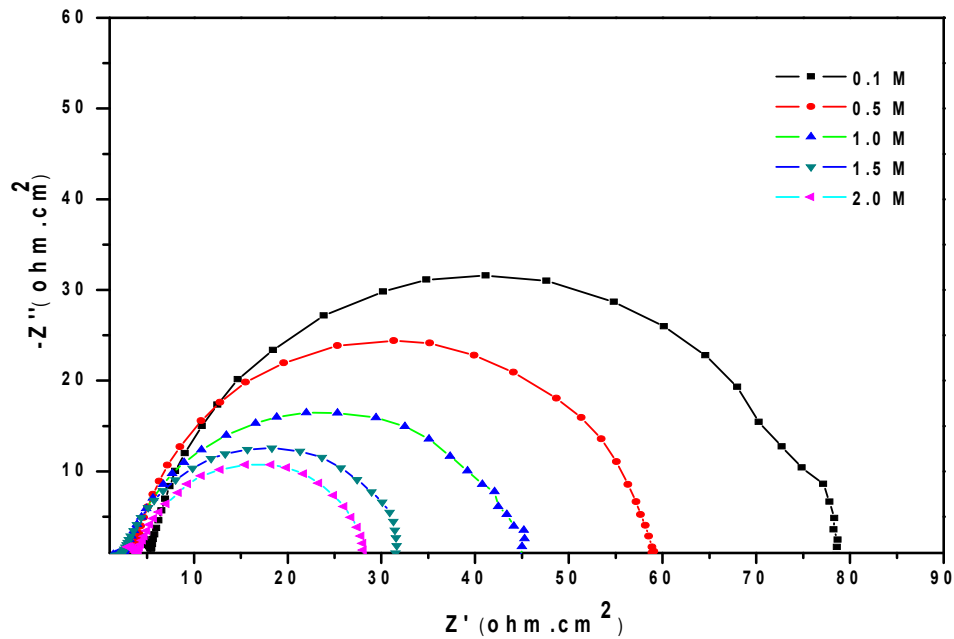


Fig. 3.2: Nyquist plots for the corrosion of welded maraging steel in different concentrations of HCl at 35 °C.

The results obtained can be interpreted in terms of the equivalent circuit of the electrical double layer. The circuit fitment was done by ZSimpWin software of version 3.21. The impedance data for the corrosion of welded maraging steel in HCl were analyzed using the circuit fitment shown in Fig. 3.3 in which R_s represents the solution resistance, R_{ct} the charge transfer resistance. The constant phase element (Q_{dl}) is substituted for the capacitive element to give a more accurate fit, as capacitive loops are depressed semi circles rather than regular semi circles (Tang et al. 2008). The results of EIS measurement are summarized in Table 3.2.

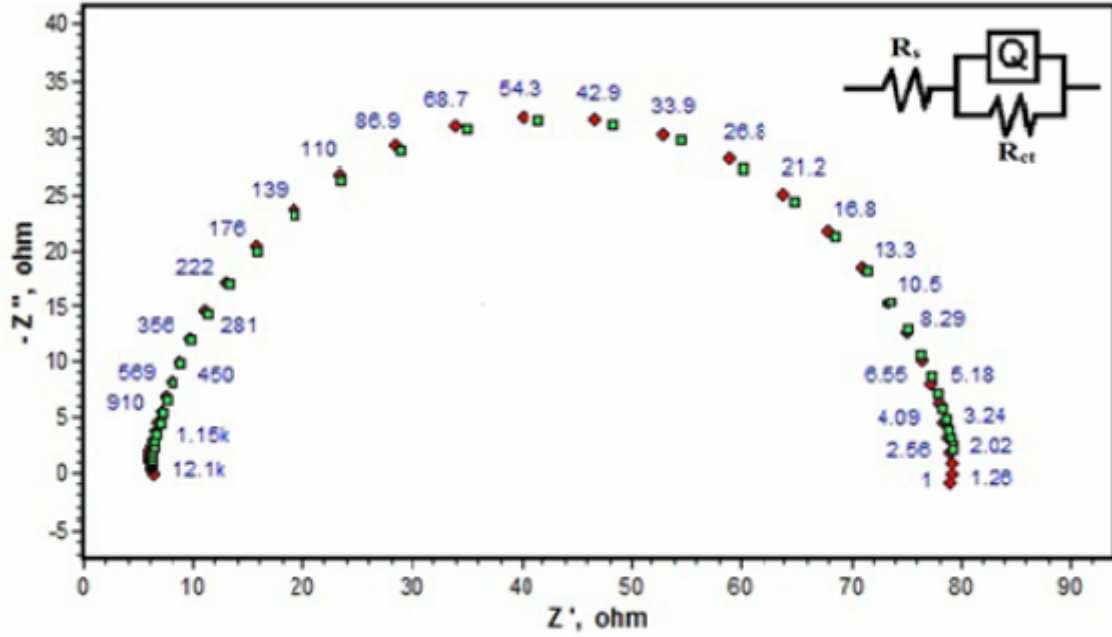


Fig. 3.3: The equivalent circuit model used to fit the experimental data for the corrosion of the welded maraging steel in 0.5 M HCl solution at 30 °C.

The impedance of constant phase (Z_Q) is described by the expression:

$$Z_Q = Y_0^{-1} (j\omega)^{-n} \quad (3.15)$$

where, Y_0 is a proportional factor, j is imaginary number and n has the meaning of a phase shift. The value of double layer capacitance (C_{dl}) can be obtained from the equation.

$$C_{dl} = Y_0 (\omega_m^n)^{n-1} \quad (3.16)$$

where, ω_m^n is the frequency at which the imaginary part of the impedance has maximum (Tang et al. 2008).

The results show that the charge transfer resistance (R_{ct}) value decreases and double layer capacitance (C_{dl}) increases with the increase in the concentration of hydrochloric acid. The increase in the C_{dl} value may be due to the desorption of the chloride ions at the metal surface causing a change in the double layer structure (Abd Ei-

Rehim et al. 1999). The Nyquist plots obtained in the real system represent a general behaviour where the double layer on the interface of metal/solution does not behave as a real capacitor. On the metal side electrons control the charge distribution whereas on the solution side it is controlled by ions. As ions are much larger than the electrons, the equivalent ions to the charge on the metal will occupy quite a large volume on the solution side of the double layer. Increase in the capacitance, which can result from an increase in local dielectric constant and/or a decrease in the thickness of the electrical double layer, suggests that the chloride ions get desorbed from the metal surface (Prabhu et al. 2007).

3.1.3 Effect of temperature

It is clear from the data presented in the Tables 3.1 and 3.2 that the corrosion rate of the welded maraging steel increases with the increase in the temperature of hydrochloric acid medium from 30 °C to 50 °C.

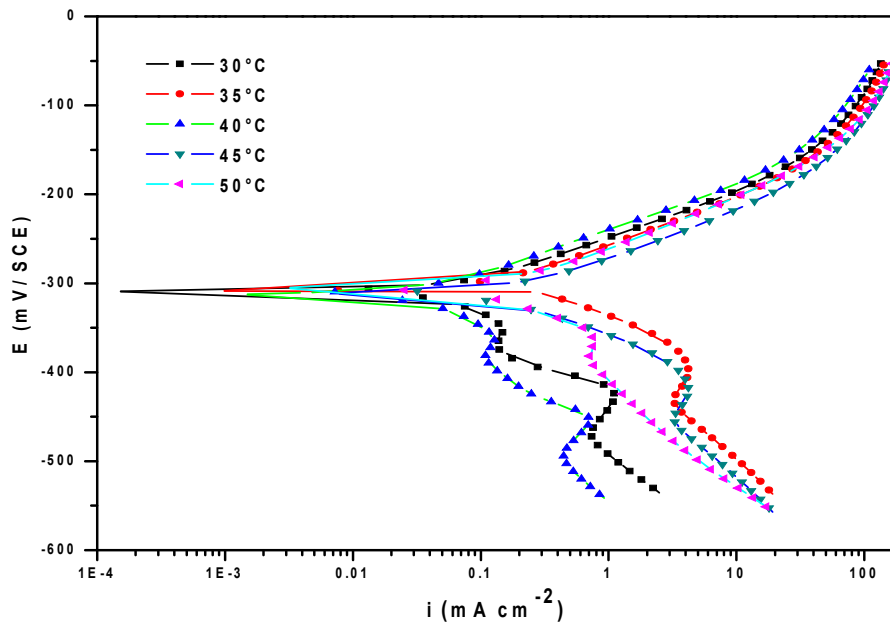


Fig. 3.4: Potentiodynamic polarization curves for the corrosion of welded maraging steel in 1.5 M HCl at different temperatures.

Fig. 3.4 and Fig. 3.5 represents the potentiodynamic polarization curves and Nyquist plots, respectively, for the corrosion of welded maraging steel in 1.5 M hydrochloric acid at different temperatures. Similar curves were obtained in other concentrations also. The increase in the corrosion rate with the increase temperature may be attributed to the fact that the hydrogen evolution overpotential decreases with the increase in temperature that leads to the increase in cathodic reaction rate (Bellanger and Rameau 1996).

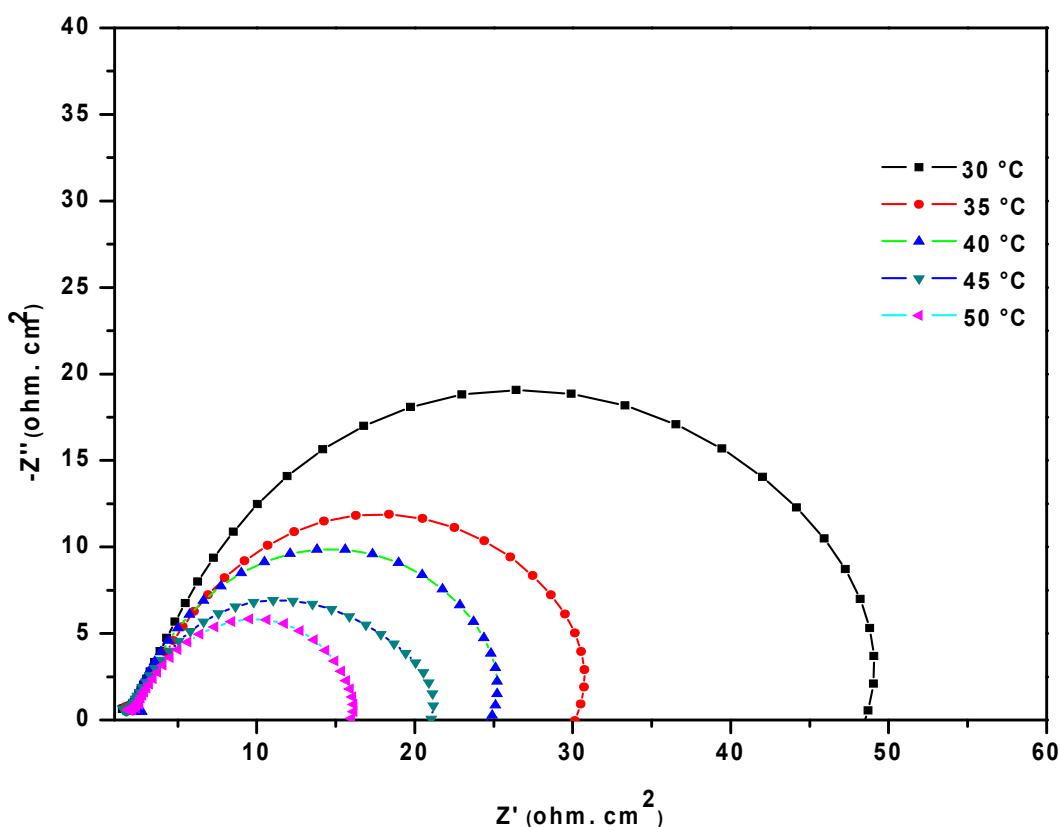


Fig. 3.5: Nyquist plots for the corrosion of welded maraging steel in 1.5 M HCl at different temperatures.

The variation of corrosion rate with temperature follows Arrhenius equation (Eqn. 2.6) which was utilized to calculate the activation energy (E_a). Enthalpy of activation (ΔH^\ddagger) and entropy of activation (ΔS^\ddagger) were calculated using transition state equation (Eqn. 2.7) from the plot of $\ln(v_{corr}/T)$ vs $1/T$. The Arrhenius plots for the corrosion of welded maraging steel in hydrochloric acid are shown in Fig.3.6.

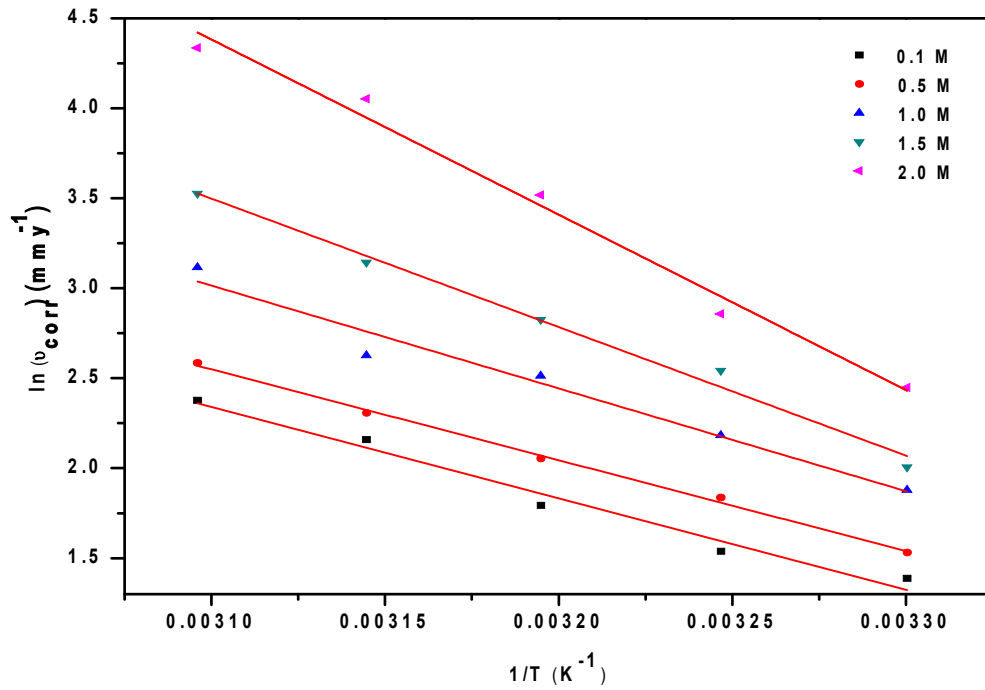


Fig. 3.6: Arrhenius plots for the corrosion of welded maraging steel in HCl.

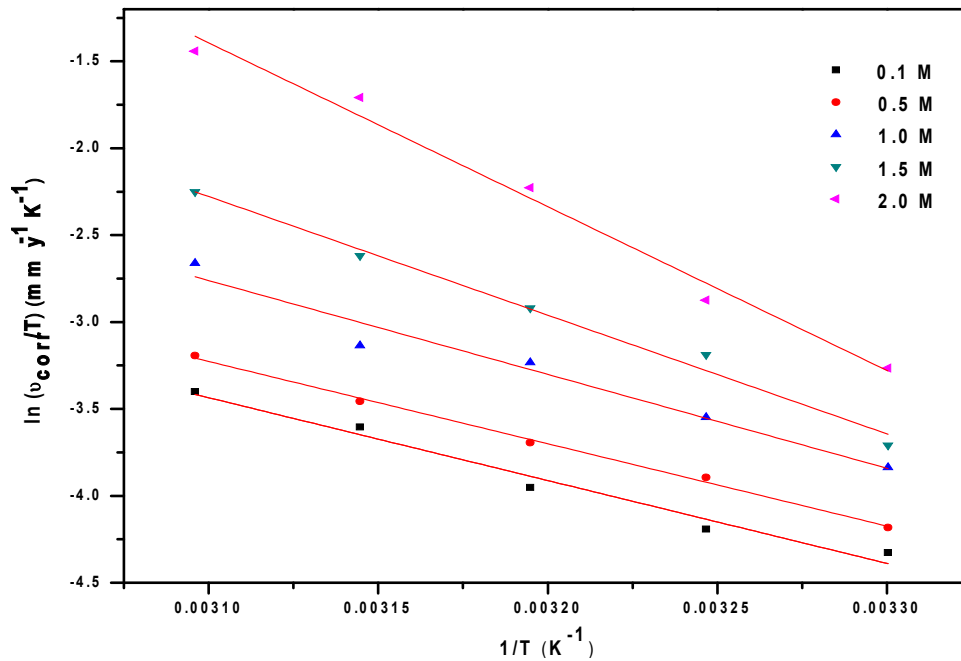


Fig. 3.7: Plots of $\ln(v_{\text{corr}}/T)$ versus $1/T$ for the corrosion of welded maraging steel in HCl.

The plots of $\ln(v_{corr}/T)$ vs $1/T$ are shown in the Fig. 3.7. The activation parameters calculated are listed in Table 3.3. The activation energy values indicate that the corrosion of the alloy is controlled by surface reaction, since the values of activation energy for the corrosion process are greater than 20 kJ mol^{-1} (Bouklah et al. 2005). The entropy of activation is negative. This implies that the activated complex in the rate-determining step represents association rather than dissociation, indicating that a decrease in randomness takes place on going from reactants to the activated complex (Prabhu et al. 2007).

3.1.4 Effect of concentration

It is clear from the Table 3.1 and 3.2 as well as from the polarisation curves (Fig.3.1) and Nyquist plots (Fig. 3.2) that the corrosion rate of the welded maraging steel increases with increase in hydrochloric acid concentration. There is no definite trend observed in E_{corr} value. This indicates that corrosion potential E_{corr} with increase in concentration of acid influences both anodic and cathodic process (El-Sayed 1997). This observation is in accordance with (Muralidharan et al. 1979) who proposed dependence of E_{corr} and i_{corr} on solution parameters. There is no significant change in the values of b_a and b_c for the welded specimen with change in concentration of acid, which implies that, there is no change in corrosion reaction mechanism with change in acid concentration. This fact is supported by similar shapes of polarisation curves at different concentrations of acid.

3.1.5 Scanning electron microscope (SEM)/EDX studies

The surface morphology of the welded maraging steel immersed in 2.0 M hydrochloric acid solution was compared with that of the non-corroded element by recording their SEM images. The SEM image of a freshly polished surface of the welded maraging steel sample is given in Fig.3.8 (a), which shows the non-corroded surface with few scratches due to improper polishing. Fig.3.8 (b) shows the SEM image of the welded maraging steel surface after immersion for 3 h in 2.0 M hydrochloric acid. The SEM images reveal that the specimen not immersed in the acid solution is in a better condition

having a smooth surface while the metal surface immersed in hydrochloric acid is deteriorated due to the acid action.

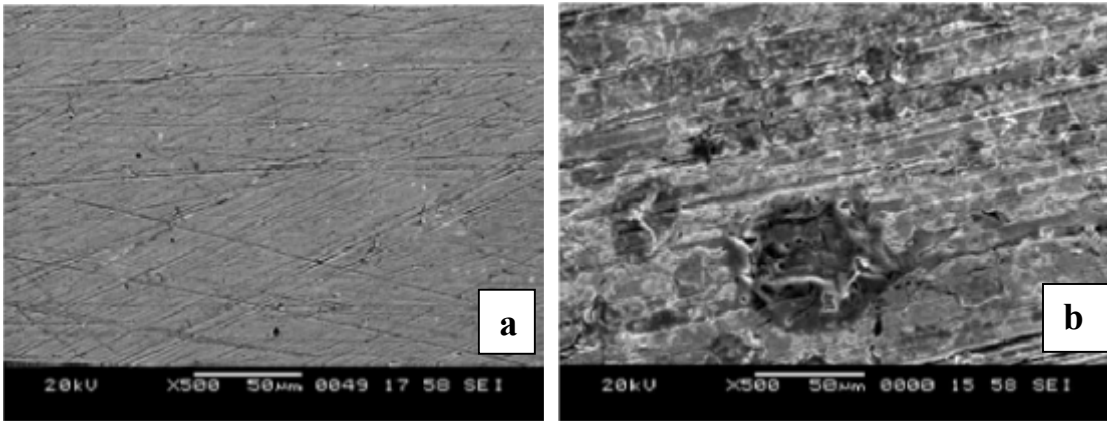


Fig. 3.8: SEM images of (a) freshly polished surface (b) corroded surface.

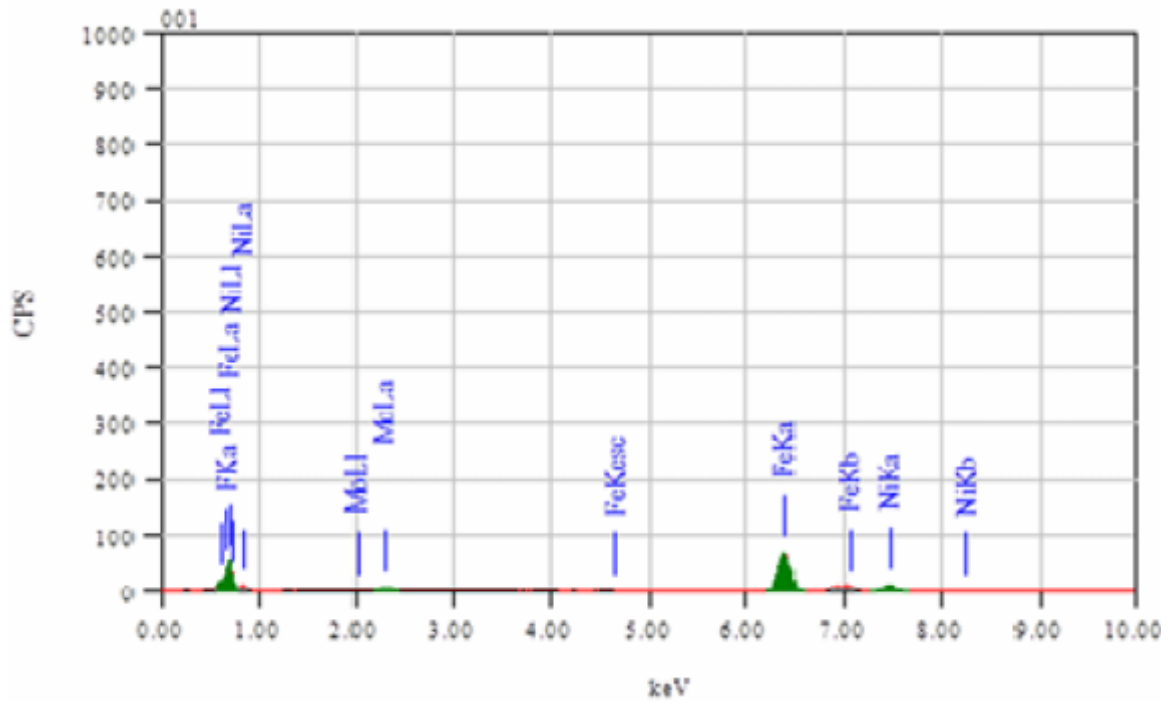


Fig. 3.9 (a): EDX spectra of the freshly polished surface of welded maraging steel.

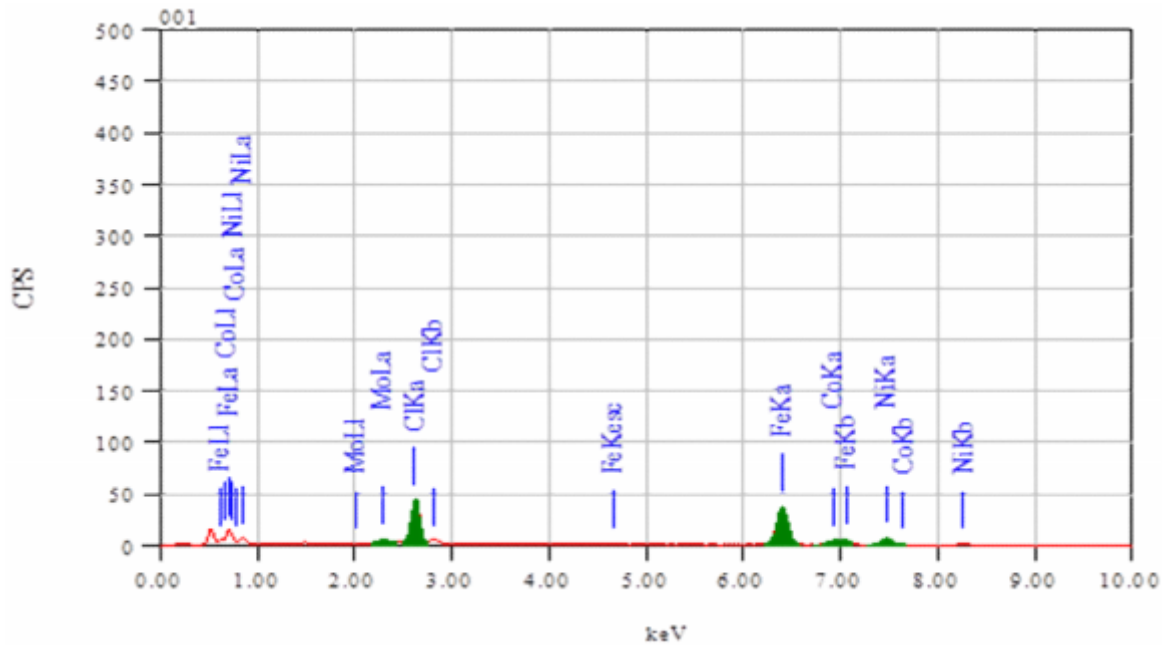


Fig. 3.9 (b): EDX spectra of the welded maraging steel after immersion in 2.0 M hydrochloric acid.

EDX spectra were used to determine the elements present on the specimen surface before and after its exposure to the acid solution. The atomic percentage of the elements found in the EDX profile for the uncorroded metal surface (Fig. 3.9(a)) was 66.5 % Fe, 17.2% Ni, 3.1% Mo, 6.7% Co, 0.07% Si and 0.22% Ti. The EDX spectra of the corroded surface is shown in Fig. 3.9 (b). The atomic percentage of the elements on the corroded metal surface was 51.63% Fe, 13.15% Ni, 27.48% Cl, 2.06% Mo and 5.68% Co. The presence of chlorine on the corroded metal surface and decreased metal content indicates the presence of metal chlorides on the corroded metal surface. The metal chlorides are formed due to the corrosion of the alloy in HCl medium.

Table 3.1: Results of potentiodynamic polarization studies for the corrosion of welded maraging steel in different concentrations of HCl at different temperatures.

| Molarity of HCl (M) | Temperature (°C) | $-E_{corr}$ (mV vs SCE) | b_a (mV dec ⁻¹) | $-b_c$ (mV dec ⁻¹) | i_{corr} (mA cm ⁻²) | U_{corr} (mm y ⁻¹) |
|---------------------|------------------|-------------------------|-------------------------------|--------------------------------|-----------------------------------|----------------------------------|
| 0.1 | 30 | 306 | 98 | 140 | 0.31 | 4.00 |
| | 35 | 310 | 101 | 146 | 0.36 | 4.64 |
| | 40 | 312 | 103 | 147 | 0.46 | 5.93 |
| | 45 | 315 | 108 | 156 | 0.67 | 8.64 |
| | 50 | 313 | 113 | 161 | 0.83 | 10.70 |
| 0.5 | 30 | 315 | 103 | 149 | 0.35 | 4.51 |
| | 35 | 323 | 105 | 152 | 0.48 | 6.19 |
| | 40 | 330 | 112 | 158 | 0.60 | 7.73 |
| | 45 | 328 | 116 | 165 | 0.77 | 9.93 |
| | 50 | 324 | 118 | 173 | 1.03 | 13.28 |
| 1.0 | 30 | 324 | 112 | 158 | 0.51 | 6.57 |
| | 35 | 328 | 118 | 163 | 0.68 | 8.77 |
| | 40 | 336 | 126 | 171 | 0.95 | 12.25 |
| | 45 | 331 | 131 | 179 | 1.07 | 13.79 |
| | 50 | 328 | 142 | 191 | 1.75 | 22.56 |
| 1.5 | 30 | 316 | 109 | 163 | 0.57 | 7.35 |
| | 35 | 320 | 117 | 171 | 0.98 | 12.63 |
| | 40 | 328 | 124 | 183 | 1.31 | 16.89 |
| | 45 | 322 | 132 | 198 | 1.80 | 23.20 |
| | 50 | 315 | 147 | 209 | 2.63 | 33.90 |
| 2.0 | 30 | 324 | 114 | 178 | 0.90 | 11.60 |
| | 35 | 316 | 129 | 186 | 1.34 | 17.27 |
| | 40 | 310 | 137 | 193 | 2.61 | 33.64 |
| | 45 | 327 | 143 | 212 | 4.46 | 57.49 |
| | 50 | 332 | 159 | 223 | 5.93 | 76.44 |

Table 3.2: EIS data for the corrosion of welded maraging steel in different concentrations of HCl at different temperatures.

| Molarity of HCl (M) | Temperature (°C) | C_{dl} (mF cm ⁻²) | R_{ct} (Ω cm ²) | v_{corr} (mm y ⁻¹) |
|---------------------|------------------|---------------------------------|---------------------------------------|----------------------------------|
| 0.1 | 30 | 0.061 | 80.6 | 4.01 |
| | 35 | 0.069 | 71.8 | 4.67 |
| | 40 | 0.135 | 56.4 | 6.01 |
| | 45 | 0.183 | 41.3 | 8.64 |
| | 50 | 0.224 | 34.5 | 10.77 |
| 0.5 | 30 | 0.071 | 73.8 | 4.61 |
| | 35 | 0.112 | 55.4 | 6.27 |
| | 40 | 0.165 | 47.1 | 7.78 |
| | 45 | 0.216 | 38.0 | 10.03 |
| | 50 | 0.279 | 29.6 | 13.26 |
| 1.0 | 30 | 0.110 | 56.1 | 6.53 |
| | 35 | 0.203 | 43.2 | 8.86 |
| | 40 | 0.276 | 32.9 | 12.34 |
| | 45 | 0.308 | 30.6 | 13.83 |
| | 50 | 0.346 | 20.2 | 22.56 |
| 1.5 | 30 | 0.166 | 49.2 | 7.43 |
| | 35 | 0.315 | 30.6 | 12.71 |
| | 40 | 0.378 | 24.5 | 16.88 |
| | 45 | 0.395 | 19.1 | 23.21 |
| | 50 | 0.402 | 14.2 | 34.01 |
| 2.0 | 30 | 0.248 | 33.6 | 11.57 |
| | 35 | 0.362 | 24.5 | 17.40 |
| | 40 | 0.399 | 13.3 | 33.72 |
| | 45 | 0.418 | 8.3 | 57.58 |
| | 50 | 0.439 | 6.8 | 76.39 |

Table 3.3: Activation parameters for the corrosion of welded maraging steel in hydrochloric acid.

| Molarity of HCl (M) | E_a (kJ mol ⁻¹) | ΔH^\ddagger (kJ mol ⁻¹) | ΔS^\ddagger (J K ⁻¹ mol ⁻¹) |
|------------------------|----------------------------------|--|---|
| 0.1 | 42.28 | 39.62 | -103.29 |
| 0.5 | 42.97 | 39.37 | -102.37 |
| 1.0 | 47.51 | 44.97 | -81.34 |
| 1.5 | 59.37 | 56.78 | -40.52 |
| 2.0 | 80.98 | 78.36 | -33.72 |

3.2 CORROSION BEHAVIOR OF 18% Ni M250 GRADE MARAGING STEEL UNDER WELDED CONDITION IN SULPHURIC ACID MEDIUM

3.2.1 Potentiodynamic polarization studies

Fig. 3.10 represents the potentiodynamic polarization curves for the corrosion of welded sample of maraging steel in sulphuric acid solutions of different concentrations at 50 °C. Similar plots were obtained at other temperatures also. The potentiodynamic polarization parameters are summarised in the Table 3.4. These results predict substantial corrosion of the welded maraging steel in sulphuric acid at all the studied temperatures and concentrations. The corrosion rate increases with the increase in the concentration of sulphuric acid. It is also observed from the results that there is no definite trend observed in the corrosion potential values as the concentration of sulphuric acid is increased.

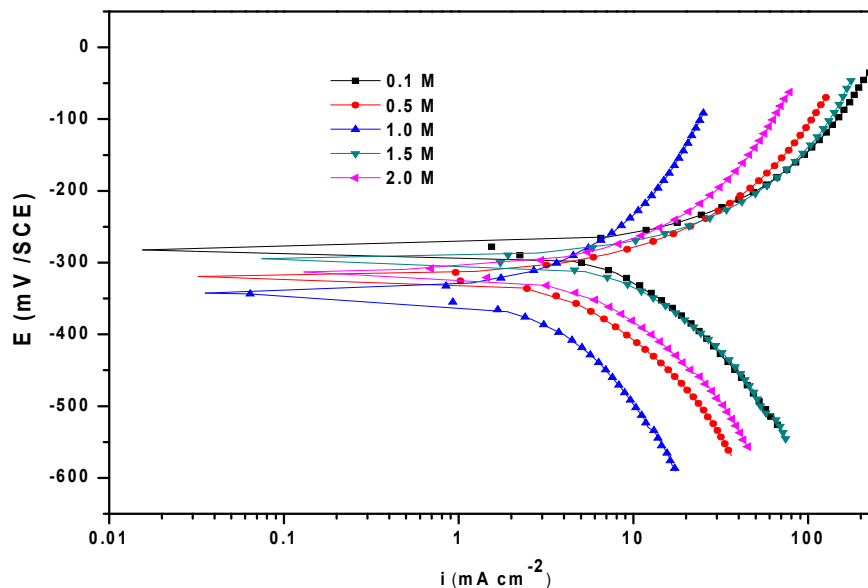


Fig. 3.10: Potentiodynamic polarisation curves for the corrosion of welded maraging steel in different concentrations of H₂SO₄ at 50 °C.

3.2.2 Electrochemical impedance spectroscopy studies

Nyquist plots for the corrosion of welded maraging steel in different concentrations of H₂SO₄ at 50 °C are shown in Fig. 3.11. Similar plots were obtained at other temperatures also. The similar semi-circular appearance of the impedance diagrams

shows that the corrosion of welded maraging steel is controlled by a charge transfer process and the mechanism of dissolution of the metal is not affected by the variation in the concentration of sulfuric acid (Larabi et al., 2005). As seen from the figure, the Nyquist plots are not perfect semicircles. The deviation has been attributed to frequency dispersion.

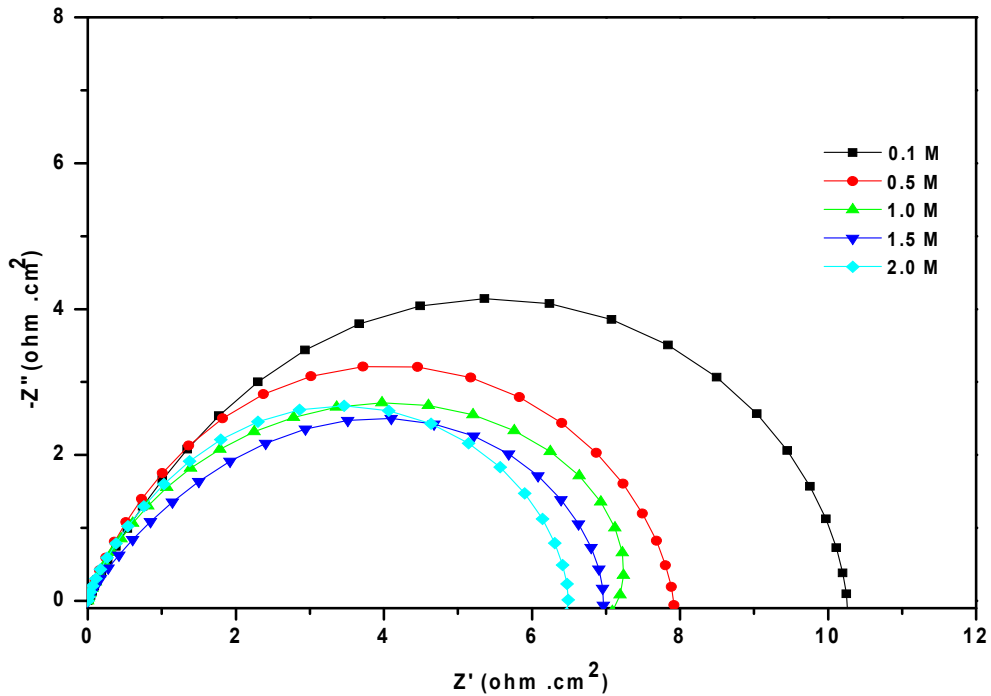


Fig. 3.11: Nyquist plots for the corrosion of welded maraging steel in different concentrations of H_2SO_4 at 50 °C.

The equivalent circuit used for the corrosion of the alloy in HCl medium shown in the Fig. 3.3 is used to fit the experimental data in the sulphuric acid medium also. The calculated values of R_{ct} , C_{dl} and corrosion rate (ν_{corr}) are listed in Table 3.5. The values of charge transfer resistance (R_{ct}) decreases and that of the double layer capacitance (C_{dl}) increases with the increase in the concentrations of sulphuric acid, indicating an increase in the corrosion rate with the increase in the concentration of sulphuric acid. This is in agreement with the results of potentiodynamic polarization studies.

3.2.3 Effect of temperature

Fig. 3.12 and Fig. 3.13 represents the potentiodynamic polarization curves and Nyquist plots, respectively, for the corrosion of welded maraging steel in 1.0 M sulphuric acid at different temperatures. Similar curves were obtained in other concentrations also. It is clear from the data presented in the Tables 3.4 and 3.5 that the corrosion rate of welded maraging steel increases with the increase in the temperature of sulphuric acid medium. This may be attributed to the fact that the hydrogen evolution overpotential decreases with the increase in temperature that leads to the increase in cathodic reaction rate (Bellanger and Rameau, 1996). The Arrhenius plots and plots of $\ln(v_{corr}/T)$ versus $1/T$ for the corrosion of welded maraging steel in sulphuric acid are presented in Fig. 3.14 and Fig. 3.15, respectively. The calculated activation parameters are given in the Table 3.6.

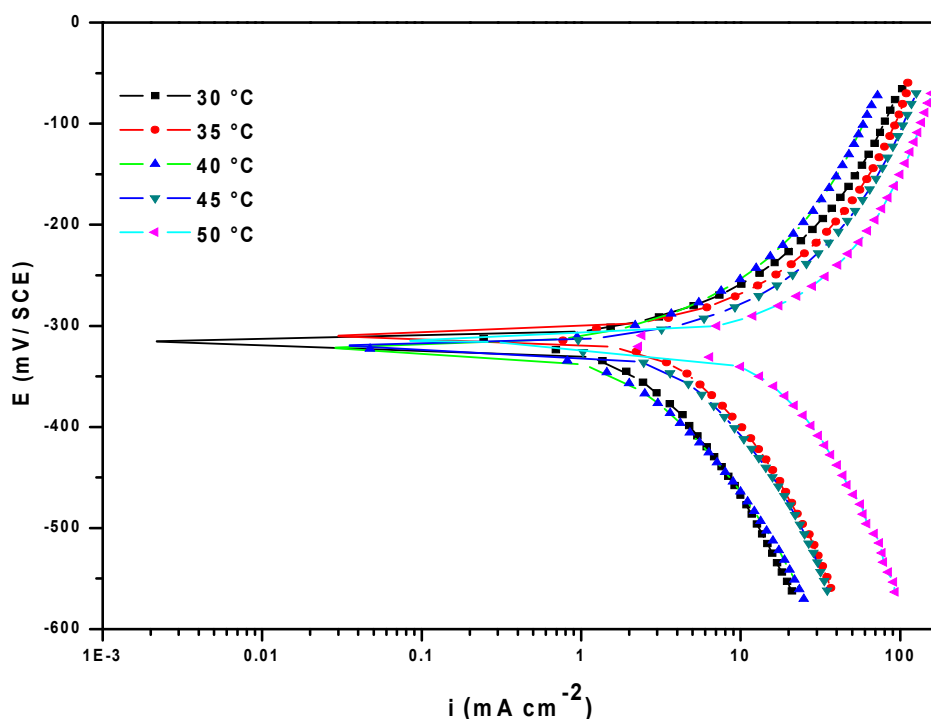


Fig. 3.12: Potentiodynamic polarization curves for the corrosion of welded maraging steel in 1.0 M H₂SO₄ at different temperatures.

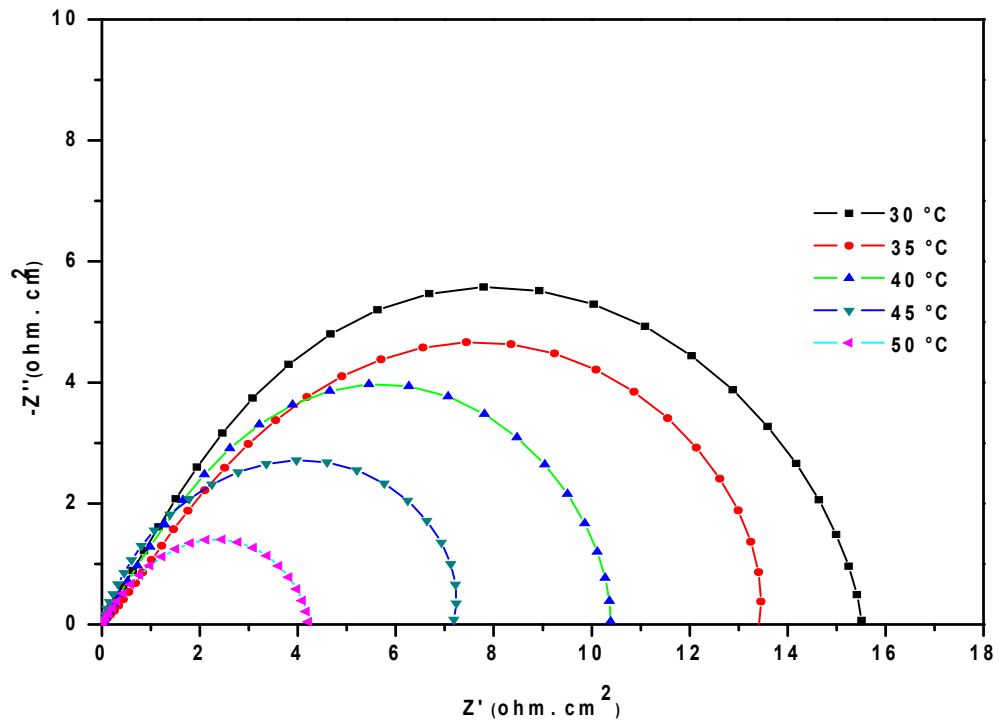


Fig. 3.13: Nyquist plots for the corrosion of welded maraging steel in 1.0 M H₂SO₄ at different temperatures.

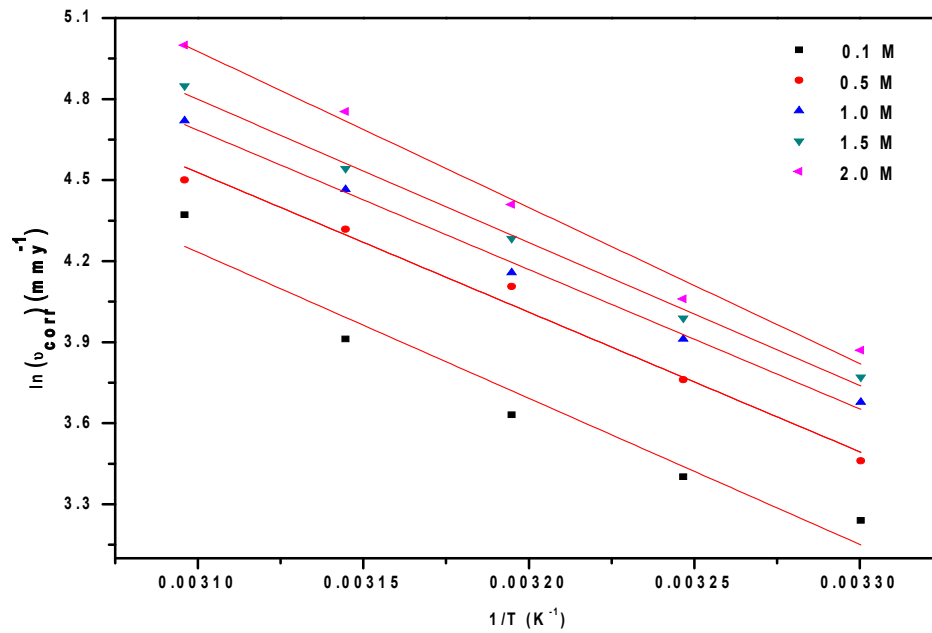


Fig. 3.14: Arrhenius plots for the corrosion of welded sample of maraging steel in H₂SO₄.

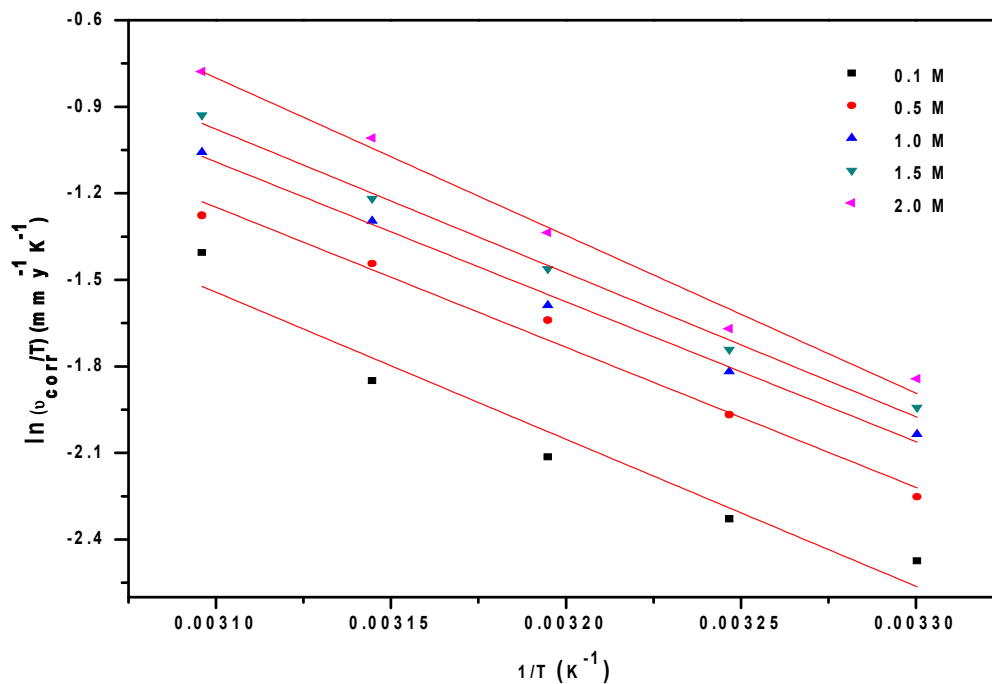


Fig. 3.15: Plots of $\ln (U_{corr} / T)$ versus $1/T$ for the corrosion of welded sample of maraging steel in H_2SO_4 .

3.2.4 Scanning electron microscope (SEM)/EDX studies

The SEM image of a freshly polished surface of the welded maraging steel sample is given in Fig.3.16 (a), which shows the non-corroded surface with few scratches due to improper polishing. Fig. 3.16 (b) shows the SEM image of welded maraging steel surface after immersion for 3 h in 2.0 M sulphuric acid, with a deteriorated surface due to the acid action. The atomic percentage of the elements found in the EDX spectra for corroded metal surface (Fig. 3.17) was 9.83% Fe, 2.41% Ni, 34.31% S, 3.34% Mo, 1.33% Co and 48.62% O and indicated that iron sulphate is existing on the corroded surface. The elemental compositions mentioned above were mean values at different regions.

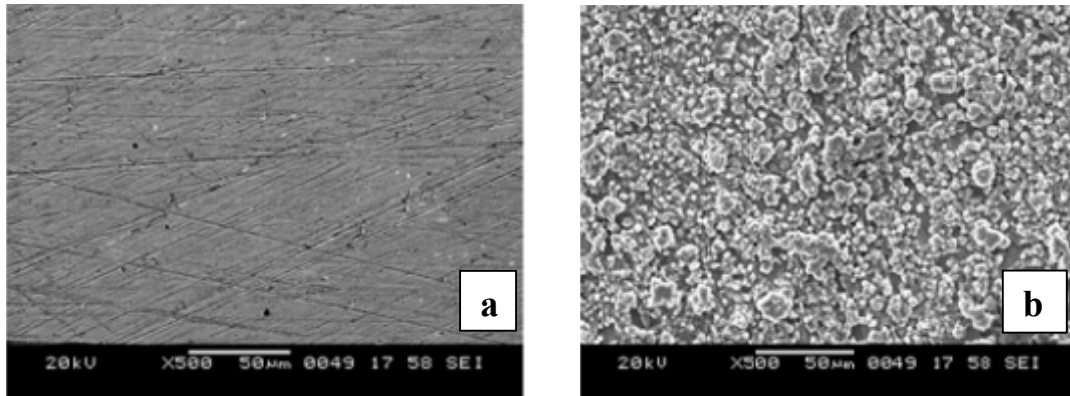


Fig. 3.16: SEM images of (a) freshly polished surface (b) corroded surface.

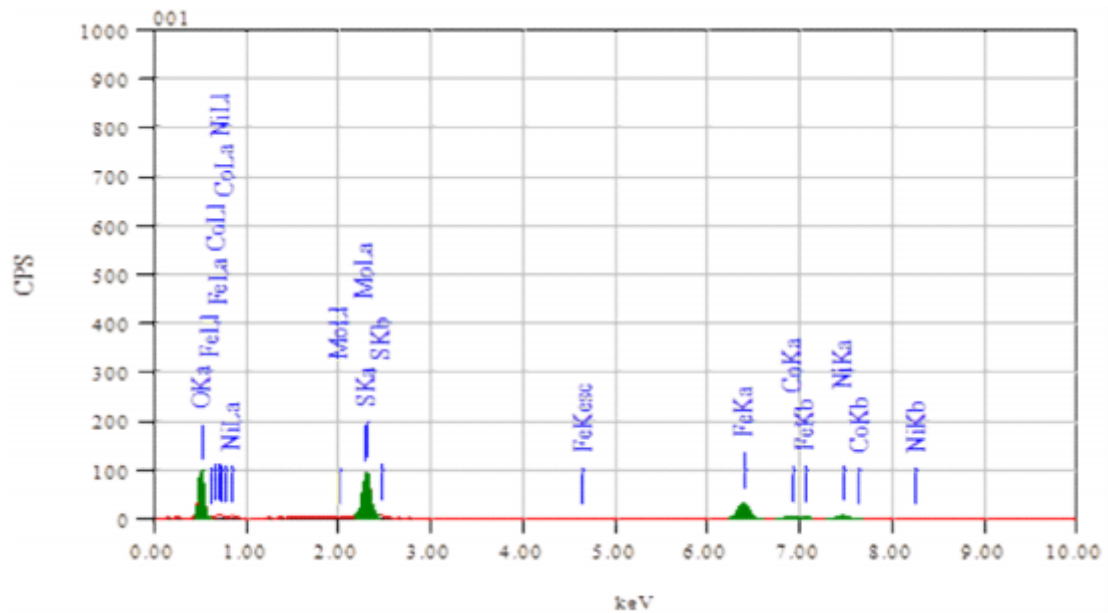


Fig. 3.17: EDX spectra of the welded maraging steel after immersion in 2.0 M sulphuric acid.

Table 3.4: Results of potentiodynamic polarization studies for the corrosion of welded maraging steel in different concentrations of H₂SO₄ at different temperatures.

| Molarity of H ₂ SO ₄ (M) | Temperature (°C) | $-E_{corr}$ (mV /SCE) | b_a (mV dec ⁻¹) | $-b_c$ (mV dec ⁻¹) | i_{corr} (mA cm ⁻²) | v_{corr} (mm y ⁻¹) |
|--|------------------|-----------------------|-------------------------------|--------------------------------|-----------------------------------|----------------------------------|
| 0.1 | 30 | 356 | 162 | 113 | 1.98 | 25.52 |
| | 35 | 353 | 171 | 124 | 2.41 | 31.07 |
| | 40 | 347 | 183 | 131 | 2.93 | 37.77 |
| | 45 | 345 | 197 | 142 | 3.47 | 44.73 |
| | 50 | 342 | 214 | 154 | 6.14 | 79.15 |
| 0.5 | 30 | 322 | 172 | 115 | 2.47 | 31.84 |
| | 35 | 321 | 191 | 132 | 2.68 | 34.55 |
| | 40 | 318 | 207 | 144 | 4.71 | 60.71 |
| | 45 | 314 | 224 | 158 | 5.38 | 69.35 |
| | 50 | 312 | 232 | 163 | 6.94 | 89.45 |
| 1.0 | 30 | 315 | 187 | 132 | 3.93 | 50.32 |
| | 35 | 313 | 198 | 147 | 4.21 | 54.12 |
| | 40 | 310 | 212 | 163 | 5.41 | 69.72 |
| | 45 | 312 | 243 | 178 | 6.70 | 86.36 |
| | 50 | 320 | 269 | 192 | 8.11 | 104.54 |
| 1.5 | 30 | 313 | 240 | 146 | 4.28 | 55.17 |
| | 35 | 308 | 242 | 151 | 5.31 | 68.45 |
| | 40 | 300 | 248 | 156 | 6.48 | 83.53 |
| | 45 | 301 | 290 | 197 | 7.54 | 97.19 |
| | 50 | 295 | 349 | 242 | 8.64 | 111.37 |
| 2.0 | 30 | 315 | 312 | 154 | 4.97 | 64.06 |
| | 35 | 313 | 283 | 208 | 6.12 | 78.89 |
| | 40 | 310 | 261 | 225 | 7.32 | 94.36 |
| | 45 | 312 | 282 | 231 | 8.23 | 106.09 |
| | 50 | 320 | 329 | 204 | 9.02 | 116.27 |

Table 3.5: EIS data for the corrosion of welded maraging steel in different concentrations of H₂SO₄ at different temperatures.

| Molarity of H ₂ SO ₄ (M) | Temperature (°C) | C _{dl} (mF cm ⁻²) | R _{ct} (Ω cm ²) | <i>v</i> _{corr} (mm y ⁻¹) |
|--|------------------|--|--------------------------------------|--|
| 0.1 | 30 | 0.324 | 20.1 | 25.26 |
| | 35 | 0.469 | 17.4 | 31.21 |
| | 40 | 0.531 | 14.1 | 38.03 |
| | 45 | 0.668 | 12.3 | 45.14 |
| | 50 | 0.830 | 10.2 | 78.11 |
| 0.5 | 30 | 0.633 | 18.7 | 30.81 |
| | 35 | 0.682 | 15.4 | 34.72 |
| | 40 | 0.727 | 11.4 | 59.29 |
| | 45 | 0.831 | 10.5 | 68.71 |
| | 50 | 0.965 | 7.9 | 89.09 |
| 1.0 | 30 | 0.641 | 16.1 | 38.02 |
| | 35 | 0.714 | 13.5 | 46.44 |
| | 40 | 0.670 | 10.3 | 62.77 |
| | 45 | 0.873 | 8.6 | 75.60 |
| | 50 | 1.123 | 7.3 | 108.17 |
| 1.5 | 30 | 0.958 | 15.9 | 41.37 |
| | 35 | 0.982 | 11.6 | 60.02 |
| | 40 | 1.070 | 9.4 | 69.61 |
| | 45 | 1.281 | 8.1 | 88.47 |
| | 50 | 1.318 | 6.9 | 124.38 |
| 2.0 | 30 | 1.093 | 13.9 | 44.89 |
| | 35 | 1.241 | 10.8 | 61.31 |
| | 40 | 1.324 | 9.2 | 80.05 |
| | 45 | 1.369 | 7.4 | 106.31 |
| | 50 | 1.508 | 6.5 | 143.16 |

Table 3.6: Activation parameters for the corrosion of welded maraging steel in H₂SO₄ medium.

| Molarity of H ₂ SO ₄ (M) | E _a (kJ mol ⁻¹) | ΔH [#] (kJ mol ⁻¹) | ΔS [#] (J K ⁻¹ mol ⁻¹) |
|---|---|--|---|
| 0.1 | 43.14 | 46.18 | -21.03 |
| 0.5 | 37.32 | 40.37 | -37.15 |
| 1.0 | 37.79 | 39.81 | -34.41 |
| 1.5 | 40.90 | 43.04 | -23.91 |
| 2.0 | 42.41 | 45.23 | -18.38 |

3.3 2,5-BIS(3,4,5-TRIMETHOXY PHENYL)-1,3,4-OXADIAZOLE (BTPO) AS INHIBITOR FOR THE CORROSION OF WELDED MARAGING STEEL IN HYDROCHLORIC ACID MEDIUM

3.3.1 Potentiodynamic polarization measurements

Polarization curves for the corrosion of maraging steel in 1.0 M HCl solution in the presence of different concentrations of BTPO are shown in Fig. 3.18. Similar results were obtained at other temperatures and in other concentrations of hydrochloric acid. The potentiodynamic polarization parameters are summarized in Tables 3.7 to 3.11.

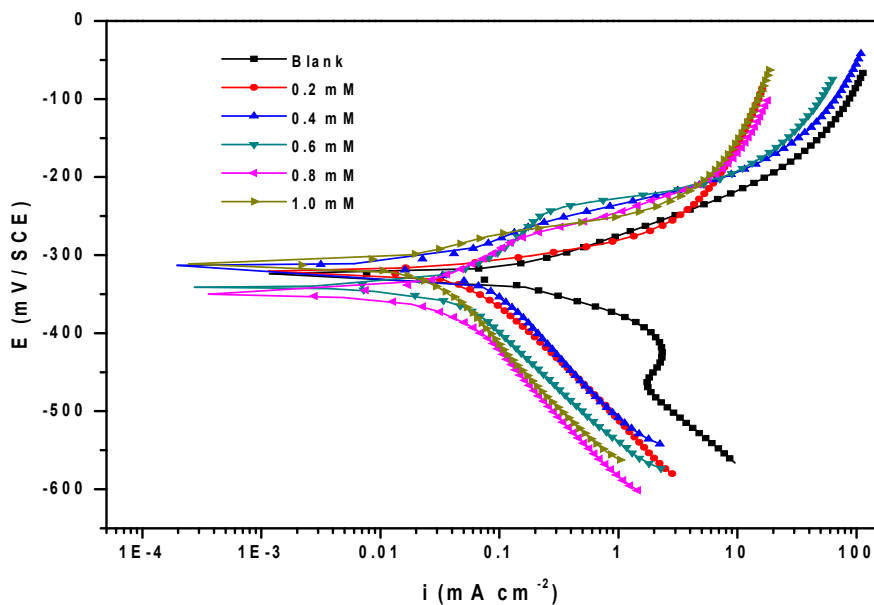


Fig. 3.18: Potentiodynamic polarization curves for the corrosion of welded maraging steel in 1.0 M hydrochloric acid containing different concentrations of BTPO at 30 °C.

It could be observed that both the anodic and cathodic reactions were suppressed with the addition of inhibitor, which suggested that the inhibitor exerted an efficient inhibitory effect both on the anodic dissolution of metal and on cathodic hydrogen evolution reaction (Tao et al. 2011). In general, according to the results presented in the Tables and also from the polarization curves in Fig. 3.18, the corrosion current density (i_{corr}) decreases significantly even on the addition of small concentration of BTPO and

the inhibition efficiency ($\eta\%$) increases with the increase in the inhibitor concentration for the welded maraging steel. The maximum efficiency of the inhibitor reported corresponds to the optimum concentration of the inhibitor. Inhibition efficiency increases with the increase in the inhibitor concentration up to an optimum value. Thereafter the increase in the inhibitor concentration does not show significant increase in inhibition efficiency.

It is seen from Tables 3.7 to 3.11, that the values of b_a and b_c do not change significantly with the increase in BTPO concentration, which indicates that the addition of BTPO does not change the mechanism of corrosion reaction (Atta et al. 2011). The small change in b_c and b_a values suggests that the BTPO was adsorbed on the metal surface and the addition of the inhibitor hindered the acid attack on the maraging steel electrode. The parallel cathodic Tafel curves showed that the hydrogen evolution was activation controlled and the reduction mechanism was not affected by the presence of the inhibitor (Tao et al. 2011). Hydrogen evolution reaction has been reported to be generally the dominant local cathodic process in the corrosion of steel alloy in aqueous acidic solutions, via H^+ ion or H_2O molecule reduction. The amounts of hydrogen evolved by the cathodic reaction are proportional to the corroded amounts of iron (Fekry et al. 2010).

The presence of inhibitor does not cause any significant shift in the E_{corr} value. According to Riggs and others (Li et al. 2008), if the change in corrosion potential is more than ± 85 mV with respect to corrosion potential of the blank, the compound could be recognised as an anodic or a cathodic type inhibitor. But the largest displacement of E_{corr} is about -34 mV, which implies that the inhibitor, BTPO, acts as a mixed type inhibitor, affecting both the metal dissolution and the hydrogen evolution reactions, but with more predominant towards cathodic action. This indicates that the inhibitive action of BTPO may be considered due to the adsorption and formation of barrier film on the electrode surface. The protective film formed on the metal surface reduces the probability that both the anodic and cathodic reactions, resulting in the decrease in the corrosion rate (Li et al. 2008). The increase in the inhibition efficiency with the increase in inhibitor

concentration is attributed to the increased surface coverage by the inhibitor molecules as the concentration is increased (El- Sayed et al. 1997).

3.3.2 Electrochemical impedance spectroscopy (EIS) studies

Nyquist plots for the corrosion of welded maraging steel in 1.0 M HCl solution in the presence of different concentrations of BTPO are given in Fig. 3.19. Similar plots were obtained in other concentrations of the acid and also at other temperatures. The impedance parameters are presented in Tables 3.12 to 3.16. It is seen from the Fig. 3.19 that the impedance spectra did not present perfect semicircles. The depressed semicircle is often attributed to the surface roughness, dislocations and distribution of the active sites or adsorption of inhibitors (Prabhu et al. 2008, El Hosary et al. 1972). The impedance data were analysed using an equivalent circuit (EC) that tentatively models the physical processes occurring at the metal-electrolyte interface (Machnikova et al. 2008).

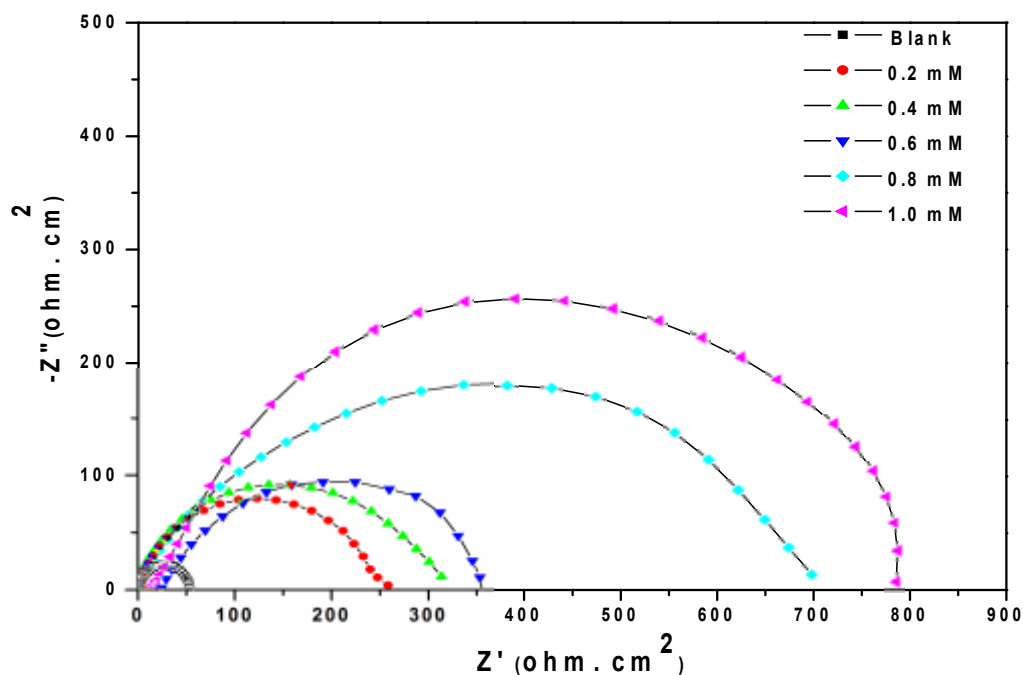


Fig. 3.19: Nyquist plots for the corrosion of welded maraging steel in 1.0 M hydrochloric acid containing different concentrations of BTPO at 30 °C.

The EC , as shown in Fig. 3.3 was used to simulate the measured impedance data for the corrosion of the alloy in 1.0 M HCl in the absence of BTPO. However, the impedance plots recorded for welded maraging steel in 1.0 M HCl solution in the presence of BTPO are modelled by using the equivalent circuit depicted in Fig. 3.20, which consists of the solution resistance (R_s), constant phase element (CPE), charge transfer resistance (R_{ct}), film resistance (R_f) and film capacitance (Q_f).

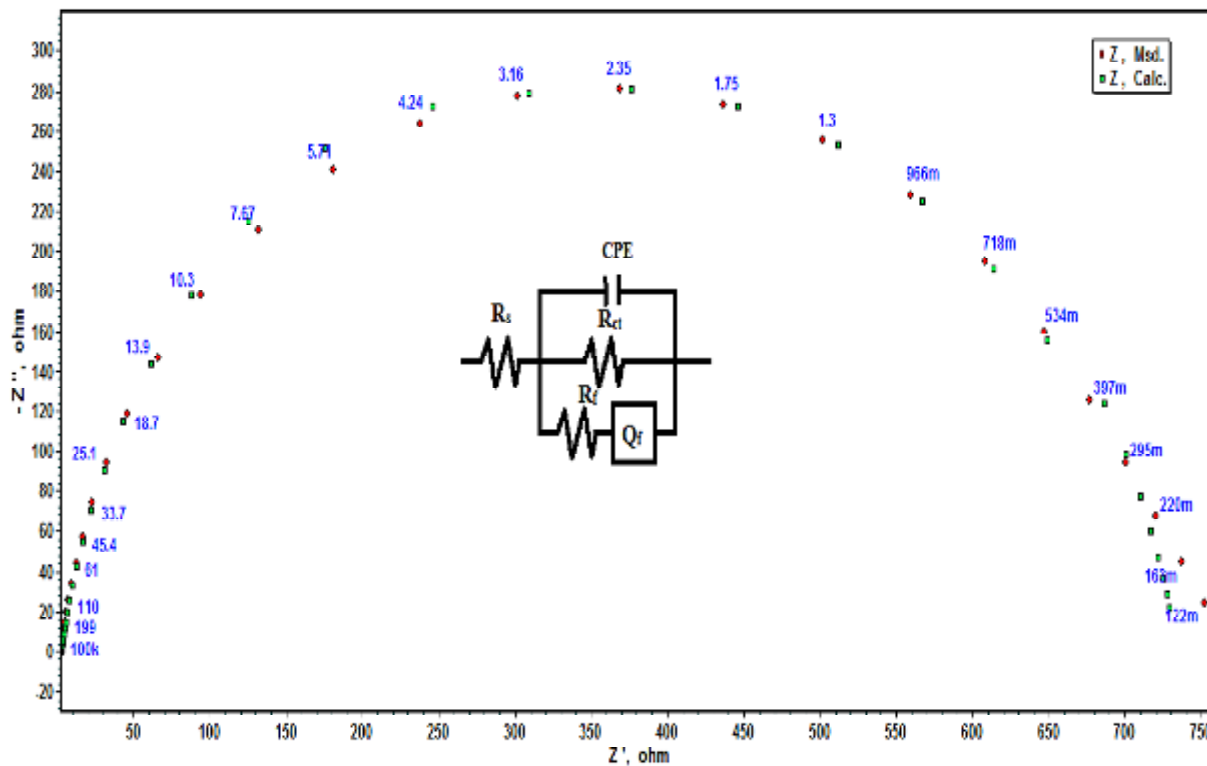


Fig. 3.20: Equivalent circuit used to fit the experimental EIS data for the corrosion of welded maraging steel in 1.0 M HCl at 30 °C in the presence of BTPO.

The film resistance and film capacitance elements appear from the adsorption of inhibitor molecules layer on the surface of the alloy. A constant-phase element (CPE) is employed instead of the double layer capacitance (C_{dl}) to describe the non-homogeneities in the system. It is seen from the data in Tables that the value of R_{ct} increases and the value of C_{dl} decreases as the concentration of BTPO increases, indicating an increased

inhibition efficiency. The double layer capacitance decreases with the increase in the concentration of BTPO can be attributed to the gradual replacement of water molecules by the adsorption of the organic molecules at metal/solution interface, which is leading to a protective film on the metal surface. In addition, the more the inhibitor is adsorbed, the more the thickness of the barrier layer, which also contributes to the decrease in the C_{dl} value according to the expression of the Helmholtz model.

$$C_{dl} = \frac{\varepsilon \varepsilon_o}{d} S \quad (3.17)$$

where, d is the thickness of the film, S is the surface area of the electrode, ε_o is the permittivity of the air, and ε is the local dielectric constant.

The R_p was used to calculate the inhibition efficiency ($\eta\%$) from the following equation.

$$\eta(\%) = \frac{R_{p(inh)} - R_p}{R_{p(inh)}} \times 100 \quad (3.18)$$

where, $R_{p(inh)}$ and R_p are the polarisation resistances obtained in inhibited and uninhibited solutions, respectively. R_p is calculated using the following equation:

$$\frac{1}{R_p} = \frac{1}{R_{ct}} + \frac{1}{R_f} \quad (3.19)$$

The increase of inhibitor concentration leads to the improved effectiveness of the protection which can be attributed to the blocking effect of the inhibitor on the surface by both adsorption and film formation reducing the effective area of attack. This modification results in an increase of charge transfer resistance where the resulting adsorption films isolate the metal surface from the corrosive medium and decrease metal dissolution (Arab et al. 2008, Ozcan et al. 2004, Machnikova et al. 2008).

The Bode plots of phase angle and amplitude for the corrosion of the alloy in 1.0 M HCl at 30 °C in the presence of BTPO, are shown in Fig. 3.21(a) and Fig. 3.21(b), respectively. Similar plots were obtained in other concentrations of HCl and at other temperatures also. The high frequency (HF) limit corresponds to R_s (Ω), while the lower

frequency (LF) limit corresponds to $(R_{ct} + R_f)$, which are associated with the dissolution processes at the metal/solution interface. Phase angle increases with the increase in concentrations of BTPO in hydrochloric acid medium. This might be due to the decrease in the dissolution of metal and decrease in the capacitive behaviour on the electrode surface. The presence of phase maximum at intermediate frequencies indicates the presence of a time constant corresponding to the impedance of the formed adsorbed film. The difference between the HF and LF for the inhibited system in the Bode plot increases with the increase in the concentration of BTPO. The impedance ($|Z|$) of maraging steel alloy is found to depend on the inhibitor type and concentration. An increase in the inhibitor concentration leads to an increase in the $|Z|$ value.

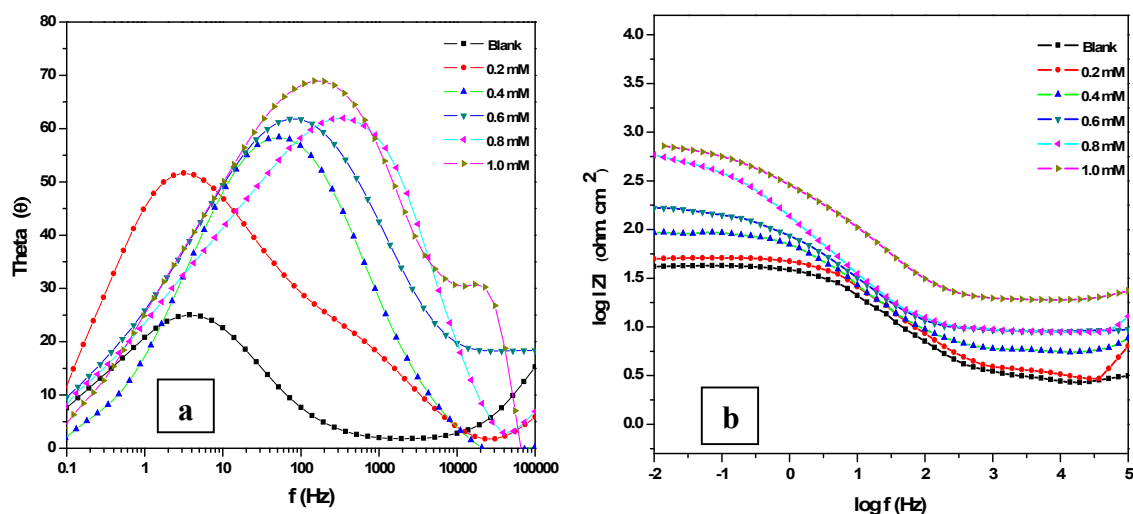


Fig. 3.21: Bode (a) phase angle plots and (b) amplitude plots for the corrosion of welded maraging steel in 1.0 M HCl containing different concentrations of BTPO at 30 °C.

3.3.3 Effect of temperature

The results in Tables 3.7 to 3.16 indicate that the inhibition efficiency of BTPO decreases with the increase in temperature. It is also seen from the data in the Tables 3.7 to 3.11, that the increase in solution temperature, does not alter the corrosion potential (E_{corr}), anodic Tafel slope (b_a) and cathodic Tafel slope (b_c) values significantly. This indicates that the increase in temperature does not change the mechanism of corrosion

reaction (Poornima et al 2011). However, i_{corr} and hence the corrosion rate of the specimen increases with the increase in temperature for both the blank and the inhibited solutions. The decrease in inhibition efficiency with the increase in temperature may be attributed to the higher dissolution rates of welded maraging steel at elevated temperature and also a possible desorption of adsorbed inhibitor due to the increased solution agitation resulting from higher rates of hydrogen gas evolution (Poornima et al. 2011). The higher rate of hydrogen gas evolution may also reduce the ability of the inhibitor to be adsorbed on the metal surface. The decrease in inhibition efficiency with the increase in temperature is also suggestive of physisorption of the inhibitor molecules on the metal surface (Geetha et al. 2011).

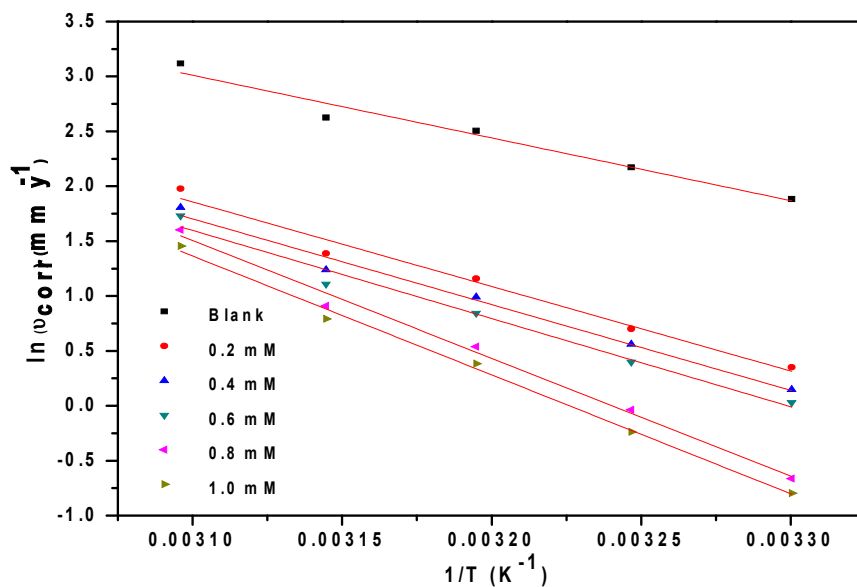


Fig. 3.22: Arrhenius Plots for the corrosion of welded maraging steel in 1.0 M hydrochloric acid containing different concentrations of BTPO.

The Arrhenius plots for the corrosion of welded maraging steel in the presence of different concentrations of BTPO in 1.0 M hydrochloric acid are shown in Fig. 3.22. The plots of $\ln(v_{\text{corr}}/T)$ versus $1/T$ for the corrosion of welded samples of maraging steel in the presence of different concentrations of BTPO in 1.0 M hydrochloric acid are shown

in Fig. 3.23. The calculated values of activation parameters are recorded in Table 3.17. The results show that the value of E_a increases with the increase in the concentration of BTPO indicating that the energy barrier for the corrosion reaction increases. It is also indicated that the whole process is controlled by surface reaction (Fouda et al. 2009), since the activation energies of the corrosion process are above 20 kJ mol⁻¹. The adsorption of the inhibitor on the electrode surface leads to the formation of a physical barrier between the metal surface and the corrosion medium, blocking the charge transfer, and thereby reducing the metal reactivity in the electrochemical reactions of corrosion.

The entropy of activation values in the absence and the presence of BTPO are large and negative; this indicates that the activated complex formation in the rate-determining step represents an association rather than dissociation, decreasing the randomness on going from the reactants to the activated complex (Abd EI Rehim et al. 2003). It is also seen from the Table that entropy of activation increases with the increase in the concentration of BTPO.

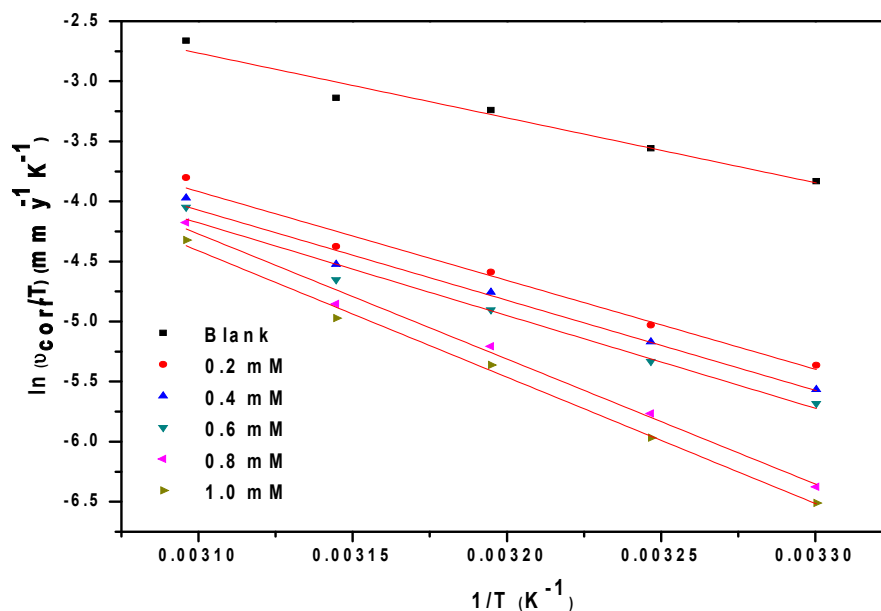


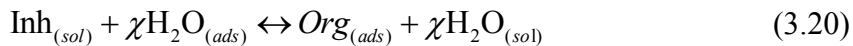
Fig. 3.23: Plots of $\ln(v_{corr}/T)$ versus $1/T$ for the corrosion of welded maraging steel in 1.0 M hydrochloric acid containing different concentrations of BTPO.

3.3.4 Effect of hydrochloric acid concentration

Table 3.18 summarises the maximum inhibition efficiencies exhibited by BTPO in the HCl solutions of different concentrations at different temperatures. It is evident from both polarization and EIS experimental results that, for a particular concentration of inhibitor, the inhibition efficiency decreases with the increase in hydrochloric acid concentration on the welded maraging steel. The highest inhibition efficiency is observed in hydrochloric acid of 0.1 M concentration. The decreased inhibition efficiency in higher concentration of hydrochloric acid can be attributed to the higher corrosivity of the medium.

3.3.5 Adsorption isotherm

The information on the interaction between the inhibitor molecules and the metal surface can be provided by the adsorption isotherms (Fekry et al. 2010). The adsorption of BTPO molecule on the metal surface can occur either through donor-acceptor interaction between the unshared electron pairs and/or π -electrons of inhibitor molecule and the vacant d-orbitals of the metal surface atoms, or through electrostatic interaction of the inhibitor molecules with already adsorbed chloride ions (Ashish Kumar et al. 2010). The adsorption bond strength is dependent on the composition of the metal, corrodent, inhibitor structure, concentration and orientation as well as temperature. The adsorption of an organic adsorbate at metal/solution interface can be presented as a substitution adsorption process between the organic molecules in aqueous solution (Org_{aq}), and the water molecules on metallic surface (H_2O_{ads}), as given below (Tao et al. 2011):



where, χ the size ratio, is the number of water molecules displaced by one molecule of organic inhibitor. χ is assumed to be independent of coverage or charge on the electrode (Tao et al. 2010, Oguzie et al. 2008).

The surface coverage (θ) was calculated from potentiodynamic polarization data using the equation:

$$\theta = \frac{\eta(\%)}{100} \quad (3.21)$$

where, η (%) is the percentage inhibition efficiency. The values of θ at different concentrations of inhibitor in the solution (C_{inh}) were applied to various isotherms including Langmuir, Temkin, Frumkin and Florye - Huggins isotherms. It was found that the data fitted best with the Langmuir adsorption isotherm, which is given by the relation:

$$\frac{C_{inh}}{\theta} = C_{inh} + \frac{1}{K} \quad (3.22)$$

where, K is the adsorption/desorption equilibrium constant, C_{inh} is the corrosion inhibitor concentration in the solution, and θ is the surface coverage. The plot of C_{inh}/θ versus C_{inh} gives a straight line with an intercept of $1/K$. The Langmuir adsorption isotherms for the adsorption of BTPO on the maraging steel surface in 1.0 M HCl at different temperatures are shown in Fig. 3.24. Similar plots were obtained in other HCl solutions also. The linear regression coefficients are close to unity and the slopes of the straight lines are nearly unity, suggesting that the adsorption of BTPO obeys Langmuir's adsorption isotherm with negligible interaction between the adsorbed molecules.

The standard free energy of adsorption, (ΔG_{ads}^0) was calculated using the relation (Fekry et al. 2010)

$$K = \frac{1}{55.5} \exp\left(\frac{-\Delta G_{ads}^0}{RT}\right) \quad (3.23)$$

where, the value 55.5 is the concentration of water in solution in mol dm⁻³, R is the universal gas constant and T is absolute temperature. Standard enthalpy of adsorption (ΔH_{ads}^0) and standard entropies of adsorption (ΔS_{ads}^0) were obtained from the plot of (ΔG_{ads}^0) versus T according to the thermodynamic equation:

$$\Delta G_{ads}^0 = \Delta H_{ads}^0 - T\Delta S_{ads}^0 \quad (3.24)$$

The thermodynamic data obtained for the adsorption of BTPO on the surface the alloy are tabulated in Table 3.19. The negative sign of ΔH^0_{ads} in HCl solution indicates that the adsorption of inhibitor molecules is an exothermic process. Generally, an exothermic adsorption process signifies either physisorption or chemisorptions while endothermic process is attributable unequivocally to chemisorption. Typically, the standard enthalpy of physisorption process is less negative than $-41.86 \text{ kJ mol}^{-1}$, while that of chemisorptions process approaches to -100 kJ mol^{-1} (Poornima et al. 2011). In the present study the value of ΔH^0_{ads} is less negative than $-41.86 \text{ kJ mol}^{-1}$, which shows that the adsorption of BTPO on welded maraging steel involves physisorption phenomenon (Ashish Kumar et al. 2010).

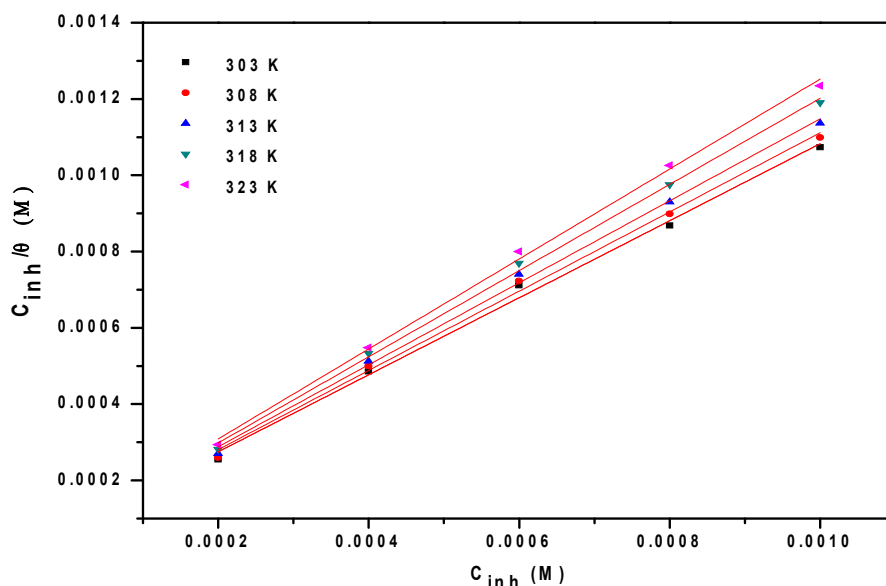


Fig. 3.24: Langmuir adsorption isotherms for the adsorption of BTPO on welded maraging steel in 1.0 M HCl at different temperatures.

The negative ΔG^0_{ads} values are consistent with the spontaneity of the adsorption process and the stability of the adsorbed layer on the alloy surface. When the value of ΔG^0_{ads} is less negative than -20 kJ mol^{-1} , the adsorption processes are associated with an electrostatic interaction between charged molecules and charged metal surface, resulting in physisorption and more negative than -40 kJ mol^{-1} involve charge transfer or sharing

from the inhibitor molecules to the metal surface to form a coordinate covalent bond, resulting in chemisorption (Hosseini et al. 2003). In the present case, the value of ΔG_{ads}^0 is -34 to -38 kJ mol⁻¹, indicating that the adsorption of BTPO is mixed adsorption, involving both physisorption and chemisorption. The decrease in inhibition efficiency with the increase in temperature also hints at physisorption of BTPO on the alloy surface. Therefore it can be concluded that the adsorption of BTPO as mixed adsorption with predominant physical mode of adsorption.

The ΔS_{ads}^0 value is negative indicating that decrease in randomness involved in the adsorption of BTPO molecules on the alloy surface. This could be the result of the adsorption of the inhibitor molecules, which could be regarded as a quasi-substitution process between the inhibitor compound in the aqueous phase and water molecules at electrode surface. In the present case, the decrease in entropy indicates that the more orderly arrangement of the inhibitor molecules on the metal surface overweighs the solvent entropy resulting from desorption of water molecules from the metal surface.

3.3.6 Mechanism of corrosion inhibition

The inhibitive effect of BTPO on the corrosion of welded maraging steel can be accounted for on the basis of its adsorption on the alloy surface. The adsorption of BTPO molecules on the metal surface can be attributed to the presence of electronegative elements like oxygen and nitrogen and also to the presence of π -electron cloud in the benzene rings of the molecule. The adsorption mechanism for a given inhibitor depends on factors, such as the nature of the metal, the corrosive medium, the pH, and the concentration of the inhibitor as well as the functional groups present in its molecule, since different groups are adsorbed to different extents (Wang et al. 2010, Taner et al. 2009). Welded maraging steel consists of segregated alloying elements along the grain boundaries. Since these segregations have different composition, their electrochemical behaviour is expected to be different from that of the matrix. Also, the lattice mismatch between the precipitate and the matrix causes strain field around the segregated

precipitates. These strain fields in combination with the galvanic effect due to the composition difference leads to the enhanced corrosion of welded maraging steel in acid medium. Considering the inhomogeneous nature, the surface of the alloy is generally characterized by multiple adsorption sites having different activation energies and enthalpies of adsorption. Inhibitor molecules may thus be adsorbed more readily at surface active sites having suitable adsorption enthalpies (Poornima et al. 2011).

To understand the mechanism of inhibition and the effect of inhibitor in aggressive acidic environment, some knowledge of interaction between the protective compound and the metal surface is required. Many organic corrosion inhibitors have at least one polar unit with a heteroatom; this polar unit is regarded as the reaction centre for the adsorption process (Gao et al. 2009). Furthermore, the size, orientation, shape and electric charge on the molecule determine the degree of adsorption and hence the effectiveness of inhibitor (Bilgic et al. 2003). On the other hand, iron is well known for its coordination affinity to ligands possessing heteroatom (Hackerman et al. 1996). Increase in inhibition efficiencies with increase in inhibitor concentration shows that the inhibition action is due to the adsorption on the maraging steel surface. Adsorption may take place by organic molecules at metal/solution interface due to electrostatic attraction between the charged molecules and charged metal, interaction of unshared electron pairs in the molecule with the metal, interaction of π -electrons with the metal or the combination of the above (Selim et al. 1996).

The presence of oxygen and nitrogen produce positive and negative charge centres on the molecules, because of higher electronegativity of these elements. In a highly acidic medium like the one in the present investigation, the metal surface is positively charged. This would cause the negatively charged chloride ions to become adsorbed on the metal surface, making the metal surface negatively charged. The positive centres of the BTPO molecules can interact electrostatically with the negatively charged chloride adsorbed metal surface, resulting in physisorption (Quraishi et al. 2003, Maayta et al. 2004, Ekpe et al. 1995). The negative charge centres of the BTPO molecules containing a lone pairs of electrons and/or π electrons can electrostatically interact with

the metal surface which is not adsorbed with chloride ions and get adsorbed. The neutral inhibitor molecules may occupy the vacant adsorption sites on the metal surface through the chemisorption mode involving the displacement of water molecules from the metal surface and sharing of electrons by the hetero atoms like oxygen, or nitrogen with iron. Chemisorption is also possible by the donor -acceptor interactions between π electrons of the aromatic ring and the vacant d orbitals of iron, providing another mode of protection (Wang et al. 2004, Barouni et al. 2008, El Azhar et al. 2001).

3.3.7 SEM/EDX studies

In order to differentiate between the surface morphology and to identify the composition of the species formed on the metal surface after its immersion in HCl in the absence and presence of BTPO, SEM/EDX investigations were carried out. Fig. 3.25 (a) represents SEM image of corroded welded maraging steel sample. The corrosion of welded alloy may be predominantly attributed to the inter-granular corrosion assisted by the galvanic effect between the precipitates and the matrix along the grain boundaries. Fig.3.25 (b) represents SEM image of welded maraging steel after the corrosion tests in a medium of hydrochloric acid containing 1.0 mM of BTPO. The image clearly shows a relatively smooth surface due to the layer of inhibitor molecules adsorbed on the surface of the alloy and thus protecting the metal from corrosion.

EDX spectral investigations were conducted in order to identify the species composition formed on the metal surface after immersion in hydrochloric acid in the absence and presence of BTPO. The atomic percentage of the elements found in the EDX profile for the inhibitor adsorbed metal surface (Fig. 3.26) were 17.67% Fe, 1.53% Ni, 6.79% Cl, 29.15% O, 13.66% N and 31.19% C and suggested the presence of BTPO on the alloy surface forming an anticorrosion protective film

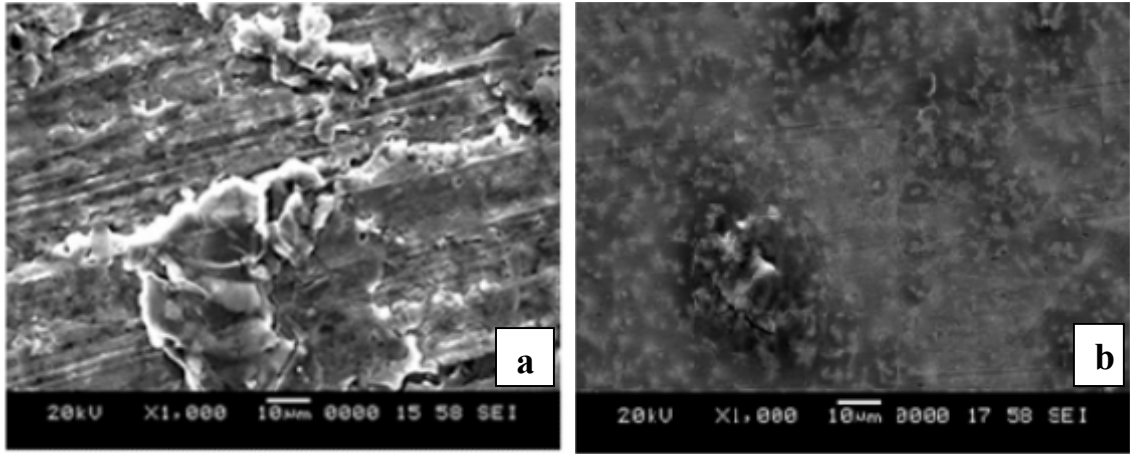


Fig. 3.25: SEM images of the welded maraging steel after immersion in 1.0 M HCl (a) in the absence and (b) in the presence of BTPO.

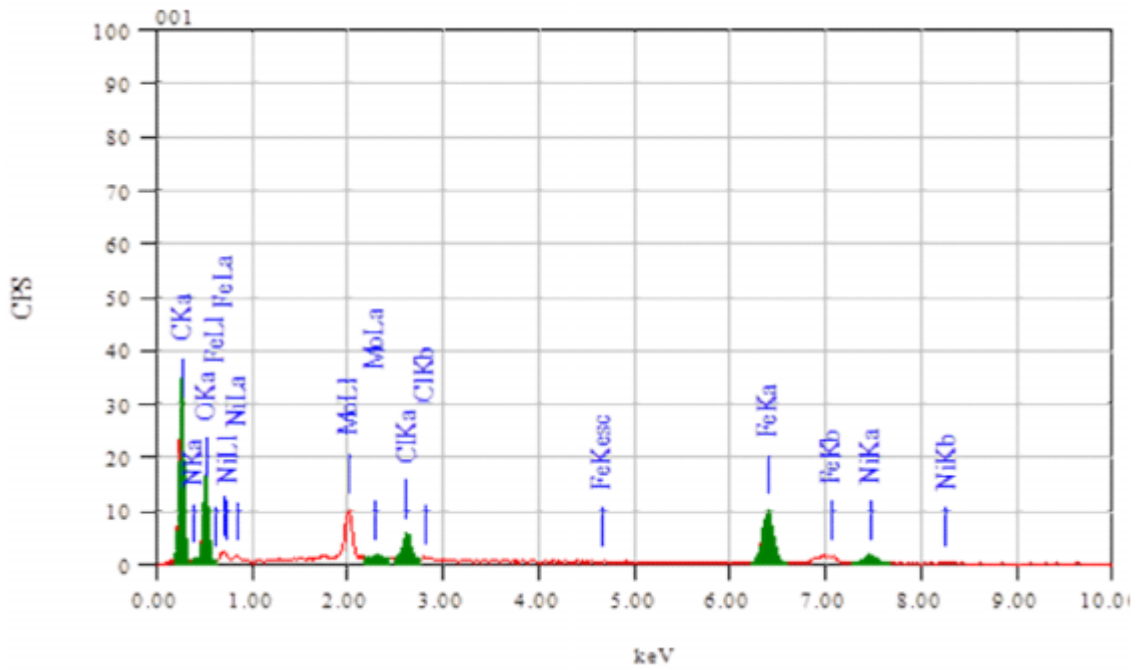


Fig. 3.26: EDX spectra of the welded maraging steel after immersion in 1.0 M HCl in the presence of BTPO.

Table 3.7: Results of potentiodynamic polarization studies for the corrosion of welded maraging steel in 0.1 M hydrochloric acid containing different concentrations of BTPO.

| Temperature (°C) | Conc. of inhibitor (mM) | $-E_{corr}$ (mV /SCE) | b_a (mV dec ⁻¹) | $-b_c$ (mV dec ⁻¹) | i_{corr} (mA cm ⁻²) | U_{corr} (mm y ⁻¹) | η (%) |
|------------------|-------------------------|-----------------------|-------------------------------|--------------------------------|-----------------------------------|----------------------------------|------------|
| 30 | Blank | 306 | 98 | 140 | 0.31 | 4.00 | |
| | 0.2 | 334 | 91 | 124 | 0.07 | 0.90 | 77.4 |
| | 0.4 | 328 | 88 | 121 | 0.05 | 0.64 | 83.9 |
| | 0.6 | 316 | 84 | 118 | 0.04 | 0.52 | 87.1 |
| | 0.8 | 323 | 83 | 116 | 0.03 | 0.39 | 90.3 |
| | 1.0 | 329 | 82 | 114 | 0.02 | 0.13 | 93.6 |
| | 35 | Blank | 310 | 101 | 146 | 0.36 | 4.64 |
| 0.2 | | 301 | 98 | 126 | 0.09 | 1.16 | 75.0 |
| 0.4 | | 317 | 95 | 124 | 0.07 | 0.90 | 80.6 |
| 0.6 | | 324 | 93 | 121 | 0.05 | 0.64 | 86.1 |
| 0.8 | | 331 | 91 | 118 | 0.04 | 0.52 | 88.9 |
| 1.0 | | 342 | 88 | 117 | 0.03 | 0.39 | 91.7 |
| 40 | | Blank | 312 | 103 | 147 | 0.46 | 5.93 |
| | 0.2 | 324 | 101 | 131 | 0.09 | 1.16 | 80.4 |
| | 0.4 | 329 | 98 | 128 | 0.08 | 1.03 | 82.6 |
| | 0.6 | 336 | 96 | 124 | 0.07 | 0.90 | 84.8 |
| | 0.8 | 341 | 94 | 119 | 0.05 | 0.64 | 89.1 |
| | 1.0 | 328 | 93 | 116 | 0.04 | 0.52 | 91.3 |
| | 45 | Blank | 315 | 108 | 156 | 0.67 | 8.64 |
| 0.2 | | 309 | 103 | 135 | 0.14 | 1.80 | 79.2 |
| 0.4 | | 321 | 99 | 133 | 0.12 | 1.55 | 82.1 |
| 0.6 | | 330 | 97 | 131 | 0.10 | 1.29 | 85.1 |
| 0.8 | | 317 | 95 | 128 | 0.09 | 1.16 | 86.4 |
| 1.0 | | 325 | 93 | 125 | 0.07 | 0.90 | 89.6 |
| 50 | | Blank | 313 | 113 | 161 | 0.83 | 10.70 |
| | 0.2 | 327 | 105 | 142 | 0.18 | 2.32 | 78.4 |
| | 0.4 | 332 | 103 | 139 | 0.16 | 2.06 | 80.7 |
| | 0.6 | 319 | 100 | 132 | 0.14 | 1.80 | 82.9 |
| | 0.8 | 348 | 98 | 129 | 0.12 | 1.55 | 85.5 |
| | 1.0 | 353 | 96 | 128 | 0.11 | 1.42 | 86.7 |

Table 3.8: Results of potentiodynamic polarization studies for the corrosion of welded maraging steel in 0.5 M hydrochloric acid containing different concentrations of BTPO.

| Temperature (°C) | Conc. of inhibitor (mM) | $-E_{corr}$ (mV /SCE) | b_a (mV dec ⁻¹) | $-b_c$ (mV dec ⁻¹) | i_{corr} (mA cm ⁻²) | U_{corr} (mm y ⁻¹) | η (%) |
|------------------|-------------------------|-----------------------|-------------------------------|--------------------------------|-----------------------------------|----------------------------------|------------|
| 30 | Blank | 315 | 103 | 149 | 0.35 | 4.51 | |
| | 0.2 | 327 | 97 | 112 | 0.07 | 0.90 | 80.1 |
| | 0.4 | 338 | 95 | 109 | 0.06 | 0.77 | 82.9 |
| | 0.6 | 346 | 93 | 108 | 0.05 | 0.64 | 85.7 |
| | 0.8 | 351 | 92 | 104 | 0.04 | 0.52 | 88.6 |
| | 1.0 | 354 | 90 | 101 | 0.03 | 0.26 | 91.4 |
| | 35 | Blank | 323 | 105 | 152 | 0.48 | 6.19 |
| 0.2 | | 318 | 101 | 121 | 0.10 | 1.29 | 79.2 |
| 0.4 | | 327 | 98 | 118 | 0.09 | 1.16 | 81.3 |
| 0.6 | | 345 | 95 | 116 | 0.07 | 0.90 | 85.4 |
| 0.8 | | 352 | 93 | 113 | 0.06 | 0.64 | 87.5 |
| 1.0 | | 357 | 92 | 111 | 0.05 | 0.52 | 89.5 |
| 40 | | Blank | 330 | 112 | 158 | 0.60 | 7.73 |
| | 0.2 | 324 | 104 | 127 | 0.14 | 1.80 | 76.7 |
| | 0.4 | 335 | 102 | 125 | 0.12 | 1.55 | 80.0 |
| | 0.6 | 343 | 99 | 123 | 0.10 | 1.29 | 83.3 |
| | 0.8 | 359 | 97 | 121 | 0.08 | 1.03 | 86.7 |
| | 1.0 | 364 | 96 | 118 | 0.07 | 0.77 | 88.3 |
| | 45 | Blank | 328 | 116 | 165 | 0.77 | 9.93 |
| 0.2 | | 316 | 104 | 131 | 0.19 | 2.40 | 75.3 |
| 0.4 | | 325 | 102 | 128 | 0.17 | 2.19 | 77.9 |
| 0.6 | | 319 | 99 | 125 | 0.14 | 1.80 | 81.8 |
| 0.8 | | 331 | 97 | 123 | 0.11 | 1.42 | 85.7 |
| 1.0 | | 343 | 94 | 119 | 0.10 | 1.29 | 87.0 |
| 50 | | Blank | 324 | 118 | 173 | 1.03 | 13.28 |
| | 0.2 | 312 | 104 | 142 | 0.26 | 3.35 | 74.8 |
| | 0.4 | 319 | 101 | 139 | 0.24 | 3.09 | 76.7 |
| | 0.6 | 328 | 98 | 137 | 0.20 | 2.58 | 80.6 |
| | 0.8 | 331 | 95 | 134 | 0.17 | 2.20 | 83.5 |
| | 1.0 | 343 | 93 | 132 | 0.15 | 1.93 | 85.4 |

Table 3.9: Results of potentiodynamic polarization studies for the corrosion of welded maraging steel in 1.0 M hydrochloric acid containing different concentrations of BTPO.

| Temperature (°C) | Conc. of inhibitor (mM) | $-E_{corr}$ (mV /SCE) | b_a (mV dec ⁻¹) | $-b_c$ (mV dec ⁻¹) | i_{corr} (mA cm ⁻²) | U_{corr} (mm y ⁻¹) | η (%) |
|------------------|-------------------------|-----------------------|-------------------------------|--------------------------------|-----------------------------------|----------------------------------|------------|
| 30 | Blank | 324 | 112 | 158 | 0.51 | 6.57 | |
| | 0.2 | 321 | 104 | 131 | 0.11 | 1.42 | 78.4 |
| | 0.4 | 314 | 101 | 128 | 0.09 | 1.16 | 82.4 |
| | 0.6 | 339 | 98 | 126 | 0.08 | 1.03 | 84.3 |
| | 0.8 | 352 | 96 | 124 | 0.06 | 0.52 | 88.2 |
| | 1.0 | 312 | 95 | 121 | 0.05 | 0.47 | 90.2 |
| | 35 | Blank | 328 | 118 | 163 | 0.68 | 8.77 |
| 0.2 | | 319 | 111 | 141 | 0.16 | 2.02 | 76.5 |
| 0.4 | | 331 | 108 | 137 | 0.14 | 1.75 | 79.4 |
| 0.6 | | 342 | 106 | 135 | 0.12 | 1.49 | 82.3 |
| 0.8 | | 349 | 103 | 132 | 0.08 | 0.96 | 86.4 |
| 1.0 | | 353 | 99 | 131 | 0.07 | 0.79 | 89.7 |
| 40 | | Blank | 336 | 126 | 171 | 0.95 | 12.25 |
| | 0.2 | 341 | 112 | 148 | 0.25 | 3.18 | 73.4 |
| | 0.4 | 348 | 109 | 143 | 0.21 | 2.69 | 77.9 |
| | 0.6 | 329 | 107 | 139 | 0.18 | 2.33 | 81.1 |
| | 0.8 | 341 | 104 | 136 | 0.13 | 1.71 | 86.3 |
| | 1.0 | 357 | 101 | 134 | 0.11 | 1.47 | 88.4 |
| | 45 | Blank | 331 | 131 | 179 | 1.07 | 13.79 |
| 0.2 | | 326 | 116 | 142 | 0.31 | 4.00 | 71.0 |
| 0.4 | | 337 | 113 | 139 | 0.27 | 3.45 | 74.8 |
| 0.6 | | 343 | 111 | 137 | 0.24 | 3.03 | 77.6 |
| 0.8 | | 351 | 108 | 132 | 0.19 | 2.48 | 82.2 |
| 1.0 | | 360 | 105 | 130 | 0.17 | 2.21 | 84.1 |
| 50 | | Blank | 328 | 142 | 191 | 1.75 | 22.56 |
| | 0.2 | 339 | 123 | 142 | 0.56 | 7.22 | 68.0 |
| | 0.4 | 343 | 119 | 139 | 0.47 | 6.09 | 73.1 |
| | 0.6 | 354 | 117 | 135 | 0.44 | 5.64 | 74.8 |
| | 0.8 | 362 | 115 | 133 | 0.39 | 4.96 | 77.7 |
| | 1.0 | 359 | 113 | 129 | 0.33 | 4.29 | 81.1 |

Table 3.10: Results of potentiodynamic polarization studies for the corrosion of welded maraging steel in 1.5 M hydrochloric acid containing different concentrations of BTPO.

| Temperature (°C) | Conc. of inhibitor (mM) | $-E_{corr}$ (mV /SCE) | b_a (mV dec ⁻¹) | $-b_c$ (mV dec ⁻¹) | i_{corr} (mA cm ⁻²) | \mathcal{U}_{corr} (mm y ⁻¹) | η (%) |
|------------------|-------------------------|-----------------------|-------------------------------|--------------------------------|-----------------------------------|--|------------|
| 30 | Blank | 316 | 109 | 163 | 0.57 | 7.35 | |
| | 0.2 | 319 | 100 | 137 | 0.13 | 1.68 | 77.2 |
| | 0.4 | 331 | 98 | 135 | 0.11 | 1.45 | 80.2 |
| | 0.6 | 342 | 96 | 131 | 0.10 | 1.33 | 81.9 |
| | 0.8 | 349 | 95 | 132 | 0.08 | 0.79 | 85.8 |
| | 1.0 | 353 | 93 | 127 | 0.06 | 0.60 | 89.4 |
| | 35 | Blank | 320 | 117 | 171 | 0.98 | 12.63 |
| 0.2 | | 324 | 112 | 142 | 0.24 | 3.13 | 75.2 |
| 0.4 | | 321 | 108 | 140 | 0.23 | 2.94 | 76.7 |
| 0.6 | | 314 | 105 | 138 | 0.20 | 2.55 | 79.8 |
| 0.8 | | 339 | 103 | 137 | 0.16 | 2.05 | 83.8 |
| 1.0 | | 352 | 100 | 132 | 0.12 | 1.53 | 87.9 |
| 40 | | Blank | 328 | 124 | 183 | 1.31 | 16.89 |
| | 0.2 | 315 | 117 | 164 | 0.37 | 4.76 | 71.8 |
| | 0.4 | 309 | 112 | 158 | 0.33 | 4.27 | 74.7 |
| | 0.6 | 321 | 109 | 154 | 0.27 | 3.50 | 79.3 |
| | 0.8 | 330 | 107 | 152 | 0.23 | 3.02 | 82.1 |
| | 1.0 | 317 | 105 | 149 | 0.18 | 2.31 | 86.3 |
| | 45 | Blank | 322 | 132 | 198 | 1.80 | 23.20 |
| 0.2 | | 312 | 119 | 173 | 0.53 | 6.84 | 70.5 |
| 0.4 | | 324 | 116 | 167 | 0.48 | 6.17 | 73.4 |
| 0.6 | | 329 | 114 | 163 | 0.45 | 5.75 | 75.2 |
| 0.8 | | 336 | 111 | 164 | 0.33 | 4.25 | 81.7 |
| 1.0 | | 341 | 105 | 156 | 0.30 | 3.85 | 83.4 |
| 50 | | Blank | 315 | 147 | 209 | 2.63 | 33.90 |
| | 0.2 | 307 | 121 | 182 | 0.86 | 11.12 | 67.2 |
| | 0.4 | 318 | 120 | 177 | 0.74 | 9.56 | 71.8 |
| | 0.6 | 324 | 119 | 175 | 0.65 | 8.34 | 76.9 |
| | 0.8 | 314 | 115 | 170 | 0.61 | 7.83 | 75.4 |
| | 1.0 | 322 | 110 | 168 | 0.54 | 6.95 | 79.5 |

Table 3.11: Results of potentiodynamic polarization studies for the corrosion of welded maraging steel in 2.0 M hydrochloric acid containing different concentrations of BTPO.

| Temperature (°C) | Conc. of inhibitor (mM) | $-E_{corr}$ (mV /SCE) | b_a (mV dec ⁻¹) | $-b_c$ (mV dec ⁻¹) | i_{corr} (mA cm ⁻²) | ν_{corr} (mm y ⁻¹) | η (%) |
|------------------|-------------------------|-----------------------|-------------------------------|--------------------------------|-----------------------------------|------------------------------------|------------|
| 30 | Blank | 324 | 114 | 178 | 0.90 | 11.60 | |
| | 0.2 | 328 | 107 | 152 | 0.22 | 2.89 | 75.1 |
| | 0.4 | 315 | 105 | 149 | 0.19 | 2.45 | 78.9 |
| | 0.6 | 309 | 101 | 144 | 0.18 | 2.29 | 80.3 |
| | 0.8 | 321 | 98 | 146 | 0.12 | 1.40 | 86.7 |
| | 1.0 | 330 | 97 | 141 | 0.10 | 1.13 | 88.9 |
| | 35 | Blank | 316 | 129 | 186 | 1.34 | 17.27 |
| 0.2 | | 331 | 124 | 163 | 0.34 | 4.44 | 74.3 |
| 0.4 | | 326 | 121 | 159 | 0.32 | 4.18 | 75.8 |
| 0.6 | | 337 | 118 | 155 | 0.29 | 3.78 | 78.1 |
| 0.8 | | 343 | 114 | 153 | 0.25 | 3.21 | 81.4 |
| 1.0 | | 351 | 112 | 147 | 0.21 | 2.66 | 84.6 |
| 40 | | Blank | 310 | 137 | 193 | 2.61 | 33.64 |
| | 0.2 | 312 | 126 | 171 | 0.78 | 10.03 | 70.2 |
| | 0.4 | 324 | 122 | 168 | 0.73 | 9.39 | 72.1 |
| | 0.6 | 329 | 118 | 164 | 0.63 | 8.18 | 75.7 |
| | 0.8 | 340 | 115 | 161 | 0.52 | 6.66 | 80.2 |
| | 1.0 | 335 | 111 | 154 | 0.45 | 5.82 | 82.7 |
| | 45 | Blank | 327 | 143 | 212 | 4.46 | 57.49 |
| 0.2 | | 315 | 129 | 187 | 1.38 | 17.76 | 69.1 |
| 0.4 | | 310 | 122 | 183 | 1.27 | 16.50 | 71.3 |
| 0.6 | | 321 | 124 | 182 | 1.15 | 14.78 | 74.3 |
| 0.8 | | 332 | 121 | 177 | 0.92 | 11.84 | 79.4 |
| 1.0 | | 317 | 115 | 172 | 0.82 | 10.58 | 81.6 |
| 50 | | Blank | 332 | 159 | 223 | 5.93 | 76.44 |
| | 0.2 | 324 | 134 | 191 | 1.99 | 25.68 | 66.4 |
| | 0.4 | 312 | 130 | 188 | 1.78 | 22.78 | 70.2 |
| | 0.6 | 319 | 126 | 183 | 1.59 | 20.49 | 73.2 |
| | 0.8 | 327 | 123 | 181 | 1.48 | 19.26 | 74.8 |
| | 1.0 | 321 | 120 | 174 | 1.29 | 16.59 | 78.3 |

Table 3.12: EIS data for the corrosion of welded maraging steel in 0.1 M hydrochloric acid containing different concentrations of BTPO.

| Temperature (°C) | Conc. of inhibitor (mM) | R_p (ohm. cm ²) | C_{dl} (mF cm ⁻²) | η (%) |
|------------------|-------------------------|-------------------------------|---------------------------------|------------|
| 30 | Blank | 80.6 | 0.061 | |
| | 0.2 | 465.9 | 0.046 | 82.7 |
| | 0.4 | 530.3 | 0.044 | 84.8 |
| | 0.6 | 688.9 | 0.040 | 88.3 |
| | 0.8 | 1168.3 | 0.038 | 93.0 |
| | 1.0 | 1366.1 | 0.035 | 94.1 |
| 35 | Blank | 71.8 | 0.069 | |
| | 0.2 | 394.5 | 0.043 | 81.8 |
| | 0.4 | 415.0 | 0.041 | 82.7 |
| | 0.6 | 502.1 | 0.037 | 85.7 |
| | 0.8 | 697.1 | 0.032 | 89.6 |
| | 1.0 | 834.9 | 0.027 | 91.4 |
| 40 | Blank | 56.4 | 0.135 | |
| | 0.2 | 272.5 | 0.127 | 79.3 |
| | 0.4 | 306.5 | 0.123 | 81.6 |
| | 0.6 | 346.0 | 0.118 | 83.7 |
| | 0.8 | 447.6 | 0.114 | 87.4 |
| | 1.0 | 547.6 | 0.107 | 89.7 |
| 45 | Blank | 41.3 | 0.183 | |
| | 0.2 | 193.9 | 0.161 | 78.7 |
| | 0.4 | 209.6 | 0.154 | 80.3 |
| | 0.6 | 269.9 | 0.152 | 84.7 |
| | 0.8 | 322.7 | 0.148 | 87.2 |
| | 1.0 | 378.9 | 0.141 | 89.1 |
| 50 | Blank | 34.5 | 0.224 | |
| | 0.2 | 159.7 | 0.201 | 78.4 |
| | 0.4 | 170.8 | 0.193 | 79.8 |
| | 0.6 | 194.9 | 0.189 | 82.3 |
| | 0.8 | 231.5 | 0.182 | 85.1 |
| | 1.0 | 263.6 | 0.180 | 86.9 |

Table 3.13: EIS data for the corrosion of welded maraging steel in 0.5 M hydrochloric acid containing different concentrations of BTPO.

| Temperature (°C) | Conc. of inhibitor (mM) | R_p (ohm. cm ²) | C_{dl} (mF cm ⁻²) | η (%) |
|------------------|-------------------------|-------------------------------|---------------------------------|------------|
| 30 | Blank | 73.8 | 0.071 | |
| | 0.2 | 386.4 | 0.058 | 80.9 |
| | 0.4 | 426.6 | 0.050 | 82.7 |
| | 0.6 | 542.6 | 0.046 | 86.4 |
| | 0.8 | 1011.0 | 0.041 | 92.7 |
| | 1.0 | 1118.2 | 0.035 | 93.4 |
| 35 | Blank | 55.4 | 0.112 | |
| | 0.2 | 272.9 | 0.104 | 79.7 |
| | 0.4 | 285.6 | 0.097 | 80.6 |
| | 0.6 | 333.7 | 0.090 | 83.4 |
| | 0.8 | 490.3 | 0.083 | 88.7 |
| | 1.0 | 571.1 | 0.077 | 90.3 |
| 40 | Blank | 47.1 | 0.165 | |
| | 0.2 | 208.4 | 0.141 | 77.4 |
| | 0.4 | 221.1 | 0.134 | 78.7 |
| | 0.6 | 266.1 | 0.127 | 82.3 |
| | 0.8 | 343.8 | 0.121 | 86.3 |
| | 1.0 | 395.8 | 0.115 | 88.1 |
| 45 | Blank | 38.0 | 0.216 | |
| | 0.2 | 153.2 | 0.174 | 75.2 |
| | 0.4 | 211.1 | 0.169 | 82.0 |
| | 0.6 | 207.7 | 0.161 | 81.7 |
| | 0.8 | 265.6 | 0.154 | 85.7 |
| | 1.0 | 296.9 | 0.149 | 87.2 |
| 50 | Blank | 29.6 | 0.279 | |
| | 0.2 | 117.5 | 0.231 | 74.8 |
| | 0.4 | 129.3 | 0.223 | 77.1 |
| | 0.6 | 149.5 | 0.217 | 80.2 |
| | 0.8 | 178.3 | 0.212 | 83.4 |
| | 1.0 | 202.7 | 0.204 | 85.4 |

Table 3.14: EIS data for the corrosion of welded maraging steel in 1.0 M hydrochloric acid containing different concentrations of BTPO.

| Temperature (°C) | Conc. of inhibitor (mM) | R_p (ohm. cm ²) | C_{dl} (mF cm ⁻²) | η (%) |
|------------------|-------------------------|-------------------------------|---------------------------------|------------|
| 30 | Blank | 56.1 | 0.110 | |
| | 0.2 | 256.2 | 0.091 | 78.1 |
| | 0.4 | 309.0 | 0.087 | 81.8 |
| | 0.6 | 352.9 | 0.080 | 84.1 |
| | 0.8 | 702.1 | 0.071 | 92.0 |
| | 1.0 | 787.3 | 0.063 | 92.9 |
| 35 | Blank | 43.2 | 0.203 | |
| | 0.2 | 194.6 | 0.175 | 77.8 |
| | 0.4 | 200.0 | 0.168 | 78.4 |
| | 0.6 | 237.4 | 0.162 | 81.8 |
| | 0.8 | 345.6 | 0.157 | 87.5 |
| | 1.0 | 407.5 | 0.151 | 89.4 |
| 40 | Blank | 32.9 | 0.276 | |
| | 0.2 | 132.7 | 0.224 | 75.2 |
| | 0.4 | 145.6 | 0.219 | 77.4 |
| | 0.6 | 170.5 | 0.212 | 80.7 |
| | 0.8 | 215.0 | 0.208 | 84.8 |
| | 1.0 | 247.4 | 0.201 | 86.7 |
| 45 | Blank | 30.6 | 0.308 | |
| | 0.2 | 104.8 | 0.252 | 70.8 |
| | 0.4 | 121.3 | 0.247 | 74.7 |
| | 0.6 | 136.4 | 0.239 | 77.6 |
| | 0.8 | 172.3 | 0.238 | 82.2 |
| | 1.0 | 190.1 | 0.229 | 83.9 |
| 50 | Blank | 20.2 | 0.346 | |
| | 0.2 | 63.1 | 0.282 | 68.0 |
| | 0.4 | 75.2 | 0.277 | 73.1 |
| | 0.6 | 80.3 | 0.274 | 74.9 |
| | 0.8 | 90.6 | 0.269 | 77.7 |
| | 1.0 | 105.8 | 0.251 | 80.9 |

Table 3.15: EIS data for the corrosion of welded maraging steel in 1.5 M hydrochloric acid containing different concentrations of BTPO.

| Temperature (°C) | Conc. of inhibitor (mM) | R_p (ohm. cm ²) | C_{dl} (mF cm ⁻²) | η (%) |
|------------------|-------------------------|-------------------------------|---------------------------------|------------|
| 30 | Blank | 49.2 | 0.166 | |
| | 0.2 | 213.0 | 0.130 | 76.9 |
| | 0.4 | 242.4 | 0.129 | 79.7 |
| | 0.6 | 257.6 | 0.123 | 80.9 |
| | 0.8 | 456.6 | 0.119 | 89.2 |
| | 1.0 | 630.8 | 0.114 | 92.2 |
| | 35 | Blank | 30.6 | 0.315 |
| 0.2 | | 119.5 | 0.244 | 74.4 |
| 0.4 | | 125.9 | 0.240 | 75.7 |
| 0.6 | | 147.8 | 0.238 | 79.3 |
| 0.8 | | 193.7 | 0.231 | 84.2 |
| 1.0 | | 214.0 | 0.221 | 85.7 |
| 40 | | Blank | 24.5 | 0.378 |
| | 0.2 | 89.7 | 0.281 | 72.7 |
| | 0.4 | 95.0 | 0.274 | 74.2 |
| | 0.6 | 115.6 | 0.267 | 78.8 |
| | 0.8 | 147.6 | 0.260 | 83.4 |
| | 1.0 | 167.8 | 0.253 | 85.4 |
| | 45 | Blank | 19.1 | 0.395 |
| 0.2 | | 62.6 | 0.294 | 69.5 |
| 0.4 | | 71.8 | 0.289 | 73.4 |
| 0.6 | | 77.0 | 0.281 | 75.2 |
| 0.8 | | 104.4 | 0.274 | 81.7 |
| 1.0 | | 115.1 | 0.269 | 83.4 |
| 50 | | Blank | 14.2 | 0.402 |
| | 0.2 | 43.3 | 0.311 | 67.2 |
| | 0.4 | 49.5 | 0.293 | 71.3 |
| | 0.6 | 61.5 | 0.288 | 75.4 |
| | 0.8 | 69.3 | 0.281 | 76.9 |
| | 1.0 | 57.7 | 0.272 | 79.5 |

Table 3.16: EIS data for the corrosion of welded maraging steel in 2.0 M hydrochloric acid containing different concentrations of BTPO.

| Temperature (°C) | Conc. of inhibitor (mM) | R_p (ohm. cm ²) | C_{dl} (mF cm ⁻²) | η (%) |
|------------------|-------------------------|-------------------------------|---------------------------------|------------|
| 30 | Blank | 33.6 | 0.248 | |
| | 0.2 | 133.3 | 0.194 | 74.8 |
| | 0.4 | 148.7 | 0.189 | 77.4 |
| | 0.6 | 166.3 | 0.183 | 79.8 |
| | 0.8 | 260.5 | 0.175 | 87.1 |
| | 1.0 | 377.5 | 0.167 | 91.1 |
| 35 | Blank | 24.5 | 0.362 | |
| | 0.2 | 93.5 | 0.270 | 73.8 |
| | 0.4 | 96.1 | 0.263 | 74.5 |
| | 0.6 | 103.8 | 0.257 | 76.4 |
| | 0.8 | 130.3 | 0.247 | 81.2 |
| | 1.0 | 145.8 | 0.240 | 83.2 |
| 40 | Blank | 13.3 | 0.399 | |
| | 0.2 | 47.2 | 0.283 | 71.8 |
| | 0.4 | 45.7 | 0.279 | 72.9 |
| | 0.6 | 51.0 | 0.272 | 75.8 |
| | 0.8 | 66.8 | 0.263 | 80.1 |
| | 1.0 | 83.6 | 0.257 | 84.1 |
| 45 | Blank | 8.3 | 0.418 | |
| | 0.2 | 26.5 | 0.312 | 68.7 |
| | 0.4 | 28.8 | 0.301 | 71.2 |
| | 0.6 | 31.2 | 0.297 | 73.4 |
| | 0.8 | 40.3 | 0.281 | 79.4 |
| | 1.0 | 45.1 | 0.274 | 81.6 |
| 50 | Blank | 6.8 | 0.439 | |
| | 0.2 | 20.2 | 0.311 | 66.4 |
| | 0.4 | 22.6 | 0.303 | 69.9 |
| | 0.6 | 25.4 | 0.292 | 73.2 |
| | 0.8 | 26.5 | 0.287 | 74.2 |
| | 1.0 | 30.2 | 0.271 | 77.5 |

Table 3.17: Activation parameters for the corrosion of welded maraging steel in hydrochloric acid containing different concentrations of BTPO.

| Molarity of HCl (M) | Conc. of inhibitor (mM) | E_a (kJ mol ⁻¹) | ΔH^\ddagger (kJ mol ⁻¹) | ΔS^\ddagger (J mol ⁻¹ K ⁻¹) |
|------------------------|----------------------------|----------------------------------|--|---|
| 0.1 | Blank | 42.28 | 39.62 | -103.29 |
| | 0.2 | 54.89 | 52.29 | -76.77 |
| | 0.4 | 54.95 | 52.35 | -77.35 |
| | 0.6 | 63.21 | 60.61 | -52.91 |
| | 0.8 | 70.82 | 68.22 | -30.55 |
| | 1.0 | 77.40 | 74.80 | -11.09 |
| 0.5 | Blank | 42.97 | 39.37 | -102.37 |
| | 0.2 | 55.71 | 53.11 | -71.04 |
| | 0.4 | 56.45 | 53.85 | -69.62 |
| | 0.6 | 60.99 | 58.39 | -58.39 |
| | 0.8 | 74.11 | 71.50 | -17.41 |
| | 1.0 | 75.87 | 73.27 | -13.02 |
| 1.0 | Blank | 47.51 | 44.97 | -81.34 |
| | 0.2 | 64.06 | 61.46 | -39.69 |
| | 0.4 | 64.93 | 62.33 | -38.19 |
| | 0.6 | 66.98 | 64.18 | -33.37 |
| | 0.8 | 89.11 | 86.47 | -15.13 |
| | 1.0 | 90.02 | 87.42 | -16.71 |
| 1.5 | Blank | 59.37 | 56.78 | -40.52 |
| | 0.2 | 58.31 | 57.69 | -33.61 |
| | 0.4 | 59.58 | 60.98 | -26.85 |
| | 0.6 | 63.07 | 61.47 | -21.51 |
| | 0.8 | 86.87 | 84.09 | -19.89 |
| | 1.0 | 87.88 | 84.28 | -11.34 |
| 2.0 | Blank | 80.98 | 78.36 | -33.72 |
| | 0.2 | 53.73 | 50.13 | -24.23 |
| | 0.4 | 55.07 | 52.47 | -17.72 |
| | 0.6 | 60.62 | 59.03 | -14.16 |
| | 0.8 | 71.60 | 68.16 | -10.31 |
| | 1.0 | 79.15 | 78.55 | -8.79 |

Table 3.18: Maximum inhibition efficiency attained in different concentrations of hydrochloric acid at different temperatures for BTPO.

| Temperature (°C) | Welded Maraging Steel | | | |
|---------------------|--|----------------------------------|---|------------|
| | Hydrochloric acid concentration (M) | Concentration of BTPO (mM) | η (%) | |
| | | | Potentiodynamic polarization method | EIS method |
| 30 | 0.1 | 1.0 | 96.8 | 94.0 |
| | 0.5 | | 93.3 | 93.4 |
| | 1.0 | | 93.1 | 93.0 |
| | 1.5 | | 91.8 | 92.2 |
| | 2.0 | | 90.3 | 91.1 |
| 35 | 0.1 | 1.0 | 91.7 | 91.4 |
| | 0.5 | | 91.5 | 90.3 |
| | 1.0 | | 91.2 | 89.4 |
| | 1.5 | | 87.9 | 85.7 |
| | 2.0 | | 84.6 | 83.2 |
| 40 | 0.1 | 1.0 | 91.3 | 89.7 |
| | 0.5 | | 90.0 | 88.1 |
| | 1.0 | | 88.4 | 86.7 |
| | 1.5 | | 86.3 | 85.4 |
| | 2.0 | | 82.7 | 84.1 |
| 45 | 0.1 | 1.0 | 89.4 | 89.1 |
| | 0.5 | | 87.0 | 87.2 |
| | 1.0 | | 84.1 | 83.9 |
| | 1.5 | | 83.4 | 83.4 |
| | 2.0 | | 81.6 | 81.2 |
| 50 | 0.1 | 1.0 | 86.7 | 86.9 |
| | 0.5 | | 85.4 | 85.4 |
| | 1.0 | | 81.1 | 80.9 |
| | 1.5 | | 79.5 | 79.4 |
| | 2.0 | | 78.3 | 77.5 |

Table 3.19: Thermodynamic parameters for the adsorption of BTPO on welded maraging steel surface in hydrochloric acid at different temperatures.

| Molarity of HCl (M) | Temperature (° C) | $-\Delta G^{\circ}_{ads}$ (kJ mol ⁻¹) | ΔH°_{ads} (kJ mol ⁻¹) | ΔS°_{ads} (J mol ⁻¹ K ⁻¹) |
|------------------------|----------------------|--|---|--|
| 0.1 | 30 | 35.11 | -27.62 | -123.44 |
| | 35 | 34.85 | | |
| | 40 | 34.67 | | |
| | 45 | 34.59 | | |
| | 50 | 34.45 | | |
| 0.5 | 30 | 34.59 | -30.58 | -112.23 |
| | 35 | 34.30 | | |
| | 40 | 34.23 | | |
| | 45 | 34.05 | | |
| | 50 | 33.92 | | |
| 1.0 | 30 | 34.12 | - 38.21 | -113.08 |
| | 35 | 33.98 | | |
| | 40 | 33.83 | | |
| | 45 | 33.71 | | |
| | 50 | 33.37 | | |
| 1.5 | 30 | 33.95 | -30.02 | -128.61 |
| | 35 | 33.76 | | |
| | 40 | 33.68 | | |
| | 45 | 33.47 | | |
| | 50 | 33.24 | | |
| 2.0 | 30 | 33.82 | -30.73 | -110.59 |
| | 35 | 33.70 | | |
| | 40 | 33.62 | | |
| | 45 | 33.47 | | |
| | 50 | 33.40 | | |

3.4 2,5-BIS(3,4,5-TRIMETHOXYPHENYL)-1,3,4-OXADIAZOLE (BTPO) AS INHIBITOR FOR THE CORROSION OF WELDED MARAGING STEEL IN SULPHURIC ACID MEDIUM

3.4.1 Potentiodynamic polarization measurements

The potentiodynamic polarization curves for the corrosion of welded maraging steel in 1.0 M sulphuric acid in the presence of different concentrations of BTPO, at 30 °C are shown in Fig. 3.27. Similar results were obtained at other temperatures and also in the other four concentrations of sulphuric acid. The potentiodynamic polarization parameters such as corrosion potential (E_{corr}), corrosion current density (i_{corr}), anodic and cathodic Tafel slopes (b_a , b_c) were calculated from the Tafel plots in the presence of different concentrations of BTPO at different temperatures are summarized in Tables 3.20 to 3.24.

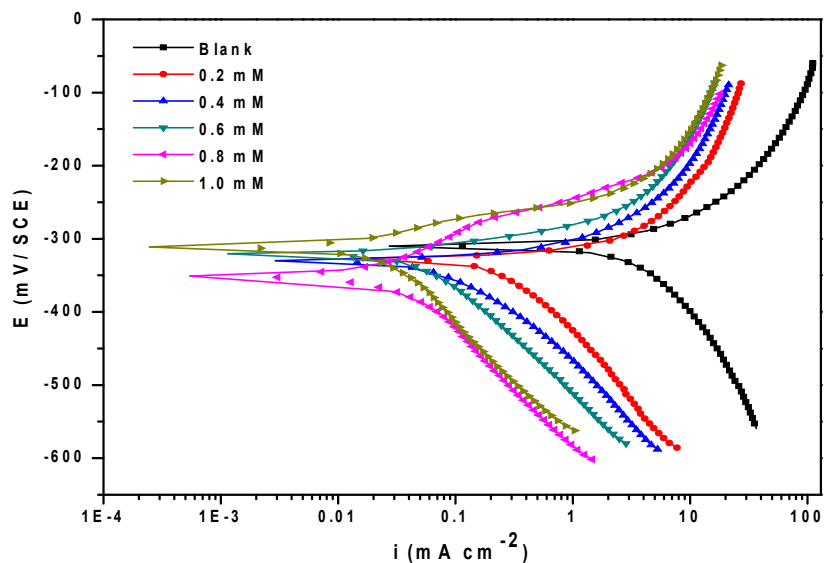


Fig. 3.27: Potentiodynamic polarization curves for the corrosion of welded maraging steel in 1.0 M sulphuric acid containing different concentrations of BTPO at 30 °C.

The presence of inhibitor brings down the corrosion rate considerably. Polarization curves are shifted to a lower current density region indicating a decrease in the corrosion rate (Li et al. 2007). Inhibition efficiency increases with the increase in

BTPO concentration. The presence of inhibitor does not cause more than 38 mV shift in the E_{corr} value and also the shift does not show any regular trend in the cathodic or anodic direction. This implies that the inhibitor, BTPO, acts as a mixed type inhibitor, affecting both metal dissolution and hydrogen evolution reactions.

3.4.2 Electrochemical impedance spectroscopy (EIS) studies

Nyquist plots for the corrosion of welded maraging steel in 1.0 M sulphuric acid solution in the presence of different concentrations of BTPO are shown in Fig. 3.28. Similar plots were obtained in other concentrations of sulphuric acid and also at other temperatures. The experimental results of EIS measurements obtained for the corrosion of welded maraging steel in 1.0 M sulphuric acid are summarized in Tables 3.25 to 3.29.

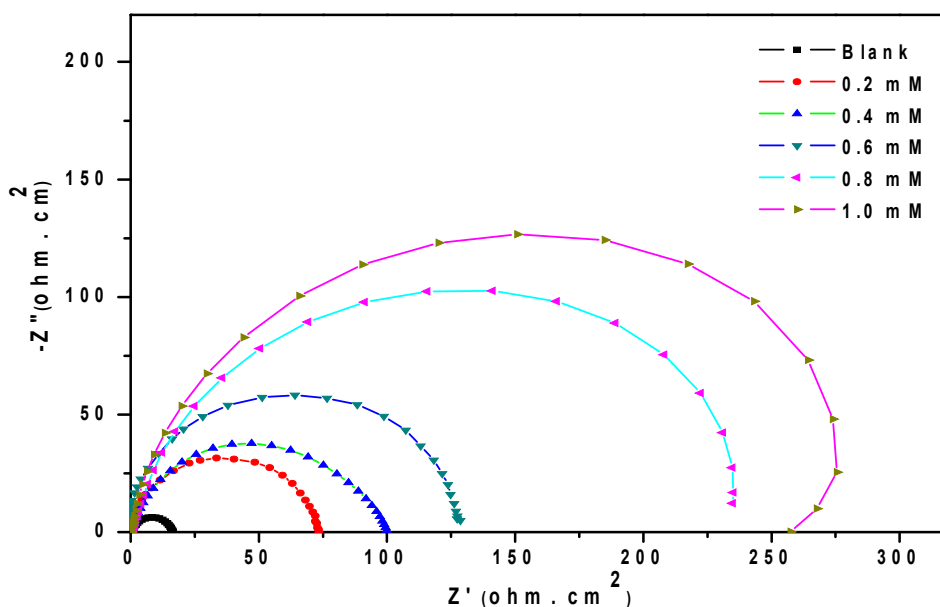


Fig. 3.28: Nyquist plots for the corrosion of welded maraging steel in 1.0 M H_2SO_4 containing different concentrations of BTPO at 30 °C.

As seen from Fig. 3.28 the Nyquist plots are semi-circular in the presence as well as in the absence of inhibitor. This indicates that the corrosion of welded maraging steel is controlled by a charge transfer process and the addition of BTPO does not change the

reaction mechanism of the corrosion of sample in H_2SO_4 solution (Amin et al. 2007). The charge transfer resistance (R_{ct}) increases and double layer capacitance decreases with the increase in the concentration of BTPO, indicating an increase in the inhibition efficiency. BTPO inhibits the corrosion primarily through its adsorption and subsequent formation of a barrier film on the metal surface (El Hosary et al. 1972, Sanaa et al. 2008). This is in accordance with the observations of Tafel polarization measurements. The equivalent circuit models shown in Fig. 3.29 is used for the interpretation of the Nyquist plots in the presence of BTPO. It consists of a solution resistance (R_s), constant phase element (Q), charge transfer resistance (R_{ct}), film resistance (R_f) and film capacitance (C_f). The film resistance and film capacitance arises due to the formation of BTPO film on the alloy surface on its adsorption.

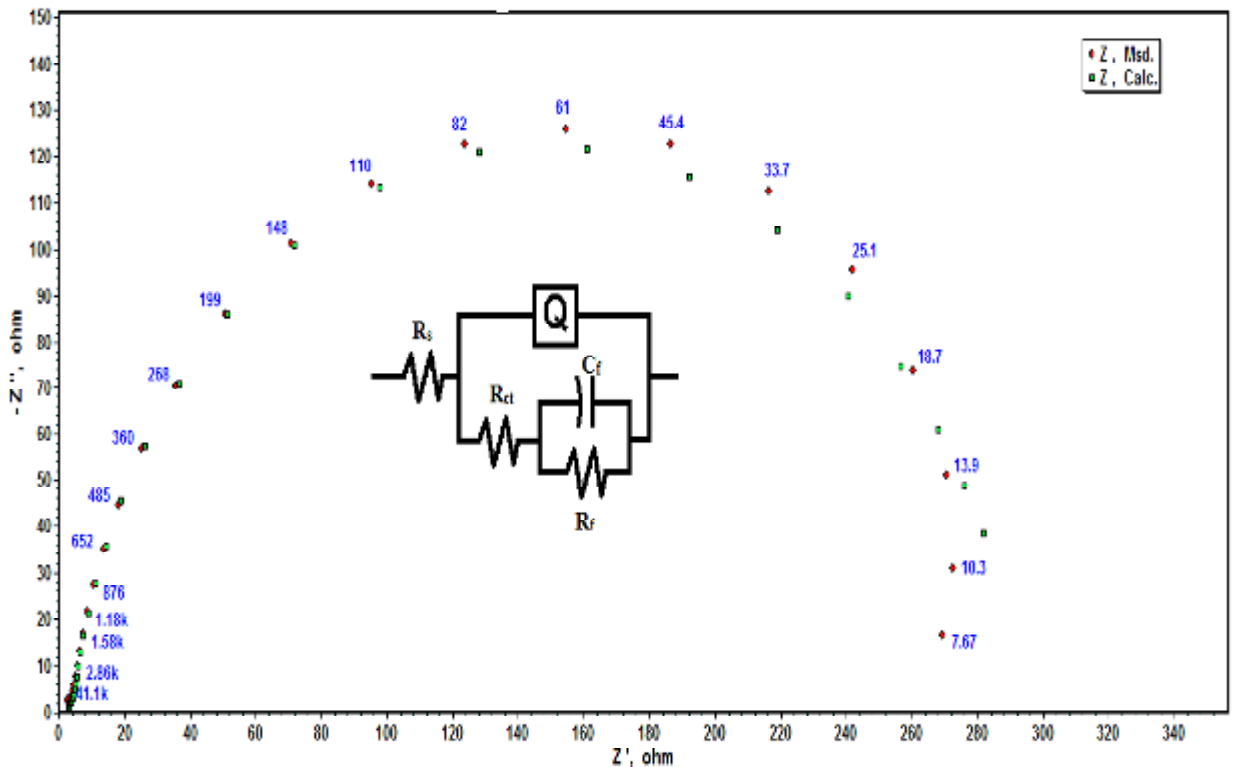


Fig. 3.29: Equivalent circuit used to fit the experimental EIS data for the corrosion of welded maraging steel in 1.0 M H_2SO_4 at 30 °C in the presence of BTPO.

The Bode plots of phase angle and amplitude for the corrosion of the alloy in 1.0 M sulphuric acid at 30 °C in the presence of BTPO are shown in Fig. 3.30 (a) and Fig. 3.30 (b), respectively. Phase angle increases with increase in concentrations of BTPO in sulphuric acid medium. The difference between the HF and LF for the inhibited system in the Bode plot increases with increase in the concentration of BTPO. The increase in phase angle with the increase in BTPO concentration suggests decrease in corrosion rate. An increase in BTPO concentration leads to an increase in the $|Z|$ value.

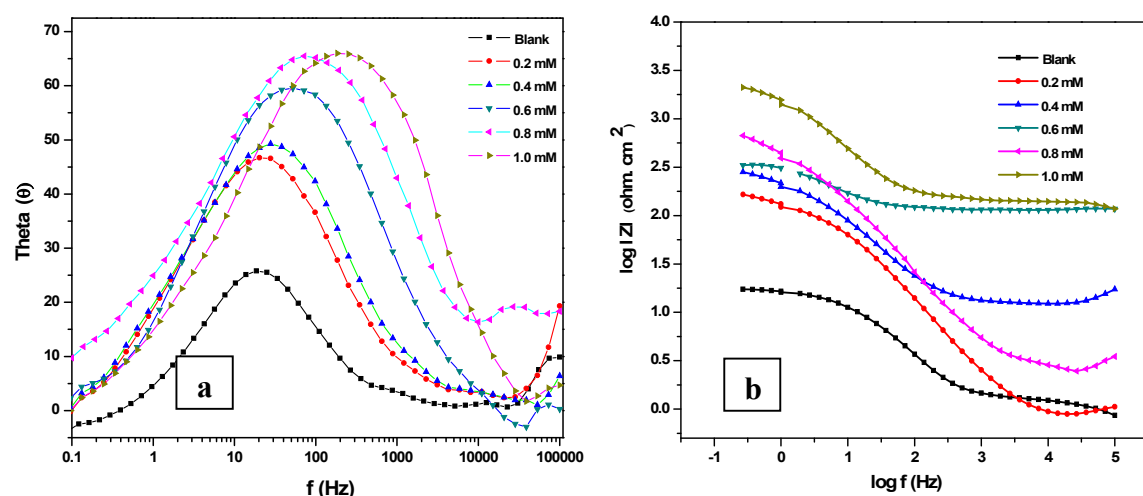


Fig. 3.30: Bode (a) phase angle plots and (b) amplitude plots for the corrosion of welded maraging steel in 1.0 M H₂SO₄ containing different concentrations of BTPO at 30 °C.

3.4.3 Effect of temperature

The potentiodynamic polarization and EIS results pertaining to different temperatures in different concentrations of sulphuric acid have been listed in the Tables 3.20 to 3.29. The decrease in inhibition efficiency with the increase in temperature indicates desorption of the inhibitor molecules from the metal surface on increasing the temperature (Poornima et al. 2011). This fact is also suggestive of physisorption of the inhibitor molecules on the metal surface.

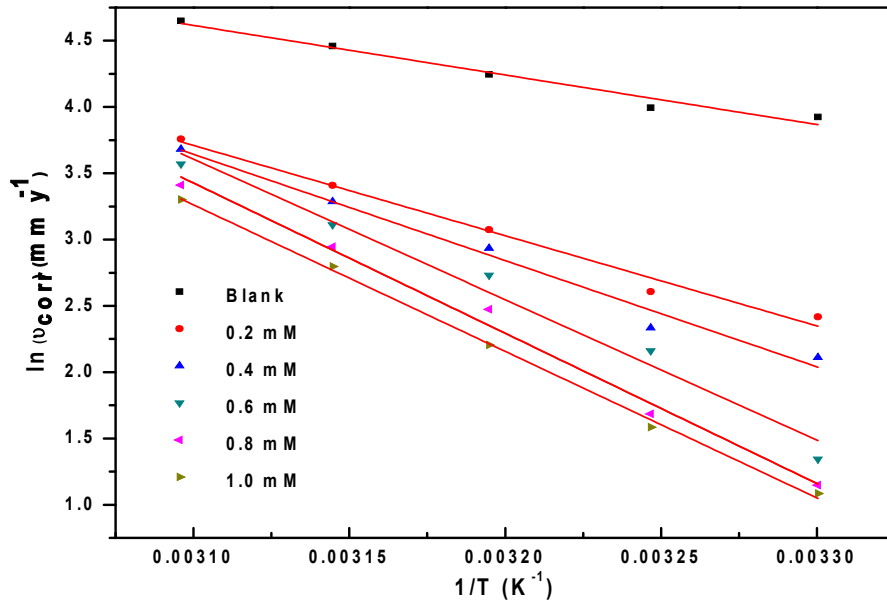


Fig. 3.31: Arrhenius plots for the corrosion of welded maraging steel in 1.0 M H₂SO₄ containing different concentrations of BTPO.

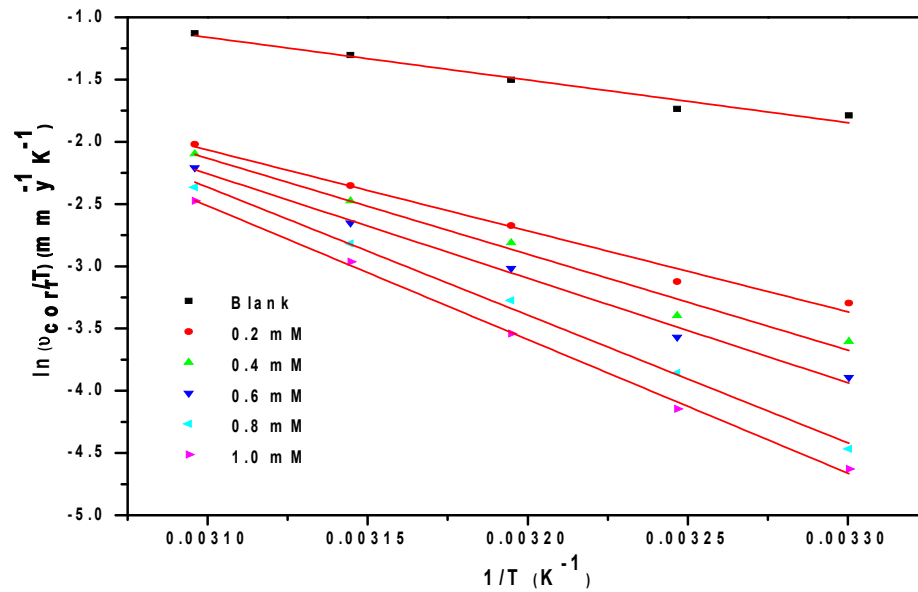


Fig. 3.32: Plots of $\ln(v_{corr}/T)$ versus $1/T$ for the corrosion of welded maraging steel in 1.0 M H₂SO₄ containing different concentrations of BTPO.

The Arrhenius plots for the corrosion of welded maraging steel in the presence of different concentrations of BTPO in 1.0 M H₂SO₄ acid are shown in Fig. 3.31. The plots of $\ln(i_{\text{corr}}/T)$ versus $1/T$ in 1.0 M H₂SO₄ in the absence and presence of various concentrations of BTPO are shown in Fig. 3.32. The calculated values of E_a , ΔH^\ddagger and ΔS^\ddagger are given in Table 3.30. The proportionate increase in the activation energy on the addition of BTPO can be attributed to the increased adsorption of BTPO providing a barrier on the alloy surface (Avci et al. 2008).

The values of entropy of activation indicates that the activated complex in the rate determining step represents an association rather than dissociation, resulting in a decrease in randomness on going from the reactants to the activated complex.

3.4.4 Effect of sulphuric acid concentration

Tables 3.31 summarises the maximum inhibition efficiencies exhibited by BTPO in the H₂SO₄ solutions of different concentrations at different temperatures. It is evident from both polarization and EIS experimental results that for a particular concentration of inhibitor, the inhibition efficiency decreases with the increase in sulphuric acid concentration on the welded maraging steel. The highest inhibition efficiency is observed in sulphuric acid of 0.1 M concentration.

3.4.5 Adsorption isotherm

The adsorption of BTPO on the surface of welded maraging steel was found to obey Langmuir adsorption isotherm. The Langmuir adsorption isotherms for the adsorption of BTPO on welded maraging steel in 1.0 M H₂SO₄ are shown in Fig. 3.33. The linear regression coefficients are close to unity and the slopes of the straight lines are nearly unity, suggesting that the adsorption of BTPO obeys Langmuir's adsorption isotherm with negligible interaction between the adsorbed molecules. The thermodynamic data obtained for the adsorption of BTPO on welded maraging steel in sulphuric acid are tabulated in Table 3.32. The exothermic ΔH_{ads}^0 values of less than $-41.86 \text{ kJ mol}^{-1}$ predict physisorption of BTPO on the alloy surfaces (Ashish Kumar et al. 2010). The ΔG_{ads}^0 values predict both physisorption and chemisorption of BTPO.

Therefore it can be concluded that the adsorption of BTPO on the welded maraging steel is predominantly through physisorption. These facts are also supported by the decrease in inhibition efficiencies with the increase in temperature as discussed under section 3.4.3.

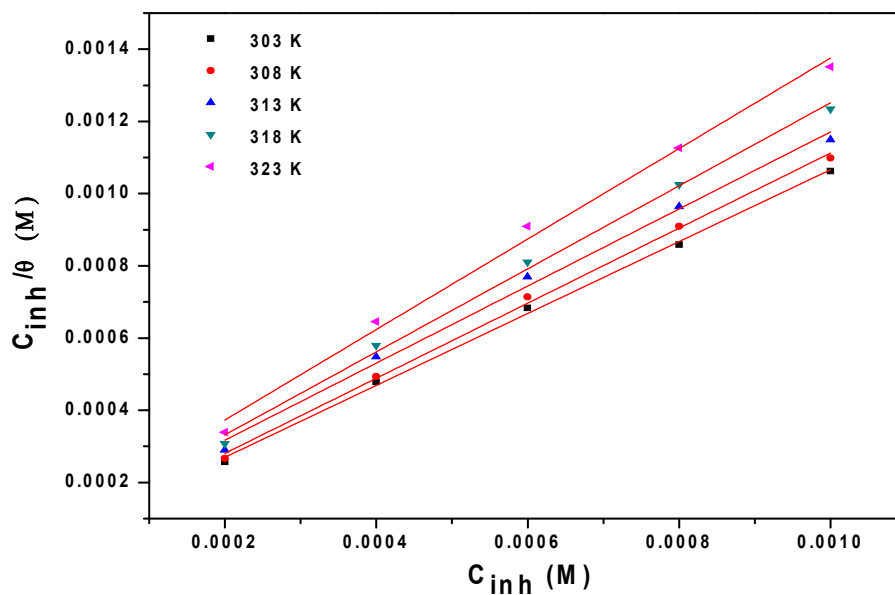


Fig. 3.33: Langmuir adsorption isotherms for the adsorption of BTPO on welded maraging steel in 1.0 M H₂SO₄ at different temperatures.

3.4.6 Mechanism of corrosion inhibition

The corrosion inhibition mechanism of BTPO in sulphuric acid solution can be explained in the same lines as that of BTPO in the section 3.3.6. The inhibitor BTPO protects the alloy surface through predominant physisorption mode in which the positive charge centers of BTPO gets adsorbed on the sulphate ion adsorbed alloy surface and the negative charge centres of BTPO gets adsorbed on positively charged blank alloy surfaces through electrostatic attraction. The protection is also to some extent through chemisorption mode involving neutral BTPO molecules as discussed in the section 3.3.6.

3.4.7 SEM/EDX studies

Fig. 3.34 (a) represents the SEM image of the corroded welded maraging steel sample. The corroded surface shows detachment of particles from the surface. The

corrosion of the alloy may be predominantly attributed to the inter-granular corrosion assisted by the galvanic effect between the precipitates and the matrix along the grain boundaries. Fig. 3.34 (b) represents the SEM image of welded maraging steel after the corrosion tests in a medium of sulphuric acid containing 1.0 mM of BTPO. The image clearly shows a smooth surface due to the adsorbed layer of inhibitor molecules on the alloy surface, thus protecting the metal from corrosion.

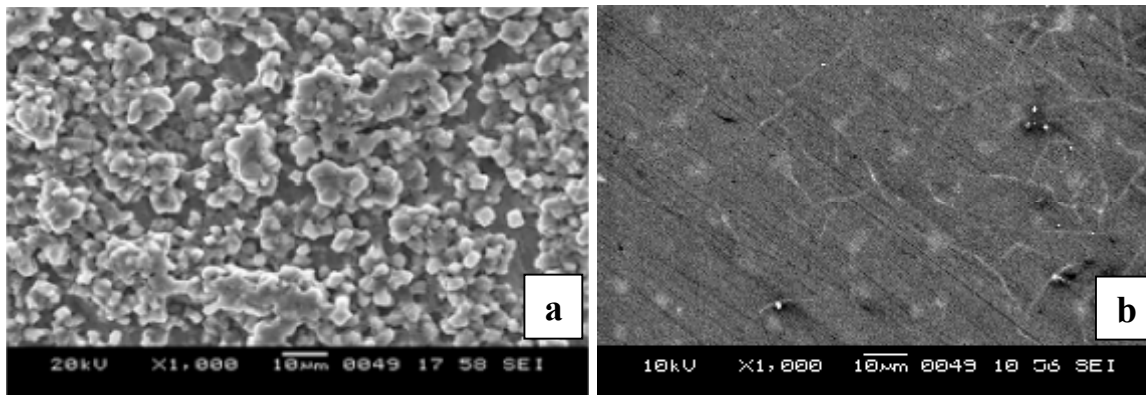


Fig.3.34: SEM images of the welded maraging steel after immersion in 1.0 M H₂SO₄ (a) in the absence and (b) in the presence of BTPO.

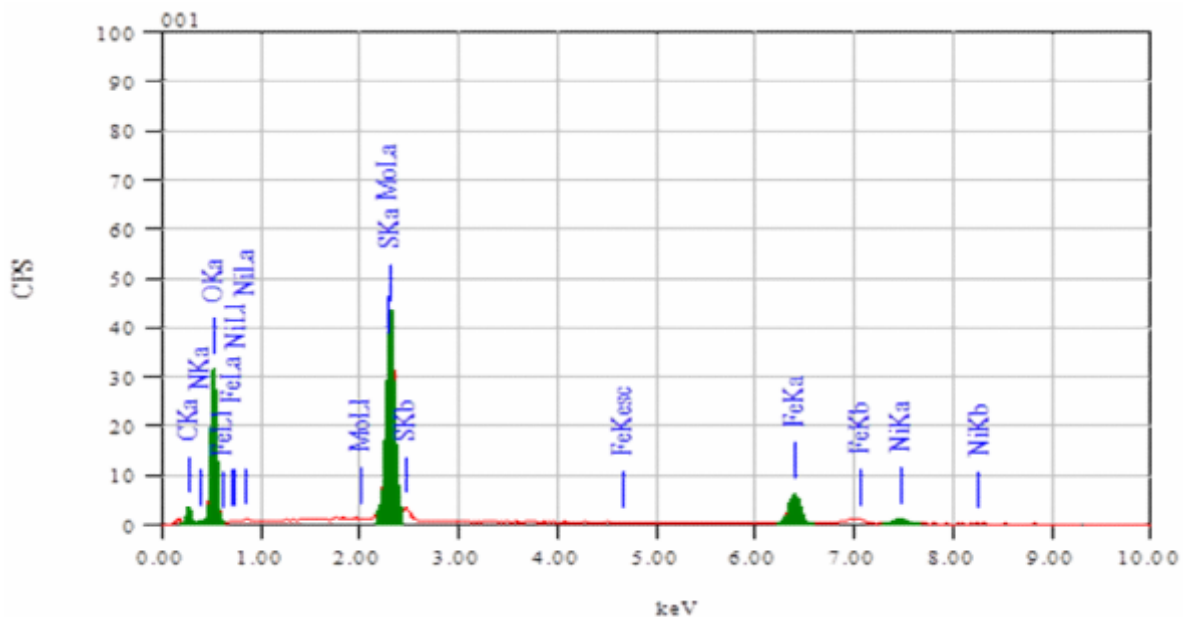


Fig. 3.35: EDX spectra of the welded maraging steel after immersion in 1.0 M H₂SO₄ in the presence of BTPO.

EDX spectral investigations were carried out in order to identify the composition of the species formed on the metal surface in 1.0 M sulphuric acid in the absence and presence of BTPO. The atomic percentage of the elements found in the EDX spectra (Fig. 3.35) for inhibited metal surface was 4.07% Fe, 0.62% Ni, 1.85% Mo, 52.90% O, 1.03% N, 34.21% C and 5.31% S and indicated the formation of inhibitor film on the surface of the alloy. The elemental compositions mentioned above were mean values of different regions.

Table 3.20: Results of potentiodynamic polarization studies for the corrosion of welded maraging steel in 0.1 M sulphuric acid containing different concentrations of BTPO.

| Temperature (°C) | Conc. of inhibitor (mM) | $-E_{corr}$ (mV /SCE) | b_a (mV dec ⁻¹) | $-b_c$ (mV dec ⁻¹) | i_{corr} (mA cm ⁻²) | U_{corr} (mm y ⁻¹) | η (%) |
|------------------|-------------------------|-----------------------|-------------------------------|--------------------------------|-----------------------------------|----------------------------------|------------|
| 30 | Blank | 356 | 162 | 113 | 1.98 | 25.52 | |
| | 0.2 | 351 | 121 | 104 | 0.37 | 4.78 | 81.2 |
| | 0.4 | 348 | 116 | 102 | 0.29 | 3.75 | 85.3 |
| | 0.6 | 357 | 113 | 99 | 0.23 | 2.90 | 88.6 |
| | 0.8 | 339 | 111 | 97 | 0.13 | 1.68 | 93.4 |
| | 1.0 | 324 | 109 | 94 | 0.10 | 1.32 | 94.8 |
| | 35 | Blank | 353 | 171 | 124 | 2.41 | 31.07 |
| 0.2 | | 348 | 138 | 118 | 0.52 | 6.74 | 78.3 |
| 0.4 | | 339 | 135 | 115 | 0.40 | 5.15 | 83.4 |
| 0.6 | | 323 | 129 | 113 | 0.34 | 4.44 | 85.7 |
| 0.8 | | 342 | 126 | 112 | 0.23 | 3.01 | 90.3 |
| 1.0 | | 361 | 124 | 109 | 0.17 | 2.20 | 92.9 |
| 40 | | Blank | 347 | 183 | 131 | 2.93 | 37.77 |
| | 0.2 | 339 | 151 | 127 | 0.75 | 9.63 | 74.5 |
| | 0.4 | 334 | 148 | 125 | 0.68 | 8.80 | 76.7 |
| | 0.6 | 342 | 144 | 123 | 0.57 | 7.44 | 80.3 |
| | 0.8 | 329 | 138 | 120 | 0.39 | 5.02 | 86.7 |
| | 1.0 | 312 | 135 | 119 | 0.31 | 4.04 | 89.3 |
| | 45 | Blank | 345 | 197 | 142 | 3.47 | 44.73 |
| 0.2 | | 325 | 164 | 131 | 1.09 | 14.00 | 68.7 |
| 0.4 | | 329 | 161 | 128 | 0.91 | 11.76 | 73.7 |
| 0.6 | | 352 | 158 | 126 | 0.79 | 10.15 | 77.3 |
| 0.8 | | 349 | 154 | 123 | 0.59 | 7.55 | 83.1 |
| 1.0 | | 312 | 151 | 119 | 0.51 | 6.61 | 85.2 |
| 50 | | Blank | 342 | 214 | 154 | 6.14 | 79.15 |
| | 0.2 | 328 | 187 | 139 | 2.10 | 26.67 | 66.3 |
| | 0.4 | 341 | 179 | 136 | 1.96 | 25.24 | 68.1 |
| | 0.6 | 337 | 171 | 132 | 1.81 | 23.26 | 70.6 |
| | 0.8 | 309 | 167 | 129 | 1.58 | 20.34 | 74.3 |
| | 1.0 | 323 | 161 | 124 | 1.09 | 18.04 | 82.5 |

Table 3.21: Results of potentiodynamic polarization studies for the corrosion of welded maraging steel in 0.5 M sulphuric acid containing different concentrations of BTPO.

| Temperature (°C) | Conc. of inhibitor (mM) | $-E_{corr}$ (mV /SCE) | b_a (mV dec ⁻¹) | $-b_c$ (mV dec ⁻¹) | i_{corr} (mA cm ⁻²) | U_{corr} (mm y ⁻¹) | η (%) |
|------------------|-------------------------|-----------------------|-------------------------------|--------------------------------|-----------------------------------|----------------------------------|------------|
| 30 | Blank | 322 | 172 | 115 | 2.47 | 31.84 | |
| | 0.2 | 319 | 139 | 109 | 0.48 | 6.24 | 80.4 |
| | 0.4 | 327 | 135 | 105 | 0.39 | 5.03 | 84.2 |
| | 0.6 | 338 | 132 | 102 | 0.29 | 3.78 | 88.1 |
| | 0.8 | 342 | 128 | 99 | 0.17 | 2.16 | 93.2 |
| | 1.0 | 298 | 126 | 97 | 0.14 | 1.78 | 94.4 |
| | 35 | Blank | 321 | 191 | 132 | 2.68 | 34.55 |
| 0.2 | | 337 | 152 | 121 | 0.62 | 7.98 | 76.9 |
| 0.4 | | 341 | 147 | 118 | 0.48 | 6.14 | 82.2 |
| 0.6 | | 316 | 143 | 115 | 0.40 | 5.21 | 84.9 |
| 0.8 | | 318 | 141 | 113 | 0.28 | 3.66 | 89.4 |
| 1.0 | | 327 | 139 | 110 | 0.22 | 2.86 | 91.7 |
| 40 | | Blank | 318 | 207 | 144 | 4.71 | 60.71 |
| | 0.2 | 329 | 171 | 129 | 1.32 | 16.93 | 72.1 |
| | 0.4 | 341 | 164 | 125 | 1.21 | 15.60 | 74.3 |
| | 0.6 | 338 | 158 | 122 | 1.01 | 12.99 | 78.6 |
| | 0.8 | 323 | 155 | 118 | 0.70 | 9.04 | 85.1 |
| | 1.0 | 309 | 152 | 116 | 0.55 | 7.04 | 88.4 |
| | 45 | Blank | 314 | 224 | 158 | 5.38 | 69.35 |
| 0.2 | | 319 | 187 | 145 | 1.76 | 22.74 | 67.2 |
| 0.4 | | 299 | 179 | 142 | 1.54 | 19.83 | 71.4 |
| 0.6 | | 308 | 173 | 138 | 1.30 | 16.78 | 75.8 |
| 0.8 | | 325 | 168 | 131 | 0.97 | 12.55 | 81.9 |
| 1.0 | | 328 | 165 | 129 | 0.89 | 11.51 | 83.4 |
| 50 | | Blank | 312 | 232 | 163 | 6.94 | 89.45 |
| | 0.2 | 318 | 191 | 154 | 2.47 | 31.84 | 64.4 |
| | 0.4 | 331 | 184 | 151 | 2.48 | 31.93 | 64.3 |
| | 0.6 | 342 | 179 | 148 | 1.51 | 19.41 | 78.3 |
| | 0.8 | 329 | 175 | 146 | 1.85 | 23.79 | 73.4 |
| | 1.0 | 332 | 168 | 143 | 1.69 | 21.73 | 75.7 |

Table 3.22: Results of potentiodynamic polarization studies for the corrosion of welded maraging steel in 1.0 M sulphuric acid containing different concentrations of BTPO.

| Temperature (°C) | Conc. of inhibitor (mM) | $-E_{corr}$ (mV /SCE) | b_a (mV dec ⁻¹) | $-b_c$ (mV dec ⁻¹) | i_{corr} (mA cm ⁻²) | U_{corr} (mm y ⁻¹) | η (%) |
|------------------|-------------------------|-----------------------|-------------------------------|--------------------------------|-----------------------------------|----------------------------------|------------|
| 30 | Blank | 315 | 187 | 132 | 3.93 | 50.32 | |
| | 0.2 | 334 | 148 | 124 | 0.87 | 11.21 | 77.9 |
| | 0.4 | 338 | 143 | 121 | 0.64 | 8.25 | 83.7 |
| | 0.6 | 322 | 139 | 117 | 0.48 | 6.19 | 87.8 |
| | 0.8 | 353 | 137 | 115 | 0.27 | 3.48 | 93.1 |
| | 1.0 | 312 | 132 | 112 | 0.23 | 2.96 | 94.1 |
| | 35 | Blank | 313 | 198 | 147 | 4.21 | 54.12 |
| 0.2 | | 327 | 161 | 135 | 1.05 | 13.57 | 75.1 |
| 0.4 | | 310 | 157 | 129 | 0.80 | 10.31 | 80.9 |
| 0.6 | | 329 | 152 | 125 | 0.67 | 8.68 | 84.1 |
| 0.8 | | 334 | 149 | 122 | 0.51 | 6.51 | 87.8 |
| 1.0 | | 337 | 147 | 118 | 0.38 | 4.88 | 90.9 |
| 40 | | Blank | 310 | 212 | 163 | 5.41 | 69.72 |
| | 0.2 | 324 | 183 | 149 | 1.68 | 21.62 | 68.9 |
| | 0.4 | 328 | 179 | 143 | 1.46 | 18.83 | 73.0 |
| | 0.6 | 331 | 175 | 139 | 1.19 | 15.34 | 78.0 |
| | 0.8 | 316 | 172 | 136 | 0.92 | 11.86 | 82.9 |
| | 1.0 | 305 | 164 | 134 | 0.70 | 9.07 | 87.1 |
| | 45 | Blank | 312 | 243 | 178 | 6.70 | 86.36 |
| 0.2 | | 327 | 201 | 153 | 2.35 | 30.23 | 64.9 |
| 0.4 | | 318 | 192 | 148 | 2.08 | 26.77 | 68.9 |
| 0.6 | | 321 | 187 | 145 | 1.74 | 22.45 | 74.0 |
| 0.8 | | 332 | 183 | 141 | 1.47 | 19.00 | 78.1 |
| 1.0 | | 309 | 177 | 138 | 1.27 | 16.41 | 81.0 |
| 50 | | Blank | 320 | 269 | 192 | 8.11 | 104.54 |
| | 0.2 | 318 | 214 | 174 | 3.33 | 42.86 | 58.9 |
| | 0.4 | 329 | 203 | 168 | 3.08 | 39.73 | 62.0 |
| | 0.6 | 333 | 195 | 164 | 2.76 | 35.54 | 65.9 |
| | 0.8 | 341 | 191 | 160 | 2.35 | 30.32 | 71.0 |
| | 1.0 | 352 | 183 | 157 | 2.11 | 27.18 | 73.9 |

Table 3.23: Results of potentiodynamic polarization studies for the corrosion of welded maraging steel in 1.5 M sulphuric acid containing different concentrations of BTPO.

| Temperature (°C) | Conc. of inhibitor (mM) | $-E_{corr}$ (mV /SCE) | b_a (mV dec ⁻¹) | $-b_c$ (mV dec ⁻¹) | i_{corr} (mA cm ⁻²) | ν_{corr} (mm y ⁻¹) | η (%) |
|------------------|-------------------------|-----------------------|-------------------------------|--------------------------------|-----------------------------------|------------------------------------|------------|
| 30 | Blank | 313 | 240 | 146 | 4.28 | 55.17 | |
| | 0.2 | 318 | 194 | 131 | 1.01 | 13.07 | 76.3 |
| | 0.4 | 332 | 188 | 125 | 0.75 | 9.71 | 82.4 |
| | 0.6 | 327 | 183 | 119 | 0.59 | 7.55 | 86.3 |
| | 0.8 | 298 | 179 | 114 | 0.31 | 4.02 | 92.7 |
| | 1.0 | 306 | 176 | 110 | 0.27 | 3.53 | 93.6 |
| 35 | Blank | 308 | 242 | 151 | 5.31 | 68.45 | |
| | 0.2 | 297 | 198 | 135 | 1.21 | 15.60 | 77.2 |
| | 0.4 | 304 | 189 | 131 | 1.07 | 13.82 | 79.8 |
| | 0.6 | 315 | 182 | 128 | 0.90 | 11.56 | 83.1 |
| | 0.8 | 322 | 177 | 122 | 0.68 | 8.82 | 87.1 |
| | 1.0 | 319 | 172 | 118 | 0.51 | 6.57 | 90.4 |
| 40 | Blank | 300 | 248 | 156 | 6.48 | 83.53 | |
| | 0.2 | 317 | 201 | 142 | 2.07 | 26.6 | 68.1 |
| | 0.4 | 321 | 195 | 134 | 1.82 | 23.55 | 71.8 |
| | 0.6 | 308 | 191 | 131 | 1.54 | 19.79 | 76.3 |
| | 0.8 | 302 | 188 | 127 | 1.21 | 15.53 | 81.4 |
| | 1.0 | 298 | 183 | 121 | 0.96 | 12.36 | 85.2 |
| 45 | Blank | 301 | 290 | 197 | 7.54 | 97.19 | |
| | 0.2 | 297 | 239 | 172 | 2.73 | 35.18 | 63.8 |
| | 0.4 | 294 | 231 | 167 | 2.47 | 31.78 | 67.3 |
| | 0.6 | 308 | 226 | 163 | 2.06 | 26.53 | 72.7 |
| | 0.8 | 305 | 222 | 157 | 1.84 | 23.71 | 75.6 |
| | 1.0 | 314 | 217 | 151 | 1.56 | 20.12 | 79.3 |
| 50 | Blank | 295 | 349 | 242 | 8.64 | 111.37 | |
| | 0.2 | 287 | 287 | 209 | 3.62 | 46.66 | 58.1 |
| | 0.4 | 301 | 279 | 201 | 3.35 | 43.21 | 61.2 |
| | 0.6 | 307 | 272 | 195 | 3.05 | 39.31 | 64.7 |
| | 0.8 | 310 | 258 | 191 | 2.65 | 34.19 | 69.3 |
| | 1.0 | 292 | 247 | 184 | 2.34 | 30.18 | 72.9 |

Table 3.24: Results of potentiodynamic polarization studies for the corrosion of welded maraging steel in 2.0 M sulphuric acid containing different concentrations of BTPO.

| Temperature (°C) | Conc. of inhibitor (mM) | $-E_{corr}$ (mV /SCE) | b_a (mV dec ⁻¹) | $-b_c$ (mV dec ⁻¹) | i_{corr} (mA cm ⁻²) | v_{corr} (mm y ⁻¹) | η (%) |
|------------------|-------------------------|-----------------------|-------------------------------|--------------------------------|-----------------------------------|----------------------------------|------------|
| 30 | Blank | 315 | 312 | 154 | 4.97 | 64.06 | |
| | 0.2 | 321 | 238 | 142 | 1.22 | 15.76 | 75.4 |
| | 0.4 | 334 | 231 | 137 | 0.93 | 12.04 | 81.2 |
| | 0.6 | 338 | 226 | 133 | 0.74 | 9.48 | 85.2 |
| | 0.8 | 327 | 219 | 128 | 0.43 | 5.51 | 91.4 |
| | 1.0 | 318 | 212 | 125 | 0.37 | 4.80 | 92.5 |
| | 35 | Blank | 313 | 283 | 208 | 6.12 | 78.89 |
| 0.2 | | 318 | 247 | 169 | 1.34 | 17.28 | 78.1 |
| 0.4 | | 325 | 241 | 162 | 1.30 | 16.80 | 78.7 |
| 0.6 | | 347 | 234 | 154 | 1.11 | 14.36 | 81.8 |
| 0.8 | | 352 | 229 | 150 | 0.81 | 10.41 | 86.8 |
| 1.0 | | 361 | 223 | 148 | 0.67 | 8.60 | 89.1 |
| 40 | | Blank | 310 | 261 | 225 | 7.32 | 94.36 |
| | 0.2 | 317 | 253 | 181 | 2.47 | 31.80 | 66.3 |
| | 0.4 | 323 | 249 | 174 | 2.16 | 27.84 | 70.5 |
| | 0.6 | 304 | 242 | 169 | 1.85 | 23.87 | 74.7 |
| | 0.8 | 333 | 239 | 166 | 1.46 | 18.78 | 80.1 |
| | 1.0 | 341 | 234 | 161 | 1.18 | 15.19 | 83.9 |
| | 45 | Blank | 312 | 282 | 231 | 8.23 | 106.09 |
| 0.2 | | 327 | 267 | 192 | 3.15 | 40.63 | 61.7 |
| 0.4 | | 329 | 259 | 187 | 2.79 | 35.96 | 66.1 |
| 0.6 | | 334 | 253 | 183 | 2.43 | 31.29 | 70.5 |
| 0.8 | | 339 | 249 | 179 | 2.15 | 27.69 | 73.9 |
| 1.0 | | 321 | 246 | 176 | 1.84 | 23.76 | 77.6 |
| 50 | | Blank | 320 | 329 | 204 | 9.02 | 116.27 |
| | 0.2 | 334 | 284 | 197 | 3.91 | 50.34 | 56.7 |
| | 0.4 | 328 | 278 | 191 | 3.58 | 46.16 | 60.3 |
| | 0.6 | 316 | 271 | 182 | 3.32 | 42.79 | 63.2 |
| | 0.8 | 309 | 266 | 178 | 2.94 | 37.90 | 67.4 |
| | 1.0 | 339 | 261 | 176 | 2.62 | 33.72 | 71.0 |

Table 3.25: EIS data for the corrosion of welded maraging steel in 0.1 M sulphuric acid containing different concentrations of BTPO.

| Temperature (°C) | Conc. of inhibitor (mM) | R_p (ohm. cm ²) | C_{dl} (mF cm ⁻²) | η (%) |
|------------------|-------------------------|-------------------------------|---------------------------------|------------|
| 30 | Blank | 20.1 | 0.324 | |
| | 0.2 | 102.5 | 0.287 | 80.4 |
| | 0.4 | 126.4 | 0.271 | 84.1 |
| | 0.6 | 160.8 | 0.234 | 87.5 |
| | 0.8 | 245.1 | 0.207 | 91.8 |
| | 1.0 | 295.5 | 0.188 | 93.2 |
| 35 | Blank | 17.4 | 0.469 | |
| | 0.2 | 75.3 | 0.380 | 76.9 |
| | 0.4 | 95.0 | 0.347 | 81.7 |
| | 0.6 | 108.1 | 0.309 | 83.9 |
| | 0.8 | 153.9 | 0.278 | 88.7 |
| | 1.0 | 193.3 | 0.260 | 91.0 |
| 40 | Blank | 14.1 | 0.531 | |
| | 0.2 | 52.4 | 0.451 | 73.1 |
| | 0.4 | 55.9 | 0.421 | 74.8 |
| | 0.6 | 69.1 | 0.389 | 79.6 |
| | 0.8 | 95.9 | 0.342 | 85.3 |
| | 1.0 | 124.7 | 0.310 | 88.7 |
| 45 | Blank | 12.3 | 0.668 | |
| | 0.2 | 36.9 | 0.532 | 66.7 |
| | 0.4 | 43.6 | 0.491 | 71.8 |
| | 0.6 | 49.7 | 0.454 | 75.3 |
| | 0.8 | 67.2 | 0.421 | 81.7 |
| | 1.0 | 84.2 | 0.376 | 85.4 |
| 50 | Blank | 10.2 | 0.830 | |
| | 0.2 | 29.8 | 0.691 | 65.8 |
| | 0.4 | 31.6 | 0.658 | 67.8 |
| | 0.6 | 35.0 | 0.621 | 70.9 |
| | 0.8 | 38.3 | 0.583 | 73.4 |
| | 1.0 | 54.1 | 0.542 | 81.5 |

Table 3.26: EIS data for the corrosion of welded maraging steel in 0.5 M sulphuric acid containing different concentrations of BTPO.

| Temperature (°C) | Conc. of inhibitor (mM) | R_p (ohm. cm ²) | C_{dl} (mF cm ⁻²) | η (%) |
|------------------|-------------------------|-------------------------------|---------------------------------|------------|
| 30 | Blank | 18.7 | 0.633 | |
| | 0.2 | 92.1 | 0.512 | 79.7 |
| | 0.4 | 111.3 | 0.481 | 83.2 |
| | 0.6 | 146.0 | 0.434 | 87.2 |
| | 0.8 | 228.0 | 0.387 | 91.8 |
| | 1.0 | 246.1 | 0.351 | 92.4 |
| 35 | Blank | 15.4 | 0.682 | |
| | 0.2 | 62.3 | 0.591 | 75.3 |
| | 0.4 | 83.7 | 0.543 | 81.6 |
| | 0.6 | 92.7 | 0.514 | 83.4 |
| | 0.8 | 135.0 | 0.432 | 88.6 |
| | 1.0 | 160.4 | 0.398 | 90.4 |
| 40 | Blank | 11.4 | 0.727 | |
| | 0.2 | 39.7 | 0.612 | 71.3 |
| | 0.4 | 43.5 | 0.570 | 73.8 |
| | 0.6 | 50.0 | 0.524 | 77.2 |
| | 0.8 | 70.3 | 0.482 | 83.8 |
| | 1.0 | 89.1 | 0.455 | 87.2 |
| 45 | Blank | 10.5 | 0.831 | |
| | 0.2 | 30.7 | 0.741 | 65.8 |
| | 0.4 | 36.5 | 0.687 | 71.3 |
| | 0.6 | 40.8 | 0.663 | 74.3 |
| | 0.8 | 53.5 | 0.621 | 80.4 |
| | 1.0 | 69.0 | 0.582 | 84.8 |
| 50 | Blank | 7.9 | 0.965 | |
| | 0.2 | 22.1 | 0.832 | 64.4 |
| | 0.4 | 22.0 | 0.801 | 64.3 |
| | 0.6 | 29.6 | 0.762 | 73.4 |
| | 0.8 | 32.5 | 0.714 | 75.7 |
| | 1.0 | 36.4 | 0.698 | 78.3 |

Table 3.27: EIS data for the corrosion of welded maraging steel in 1.0 M sulphuric acid containing different concentrations of BTPO.

| Temperature (°C) | Conc. of inhibitor (mM) | R_p (ohm. cm ²) | C_{dl} (mF cm ⁻²) | η (%) |
|------------------|-------------------------|-------------------------------|---------------------------------|------------|
| 30 | Blank | 16.1 | 0.641 | |
| | 0.2 | 69.3 | 0.573 | 76.7 |
| | 0.4 | 97.4 | 0.541 | 83.5 |
| | 0.6 | 126.9 | 0.512 | 87.3 |
| | 0.8 | 214.2 | 0.459 | 91.4 |
| | 1.0 | 262.7 | 0.432 | 91.8 |
| 35 | Blank | 13.5 | 0.714 | |
| | 0.2 | 52.1 | 0.623 | 74.1 |
| | 0.4 | 68.5 | 0.592 | 80.3 |
| | 0.6 | 78.0 | 0.571 | 82.7 |
| | 0.8 | 106.2 | 0.520 | 87.3 |
| | 1.0 | 123.8 | 0.508 | 89.1 |
| 40 | Blank | 10.3 | 0.670 | |
| | 0.2 | 33.2 | 0.653 | 68.7 |
| | 0.4 | 36.6 | 0.632 | 71.6 |
| | 0.6 | 44.1 | 0.608 | 76.4 |
| | 0.8 | 59.0 | 0.582 | 82.4 |
| | 1.0 | 75.9 | 0.553 | 86.3 |
| 45 | Blank | 8.6 | 0.873 | |
| | 0.2 | 24.3 | 0.712 | 64.7 |
| | 0.4 | 29.5 | 0.680 | 70.9 |
| | 0.6 | 32.8 | 0.663 | 73.8 |
| | 0.8 | 41.1 | 0.631 | 79.1 |
| | 1.0 | 51.8 | 0.603 | 83.4 |
| 50 | Blank | 7.3 | 1.123 | |
| | 0.2 | 18.2 | 1.031 | 60.1 |
| | 0.4 | 19.1 | 0.922 | 61.8 |
| | 0.6 | 21.5 | 0.843 | 66.1 |
| | 0.8 | 25.0 | 0.791 | 70.8 |
| | 1.0 | 27.9 | 0.763 | 73.9 |

Table 3.28: EIS data for the corrosion of welded maraging steel in 1.5 M sulphuric acid containing different concentrations of BTPO.

| Temperature (°C) | Conc. of inhibitor (mM) | R_p (ohm. cm ²) | C_{dl} (mF cm ⁻²) | η (%) |
|------------------|-------------------------|-------------------------------|---------------------------------|------------|
| 30 | Blank | 15.9 | 0.958 | |
| | 0.2 | 65.7 | 0.812 | 75.8 |
| | 0.4 | 86.8 | 0.783 | 81.7 |
| | 0.6 | 111.9 | 0.720 | 85.8 |
| | 0.8 | 172.8 | 0.697 | 90.8 |
| | 1.0 | 191.5 | 0.654 | 91.3 |
| 35 | Blank | 11.6 | 0.982 | |
| | 0.2 | 43.6 | 0.874 | 73.4 |
| | 0.4 | 55.7 | 0.823 | 79.2 |
| | 0.6 | 62.3 | 0.782 | 81.4 |
| | 0.8 | 85.2 | 0.730 | 86.4 |
| | 1.0 | 100.0 | 0.715 | 88.3 |
| 40 | Blank | 9.4 | 1.070 | |
| | 0.2 | 28.8 | 0.983 | 67.4 |
| | 0.4 | 32.3 | 0.941 | 70.9 |
| | 0.6 | 39.0 | 0.922 | 75.9 |
| | 0.8 | 51.3 | 0.894 | 81.7 |
| | 1.0 | 62.2 | 0.851 | 84.9 |
| 45 | Blank | 8.1 | 1.281 | |
| | 0.2 | 22.5 | 1.132 | 64.1 |
| | 0.4 | 26.2 | 1.071 | 69.2 |
| | 0.6 | 29.7 | 1.014 | 72.8 |
| | 0.8 | 34.0 | 0.942 | 76.2 |
| | 1.0 | 38.3 | 0.891 | 78.9 |
| 50 | Blank | 6.9 | 1.318 | |
| | 0.2 | 16.7 | 1.212 | 58.7 |
| | 0.4 | 17.6 | 1.154 | 60.9 |
| | 0.6 | 19.3 | 1.114 | 64.3 |
| | 0.8 | 22.0 | 1.057 | 68.7 |
| | 1.0 | 24.4 | 0.983 | 71.8 |

Table 3.29: EIS data for the corrosion of welded maraging steel in 2.0 M sulphuric acid containing different concentrations of BTPO.

| Temperature (°C) | Conc. of inhibitor (mM) | R_p (ohm. cm ²) | C_{dl} (mF cm ⁻²) | η (%) |
|------------------|-------------------------|-------------------------------|---------------------------------|------------|
| 30 | Blank | 13.9 | 1.093 | |
| | 0.2 | 55.1 | 1.032 | 74.8 |
| | 0.4 | 72.0 | 0.981 | 80.7 |
| | 0.6 | 88.5 | 0.947 | 84.3 |
| | 0.8 | 141.8 | 0.894 | 90.2 |
| | 1.0 | 152.7 | 0.831 | 90.9 |
| 35 | Blank | 10.8 | 1.241 | |
| | 0.2 | 38.9 | 1.182 | 72.3 |
| | 0.4 | 50.7 | 1.135 | 78.7 |
| | 0.6 | 55.3 | 1.078 | 80.5 |
| | 0.8 | 73.4 | 1.031 | 85.3 |
| | 1.0 | 84.3 | 0.943 | 87.2 |
| 40 | Blank | 9.2 | 1.324 | |
| | 0.2 | 27.2 | 1.191 | 66.3 |
| | 0.4 | 30.4 | 1.162 | 69.8 |
| | 0.6 | 35.7 | 1.147 | 74.3 |
| | 0.8 | 48.6 | 1.105 | 81.1 |
| | 1.0 | 58.2 | 1.041 | 84.2 |
| 45 | Blank | 7.4 | 1.369 | |
| | 0.2 | 20.1 | 1.211 | 63.2 |
| | 0.4 | 21.6 | 1.142 | 65.8 |
| | 0.6 | 25.7 | 1.084 | 71.3 |
| | 0.8 | 28.5 | 1.032 | 74.1 |
| | 1.0 | 32.4 | 0.974 | 77.2 |
| 50 | Blank | 6.5 | 1.508 | |
| | 0.2 | 15.1 | 1.341 | 57.1 |
| | 0.4 | 16.2 | 1.293 | 59.8 |
| | 0.6 | 18.0 | 1.234 | 63.9 |
| | 0.8 | 20.0 | 1.151 | 67.5 |
| | 1.0 | 21.8 | 1.080 | 70.3 |

Table 3.30: Activation parameters for the corrosion of welded maraging steel in sulphuric acid containing different concentrations of BTPO.

| Molarity of H ₂ SO ₄ (M) | Conc. of inhibitor (mM) | E_a (kJ mol ⁻¹) | ΔH^\ddagger (kJ mol ⁻¹) | ΔS^\ddagger (J mol ⁻¹ K ⁻¹) |
|--|-------------------------|-------------------------------|---|--|
| 0.1 | Blank | 43.14 | 46.18 | -21.03 |
| | 0.2 | 67.68 | 65.07 | -17.99 |
| | 0.4 | 75.31 | 72.41 | -15.04 |
| | 0.6 | 71.79 | 78.45 | -12.08 |
| | 0.8 | 85.76 | 93.22 | -8.73 |
| | 1.0 | 102.74 | 100.17 | -5.65 |
| 0.5 | Blank | 37.32 | 40.37 | -37.15 |
| | 0.2 | 70.14 | 67.54 | -34.26 |
| | 0.4 | 79.25 | 76.65 | -28.67 |
| | 0.6 | 72.03 | 69.93 | -20.92 |
| | 0.8 | 89.48 | 95.61 | -16.87 |
| | 1.0 | 104.09 | 101.49 | -4.16 |
| 1.0 | Blank | 37.79 | 39.81 | -34.41 |
| | 0.2 | 56.61 | 54.01 | -47.31 |
| | 0.4 | 66.64 | 64.04 | -26.79 |
| | 0.6 | 88.13 | 79.77 | -20.12 |
| | 0.8 | 94.23 | 85.38 | -17.36 |
| | 1.0 | 91.89 | 89.28 | -8.25 |
| 1.5 | Blank | 40.90 | 43.04 | -23.91 |
| | 0.2 | 54.65 | 52.05 | -52.41 |
| | 0.4 | 62.21 | 59.61 | -29.38 |
| | 0.6 | 67.87 | 64.69 | -24.58 |
| | 0.8 | 86.01 | 83.40 | -16.87 |
| | 1.0 | 88.19 | 85.59 | -12.27 |
| 2.0 | Blank | 42.41 | 45.23 | -18.38 |
| | 0.2 | 51.73 | 49.13 | -60.56 |
| | 0.4 | 56.22 | 53.62 | -47.26 |
| | 0.6 | 61.83 | 59.23 | -30.63 |
| | 0.8 | 78.23 | 76.29 | -24.67 |
| | 1.0 | 80.12 | 77.52 | -21.01 |

Table 3.31: Maximum inhibition efficiency attained in different concentrations of sulphuric acid at different temperatures for BTPO.

| Temperature (°C) | Welded Maraging Steel | | | |
|---------------------|-------------------------------------|----------------------------------|---|------------|
| | Sulphuric acid concentration (M) | Concentration of BTPO (Mm) | η (%) | |
| | | | Potentiodynamic polarization method | EIS method |
| 30 | 0.1 | 1.0 | 94.8 | 93.2 |
| | 0.5 | | 94.4 | 92.4 |
| | 1.0 | | 94.1 | 91.8 |
| | 1.5 | | 93.6 | 91.3 |
| | 2.0 | | 92.5 | 90.9 |
| 35 | 0.1 | 1.0 | 92.9 | 91.0 |
| | 0.5 | | 91.7 | 90.4 |
| | 1.0 | | 90.9 | 89.1 |
| | 1.5 | | 90.4 | 88.3 |
| | 2.0 | | 89.1 | 87.2 |
| 40 | 0.1 | 1.0 | 89.3 | 88.7 |
| | 0.5 | | 88.4 | 87.2 |
| | 1.0 | | 87.1 | 86.3 |
| | 1.5 | | 85.2 | 84.9 |
| | 2.0 | | 83.9 | 84.2 |
| 45 | 0.1 | 1.0 | 85.2 | 85.4 |
| | 0.5 | | 83.4 | 84.8 |
| | 1.0 | | 81.0 | 83.4 |
| | 1.5 | | 79.3 | 78.9 |
| | 2.0 | | 77.6 | 77.2 |
| 50 | 0.1 | 1.0 | 82.5 | 81.5 |
| | 0.5 | | 75.7 | 78.3 |
| | 1.0 | | 73.9 | 73.9 |
| | 1.5 | | 72.9 | 71.8 |
| | 2.0 | | 71.0 | 70.3 |

Table 3.32: Thermodynamic parameters for the adsorption of BTPO on welded maraging steel surface in sulphuric acid at different temperatures.

| Molarity of H ₂ SO ₄ (M) | Temperature (° C) | $-\Delta G^{\circ}_{ads}$ (kJ mol ⁻¹) | ΔH°_{ads} (kJ mol ⁻¹) | ΔS°_{ads} (J mol ⁻¹ K ⁻¹) |
|--|-------------------|---|--|---|
| 0.1 | 30 | 34.63 | -15.05 | -64.21 |
| | 35 | 34.27 | | |
| | 40 | 34.15 | | |
| | 45 | 34.04 | | |
| | 50 | 33.86 | | |
| 0.5 | 30 | 34.48 | -19.21 | -32.10 |
| | 35 | 34.34 | | |
| | 40 | 34.29 | | |
| | 45 | 34.13 | | |
| | 50 | 34.06 | | |
| 1.0 | 30 | 34.21 | -22.76 | -37.6 |
| | 35 | 34.15 | | |
| | 40 | 33.93 | | |
| | 45 | 33.69 | | |
| | 50 | 33.52 | | |
| 1.5 | 30 | 33.95 | -21.83 | -40.8 |
| | 35 | 33.86 | | |
| | 40 | 33.74 | | |
| | 45 | 33.60 | | |
| | 50 | 33.55 | | |
| 2.0 | 30 | 33.90 | -22.36 | -39.0 |
| | 35 | 33.79 | | |
| | 40 | 33.63 | | |
| | 45 | 33.56 | | |
| | 50 | 33.12 | | |

3.5 1-PHENYL-4-(4-NITROPHENYL)THIOSEMICARBAZIDE (PNPT) AS INHIBITOR FOR THE CORROSION OF WELDED MARAGING STEEL IN HYDROCHLORIC ACID MEDIUM

3.5.1 Potentiodynamic polarization measurements

Polarization curves for the corrosion of maraging steel in 1.0 M HCl solution in the presence of different concentrations of PNPT are shown in Fig. 3.36. Similar results were obtained at other temperatures and in other concentrations of hydrochloric acid. The potentiodynamic polarization parameters are summarized in Tables 3.33 to 3.37.

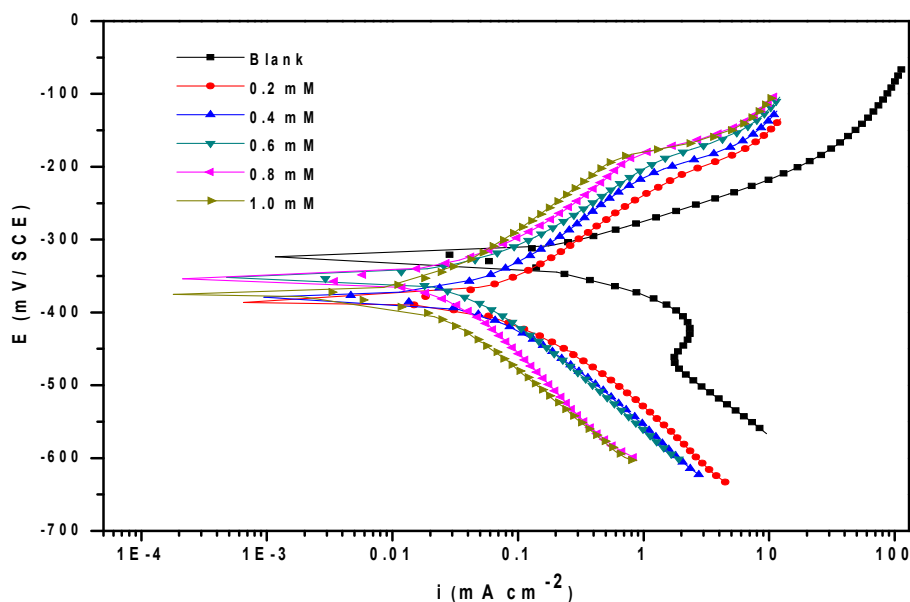


Fig. 3.36: Potentiodynamic polarization curves for the corrosion of welded maraging steel in 1.0 M hydrochloric acid containing different concentrations of PNPT at 30 °C.

It could be observed that both the anodic and cathodic reactions were suppressed with the addition of inhibitor, which suggested that the inhibitor exerted an efficient inhibitory effect both on the anodic dissolution of metal and on cathodic hydrogen evolution reaction (Tao et al. 2011). In general, according to the results presented in Tables 3.33 to 3.37 and also from polarization curves in Fig. 3.36, the corrosion current density (i_{corr}) decreased significantly even on the addition of small concentration of

PNPT and the inhibition efficiency ($\eta\%$) increases with the increase in the inhibitor concentration of PNPT. The presence of PNPT shifts E_{corr} slightly towards negative direction. However, the maximum displacement in the present study is -64 mV, therefore it can be concluded that PNPT acts as a mixed type inhibitor on welded maraging steel with a predominant cathodic effect. The rest of the discussion is similar to the discussion regarding the inhibition behaviour of BTPO for the corrosion of welded maraging steel in hydrochloric acid medium, under the section 3.3.1.

3.5.2 Electrochemical impedance spectroscopy (EIS) studies

Nyquist plots for the corrosion of welded maraging steel in 1.0 M HCl solution in the presence of different concentrations of PNPT are given in Fig. 3.37. Similar results were obtained in other concentrations of the acid and also at other temperatures. The impedance parameters are presented in Tables 3.38 to 3.42. It can be observed that the diameter of the semicircle increases with the increasing PNPT concentration and the impedance spectra did not present perfect semicircles at higher concentration of inhibitor.

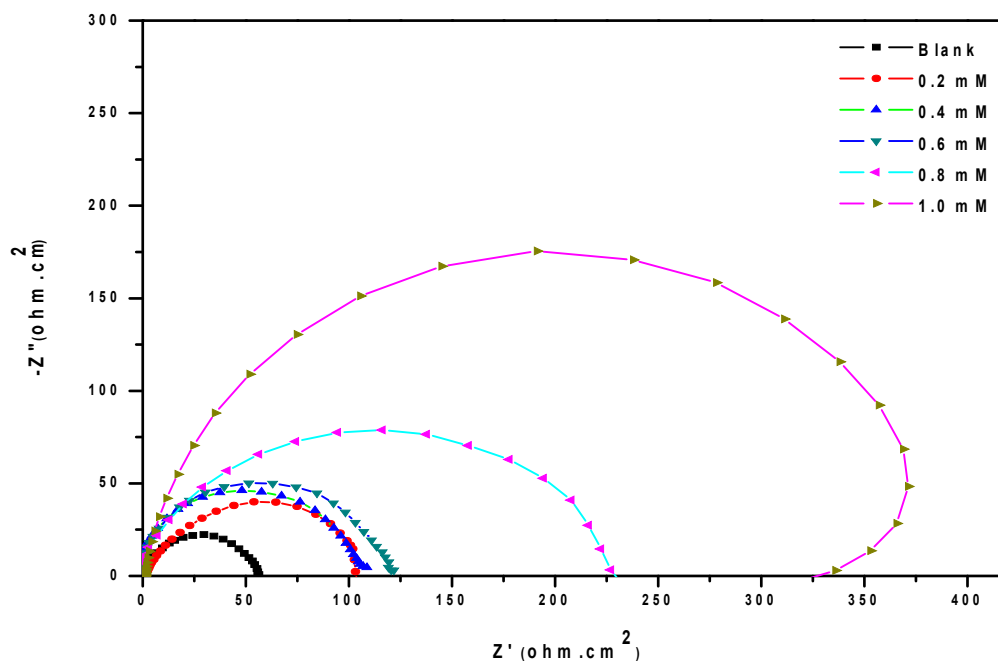


Fig. 3.37: Nyquist plots for the corrosion of welded maraging steel in 1.0 M hydrochloric acid containing different concentrations of PNPT at 30 °C.

It is seen from the data in Tables 3.38 to 3.42 that the value of R_{ct} increases and the value of C_{dl} decreases as the concentration of PNPT increases, indicating an increased inhibition efficiency. The equivalent circuit given in Fig. 3.17 is used to fit the experimental data for the corrosion of welded maraging steel in hydrochloric acid in the presence of PNPT.

The increase of inhibitor concentration leads to improved effectiveness of the protection which can be attributed to the blocking effect of the inhibitor on the surface by both adsorption and film formation reducing the effective area of attack. This modification results in an increase of charge transfer resistance where the resulting adsorption films isolate the metal surface from the corrosive medium and decrease metal dissolution (Arab et al. 2008, Ozcan et al. 2004, Machnikova et al. 2008).

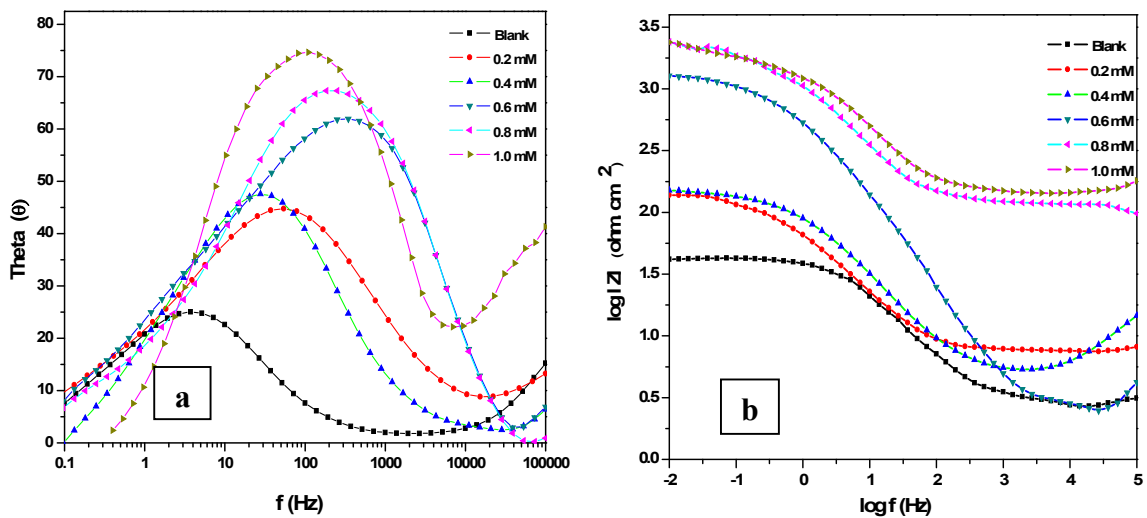


Fig. 3.38: Bode (a) Phase angle plots and (b) amplitude plots for the corrosion of welded maraging steel in 1.0 M HCl containing different concentrations of PNPT at 30 °C.

The Bode plots of phase angle and amplitude for the corrosion of the alloy in the presence of PNPT, are shown in Fig. 3.38 (a) and Fig. 3.38 (b), respectively. The high frequency (HF) limits correspond to R_s (Ω), while the lower frequency (LF) limits corresponds to $(R_{ct} + R_f)$, which is associated with the dissolution processes at the metal/solution interface. Phase angle increases with increase in concentrations of PNPT

in hydrochloric acid medium. This might be due to the decrease in dissolution of metal and decrease in capacitive behaviour on the electrode surface. The presence of phase maximum at intermediate frequencies indicates the presence of a time constant corresponding to the impedance of the formed adsorbed film. An increase in PNPT concentration leads to an increase in the $|Z|$ value.

3.5.2 Effect of temperature

The data's in Tables 3.33 to 3.42 indicate that the inhibition efficiency of PNPT decreases with the increase in temperature. The decrease in inhibition efficiency with the increase in temperature may be attributed to the higher dissolution rates of welded maraging steel at elevated temperature and also a possible desorption of adsorbed inhibitor due to the increased solution agitation resulting from higher rates of hydrogen gas evolution (Poornima et al. 2011). The decrease in inhibition efficiency with the increase in temperature is also suggestive of physisorption of the inhibitor molecules on the metal surface (Geetha et al. 2011).

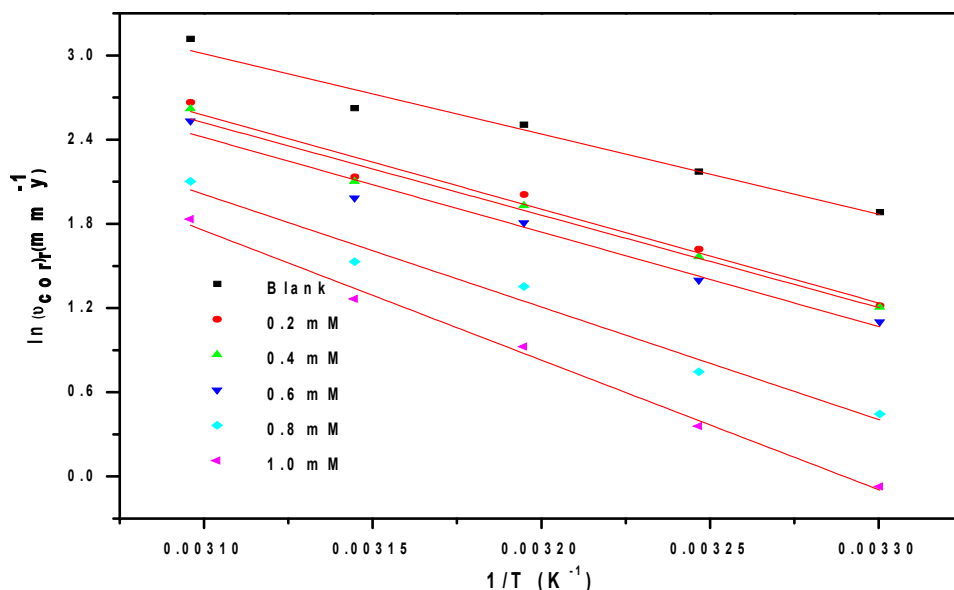


Fig. 3.39: Arrhenius Plots for the corrosion of welded maraging steel in 1.0 M hydrochloric acid containing different concentrations of PNPT.

The Arrhenius plots for the corrosion of welded maraging steel in the presence of different concentrations of PNPT in 1.0 M hydrochloric acid are shown in Fig. 3.39. The plots of $\ln(v_{\text{corr}}/T)$ versus $1/T$ for the corrosion of welded samples of maraging steel in the presence of different concentrations of PNPT in 1.0M hydrochloric acid are shown in Fig. 3.40. The calculated values of activation parameters are recorded in Table 3.43

The results show that the value of E_a increases with the increase in the concentration of inhibitor indicating that the energy barrier for the corrosion reaction increases. It is also indicated that the whole process is controlled by surface reaction (Fouda et al. 2009), since the activation energies of the corrosion process are above 20 kJ mol⁻¹.

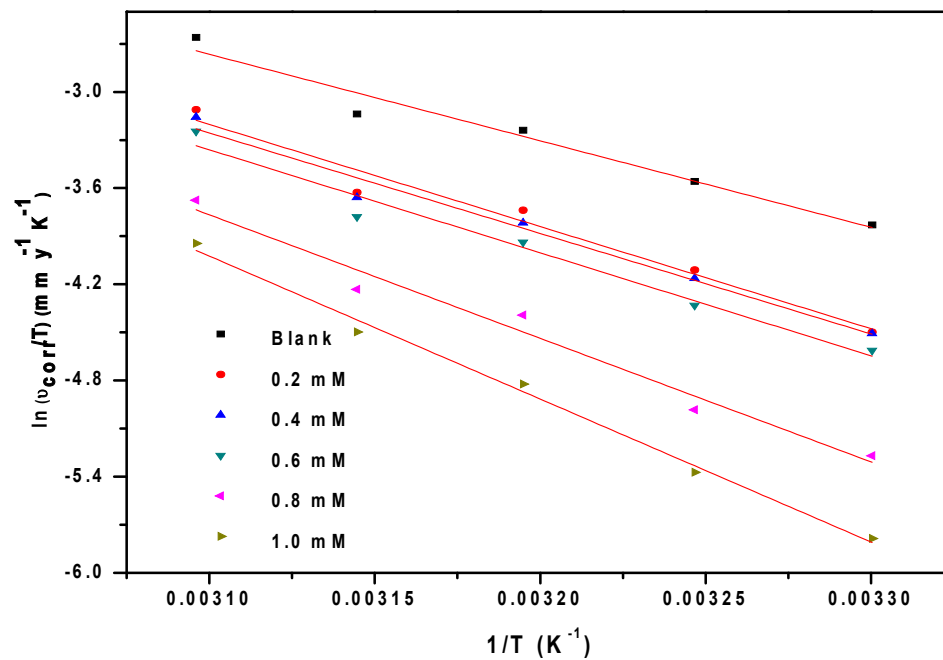


Fig. 3.40: Plots of $\ln(v_{\text{corr}}/T)$ versus $1/T$ for the corrosion of welded maraging steel in 1.0 M hydrochloric acid containing different concentrations of PNPT.

The entropy of activation values in the absence and the presence of PNPT are large and negative; this indicates that the activated complex formation in the rate-determining step represents an association rather than dissociation, decreasing the

randomness on going from the reactants to the activated complex (Abd EI Rehim et al. 2003). It is also seen from the Table that entropy of activation increases with the increase in the concentration of PNPT.

3.5.4 Effect of hydrochloric acid concentration

Table 3.44 summarises the maximum inhibition efficiencies exhibited by PNPT in the HCl solutions of different concentrations. It is evident from both polarization and EIS experimental results that, for a particular concentration of inhibitor, the inhibition efficiency decreases with the increase in hydrochloric acid concentration. The highest inhibition efficiency is observed in hydrochloric acid of 0.1 M concentration.

3.5.5 Adsorption isotherm

The adsorption of PNPT on the surface of welded maraging steel was found to obey Langmuir adsorption isotherm. The linear regression coefficients are close to unity and the slopes of the straight lines are nearly unity, suggesting that the adsorption of PNPT obeys Langmuir's adsorption isotherm with negligible interaction between the adsorbed molecules. The Langmuir adsorption isotherms for the adsorption of PNPT on welded maraging steel in 1.0 M HCl are shown in Fig. 3.41. The thermodynamic data obtained for the adsorption of PNPT on welded maraging steel are tabulated in Table 3.45. The exothermic ΔH_{ads}^0 values of less than $-41.86 \text{ kJ mol}^{-1}$ predict physisorption of PNPT on the alloy surfaces (Ashish Kumar et al. 2010). The ΔG_{ads}^0 values predict both physisorption and chemisorption of PNPT. Therefore it can be concluded that the adsorption of PNPT on the welded maraging steel is predominantly through physisorption. These facts are also supported by the variation of inhibition efficiencies with temperature on the alloy surface as discussed under section 3.5.3.

The ΔS_{ads}^0 value is negative, indicating the decrease in randomness involved in the adsorption of PNPT molecules on the alloy surface. In the present case, the more orderly arrangement of the inhibitor molecules on the metal surface overweighs the solvent entropy resulting from the desorption of water molecules from the metal surface.

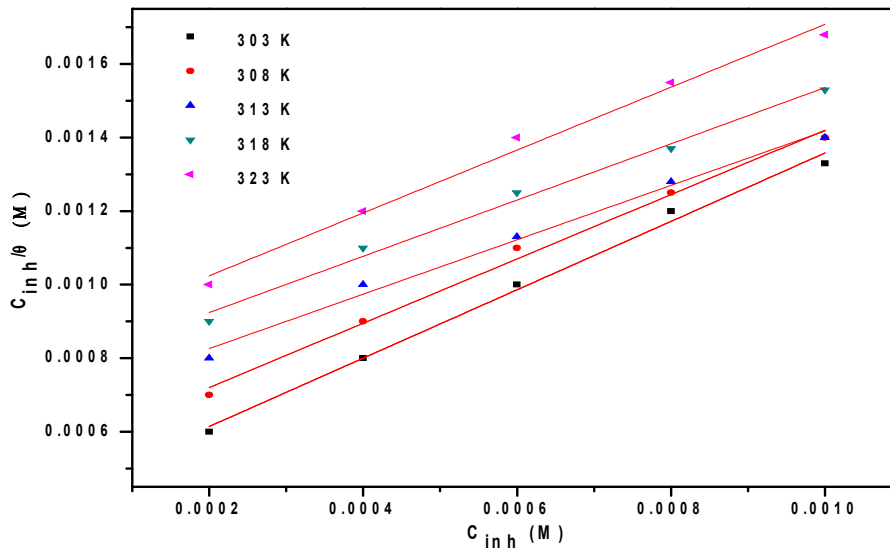


Fig. 3.41: Langmuir adsorption isotherms for the adsorption of PNPT on the welded maraging steel in 1.0 M HCl at different temperatures.

3.5.6 Mechanism of corrosion inhibition

The inhibitive effect of PNPT on the corrosion of welded maraging steel can be accounted for on the basis of its adsorption on the alloy surface. The adsorption of PNPT molecules on the metal surface can be attributed to the presence of electronegative elements like oxygen, sulphur and nitrogen and also to the presence of π -electron cloud in the benzene rings of the molecule. The electronegative elements develop positive and negative charge centers on the molecule. Also, in the acidic medium employed in the present study, the amine groups present in PNPT get protonated. The positive charge center in the PNPT molecule can electrostatically interact with the negatively charged chloride adsorbed metal surface, resulting in physisorption. The negative charge centers of the PNPT molecules containing lone pairs of electrons and/or π electrons can electrostatically interact with the positively charged metal surface, which is not adsorbed with chloride ions, and get physically adsorbed. The neutral inhibitor molecule may occupy the vacant adsorption sites on the metal surface through chemisorption mode.

3.5.7 SEM/EDX studies

Fig. 3.42 represents SEM image of welded maraging steel after the corrosion tests in a medium of hydrochloric acid containing 1.0 mM of PNPT. The image clearly shows a relatively smooth surface due to the presence of adsorbed inhibitor layer on the surface of the alloy.

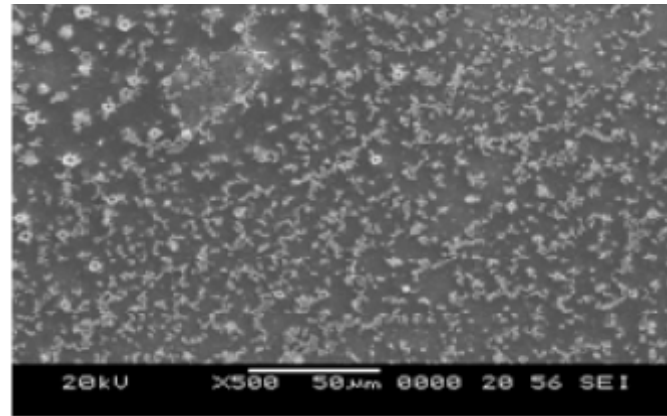


Fig. 3.42: SEM images of the welded maraging steel after immersion in 1.0 M HCl in the presence of PNPT.

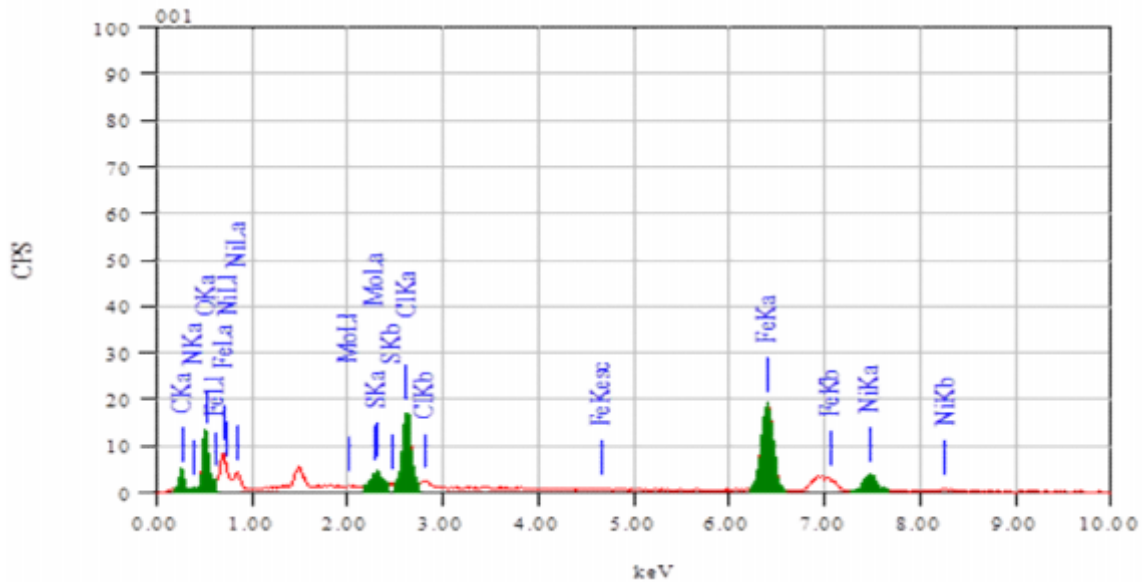


Fig. 3.43: EDX spectra of the welded maraging steel after immersion in 1.0 M HCl in the presence of PNPT.

The EDX spectra for the selected areas on the SEM image of 3.42 is shown in Fig. 3.43. The atomic percentage of the elements found in the EDX spectra for PNPT adsorbed metal surface were 28.41% Fe, 4.54% Co, 7.27% Ni, 0.06% Cl, 27.83% O, 7.05% N, 8.58% S and 16.27% C and suggested that formation of anticorrosion protective film of PNPT on the alloy surface.

Table 3.33: Results of potentiodynamic polarization studies for the corrosion of welded maraging steel in 0.1 M hydrochloric acid containing different concentrations of PNPT.

| Temperature (°C) | Conc. of inhibitor (mM) | $-E_{corr}$ (mV /SCE) | b_a (mV dec ⁻¹) | $-b_c$ (mV dec ⁻¹) | i_{corr} (mA cm ⁻²) | U_{corr} (mm y ⁻¹) | η (%) |
|------------------|-------------------------|-----------------------|-------------------------------|--------------------------------|-----------------------------------|----------------------------------|------------|
| 30 | Blank | 306 | 98 | 140 | 0.31 | 4.00 | |
| | 0.2 | 320 | 94 | 133 | 0.14 | 1.80 | 54.8 |
| | 0.4 | 322 | 92 | 128 | 0.13 | 1.68 | 58.2 |
| | 0.6 | 327 | 87 | 123 | 0.11 | 1.43 | 64.5 |
| | 0.8 | 331 | 78 | 109 | 0.04 | 0.52 | 87.1 |
| | 1.0 | 335 | 72 | 98 | 0.03 | 0.39 | 90.3 |
| | 35 | Blank | 310 | 101 | 146 | 0.36 | 4.64 |
| 0.2 | | 331 | 97 | 141 | 0.19 | 2.45 | 47.2 |
| 0.4 | | 329 | 95 | 137 | 0.18 | 2.32 | 49.9 |
| 0.6 | | 334 | 91 | 134 | 0.15 | 1.93 | 58.2 |
| 0.8 | | 338 | 82 | 123 | 0.06 | 0.77 | 83.1 |
| 1.0 | | 342 | 76 | 116 | 0.04 | 0.52 | 88.8 |
| 40 | | Blank | 312 | 103 | 147 | 0.46 | 5.93 |
| | 0.2 | 327 | 101 | 145 | 0.25 | 3.22 | 45.7 |
| | 0.4 | 334 | 97 | 139 | 0.24 | 3.09 | 47.8 |
| | 0.6 | 337 | 94 | 137 | 0.21 | 2.71 | 54.3 |
| | 0.8 | 339 | 89 | 135 | 0.10 | 1.29 | 78.1 |
| | 1.0 | 343 | 87 | 132 | 0.07 | 0.90 | 84.5 |
| | 45 | Blank | 315 | 108 | 156 | 0.67 | 8.64 |
| 0.2 | | 343 | 106 | 153 | 0.38 | 4.90 | 43.8 |
| 0.4 | | 348 | 103 | 151 | 0.36 | 4.64 | 46.1 |
| 0.6 | | 351 | 98 | 147 | 0.32 | 4.12 | 52.4 |
| 0.8 | | 357 | 94 | 142 | 0.15 | 1.93 | 77.4 |
| 1.0 | | 361 | 90 | 138 | 0.12 | 1.55 | 82.7 |
| 50 | | Blank | 313 | 113 | 161 | 0.83 | 10.70 |
| | 0.2 | 348 | 111 | 158 | 0.49 | 6.32 | 41.2 |
| | 0.4 | 351 | 108 | 154 | 0.46 | 5.93 | 44.3 |
| | 0.6 | 354 | 104 | 149 | 0.41 | 5.29 | 51.2 |
| | 0.8 | 358 | 99 | 146 | 0.21 | 2.71 | 75.2 |
| | 1.0 | 363 | 94 | 141 | 0.17 | 2.19 | 79.5 |

Table 3.34: Results of potentiodynamic polarization studies for the corrosion of welded maraging steel in 0.5 M hydrochloric acid containing different concentrations of PNPT.

| Temperature (°C) | Conc. of inhibitor (mM) | $-E_{corr}$ (mV /SCE) | b_a (mV dec ⁻¹) | $-b_c$ (mV dec ⁻¹) | i_{corr} (mA cm ⁻²) | U_{corr} (mm y ⁻¹) | η (%) |
|------------------|-------------------------|-----------------------|-------------------------------|--------------------------------|-----------------------------------|----------------------------------|------------|
| 30 | Blank | 315 | 103 | 149 | 0.35 | 4.51 | |
| | 0.2 | 328 | 98 | 138 | 0.18 | 2.29 | 49.3 |
| | 0.4 | 334 | 95 | 134 | 0.17 | 2.20 | 51.2 |
| | 0.6 | 338 | 93 | 129 | 0.14 | 1.86 | 58.7 |
| | 0.8 | 339 | 82 | 113 | 0.07 | 0.93 | 79.4 |
| | 1.0 | 342 | 76 | 104 | 0.04 | 0.57 | 87.4 |
| | 35 | Blank | 323 | 105 | 152 | 0.48 | 6.19 |
| 0.2 | | 341 | 103 | 147 | 0.27 | 3.48 | 43.8 |
| 0.4 | | 344 | 98 | 144 | 0.25 | 3.27 | 47.1 |
| 0.6 | | 346 | 93 | 142 | 0.23 | 2.97 | 52.0 |
| 0.8 | | 349 | 85 | 139 | 0.12 | 1.53 | 75.2 |
| 1.0 | | 351 | 79 | 128 | 0.08 | 0.97 | 84.3 |
| 40 | | Blank | 330 | 112 | 158 | 0.6 | 7.73 |
| | 0.2 | 339 | 108 | 155 | 0.35 | 4.51 | 41.7 |
| | 0.4 | 341 | 103 | 151 | 0.33 | 4.31 | 44.3 |
| | 0.6 | 343 | 94 | 146 | 0.29 | 3.74 | 51.6 |
| | 0.8 | 346 | 92 | 142 | 0.17 | 2.20 | 71.4 |
| | 1.0 | 348 | 89 | 139 | 0.11 | 1.43 | 81.5 |
| | 45 | Blank | 328 | 116 | 165 | 0.77 | 9.93 |
| 0.2 | | 343 | 112 | 163 | 0.47 | 6.01 | 39.4 |
| 0.4 | | 347 | 109 | 159 | 0.44 | 5.71 | 42.5 |
| 0.6 | | 353 | 104 | 155 | 0.40 | 5.13 | 48.3 |
| 0.8 | | 362 | 101 | 151 | 0.25 | 3.17 | 68.1 |
| 1.0 | | 365 | 95 | 147 | 0.17 | 2.14 | 78.4 |
| 50 | | Blank | 324 | 118 | 173 | 1.03 | 13.28 |
| | 0.2 | 352 | 113 | 162 | 0.64 | 8.22 | 38.1 |
| | 0.4 | 357 | 110 | 157 | 0.60 | 7.74 | 41.7 |
| | 0.6 | 363 | 107 | 153 | 0.55 | 7.13 | 46.3 |
| | 0.8 | 367 | 104 | 149 | 0.35 | 4.53 | 65.9 |
| | 1.0 | 371 | 102 | 147 | 0.24 | 3.17 | 76.1 |

Table 3.35: Results of potentiodynamic polarization studies for the corrosion of welded maraging steel in 1.0 M hydrochloric acid containing different concentrations of PNPT.

| Temperature (°C) | Conc. of inhibitor (mM) | $-E_{corr}$ (mV /SCE) | b_a (mV dec ⁻¹) | $-b_c$ (mV dec ⁻¹) | i_{corr} (mA cm ⁻²) | ν_{corr} (mm y ⁻¹) | η (%) |
|------------------|-------------------------|-----------------------|-------------------------------|--------------------------------|-----------------------------------|------------------------------------|------------|
| 30 | Blank | 324 | 112 | 158 | 0.51 | 6.57 | |
| | 0.2 | 388 | 109 | 143 | 0.26 | 3.37 | 48.7 |
| | 0.4 | 383 | 104 | 140 | 0.26 | 3.34 | 49.2 |
| | 0.6 | 361 | 101 | 136 | 0.23 | 3.01 | 54.2 |
| | 0.8 | 362 | 98 | 128 | 0.12 | 1.56 | 76.3 |
| | 1.0 | 376 | 91 | 121 | 0.07 | 0.93 | 85.8 |
| | 35 | Blank | 328 | 118 | 163 | 0.68 | 8.77 |
| 0.2 | | 337 | 113 | 159 | 0.39 | 5.05 | 42.4 |
| 0.4 | | 339 | 109 | 153 | 0.37 | 4.79 | 45.3 |
| 0.6 | | 344 | 102 | 148 | 0.31 | 4.05 | 53.8 |
| 0.8 | | 349 | 97 | 142 | 0.16 | 2.11 | 75.9 |
| 1.0 | | 353 | 84 | 134 | 0.11 | 1.43 | 83.7 |
| 40 | | Blank | 336 | 126 | 171 | 0.95 | 12.25 |
| | 0.2 | 341 | 121 | 164 | 0.58 | 7.45 | 39.2 |
| | 0.4 | 344 | 116 | 163 | 0.53 | 6.88 | 43.8 |
| | 0.6 | 351 | 112 | 157 | 0.47 | 6.10 | 50.2 |
| | 0.8 | 352 | 106 | 148 | 0.30 | 3.87 | 68.3 |
| | 1.0 | 358 | 98 | 142 | 0.19 | 2.52 | 79.4 |
| | 45 | Blank | 331 | 131 | 179 | 1.07 | 13.79 |
| 0.2 | | 339 | 124 | 168 | 0.66 | 8.45 | 38.7 |
| 0.4 | | 341 | 117 | 164 | 0.64 | 8.19 | 40.6 |
| 0.6 | | 347 | 113 | 163 | 0.56 | 7.27 | 47.3 |
| 0.8 | | 353 | 108 | 158 | 0.36 | 4.62 | 66.5 |
| 1.0 | | 357 | 102 | 153 | 0.27 | 3.54 | 74.3 |
| 50 | | Blank | 328 | 142 | 191 | 1.75 | 22.56 |
| | 0.2 | 343 | 124 | 168 | 1.11 | 14.37 | 36.3 |
| | 0.4 | 348 | 117 | 164 | 1.07 | 13.74 | 39.1 |
| | 0.6 | 349 | 113 | 163 | 0.98 | 12.59 | 44.2 |
| | 0.8 | 356 | 108 | 158 | 0.64 | 8.19 | 63.7 |
| | 1.0 | 361 | 102 | 153 | 0.48 | 6.25 | 72.3 |

Table 3.36: Results of potentiodynamic polarization studies for the corrosion of welded maraging steel in 1.5 M hydrochloric acid containing different concentrations of PNPT.

| Temperature (°C) | Conc. of inhibitor (mM) | $-E_{corr}$ (mV /SCE) | b_a (mV dec ⁻¹) | $-b_c$ (mV dec ⁻¹) | i_{corr} (mA cm ⁻²) | \mathcal{U}_{corr} (mm y ⁻¹) | η (%) |
|------------------|-------------------------|-----------------------|-------------------------------|--------------------------------|-----------------------------------|--|------------|
| 30 | Blank | 316 | 109 | 163 | 0.57 | 7.35 | |
| | 0.2 | 343 | 107 | 154 | 0.32 | 4.09 | 44.3 |
| | 0.4 | 344 | 105 | 151 | 0.30 | 3.86 | 47.5 |
| | 0.6 | 347 | 104 | 143 | 0.27 | 3.45 | 53.0 |
| | 0.8 | 351 | 101 | 137 | 0.14 | 1.85 | 74.8 |
| | 1.0 | 352 | 94 | 129 | 0.10 | 1.23 | 83.2 |
| 35 | Blank | 320 | 117 | 171 | 0.98 | 12.63 | |
| | 0.2 | 343 | 107 | 154 | 0.58 | 7.45 | 41.0 |
| | 0.4 | 346 | 105 | 151 | 0.55 | 7.09 | 43.9 |
| | 0.6 | 348 | 104 | 143 | 0.47 | 6.01 | 52.4 |
| | 0.8 | 353 | 101 | 137 | 0.26 | 3.32 | 73.7 |
| | 1.0 | 354 | 94 | 129 | 0.18 | 2.26 | 82.1 |
| 40 | Blank | 328 | 124 | 183 | 1.31 | 16.89 | |
| | 0.2 | 339 | 122 | 171 | 0.81 | 10.50 | 37.8 |
| | 0.4 | 343 | 118 | 169 | 0.76 | 9.76 | 42.2 |
| | 0.6 | 346 | 115 | 163 | 0.67 | 8.60 | 49.1 |
| | 0.8 | 351 | 108 | 155 | 0.44 | 5.71 | 66.2 |
| | 1.0 | 362 | 103 | 147 | 0.32 | 4.17 | 75.3 |
| 45 | Blank | 322 | 132 | 198 | 1.80 | 23.20 | |
| | 0.2 | 341 | 128 | 183 | 1.17 | 15.06 | 35.1 |
| | 0.4 | 343 | 123 | 178 | 1.09 | 14.08 | 39.3 |
| | 0.6 | 348 | 121 | 172 | 0.97 | 12.46 | 46.3 |
| | 0.8 | 351 | 113 | 164 | 0.66 | 8.56 | 63.1 |
| | 1.0 | 358 | 109 | 159 | 0.45 | 5.82 | 74.9 |
| 50 | Blank | 315 | 147 | 209 | 2.63 | 33.90 | |
| | 0.2 | 339 | 138 | 201 | 1.71 | 22.07 | 34.9 |
| | 0.4 | 343 | 135 | 192 | 1.62 | 20.88 | 38.4 |
| | 0.6 | 348 | 128 | 189 | 1.48 | 19.02 | 43.9 |
| | 0.8 | 355 | 121 | 172 | 1.00 | 12.85 | 62.1 |
| | 1.0 | 361 | 114 | 164 | 1.74 | 9.59 | 71.7 |

Table 3.37: Results of potentiodynamic polarization studies for the corrosion of welded maraging steel in 2.0 M hydrochloric acid containing different concentrations of PNPT.

| Temperature (°C) | Conc. of inhibitor (mM) | $-E_{corr}$ (mV /SCE) | b_a (mV dec ⁻¹) | $-b_c$ (mV dec ⁻¹) | i_{corr} (mA cm ⁻²) | ν_{corr} (mm y ⁻¹) | η (%) |
|------------------|-------------------------|-----------------------|-------------------------------|--------------------------------|-----------------------------------|------------------------------------|------------|
| 30 | Blank | 324 | 114 | 178 | 0.90 | 11.60 | |
| | 0.2 | 351 | 112 | 163 | 0.51 | 6.64 | 42.8 |
| | 0.4 | 355 | 109 | 157 | 0.49 | 6.25 | 46.1 |
| | 0.6 | 357 | 105 | 148 | 0.43 | 5.59 | 51.8 |
| | 0.8 | 356 | 103 | 142 | 0.24 | 3.05 | 73.7 |
| | 1.0 | 363 | 99 | 134 | 0.17 | 2.19 | 81.1 |
| | 35 | Blank | 316 | 129 | 186 | 1.34 | 17.27 |
| 0.2 | | 357 | 119 | 173 | 0.81 | 10.48 | 39.3 |
| 0.4 | | 359 | 114 | 161 | 0.78 | 10.00 | 42.1 |
| 0.6 | | 361 | 109 | 157 | 0.66 | 8.52 | 50.7 |
| 0.8 | | 364 | 107 | 143 | 0.38 | 4.94 | 71.4 |
| 1.0 | | 367 | 99 | 132 | 0.27 | 3.42 | 80.2 |
| 40 | | Blank | 310 | 137 | 193 | 2.61 | 33.64 |
| | 0.2 | 363 | 131 | 183 | 1.68 | 21.63 | 35.7 |
| | 0.4 | 365 | 123 | 175 | 1.56 | 20.05 | 40.4 |
| | 0.6 | 357 | 119 | 172 | 1.38 | 17.73 | 47.3 |
| | 0.8 | 360 | 113 | 163 | 0.93 | 12.01 | 64.3 |
| | 1.0 | 368 | 108 | 148 | 0.69 | 8.85 | 73.7 |
| | 45 | Blank | 327 | 143 | 212 | 4.46 | 57.49 |
| 0.2 | | 364 | 136 | 194 | 2.97 | 38.29 | 33.4 |
| 0.4 | | 367 | 132 | 183 | 2.81 | 36.16 | 37.1 |
| 0.6 | | 369 | 129 | 172 | 2.47 | 31.79 | 44.7 |
| 0.8 | | 371 | 124 | 167 | 1.77 | 22.82 | 60.3 |
| 1.0 | | 371 | 119 | 162 | 1.24 | 15.92 | 72.3 |
| 50 | | Blank | 332 | 159 | 223 | 5.93 | 76.44 |
| | 0.2 | 344 | 143 | 217 | 3.97 | 51.14 | 33.1 |
| | 0.4 | 348 | 137 | 204 | 3.78 | 48.69 | 36.3 |
| | 0.6 | 348 | 131 | 197 | 3.46 | 44.56 | 41.7 |
| | 0.8 | 363 | 127 | 188 | 2.47 | 31.88 | 58.3 |
| | 1.0 | 369 | 121 | 179 | 1.70 | 21.86 | 71.4 |

Table 3.38: EIS data for the corrosion of welded maraging steel in 0.1 M hydrochloric acid containing different concentrations of PNPT.

| Temperature (°C) | Conc. of inhibitor (mM) | R_p (ohm. cm ²) | C_{dl} (mF cm ⁻²) | η (%) |
|------------------|-------------------------|-------------------------------|---------------------------------|------------|
| 30 | Blank | 80.6 | 0.061 | |
| | 0.2 | 170.4 | 0.054 | 52.7 |
| | 0.4 | 193.3 | 0.053 | 58.3 |
| | 0.6 | 208.8 | 0.050 | 61.4 |
| | 0.8 | 533.8 | 0.048 | 84.9 |
| | 1.0 | 739.4 | 0.043 | 89.1 |
| 35 | Blank | 71.8 | 0.069 | |
| | 0.2 | 126.2 | 0.063 | 43.1 |
| | 0.4 | 140.1 | 0.059 | 48.8 |
| | 0.6 | 169.3 | 0.055 | 57.6 |
| | 0.8 | 419.9 | 0.053 | 82.9 |
| | 1.0 | 619.0 | 0.048 | 88.4 |
| 40 | Blank | 56.4 | 0.135 | |
| | 0.2 | 102.0 | 0.133 | 44.7 |
| | 0.4 | 106.2 | 0.129 | 46.9 |
| | 0.6 | 122.9 | 0.127 | 54.1 |
| | 0.8 | 240.0 | 0.123 | 76.5 |
| | 1.0 | 339.8 | 0.116 | 83.4 |
| 45 | Blank | 41.3 | 0.183 | |
| | 0.2 | 72.4 | 0.175 | 42.9 |
| | 0.4 | 75.5 | 0.173 | 45.3 |
| | 0.6 | 85.9 | 0.169 | 51.9 |
| | 0.8 | 174.3 | 0.165 | 76.3 |
| | 1.0 | 225.7 | 0.159 | 81.7 |
| 50 | Blank | 34.5 | 0.224 | |
| | 0.2 | 58.5 | 0.219 | 41.0 |
| | 0.4 | 61.4 | 0.216 | 43.8 |
| | 0.6 | 67.1 | 0.212 | 48.6 |
| | 0.8 | 137.5 | 0.209 | 74.9 |
| | 1.0 | 162.0 | 0.203 | 78.7 |

Table 3.39: EIS data for the corrosion of welded maraging steel in 0.5 M hydrochloric acid containing different concentrations of PNPT.

| Temperature (°C) | Conc. of inhibitor (mM) | R_p (ohm. cm ²) | C_{dl} (mF cm ⁻²) | η (%) |
|------------------|-------------------------|-------------------------------|---------------------------------|------------|
| 30 | Blank | 73.8 | 0.071 | |
| | 0.2 | 144.4 | 0.069 | 48.9 |
| | 0.4 | 148.8 | 0.064 | 50.4 |
| | 0.6 | 170.4 | 0.059 | 56.7 |
| | 0.8 | 344.9 | 0.057 | 78.6 |
| | 1.0 | 572.1 | 0.052 | 87.1 |
| | 35 | Blank | 55.4 | 0.112 |
| 0.2 | | 96.5 | 0.107 | 42.6 |
| 0.4 | | 103.2 | 0.104 | 46.3 |
| 0.6 | | 114.0 | 0.101 | 51.4 |
| 0.8 | | 212.3 | 0.097 | 73.9 |
| 1.0 | | 309.5 | 0.094 | 82.1 |
| 40 | | Blank | 47.1 | 0.165 |
| | 0.2 | 81.6 | 0.161 | 42.3 |
| | 0.4 | 82.8 | 0.157 | 43.1 |
| | 0.6 | 95.0 | 0.154 | 50.4 |
| | 0.8 | 157.5 | 0.152 | 70.1 |
| | 1.0 | 227.5 | 0.147 | 79.3 |
| | 45 | Blank | 38.0 | 0.216 |
| 0.2 | | 61.7 | 0.212 | 38.4 |
| 0.4 | | 66.8 | 0.207 | 43.1 |
| 0.6 | | 72.2 | 0.203 | 47.4 |
| 0.8 | | 103.3 | 0.195 | 63.2 |
| 1.0 | | 173.5 | 0.191 | 78.1 |
| 50 | | Blank | 29.6 | 0.279 |
| | 0.2 | 47.4 | 0.273 | 37.6 |
| | 0.4 | 50.0 | 0.269 | 40.8 |
| | 0.6 | 53.9 | 0.266 | 45.1 |
| | 0.8 | 80.9 | 0.263 | 63.4 |
| | 1.0 | 117.8 | 0.258 | 74.9 |

Table 3.40: EIS data for the corrosion of welded maraging steel in 1.0 M hydrochloric acid containing different concentrations of PNPT.

| Temperature (°C) | Conc. of inhibitor (mM) | R_p (ohm. cm ²) | C_{dl} (mF cm ⁻²) | η (%) |
|------------------|-------------------------|-------------------------------|---------------------------------|------------|
| 30 | Blank | 56.1 | 0.110 | |
| | 0.2 | 106.5 | 0.106 | 47.3 |
| | 0.4 | 108.7 | 0.103 | 48.4 |
| | 0.6 | 119.6 | 0.098 | 53.1 |
| | 0.8 | 228.0 | 0.095 | 75.4 |
| | 1.0 | 357.3 | 0.093 | 84.3 |
| | 35 | Blank | 43.2 | 0.203 |
| 0.2 | | 73.0 | 0.197 | 40.8 |
| 0.4 | | 75.9 | 0.195 | 43.1 |
| 0.6 | | 89.4 | 0.193 | 51.7 |
| 0.8 | | 161.2 | 0.187 | 73.2 |
| 1.0 | | 232.3 | 0.182 | 81.4 |
| 40 | | Blank | 32.9 | 0.276 |
| | 0.2 | 52.6 | 0.264 | 37.4 |
| | 0.4 | 56.8 | 0.261 | 42.1 |
| | 0.6 | 65.4 | 0.254 | 49.7 |
| | 0.8 | 97.9 | 0.251 | 66.4 |
| | 1.0 | 150.2 | 0.246 | 78.1 |
| | 45 | Blank | 30.6 | 0.308 |
| 0.2 | | 48.4 | 0.301 | 36.8 |
| 0.4 | | 50.2 | 0.293 | 39.1 |
| 0.6 | | 57.1 | 0.285 | 46.4 |
| 0.8 | | 84.5 | 0.279 | 63.8 |
| 1.0 | | 122.9 | 0.271 | 75.1 |
| 50 | | Blank | 20.2 | 0.346 |
| | 0.2 | 31.4 | 0.341 | 35.7 |
| | 0.4 | 32.8 | 0.336 | 38.4 |
| | 0.6 | 34.9 | 0.334 | 42.1 |
| | 0.8 | 52.9 | 0.330 | 61.8 |
| | 1.0 | 68.2 | 0.324 | 70.4 |

Table 3.41: EIS data for the corrosion of welded maraging steel in 1.5 M hydrochloric acid containing different concentrations of PNPT.

| Temperature (°C) | Conc. of inhibitor (mM) | R_p (ohm. cm ²) | C_{dl} (mF cm ⁻²) | η (%) |
|------------------|-------------------------|-------------------------------|---------------------------------|------------|
| 30 | Blank | 49.2 | 0.166 | |
| | 0.2 | 86.6 | 0.162 | 43.2 |
| | 0.4 | 92.3 | 0.157 | 46.7 |
| | 0.6 | 102.1 | 0.154 | 51.8 |
| | 0.8 | 183.6 | 0.152 | 73.2 |
| | 1.0 | 268.9 | 0.147 | 81.7 |
| | 35 | Blank | 30.6 | 0.315 |
| 0.2 | | 52.0 | 0.312 | 41.2 |
| 0.4 | | 53.0 | 0.310 | 42.3 |
| 0.6 | | 63.5 | 0.307 | 51.8 |
| 0.8 | | 106.6 | 0.304 | 71.3 |
| 1.0 | | 161.1 | 0.301 | 81.0 |
| 40 | | Blank | 24.5 | 0.378 |
| | 0.2 | 38.5 | 0.374 | 36.4 |
| | 0.4 | 42.0 | 0.372 | 41.7 |
| | 0.6 | 46.7 | 0.371 | 47.5 |
| | 0.8 | 70.4 | 0.366 | 65.2 |
| | 1.0 | 98.4 | 0.364 | 75.1 |
| | 45 | Blank | 19.1 | 0.395 |
| 0.2 | | 29.0 | 0.392 | 34.2 |
| 0.4 | | 31.2 | 0.387 | 38.7 |
| 0.6 | | 35.3 | 0.381 | 45.9 |
| 0.8 | | 50.0 | 0.379 | 61.8 |
| 1.0 | | 71.3 | 0.376 | 73.2 |
| 50 | | Blank | 14.2 | 0.402 |
| | 0.2 | 21.3 | 0.393 | 33.2 |
| | 0.4 | 22.5 | 0.391 | 36.8 |
| | 0.6 | 24.3 | 0.384 | 41.6 |
| | 0.8 | 37.1 | 0.382 | 61.7 |
| | 1.0 | 48.8 | 0.374 | 70.9 |

Table 3.42: EIS data for the corrosion of welded maraging steel in 2.0 M hydrochloric acid containing different concentrations of PNPT.

| Temperature (°C) | Conc. of inhibitor (mM) | R_p (ohm. cm ²) | C_{dl} (mF cm ⁻²) | η (%) |
|------------------|-------------------------|-------------------------------|---------------------------------|------------|
| 30 | Blank | 33.6 | 0.248 | |
| | 0.2 | 56.9 | 0.243 | 40.9 |
| | 0.4 | 60.9 | 0.239 | 44.8 |
| | 0.6 | 68.4 | 0.232 | 50.9 |
| | 0.8 | 119.1 | 0.228 | 71.8 |
| | 1.0 | 170.6 | 0.221 | 80.3 |
| 35 | Blank | 24.5 | 0.362 | |
| | 0.2 | 39.0 | 0.358 | 37.1 |
| | 0.4 | 41.5 | 0.351 | 40.9 |
| | 0.6 | 48.8 | 0.347 | 49.8 |
| | 0.8 | 82.5 | 0.344 | 70.3 |
| | 1.0 | 121.3 | 0.338 | 79.8 |
| 40 | Blank | 13.3 | 0.399 | |
| | 0.2 | 20.2 | 0.393 | 34.2 |
| | 0.4 | 21.6 | 0.387 | 38.4 |
| | 0.6 | 24.9 | 0.385 | 46.5 |
| | 0.8 | 35.8 | 0.383 | 62.8 |
| | 1.0 | 49.6 | 0.381 | 73.2 |
| 45 | Blank | 8.3 | 0.418 | |
| | 0.2 | 12.6 | 0.414 | 33.9 |
| | 0.4 | 13.0 | 0.411 | 36.2 |
| | 0.6 | 14.6 | 0.405 | 43.1 |
| | 0.8 | 21.1 | 0.403 | 60.6 |
| | 1.0 | 29.0 | 0.394 | 71.4 |
| 50 | Blank | 6.8 | 0.439 | |
| | 0.2 | 10.2 | 0.432 | 33.4 |
| | 0.4 | 10.5 | 0.431 | 35.2 |
| | 0.6 | 11.4 | 0.426 | 40.2 |
| | 0.8 | 16.0 | 0.423 | 57.5 |
| | 1.0 | 23.2 | 0.417 | 70.7 |

Table 3.43: Activation parameters for the corrosion of welded maraging steel in hydrochloric acid containing different concentrations of PNPT.

| Molarity of HCl (M) | Conc. of inhibitor (mM) | E_a (kJ mol ⁻¹) | ΔH^\ddagger (kJ mol ⁻¹) | ΔS^\ddagger (J mol ⁻¹ K ⁻¹) |
|------------------------|----------------------------|----------------------------------|--|---|
| 0.1 | Blank | 42.28 | 39.62 | -103.29 |
| | 0.2 | 50.78 | 48.18 | -81.18 |
| | 0.4 | 53.36 | 50.76 | -73.45 |
| | 0.6 | 54.35 | 51.75 | -71.45 |
| | 0.8 | 66.73 | 64.13 | -38.61 |
| | 1.0 | 74.99 | 72.39 | -14.83 |
| 0.5 | Blank | 42.97 | 39.37 | -102.37 |
| | 0.2 | 50.53 | 47.93 | -79.68 |
| | 0.4 | 50.05 | 47.45 | -81.68 |
| | 0.6 | 52.67 | 50.07 | -74.28 |
| | 0.8 | 63.45 | 60.85 | -44.51 |
| | 1.0 | 68.73 | 66.18 | -30.96 |
| 1.0 | Blank | 47.51 | 44.97 | -81.34 |
| | 0.2 | 56.47 | 54.87 | -60.47 |
| | 0.4 | 58.47 | 58.87 | -57.81 |
| | 0.6 | 69.79 | 67.19 | -31.29 |
| | 0.8 | 79.77 | 77.17 | -21.31 |
| | 1.0 | 97.18 | 95.58 | -18.66 |
| 1.5 | Blank | 59.37 | 56.78 | -40.52 |
| | 0.2 | 48.15 | 50.74 | -82.67 |
| | 0.4 | 51.42 | 53.97 | -74.52 |
| | 0.6 | 58.59 | 61.20 | -53.07 |
| | 0.8 | 70.61 | 73.22 | -22.97 |
| | 1.0 | 76.66 | 79.26 | -6.35 |
| 2.0 | Blank | 80.98 | 78.36 | -33.72 |
| | 0.2 | 18.16 | 15.77 | -169.5 |
| | 0.4 | 18.94 | 16.35 | -164.8 |
| | 0.6 | 27.89 | 25.29 | -130.4 |
| | 0.8 | 38.29 | 35.67 | -112.4 |
| | 1.0 | 40.52 | 37.92 | -107.1 |

Table 3.44: Maximum inhibition efficiency attained in different concentrations of hydrochloric acid at different temperatures for PNPT.

| Temperature (°C) | Welded Maraging Steel | | | |
|---------------------|--|----------------------------------|---|------------|
| | Hydrochloric acid concentration (M) | Concentration of PNPT (mM) | η (%) | |
| | | | Potentiodynamic polarization method | EIS method |
| 30 | 0.1 | 1.0 | 90.3 | 89.1 |
| | 0.5 | | 87.4 | 87.1 |
| | 1.0 | | 85.8 | 84.3 |
| | 1.5 | | 83.2 | 81.7 |
| | 2.0 | | 81.1 | 80.3 |
| 35 | 0.1 | 1.0 | 88.8 | 88.4 |
| | 0.5 | | 84.3 | 82.1 |
| | 1.0 | | 83.7 | 81.4 |
| | 1.5 | | 82.1 | 81.0 |
| | 2.0 | | 80.2 | 79.8 |
| 40 | 0.1 | 1.0 | 84.5 | 83.4 |
| | 0.5 | | 81.5 | 79.3 |
| | 1.0 | | 79.4 | 78.1 |
| | 1.5 | | 75.3 | 75.1 |
| | 2.0 | | 73.7 | 73.2 |
| 45 | 0.1 | 1.0 | 82.7 | 81.7 |
| | 0.5 | | 78.4 | 78.1 |
| | 1.0 | | 74.3 | 75.1 |
| | 1.5 | | 74.9 | 73.2 |
| | 2.0 | | 72.3 | 71.4 |
| 50 | 0.1 | 1.0 | 79.5 | 78.7 |
| | 0.5 | | 76.1 | 74.9 |
| | 1.0 | | 72.3 | 70.4 |
| | 1.5 | | 71.7 | 70.9 |
| | 2.0 | | 71.4 | 70.7 |

Table 3.45: Thermodynamic parameters for the adsorption of PNPT on welded maraging steel surface in hydrochloric acid at different temperatures.

| Molarity of HCl (M) | Temperature (° C) | $-\Delta G^{\circ}_{ads}$ (kJ mol ⁻¹) | ΔH°_{ads} (kJ mol ⁻¹) | ΔS°_{ads} (J mol ⁻¹ K ⁻¹) |
|------------------------|----------------------|--|---|--|
| 0.1 | 30 | 39.71 | -18.75 | -76.6 |
| | 35 | 39.07 | | |
| | 40 | 38.54 | | |
| | 45 | 38.08 | | |
| | 50 | 37.67 | | |
| 0.5 | 30 | 36.24 | -16.82 | -83.0 |
| | 35 | 36.02 | | |
| | 40 | 35.18 | | |
| | 45 | 34.67 | | |
| | 50 | 34.41 | | |
| 1.0 | 30 | 33.84 | - 38.21 | -56.13 |
| | 35 | 32.70 | | |
| | 40 | 31.69 | | |
| | 45 | 31.43 | | |
| | 50 | 30.57 | | |
| 1.5 | 30 | 31.81 | - 29.14 | -57.23 |
| | 35 | 31.31 | | |
| | 40 | 31.17 | | |
| | 45 | 30.80 | | |
| | 50 | 30.63 | | |
| 2.0 | 30 | 31.49 | -33.21 | -66.20 |
| | 35 | 31.22 | | |
| | 40 | 30.79 | | |
| | 45 | 30.51 | | |
| | 50 | 30.19 | | |

3.6 1-PHENYL-4-(4-NITROPHENYL) THIOSEMICARBAZIDE (PNPT) AS INHIBITOR FOR THE CORROSION OF WELDED MARAGING STEEL IN SULPHURIC ACID MEDIUM

3.6.1 Potentiodynamic polarization measurements

The potentiodynamic polarization curves for the corrosion of welded maraging steel in 1.0 M sulphuric acid in the presence of different concentrations of PNPT, at 30 °C are shown in Fig. 3.44. Similar results were obtained at other temperatures and also in the other four concentrations of sulphuric acid. The potentiodynamic polarization parameters such as corrosion potential (E_{corr}), corrosion current density (i_{corr}), anodic and cathodic Tafel slopes (b_a , b_c) were calculated from Tafel plots in the presence of different concentrations of PNPT at different temperatures are summarized in Tables 3.46 to 3.50.

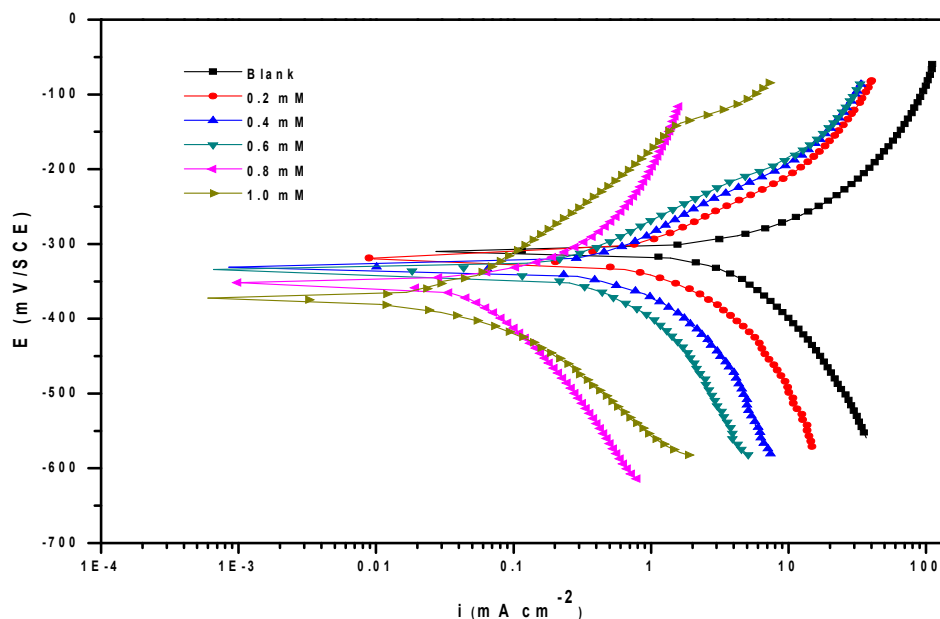


Fig. 3.44: Potentiodynamic polarization curves for the corrosion of welded maraging steel in 1.0 M H₂SO₄ containing different concentrations of PNPT at 30 °C.

Inhibition efficiency increases with the increase in PNPT concentration. There is only a slight shift in E_{corr} value towards more negative side in the presence of inhibitor,

which implies that the inhibitor, PNPT, acts as a mixed type inhibitor, affecting both metal dissolution and hydrogen evolution reactions with predominant cathodic action.

3.6.2 Electrochemical impedance spectroscopy (EIS) studies

Nyquist plots for the corrosion of welded maraging steel in 1.0 M sulphuric acid solution in the presence of different concentrations of PNPT are shown in Fig. 3.40. Similar plots were obtained in other concentrations of sulphuric acid and also at other temperatures. The experimental results of EIS measurements obtained for the corrosion of welded maraging steel in various concentration of sulphuric acid are summarized in Tables 3.51 to 3.55. The equivalent circuit given in Fig. 3.29 is used to fit the experimental data for the corrosion of welded maraging steel in sulphuric acid in the presence of PNPT.

As seen from Fig. 3.45 the Nyquist plots are semi-circular in the presence as well as in the absence of inhibitor. This indicates that the corrosion of welded maraging steel is controlled by a charge transfer process and the addition of PNPT does not change the reaction mechanism of the corrosion of sample in H_2SO_4 solution (Amin et al. 2007). The charge transfer resistance (R_{ct}) increases and double layer capacitance decreases with the increase in the concentration of PNPT, indicating an increase in the inhibition efficiency. PNPT inhibits the corrosion primarily through its adsorption and subsequent formation of a barrier film on the metal surface (El Hosary et al. 1972, Sanaa et al. 2008). This is in accordance with the observations of potentiodynamic polarization measurements.

The Bode plots of phase angle and amplitude for the corrosion of the alloy in the presence of PNPT in 1.0 M sulphuric acid are shown in Fig. 3.46 (a) and Fig. 3.46 (b), respectively. Phase angle increases with increase in concentrations of PNPT in sulphuric acid medium. The difference between the HF and LF for the inhibited system in the Bode plot increases with increase in the concentration of PNPT. The increase in phase angle with the increase in PNPT concentration suggests decrease in corrosion rate. An increase in PNPT concentration leads to an increase in the $|Z|$ value.

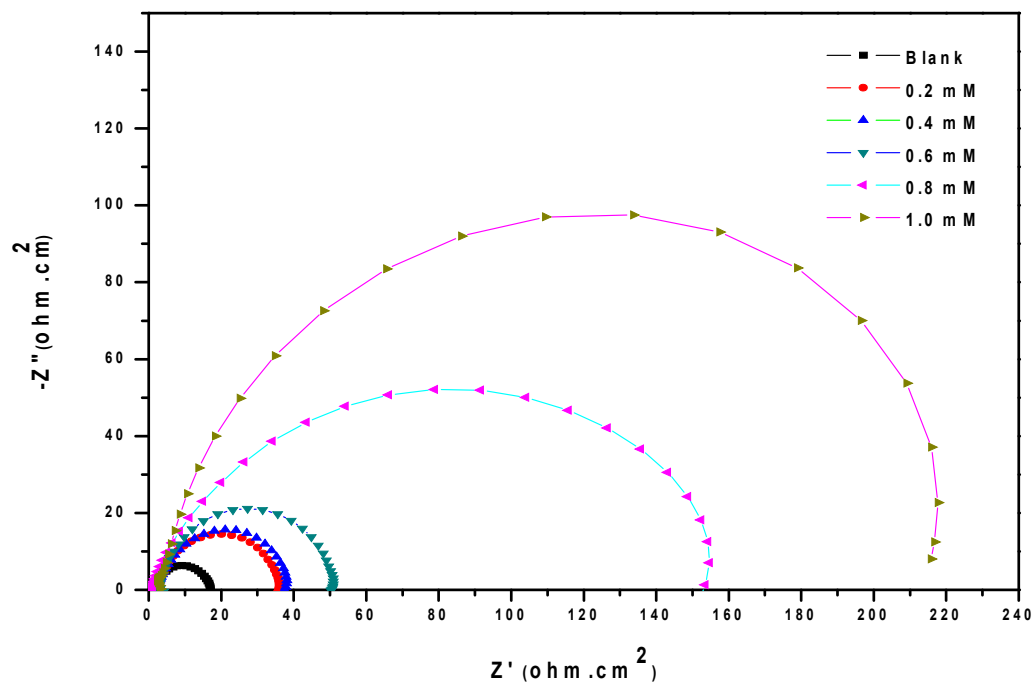


Fig. 3.45: Nyquist plots for the corrosion of welded maraging steel in 1.0 M H₂SO₄ containing different concentrations of PNPT at 30 °C.

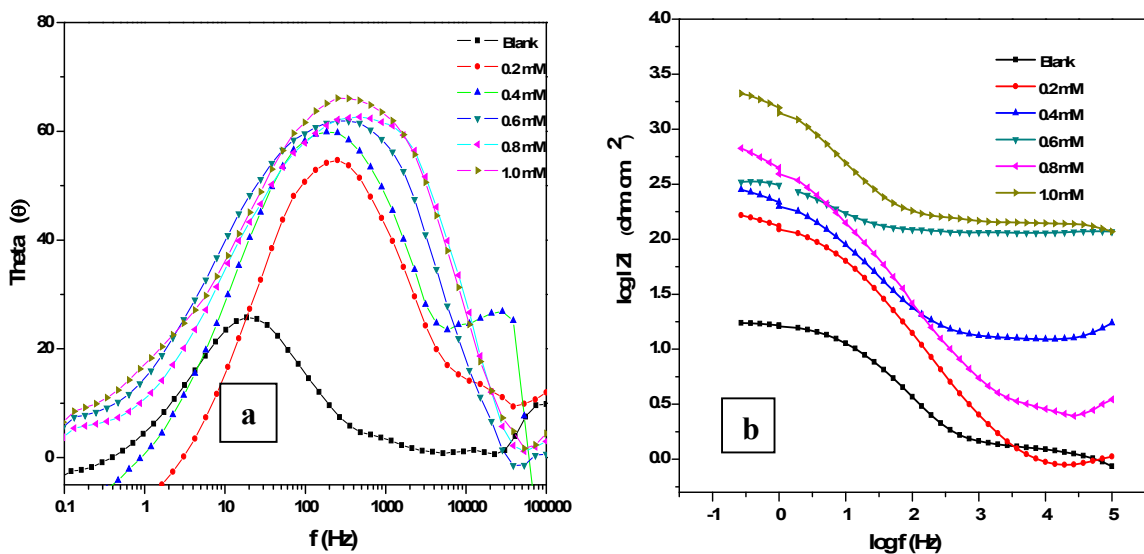


Fig. 3.46: Bode (a) phase angle plots and (b) amplitude plots for the corrosion of welded maraging steel in 1.0 M H₂SO₄ containing different concentrations of PNPT at 30 °C.

3.6.3 Effect of temperature

The Potentiodynamic polarization and EIS results pertaining to different temperatures in different concentrations of sulphuric acid have been listed in the Tables 3.46 to 3.55. The decrease in inhibition efficiency with the increase in temperature indicates desorption of the inhibitor molecules from the metal surface on increasing the temperature (Poornima et al. 2011). This fact is also suggestive of physisorption of the inhibitor molecules on the metal surface.

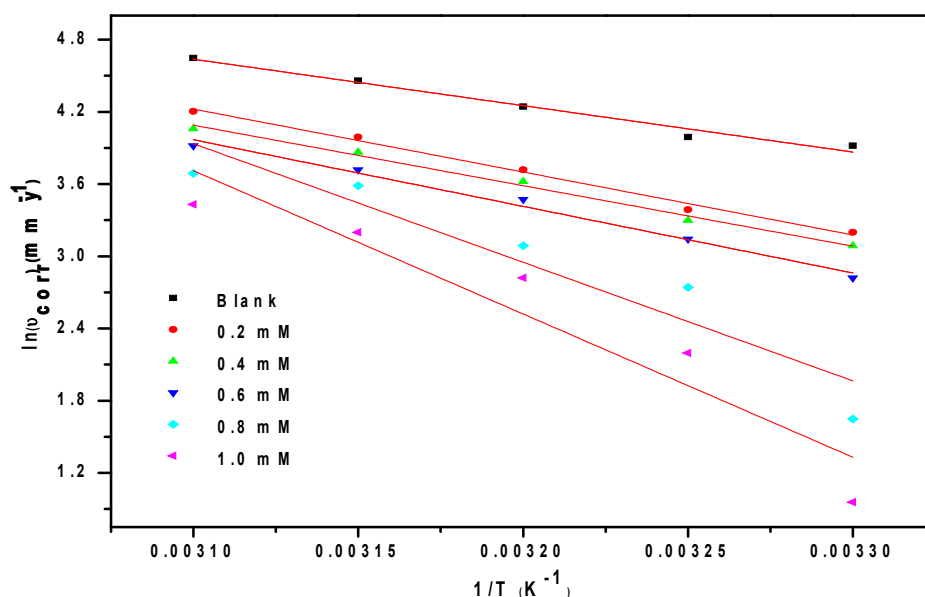


Fig. 3.47: Arrhenius plots for the corrosion of welded maraging steel in 1.0 M H₂SO₄ containing different concentrations of PNPT.

The Arrhenius plots for the corrosion of welded maraging steel in the presence of different concentrations of PNPT in 1.0 M H₂SO₄ acid are shown in Fig. 3.47. The plots of $\ln(v_{\text{corr}}/T)$ versus $1/T$ in 1.0 M H₂SO₄ acid in the presence of various concentrations of PNPT are shown in Fig. 3.48. The calculated values of E_a , ΔH^\ddagger and ΔS^\ddagger are given in Table 3.56. The proportionate increase in the activation energy on the addition of PNPT can be attributed to the increased adsorption of PNPT providing a barrier on the alloy surface (Avci et al. 2008). The values of entropy of activation indicates that the activated

complex in the rate determining step represents an association rather than dissociation, resulting in a decrease in randomness on going from the reactants to the activated complex.

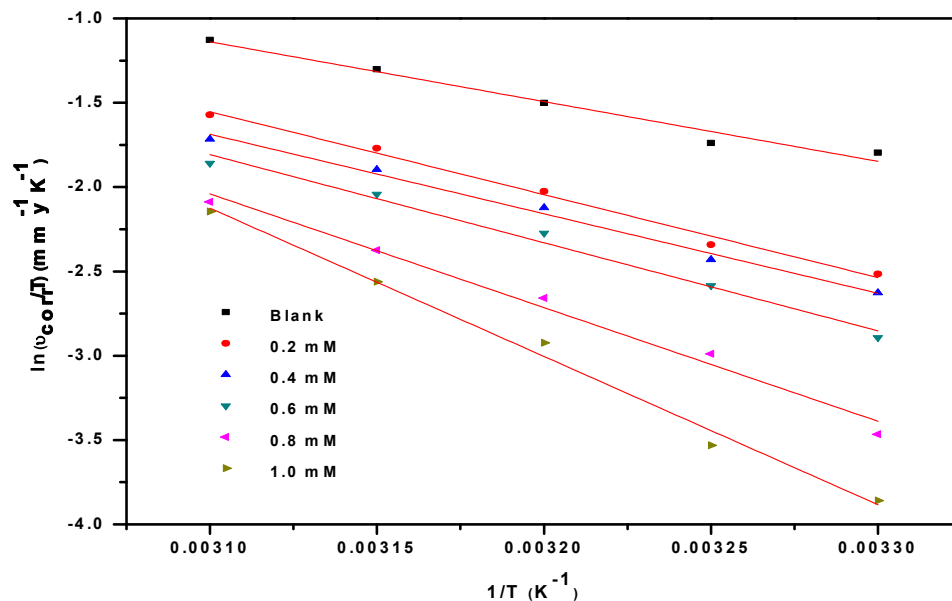


Fig. 3.48: Plots of $\ln(v_{corr}/T)$ versus $1/T$ for the corrosion of welded maraging steel in 1.0 M H_2SO_4 containing different concentrations of PNPT.

3.6.4 Effect of acid concentration

Table 3.57 summarises the maximum inhibition efficiencies exhibited by the PNPT in the H_2SO_4 solution of different concentrations. It is evident from both polarization and EIS experimental results that, for a particular concentration of inhibitor, the inhibition efficiency decreases with the increase in sulphuric acid concentration on the welded maraging steel. The highest inhibition efficiency is observed in sulphuric acid of 0.1 M concentration.

3.6.5 Adsorption isotherm

The adsorption of PNPT on the surface of welded maraging steel was found to obey Langmuir adsorption isotherm. The Langmuir adsorption isotherms for the adsorption of PNPT on welded maraging steel in 1.0 M H_2SO_4 are shown in Fig. 3.49.

The linear regression coefficients are close to unity and the slopes of the straight lines are nearly unity, suggesting that the adsorption of PNPT obeys Langmuir's adsorption isotherm with negligible interaction between the adsorbed molecules. The thermodynamic data obtained for the adsorption of PNPT on welded maraging steel are tabulated in Table 3.58. The exothermic ΔH^0_{ads} values of less than $-41.86 \text{ kJ mol}^{-1}$ predict physisorption of PNPT on the alloy surfaces (Ashish Kumar et al. 2010). The ΔG^0_{ads} values predict both physisorption and chemisorption of PNPT. Therefore it can be concluded that the adsorption of PNPT on the welded maraging steel is predominantly through physisorption. These facts are also supported by the variation of inhibition efficiencies with temperature on the alloy surface as discussed under section 3.6.3.

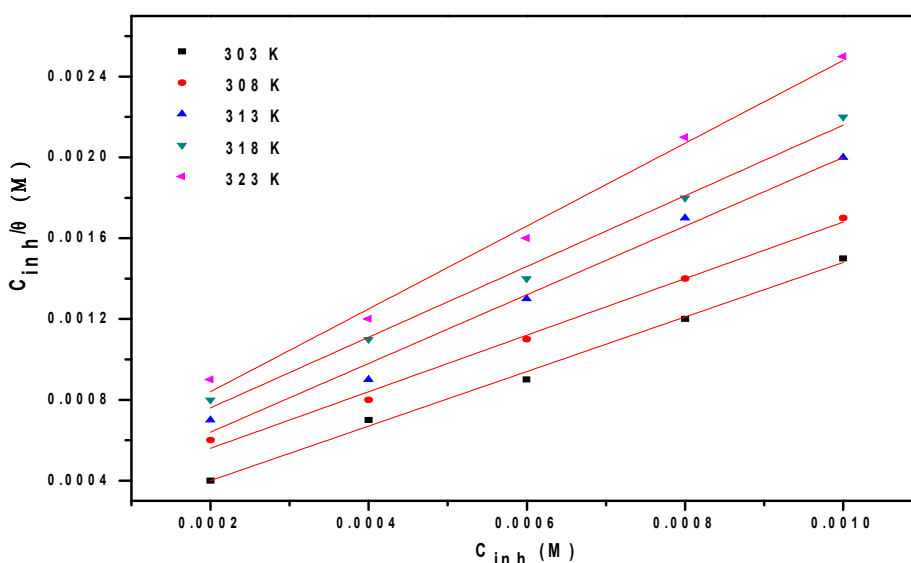


Fig. 3.49: Langmuir adsorption isotherms for the adsorption of PNPT on welded maraging steel in 1.0 M H_2SO_4 at different temperatures.

3.6.6 Mechanism of corrosion inhibition

The corrosion inhibition mechanism of PNPT in sulphuric acid solution can be explained in the same lines as that of PNPT in the section 3.5.6. The inhibitor PNPT protects the alloy surface through predominant physisorption mode in which the positive charge centers of PNPT gets adsorbed on the alloy surface through electrostatic attraction

and also to some extent through chemisorption mode involving neutral PNPT molecules as discussed in the section 3.5.6.

3.6.7 SEM/EDX studies

Fig. 3.50 represents the SEM image of the welded maraging steel after the corrosion tests in a medium of sulfuric acid containing 1.0 mM of PNPT.

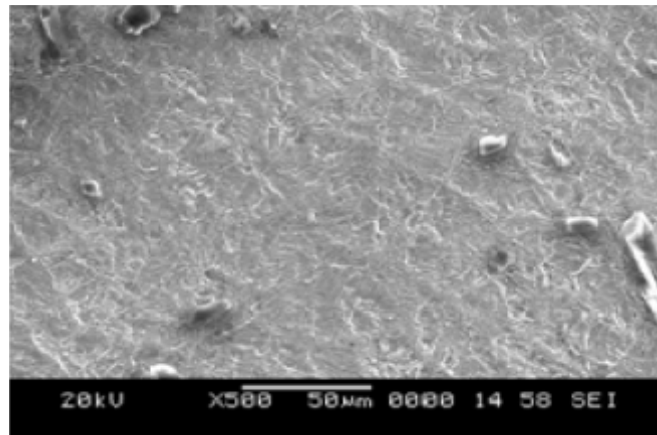


Fig.3.50: SEM image of the welded maraging steel after immersion in 1.0 M H₂SO₄ in the presence of PNPT.

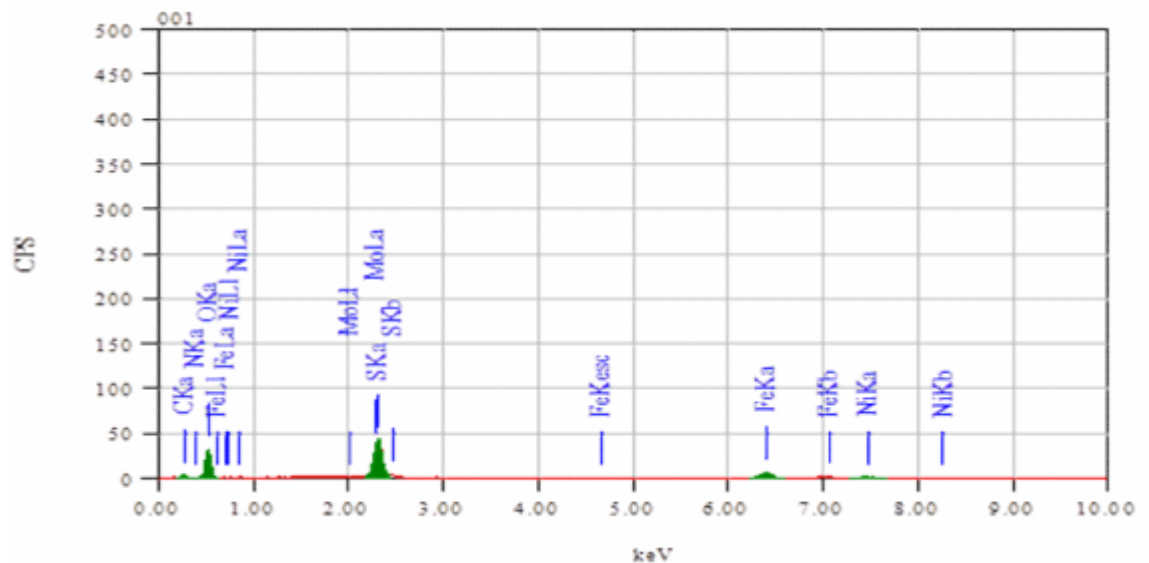


Fig. 3.51: EDX spectra of the welded maraging steel after immersion in 1.0 M H₂SO₄ in the presence of PNPT.

The image clearly shows a smooth surface due to the adsorbed layer of inhibitor molecules on the alloy surface, thus protecting the metal from corrosion. The corresponding EDX spectra for the selected areas on the SEM images of Fig. 3.50 is shown in Fig. 3.51. The atomic percentage of the elements found in the EDX spectra for the inhibited metal surface was 3.05% Fe, 0.62% Ni, 0.40% Mo, 53.97% O, 1.03% N, 19.99% C and 8.25% S and indicated the formation of inhibitor film on the surface of the alloy. The elemental compositions mentioned above were mean values of different regions.

Table 3.46: Results of potentiodynamic polarization studies for the corrosion of welded maraging steel in 0.1 M sulphuric acid containing different concentrations of PNPT.

| Temperature (°C) | Conc. of inhibitor (mM) | $-E_{corr}$ (mV /SCE) | b_a (mV dec ⁻¹) | $-b_c$ (mV dec ⁻¹) | i_{corr} (mA cm ⁻²) | \mathcal{U}_{corr} (mm y ⁻¹) | η (%) |
|------------------|-------------------------|-----------------------|-------------------------------|--------------------------------|-----------------------------------|--|------------|
| 30 | Blank | 356 | 162 | 113 | 1.98 | 25.52 | |
| | 0.2 | 359 | 158 | 102 | 0.89 | 11.34 | 55.6 |
| | 0.4 | 361 | 151 | 97 | 0.73 | 9.41 | 63.1 |
| | 0.6 | 368 | 142 | 94 | 0.64 | 8.12 | 68.2 |
| | 0.8 | 373 | 127 | 83 | 0.17 | 2.19 | 91.4 |
| | 1.0 | 382 | 118 | 78 | 0.11 | 1.42 | 93.5 |
| 35 | Blank | 353 | 171 | 124 | 2.41 | 31.07 | |
| | 0.2 | 354 | 165 | 118 | 1.22 | 15.73 | 49.4 |
| | 0.4 | 348 | 158 | 109 | 1.09 | 14.05 | 54.8 |
| | 0.6 | 359 | 149 | 98 | 0.83 | 10.70 | 65.6 |
| | 0.8 | 360 | 134 | 95 | 0.32 | 4.12 | 86.7 |
| | 1.0 | 362 | 127 | 81 | 0.24 | 3.09 | 90.0 |
| 40 | Blank | 347 | 183 | 131 | 2.93 | 37.77 | |
| | 0.2 | 349 | 173 | 128 | 1.51 | 19.46 | 48.5 |
| | 0.4 | 352 | 165 | 123 | 1.43 | 18.43 | 51.2 |
| | 0.6 | 354 | 157 | 118 | 1.07 | 13.79 | 63.5 |
| | 0.8 | 363 | 148 | 101 | 0.54 | 6.96 | 81.6 |
| | 1.0 | 375 | 134 | 87 | 0.38 | 4.90 | 87.0 |
| 45 | Blank | 345 | 197 | 142 | 3.47 | 44.73 | |
| | 0.2 | 346 | 191 | 135 | 2.08 | 26.81 | 40.1 |
| | 0.4 | 351 | 184 | 129 | 1.88 | 24.23 | 45.8 |
| | 0.6 | 354 | 176 | 124 | 1.62 | 20.88 | 53.3 |
| | 0.8 | 354 | 159 | 109 | 0.99 | 12.76 | 71.5 |
| | 1.0 | 361 | 141 | 94 | 0.54 | 6.96 | 84.4 |
| 50 | Blank | 342 | 214 | 154 | 6.14 | 79.15 | |
| | 0.2 | 344 | 208 | 148 | 3.87 | 49.89 | 36.9 |
| | 0.4 | 347 | 207 | 136 | 3.52 | 45.37 | 42.7 |
| | 0.6 | 348 | 189 | 131 | 2.94 | 37.90 | 52.1 |
| | 0.8 | 351 | 167 | 117 | 1.85 | 23.85 | 69.9 |
| | 1.0 | 343 | 161 | 113 | 1.2 | 15.47 | 80.5 |

Table 3.47: Results of potentiodynamic polarization studies for the corrosion of welded maraging steel in 0.5 M sulphuric acid containing different concentrations of PNPT.

| Temperature (°C) | Conc. of inhibitor (mM) | $-E_{corr}$ (mV /SCE) | b_a (mV dec ⁻¹) | $-b_c$ (mV dec ⁻¹) | i_{corr} (mA cm ⁻²) | ν_{corr} (mm y ⁻¹) | η (%) |
|------------------|-------------------------|-----------------------|-------------------------------|--------------------------------|-----------------------------------|------------------------------------|------------|
| 30 | Blank | 322 | 172 | 115 | 2.47 | 31.84 | |
| | 0.2 | 324 | 163 | 104 | 1.17 | 15.08 | 52.6 |
| | 0.4 | 328 | 154 | 98 | 1.04 | 13.41 | 57.9 |
| | 0.6 | 326 | 144 | 94 | 0.81 | 10.44 | 67.2 |
| | 0.8 | 331 | 130 | 87 | 0.23 | 2.96 | 90.7 |
| | 1.0 | 339 | 124 | 81 | 0.18 | 2.30 | 92.8 |
| 35 | Blank | 321 | 191 | 132 | 2.68 | 34.55 | |
| | 0.2 | 323 | 183 | 129 | 1.41 | 18.17 | 47.4 |
| | 0.4 | 328 | 174 | 118 | 1.32 | 17.02 | 50.7 |
| | 0.6 | 334 | 163 | 109 | 0.97 | 12.50 | 63.8 |
| | 0.8 | 337 | 151 | 103 | 0.68 | 8.76 | 74.6 |
| | 1.0 | 349 | 135 | 97 | 0.32 | 4.12 | 88.1 |
| 40 | Blank | 318 | 207 | 144 | 4.71 | 60.71 | |
| | 0.2 | 321 | 194 | 136 | 2.57 | 33.13 | 45.4 |
| | 0.4 | 331 | 183 | 127 | 2.37 | 30.55 | 49.7 |
| | 0.6 | 334 | 178 | 118 | 1.87 | 24.10 | 60.3 |
| | 0.8 | 339 | 159 | 110 | 1.24 | 15.98 | 73.7 |
| | 1.0 | 351 | 147 | 103 | 0.79 | 10.18 | 83.2 |
| 45 | Blank | 314 | 224 | 158 | 5.38 | 69.35 | |
| | 0.2 | 323 | 216 | 147 | 3.32 | 42.80 | 38.3 |
| | 0.4 | 331 | 203 | 136 | 3.08 | 39.71 | 42.8 |
| | 0.6 | 339 | 191 | 129 | 2.54 | 32.74 | 52.8 |
| | 0.8 | 348 | 183 | 113 | 1.96 | 25.26 | 63.6 |
| | 1.0 | 357 | 165 | 108 | 0.98 | 12.63 | 81.8 |
| 50 | Blank | 312 | 232 | 163 | 6.94 | 89.45 | |
| | 0.2 | 319 | 227 | 157 | 4.41 | 56.84 | 36.5 |
| | 0.4 | 328 | 216 | 149 | 4.08 | 52.59 | 41.2 |
| | 0.6 | 347 | 197 | 132 | 3.75 | 48.34 | 46.0 |
| | 0.8 | 351 | 192 | 129 | 2.54 | 32.74 | 63.4 |
| | 1.0 | 358 | 178 | 117 | 1.51 | 19.46 | 78.2 |

Table 3.48: Results of potentiodynamic polarization studies for the corrosion of welded maraging steel in 1.0 M sulphuric acid containing different concentrations of PNPT.

| Temperature (°C) | Conc. of inhibitor (mM) | $-E_{corr}$ (mV /SCE) | b_a (mV dec ⁻¹) | $-b_c$ (mV dec ⁻¹) | i_{corr} (mA cm ⁻²) | ν_{corr} (mm y ⁻¹) | η (%) |
|------------------|-------------------------|-----------------------|-------------------------------|--------------------------------|-----------------------------------|------------------------------------|------------|
| 30 | Blank | 315 | 187 | 132 | 3.93 | 50.32 | |
| | 0.2 | 317 | 164 | 104 | 1.92 | 24.75 | 51.3 |
| | 0.4 | 319 | 157 | 101 | 1.69 | 21.78 | 56.4 |
| | 0.6 | 327 | 146 | 98 | 1.34 | 17.27 | 66.7 |
| | 0.8 | 324 | 134 | 94 | 0.39 | 5.03 | 89.7 |
| | 1.0 | 342 | 129 | 89 | 0.31 | 4.01 | 92.3 |
| 35 | Blank | 313 | 198 | 147 | 4.21 | 54.12 | |
| | 0.2 | 315 | 169 | 114 | 2.30 | 29.65 | 45.2 |
| | 0.4 | 322 | 152 | 107 | 2.13 | 27.46 | 50.0 |
| | 0.6 | 318 | 135 | 105 | 1.81 | 23.33 | 57.1 |
| | 0.8 | 338 | 127 | 102 | 1.22 | 15.73 | 71.4 |
| | 1.0 | 345 | 112 | 97 | 0.71 | 9.15 | 83.3 |
| 40 | Blank | 310 | 212 | 163 | 5.41 | 69.72 | |
| | 0.2 | 319 | 163 | 132 | 3.23 | 41.64 | 40.7 |
| | 0.4 | 332 | 148 | 112 | 2.91 | 37.51 | 46.1 |
| | 0.6 | 334 | 132 | 109 | 2.53 | 32.60 | 53.7 |
| | 0.8 | 373 | 127 | 106 | 1.71 | 22.04 | 68.5 |
| | 1.0 | 375 | 125 | 102 | 1.32 | 17.02 | 75.9 |
| 45 | Blank | 312 | 243 | 178 | 6.70 | 86.36 | |
| | 0.2 | 317 | 205 | 123 | 4.19 | 54.01 | 37.3 |
| | 0.4 | 328 | 194 | 119 | 3.71 | 47.82 | 44.8 |
| | 0.6 | 347 | 188 | 114 | 3.22 | 41.51 | 52.3 |
| | 0.8 | 354 | 184 | 109 | 2.84 | 36.62 | 59.2 |
| | 1.0 | 359 | 173 | 104 | 1.93 | 24.88 | 71.6 |
| 50 | Blank | 320 | 269 | 192 | 8.11 | 104.54 | |
| | 0.2 | 317 | 208 | 122 | 5.23 | 67.42 | 35.8 |
| | 0.4 | 334 | 198 | 124 | 4.52 | 58.26 | 44.4 |
| | 0.6 | 343 | 193 | 120 | 3.89 | 50.14 | 51.9 |
| | 0.8 | 357 | 187 | 112 | 3.08 | 39.70 | 61.7 |
| | 1.0 | 362 | 179 | 109 | 2.31 | 29.78 | 70.3 |

Table 3.49: Results of potentiodynamic polarization studies for the corrosion of welded maraging steel in 1.5 M sulphuric acid containing different concentrations of PNPT.

| Temperature (°C) | Conc. of inhibitor (mM) | $-E_{corr}$ (mV /SCE) | b_a (mV dec ⁻¹) | $-b_c$ (mV dec ⁻¹) | i_{corr} (mA cm ⁻²) | U_{corr} (mm y ⁻¹) | η (%) |
|------------------|-------------------------|-----------------------|-------------------------------|--------------------------------|-----------------------------------|----------------------------------|------------|
| 30 | Blank | 313 | 240 | 146 | 4.28 | 55.17 | |
| | 0.2 | 317 | 238 | 142 | 2.14 | 27.59 | 50.0 |
| | 0.4 | 319 | 234 | 143 | 1.89 | 24.36 | 55.8 |
| | 0.6 | 327 | 232 | 138 | 1.62 | 20.88 | 62.1 |
| | 0.8 | 324 | 229 | 135 | 0.82 | 10.57 | 80.8 |
| | 1.0 | 342 | 223 | 128 | 0.52 | 6.70 | 87.9 |
| | 35 | Blank | 308 | 242 | 151 | 5.31 | 68.45 |
| 0.2 | | 315 | 241 | 148 | 3.14 | 40.48 | 40.9 |
| 0.4 | | 322 | 238 | 146 | 3.03 | 39.06 | 43.0 |
| 0.6 | | 318 | 236 | 142 | 2.57 | 33.13 | 51.6 |
| 0.8 | | 338 | 233 | 138 | 1.89 | 24.36 | 64.4 |
| 1.0 | | 345 | 228 | 131 | 1.03 | 13.28 | 80.6 |
| 40 | | Blank | 300 | 248 | 156 | 6.48 | 83.53 |
| | 0.2 | 319 | 245 | 152 | 4.18 | 53.88 | 35.5 |
| | 0.4 | 332 | 243 | 149 | 3.72 | 47.95 | 42.6 |
| | 0.6 | 334 | 240 | 147 | 3.14 | 40.48 | 51.5 |
| | 0.8 | 373 | 239 | 145 | 2.37 | 30.54 | 63.4 |
| | 1.0 | 375 | 232 | 138 | 1.82 | 23.46 | 71.9 |
| | 45 | Blank | 301 | 290 | 197 | 7.54 | 97.19 |
| 0.2 | | 317 | 274 | 164 | 5.38 | 69.34 | 28.6 |
| 0.4 | | 328 | 267 | 157 | 4.79 | 61.74 | 36.5 |
| 0.6 | | 347 | 252 | 153 | 3.78 | 48.85 | 49.7 |
| 0.8 | | 354 | 248 | 149 | 3.12 | 40.21 | 58.6 |
| 1.0 | | 359 | 243 | 146 | 2.37 | 30.55 | 67.9 |
| 50 | | Blank | 295 | 349 | 242 | 8.64 | 111.37 |
| | 0.2 | 317 | 328 | 227 | 6.31 | 81.34 | 30.0 |
| | 0.4 | 334 | 317 | 208 | 5.63 | 72.57 | 34.8 |
| | 0.6 | 343 | 309 | 193 | 4.47 | 57.62 | 48.3 |
| | 0.8 | 357 | 302 | 174 | 3.93 | 50.66 | 54.5 |
| | 1.0 | 362 | 284 | 158 | 2.84 | 36.61 | 67.1 |

Table 3.50: Results of potentiodynamic polarization studies for the corrosion of welded maraging steel in 2.0 M sulphuric acid containing different concentrations of PNPT.

| Temperature (°C) | Conc. of inhibitor (mM) | $-E_{corr}$ (mV /SCE) | b_a (mV dec ⁻¹) | $-b_c$ (mV dec ⁻¹) | i_{corr} (mA cm ⁻²) | ν_{corr} (mm y ⁻¹) | η (%) |
|------------------|-------------------------|-----------------------|-------------------------------|--------------------------------|-----------------------------------|------------------------------------|------------|
| 30 | Blank | 315 | 312 | 154 | 4.97 | 64.06 | |
| | 0.2 | 317 | 303 | 142 | 3.25 | 41.89 | 34.6 |
| | 0.4 | 319 | 297 | 131 | 2.47 | 31.84 | 50.3 |
| | 0.6 | 327 | 271 | 124 | 1.94 | 25.01 | 60.9 |
| | 0.8 | 324 | 264 | 121 | 1.04 | 13.41 | 79.1 |
| | 1.0 | 342 | 227 | 114 | 0.78 | 10.05 | 84.3 |
| | 35 | Blank | 313 | 283 | 208 | 6.12 | 78.89 |
| 0.2 | | 315 | 274 | 194 | 4.12 | 53.11 | 32.7 |
| 0.4 | | 322 | 257 | 174 | 3.71 | 47.82 | 39.4 |
| 0.6 | | 318 | 224 | 154 | 3.09 | 39.83 | 49.5 |
| 0.8 | | 338 | 208 | 137 | 2.43 | 31.32 | 60.1 |
| 1.0 | | 345 | 196 | 126 | 1.64 | 21.14 | 73.2 |
| 40 | | Blank | 310 | 261 | 225 | 7.32 | 94.36 |
| | 0.2 | 319 | 268 | 216 | 5.45 | 70.25 | 25.5 |
| | 0.4 | 332 | 254 | 208 | 4.57 | 58.90 | 37.6 |
| | 0.6 | 334 | 230 | 196 | 3.83 | 49.37 | 47.7 |
| | 0.8 | 373 | 217 | 148 | 2.94 | 37.89 | 59.8 |
| | 1.0 | 375 | 203 | 131 | 2.24 | 28.87 | 69.4 |
| | 45 | Blank | 312 | 282 | 231 | 8.23 | 106.09 |
| 0.2 | | 317 | 276 | 224 | 6.59 | 84.95 | 19.9 |
| 0.4 | | 328 | 263 | 217 | 6.01 | 77.47 | 27.0 |
| 0.6 | | 347 | 242 | 203 | 4.94 | 63.68 | 39.9 |
| 0.8 | | 354 | 228 | 159 | 3.87 | 49.89 | 53.0 |
| 1.0 | | 359 | 214 | 143 | 2.93 | 37.76 | 64.4 |
| 50 | | Blank | 320 | 329 | 204 | 9.02 | 116.27 |
| | 0.2 | 317 | 304 | 216 | 7.34 | 94.61 | 18.6 |
| | 0.4 | 334 | 287 | 209 | 6.75 | 87.01 | 25.2 |
| | 0.6 | 343 | 258 | 198 | 5.68 | 73.20 | 37.0 |
| | 0.8 | 357 | 237 | 173 | 4.63 | 59.68 | 48.6 |
| | 1.0 | 362 | 228 | 156 | 3.65 | 47.05 | 59.5 |

Table 3.51: EIS data for the corrosion of welded maraging steel in 0.1 M sulphuric acid containing different concentrations of PNPT.

| Temperature (°C) | Conc. of inhibitor (mM) | R_p (ohm. cm ²) | C_{dl} (mF cm ⁻²) | η (%) |
|------------------|-------------------------|-------------------------------|---------------------------------|------------|
| 30 | Blank | 20.1 | 0.324 | |
| | 0.2 | 46.1 | 0.271 | 56.4 |
| | 0.4 | 55.2 | 0.240 | 63.6 |
| | 0.6 | 63.2 | 0.235 | 68.4 |
| | 0.8 | 275.1 | 0.182 | 91.7 |
| | 1.0 | 386.5 | 0.171 | 92.4 |
| 35 | Blank | 17.4 | 0.469 | |
| | 0.2 | 34.4 | 0.322 | 49.4 |
| | 0.4 | 38.8 | 0.291 | 55.2 |
| | 0.6 | 51.8 | 0.241 | 66.4 |
| | 0.8 | 121.7 | 0.220 | 85.7 |
| | 1.0 | 202.3 | 0.194 | 91.4 |
| 40 | Blank | 14.1 | 0.531 | |
| | 0.2 | 27.8 | 0.491 | 49.3 |
| | 0.4 | 29.8 | 0.462 | 52.7 |
| | 0.6 | 38.9 | 0.437 | 63.8 |
| | 0.8 | 79.7 | 0.385 | 82.3 |
| | 1.0 | 118.5 | 0.349 | 88.1 |
| 45 | Blank | 12.3 | 0.668 | |
| | 0.2 | 21.0 | 0.644 | 41.5 |
| | 0.4 | 22.7 | 0.521 | 45.9 |
| | 0.6 | 26.0 | 0.482 | 52.7 |
| | 0.8 | 47.5 | 0.467 | 74.1 |
| | 1.0 | 86.0 | 0.374 | 85.7 |
| 50 | Blank | 10.2 | 0.830 | |
| | 0.2 | 16.3 | 0.741 | 37.4 |
| | 0.4 | 17.9 | 0.671 | 43.1 |
| | 0.6 | 21.8 | 0.595 | 53.4 |
| | 0.8 | 34.1 | 0.483 | 70.1 |
| | 1.0 | 54.5 | 0.351 | 81.3 |

Table 3.52: EIS data for the corrosion of welded maraging steel in 0.5 M sulphuric acid containing different concentrations of PNPT.

| Temperature (°C) | Conc. of inhibitor (mM) | R_p (ohm. cm ²) | C_{dl} (mF cm ⁻²) | η (%) |
|------------------|-------------------------|-------------------------------|---------------------------------|------------|
| 30 | Blank | 18.7 | 0.633 | |
| | 0.2 | 39.9 | 0.582 | 53.1 |
| | 0.4 | 44.9 | 0.531 | 58.4 |
| | 0.6 | 58.6 | 0.424 | 68.1 |
| | 0.8 | 225.3 | 0.384 | 91.7 |
| | 1.0 | 246.1 | 0.315 | 92.4 |
| 35 | Blank | 15.4 | 0.682 | |
| | 0.2 | 29.6 | 0.611 | 48.1 |
| | 0.4 | 31.3 | 0.578 | 50.9 |
| | 0.6 | 43.0 | 0.529 | 64.2 |
| | 0.8 | 62.3 | 0.474 | 75.3 |
| | 1.0 | 141.3 | 0.443 | 89.1 |
| 40 | Blank | 11.4 | 0.727 | |
| | 0.2 | 21.2 | 0.691 | 46.1 |
| | 0.4 | 23.1 | 0.635 | 50.8 |
| | 0.6 | 29.4 | 0.614 | 61.3 |
| | 0.8 | 44.0 | 0.546 | 74.1 |
| | 1.0 | 72.2 | 0.497 | 84.2 |
| 45 | Blank | 10.5 | 0.831 | |
| | 0.2 | 16.8 | 0.812 | 37.6 |
| | 0.4 | 18.6 | 0.761 | 43.5 |
| | 0.6 | 22.4 | 0.712 | 53.1 |
| | 0.8 | 29.7 | 0.674 | 64.7 |
| | 1.0 | 59.3 | 0.647 | 82.3 |
| 50 | Blank | 7.9 | 0.965 | |
| | 0.2 | 12.6 | 0.954 | 37.6 |
| | 0.4 | 13.6 | 0.931 | 41.9 |
| | 0.6 | 14.8 | 0.845 | 46.7 |
| | 0.8 | 22.0 | 0.719 | 64.1 |
| | 1.0 | 38.3 | 0.627 | 79.4 |

Table 3.53: EIS data for the corrosion of welded maraging steel in 1.0 M sulphuric acid containing different concentrations of PNPT.

| Temperature (°C) | Conc. of inhibitor (mM) | R_p (ohm. cm ²) | C_{dl} (mF cm ⁻²) | η (%) |
|------------------|-------------------------|-------------------------------|---------------------------------|------------|
| 30 | Blank | 16.1 | 0.641 | |
| | 0.2 | 33.7 | 0.692 | 52.2 |
| | 0.4 | 36.5 | 0.513 | 55.9 |
| | 0.6 | 48.5 | 0.484 | 66.8 |
| | 0.8 | 146 | 0.431 | 88.9 |
| | 1.0 | 218 | 0.365 | 92.6 |
| 35 | Blank | 13.5 | 0.714 | |
| | 0.2 | 24.5 | 0.682 | 44.9 |
| | 0.4 | 27.0 | 0.621 | 50.0 |
| | 0.6 | 31.4 | 0.570 | 57.0 |
| | 0.8 | 46.5 | 0.528 | 70.9 |
| | 1.0 | 79.4 | 0.461 | 82.3 |
| 40 | Blank | 10.4 | 0.670 | |
| | 0.2 | 17.3 | 0.651 | 39.8 |
| | 0.4 | 19.4 | 0.634 | 46.3 |
| | 0.6 | 22.1 | 0.609 | 52.9 |
| | 0.8 | 33.5 | 0.578 | 68.8 |
| | 1.0 | 43.4 | 0.514 | 76.1 |
| 45 | Blank | 8.6 | 0.873 | |
| | 0.2 | 13.6 | 0.791 | 36.7 |
| | 0.4 | 15.7 | 0.732 | 45.3 |
| | 0.6 | 17.9 | 0.684 | 51.9 |
| | 0.8 | 20.8 | 0.652 | 58.7 |
| | 1.0 | 30.7 | 0.614 | 71.9 |
| 50 | Blank | 7.3 | 1.123 | |
| | 0.2 | 11.4 | 0.981 | 35.8 |
| | 0.4 | 13.1 | 0.860 | 44.3 |
| | 0.6 | 15.2 | 0.773 | 51.9 |
| | 0.8 | 18.7 | 0.694 | 60.8 |
| | 1.0 | 24.3 | 0.639 | 69.7 |

Table 3.54: EIS data for the corrosion of welded maraging steel in 1.5 M sulphuric acid containing different concentrations of PNPT.

| Temperature (°C) | Conc. of inhibitor (mM) | R_p (ohm. cm ²) | C_{dl} (mF cm ⁻²) | η (%) |
|------------------|-------------------------|-------------------------------|---------------------------------|------------|
| 30 | Blank | 15.9 | 0.958 | |
| | 0.2 | 32.4 | 0.891 | 50.9 |
| | 0.4 | 35.1 | 0.712 | 54.7 |
| | 0.6 | 41.2 | 0.647 | 61.4 |
| | 0.8 | 89.8 | 0.589 | 82.3 |
| | 1.0 | 116.1 | 0.474 | 86.3 |
| 35 | Blank | 11.6 | 0.982 | |
| | 0.2 | 19.8 | 0.931 | 41.4 |
| | 0.4 | 20.5 | 0.844 | 43.4 |
| | 0.6 | 24.4 | 0.718 | 52.3 |
| | 0.8 | 33.2 | 0.679 | 65.1 |
| | 1.0 | 62.0 | 0.596 | 81.3 |
| 40 | Blank | 9.4 | 1.070 | |
| | 0.2 | 14.7 | 0.991 | 36.1 |
| | 0.4 | 16.6 | 0.875 | 43.4 |
| | 0.6 | 19.7 | 0.818 | 52.3 |
| | 0.8 | 25.3 | 0.739 | 62.8 |
| | 1.0 | 34.1 | 0.644 | 72.4 |
| 45 | Blank | 8.1 | 1.281 | |
| | 0.2 | 11.4 | 1.162 | 29.1 |
| | 0.4 | 13.0 | 1.077 | 37.5 |
| | 0.6 | 15.9 | 0.946 | 49.2 |
| | 0.8 | 18.4 | 0.824 | 56.1 |
| | 1.0 | 24.3 | 0.765 | 66.7 |
| 50 | Blank | 6.9 | 1.318 | |
| | 0.2 | 9.5 | 1.272 | 26.9 |
| | 0.4 | 10.4 | 1.214 | 33.7 |
| | 0.6 | 13.1 | 1.089 | 47.5 |
| | 0.8 | 14.7 | 0.977 | 53.2 |
| | 1.0 | 20.2 | 0.826 | 65.8 |

Table 3.55: EIS data for the corrosion of welded maraging steel in 2.0 M sulphuric acid containing different concentrations of PNPT.

| Temperature (°C) | Conc. of inhibitor (mM) | R_p (ohm. cm ²) | C_{dl} (mF cm ⁻²) | η (%) |
|------------------|-------------------------|-------------------------------|---------------------------------|------------|
| 30 | Blank | 13.9 | 1.093 | |
| | 0.2 | 21.3 | 1.042 | 35.1 |
| | 0.4 | 27.9 | 0.871 | 51.2 |
| | 0.6 | 35.6 | 0.738 | 60.3 |
| | 0.8 | 66.4 | 0.696 | 79.2 |
| | 1.0 | 88.6 | 0.574 | 83.1 |
| 35 | Blank | 10.8 | 1.241 | |
| | 0.2 | 16.1 | 1.175 | 33.1 |
| | 0.4 | 17.8 | 1.148 | 40.1 |
| | 0.6 | 21.4 | 0.986 | 48.7 |
| | 0.8 | 27.2 | 0.864 | 60.3 |
| | 1.0 | 40.3 | 0.799 | 71.7 |
| 40 | Blank | 9.2 | 1.324 | |
| | 0.2 | 12.2 | 1.285 | 24.7 |
| | 0.4 | 14.6 | 1.217 | 36.8 |
| | 0.6 | 17.1 | 1.156 | 46.3 |
| | 0.8 | 22.0 | 1.022 | 58.1 |
| | 1.0 | 29.0 | 0.940 | 68.3 |
| 45 | Blank | 7.4 | 1.369 | |
| | 0.2 | 9.1 | 1.292 | 18.7 |
| | 0.4 | 9.8 | 1.248 | 24.3 |
| | 0.6 | 12.0 | 1.175 | 38.1 |
| | 0.8 | 15.9 | 1.086 | 53.4 |
| | 1.0 | 19.8 | 0.974 | 62.7 |
| 50 | Blank | 6.5 | 1.508 | |
| | 0.2 | 8.1 | 1.484 | 19.2 |
| | 0.4 | 8.6 | 1.365 | 24.7 |
| | 0.6 | 10.2 | 1.276 | 36.4 |
| | 0.8 | 12.2 | 1.192 | 46.7 |
| | 1.0 | 15.6 | 1.131 | 58.4 |

Table 3.56: Activation parameters for the corrosion of welded maraging steel in sulphuric acid containing different concentrations of PNPT.

| Molarity of H ₂ SO ₄ (M) | Conc. of inhibitor (mM) | E_a (kJ mol ⁻¹) | ΔH^\ddagger (kJ mol ⁻¹) | ΔS^\ddagger (J mol ⁻¹ K ⁻¹) |
|--|-------------------------|-------------------------------|---|--|
| 0.1 | Blank | 42.58 | 39.98 | -86.83 |
| | 0.2 | 56.71 | 54.10 | -46.38 |
| | 0.4 | 54.94 | 57.34 | -37.45 |
| | 0.6 | 60.80 | 58.20 | -36.48 |
| | 0.8 | 66.08 | 63.48 | -29.87 |
| | 1.0 | 85.55 | 82.93 | -22.89 |
| 0.5 | Blank | 44.97 | 42.37 | -77.02 |
| | 0.2 | 57.15 | 54.55 | -42.85 |
| | 0.4 | 58.31 | 55.71 | -39.86 |
| | 0.6 | 65.52 | 62.91 | -28.57 |
| | 0.8 | 75.91 | 73.31 | -24.04 |
| | 1.0 | 87.96 | 85.37 | -15.28 |
| 1.0 | Blank | 32.07 | 29.46 | -115.68 |
| | 0.2 | 43.48 | 40.87 | -103.76 |
| | 0.4 | 49.79 | 47.19 | -90.07 |
| | 0.6 | 56.02 | 54.41 | -78.02 |
| | 0.8 | 81.90 | 79.30 | -32.97 |
| | 1.0 | 98.96 | 96.36 | -24.02 |
| 1.5 | Blank | 30.55 | 29.12 | -120.54 |
| | 0.2 | 40.15 | 38.74 | -97.67 |
| | 0.4 | 46.42 | 44.97 | -84.52 |
| | 0.6 | 52.59 | 51.20 | -53.07 |
| | 0.8 | 70.61 | 73.22 | -40.97 |
| | 1.0 | 76.66 | 79.26 | -34.38 |
| 2.0 | Blank | 28.24 | 26.21 | -122.45 |
| | 0.2 | 39.59 | 39.47 | -109.51 |
| | 0.4 | 44.32 | 42.13 | -84.82 |
| | 0.6 | 50.41 | 51.24 | -78.47 |
| | 0.8 | 62.17 | 60.17 | -57.42 |
| | 1.0 | 68.13 | 64.13 | -20.31 |

Table 3.57: Maximum inhibition efficiency attained in different concentrations of sulphuric acid at different temperatures for PNPT.

| Temperature (°C) | Welded Maraging Steel | | | |
|---------------------|-------------------------------------|----------------------------------|---|------------|
| | Sulphuric acid concentration (M) | Concentration of PNPT (mM) | η (%) | |
| | | | Potentiodynamic polarization method | EIS method |
| 30 | 0.1 | 1.0 | 94.5 | 94.8 |
| | 0.5 | | 92.8 | 92.4 |
| | 1.0 | | 92.3 | 92.6 |
| | 1.5 | | 87.9 | 86.3 |
| | 2.0 | | 84.3 | 83.1 |
| 35 | 0.1 | 1.0 | 90.0 | 91.4 |
| | 0.5 | | 88.1 | 89.1 |
| | 1.0 | | 83.3 | 82.3 |
| | 1.5 | | 80.6 | 81.3 |
| | 2.0 | | 73.2 | 71.7 |
| 40 | 0.1 | 1.0 | 87.0 | 88.1 |
| | 0.5 | | 83.2 | 84.2 |
| | 1.0 | | 75.9 | 76.1 |
| | 1.5 | | 71.9 | 72.4 |
| | 2.0 | | 69.4 | 68.3 |
| 45 | 0.1 | 1.0 | 84.4 | 85.7 |
| | 0.5 | | 81.8 | 82.3 |
| | 1.0 | | 71.6 | 71.9 |
| | 1.5 | | 67.9 | 66.7 |
| | 2.0 | | 64.4 | 62.7 |
| 50 | 0.1 | 1.0 | 80.5 | 81.3 |
| | 0.5 | | 78.2 | 79.4 |
| | 1.0 | | 70.3 | 69.7 |
| | 1.5 | | 67.1 | 65.8 |
| | 2.0 | | 59.5 | 58.4 |

Table 3.58: Thermodynamic parameters for the adsorption of PNPT on welded maraging steel surface in sulphuric acid at different temperatures.

| Molarity of H ₂ SO ₄ (M) | Temperature (° C) | $-\Delta G^{\circ}_{ads}$ (kJ mol ⁻¹) | ΔH°_{ads} (kJ mol ⁻¹) | ΔS°_{ads} (J mol ⁻¹ K ⁻¹) |
|--|-------------------|---|--|---|
| 0.1 | 30 | 42.43 | -25.43 | -56.31 |
| | 35 | 42.37 | | |
| | 40 | 42.14 | | |
| | 45 | 42.03 | | |
| | 50 | 41.84 | | |
| 0.5 | 30 | 42.09 | -24.09 | -59.61 |
| | 35 | 41.88 | | |
| | 40 | 41.73 | | |
| | 45 | 41.61 | | |
| | 50 | 41.42 | | |
| 1.0 | 30 | 23.79 | -4.27 | -30.7 |
| | 35 | 23.62 | | |
| | 40 | 23.56 | | |
| | 45 | 23.43 | | |
| | 50 | 23.31 | | |
| 1.5 | 30 | 25.54 | -7.23 | -38.6 |
| | 35 | 25.43 | | |
| | 40 | 25.36 | | |
| | 45 | 25.28 | | |
| | 50 | 25.03 | | |
| 2.0 | 30 | 24.08 | -9.41 | -41.47 |
| | 35 | 23.79 | | |
| | 40 | 23.62 | | |
| | 45 | 23.47 | | |
| | 50 | 23.39 | | |

3.7 3,4,5-TRIMETHOXY-BENZOICACID-(3,4,5-TRIMETHOXY BENZYLIDENE) HYDRAZIDE (TBTBH) AS INHIBITOR FOR THE CORROSION OF WELDED MARAGING STEEL IN HYDROCHLORIC ACID MEDIUM

3.7.1 Potentiodynamic polarization measurements

Polarization curves for the corrosion of maraging steel in 1.0 M HCl solution in the presence of different concentrations of TBTBH are shown in Fig. 3.52. Similar results were obtained at other temperatures and in other concentrations of hydrochloric acid. The potentiodynamic polarization parameters are summarized in Tables 3.59 to 3.63.

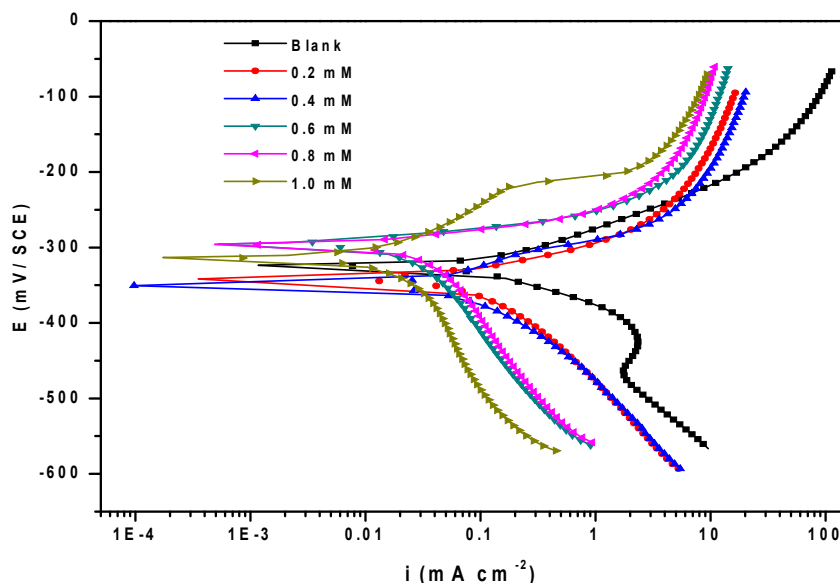


Fig. 3.52: Potentiodynamic polarization curves for the corrosion of welded maraging steel in 1.0 M hydrochloric acid containing different concentrations of TBTBH at 30 °C.

It could be observed that both the anodic and cathodic reactions were suppressed with the addition of inhibitor. There is no significant shift observed in E_{CORR} value, therefore, it can be concluded that TBTBH acts as a mixed type inhibitor on welded maraging steel. The rest of the discussion is similar to the discussion as under the section 3.3.1.

3.7.2 Electrochemical impedance spectroscopy (EIS) studies

Nyquist plots for the corrosion of welded maraging steel in 1.0 M HCl solution in the presence of different concentrations of TBTBH are given in Fig. 3.53. Similar plots were obtained in other concentrations of the acid and also at other temperatures. The impedance parameters are presented in Tables 3.64 to 3.68.

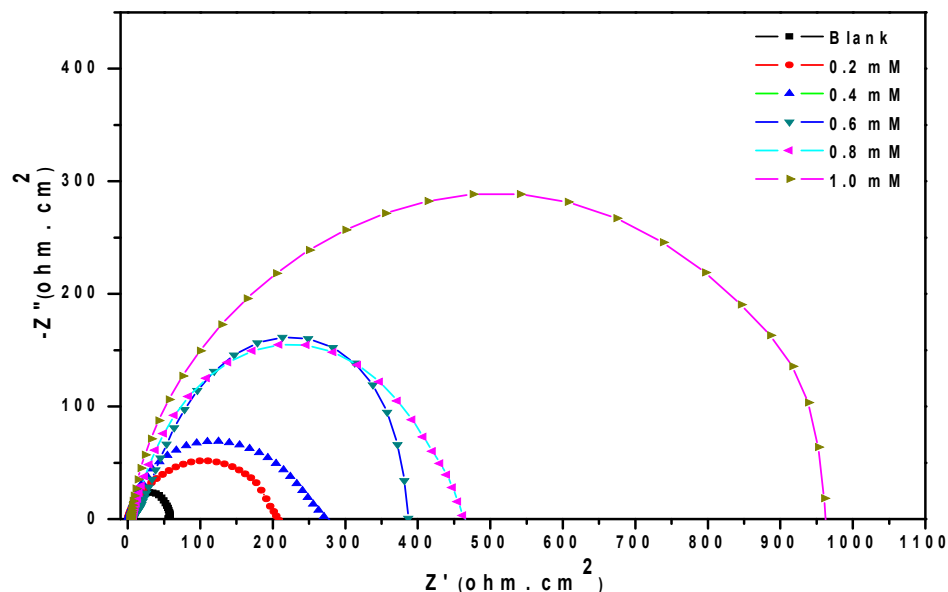


Fig. 3.53: Nyquist plots for the corrosion of welded maraging steel in 1.0 M hydrochloric acid containing different concentrations of TBTBH at 30 °C.

It is clear from Fig. 3.53 that the shapes of the impedance plots for the corrosion of welded maraging steel in the presence of inhibitor are not substantially different from those of the uninhibited one. The plots are similar to those obtained in the presence of BTPO as discussed in the section 3.3.2. The equivalent circuit given in Fig. 3.17 is used to fit the experimental data for the corrosion of welded maraging steel in hydrochloric acid in the presence of TBTBH. As can be seen from the Tables, R_{ct} , R_f value increases and C_{dl} value decreases with the increase in the concentration of TBTBH which suggests the decrease in corrosion rate.

The Bode plots of phase angle and amplitude for the corrosion of the alloy in the presence of different concentrations of TBTBH are shown in Fig. 3.54 (a) and

Fig. 3.54 (b), respectively. Phase angle increases with the increase in the concentrations of TBTBH in hydrochloric acid this might be attributed to the decrease in the capacitive behavior on the metal surface due to the decrease in the dissolution rate of the metal. Hence the discussion regarding the Bode plots under the section 3.3.2 holds good for TBTBH also.

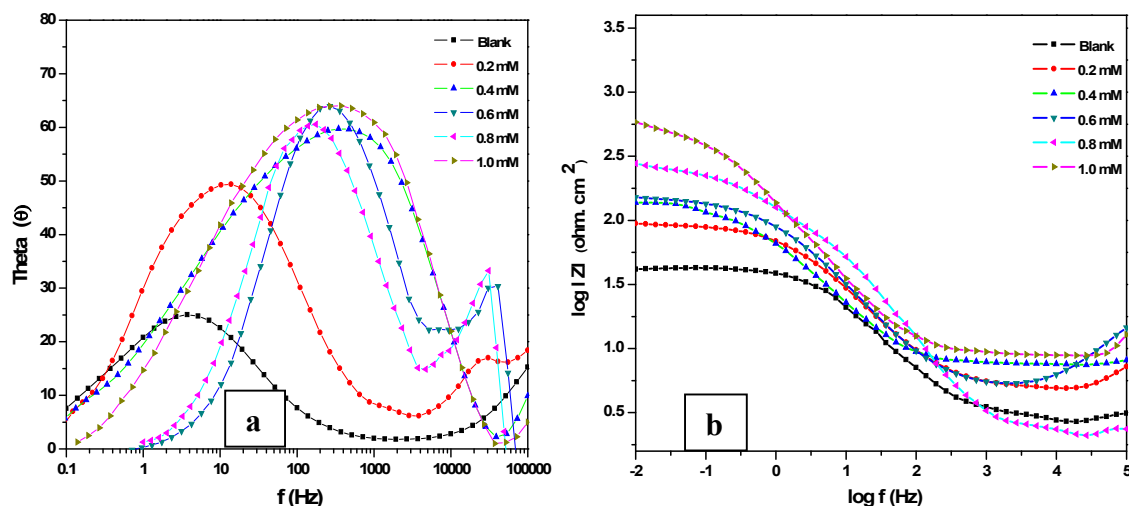


Fig. 3.54: Bode (a) phase angle plots and (b) amplitude plots for the corrosion of welded maraging steel in 1.0 M HCl containing different concentrations of TBTBH at 30 °C.

3.7.3 Effect of temperature

The potentiodynamic polarization and EIS results pertaining to different temperatures in different concentrations of hydrochloric acid in the presence of TBTBH have already been listed in Tables 3.59 to 3.68. The effect of temperature on corrosion inhibition behaviour of TBTBH is similar to that of BTPO on welded maraging steel as discussed in the section 3.3.3. The decrease in the inhibition efficiency of TBTBH with the increase in temperature on welded maraging steel surface may be attributed to the physisorption of TBTBH. The Arrhenius plots for the corrosion of welded maraging steel in 1.0 M hydrochloric acid in the presence of different concentrations of TBTBH are shown in Fig. 3.55. The plots of $\ln(v_{corr}/T)$ versus $(1/T)$ for the corrosion of

welded maraging steel are shown in Fig. 3.56. The calculated values of activation parameters are given in Table 3.69. The observations are similar to the ones obtained in the presence of BTPO and PNPT.

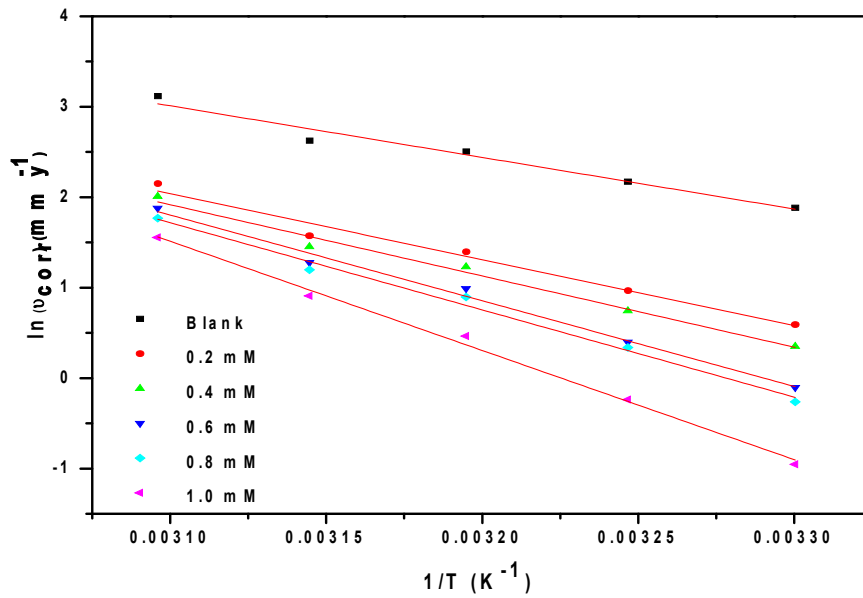


Fig. 3.55: Arrhenius Plots for the corrosion of welded maraging steel in 1.0 M hydrochloric acid containing different concentrations of TBTBH.

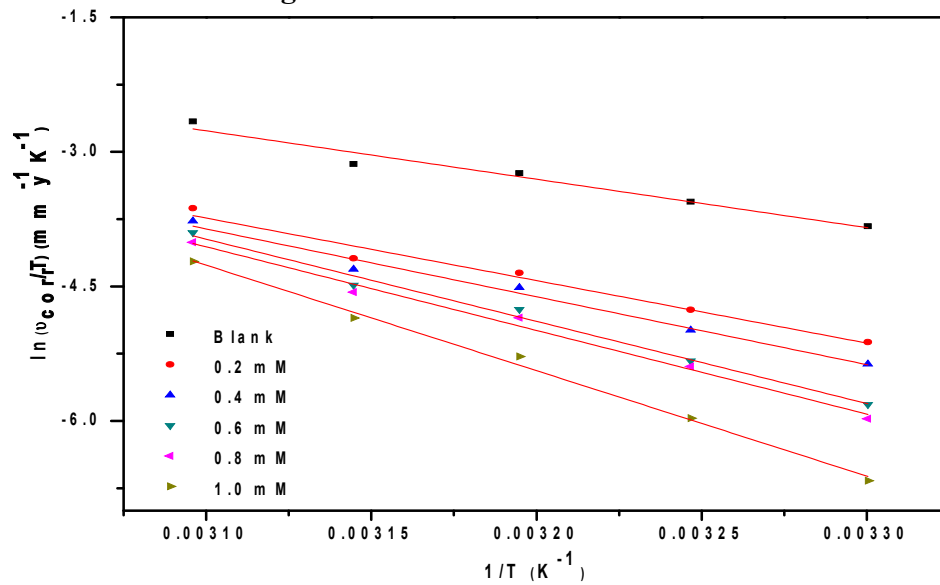


Fig. 3.56: Plots of $\ln(v_{corr}/T)$ versus $1/T$ for the corrosion of welded maraging steel in 1.0 M hydrochloric acid containing different concentrations of TBTBH.

The increase in the E_a values with the increase in TBTBH concentration indicates the increase in energy barrier for the corrosion reaction as discussed in earlier sections. The entropy of activation in the absence and presence of TBTBH is large and negative for the corrosion of alloy. This implies that the activated complex in the rate determining step represents an association rather than dissociation step, indicating that a decrease in disordering takes place on going from reactants to activated complex (Gomma and Wahdan 1995, Marsh 1988). The entropies of activation are higher for the corrosion of welded maraging steel in inhibited solutions than that in the uninhibited solutions.

3.7.4 Effect of acid concentration

Table 3.70 summarises the maximum inhibition efficiencies exhibited by TBTBH in the HCl solution of different concentrations. It is evident from both polarization and EIS experimental results that, for a particular concentration of inhibitor, the inhibition efficiency decreases with the increase in hydrochloric acid concentration on the welded maraging steel. The highest inhibition efficiency is observed in hydrochloric acid of 0.1 M concentration.

3.7.5 Adsorption isotherm

The adsorption of TBTBH on the surfaces of welded maraging steel was found to obey Langmuir adsorption isotherm. The Langmuir adsorption isotherms for the adsorption of TBTBH on welded maraging steel in 1.0 M hydrochloric acid are shown in Fig. 3.57. The thermodynamic parameters for the adsorption of TBTBH on welded maraging steel are tabulated in Tables 3.71. The values of ΔG_{ads}^0 and ΔH_{ads}^0 indicate both physisorption and chemisorption of TBTBH on welded maraging steel with predominant physisorption. The ΔS_{ads}^0 values indicate the decrease in randomness on going from the reactants to the metal adsorbed species.

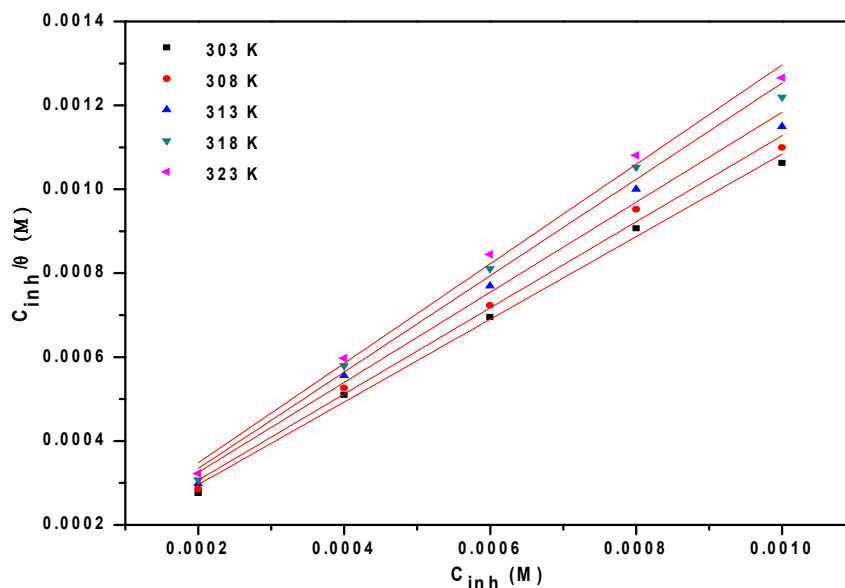


Fig. 3.57: Langmuir adsorption isotherms for the adsorption of TBTBH on welded maraging steel in 1.0 M HCl at different temperatures.

3.7.6 Mechanism of corrosion inhibition

The mechanism of corrosion inhibition of welded maraging steel in the presence of TBTBH is similar to that in the presence of PNPT as discussed under section 3.5.6. The adsorption of TBTBH molecules on the metal surface can be attributed to the presence of nitrogen, electron donating methoxy groups and delocalised benzene rings. The molecules of TBTBH get adsorbed on the alloy surface predominantly by physisorption and to a small extent by chemisorption.

3.7.7 SEM/EDX studies

Fig. 3.58 shows the SEM image of the sample after immersion in 1.0 M hydrochloric acid in the presence of TBTBH. It can be seen that the alloy surface is smooth without any visible corrosion attack. Thus, it can be concluded that TBTBH protects the alloy from corrosion by forming a uniform film on the alloy surface. The EDX spectra of the corroded surface of the alloy in the presence of TBTBH is shown in Fig. 3.59. The atomic percentages of the elements found in the

EDX profile for the inhibited metal surface was 2.61% Fe, 0.58% Ni, 0.10% Mo, 24.86% O, 41.88% C, 0.51% Cl and 29.45% N and indicated the formation of inhibitor film on the surface of the alloy.

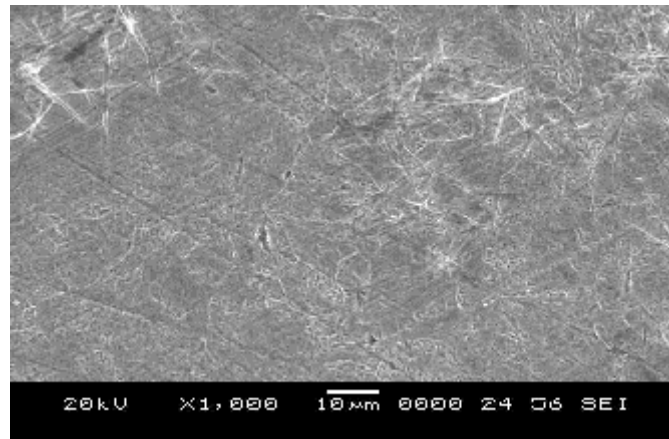


Fig. 3.58: SEM image of the welded maraging steel after immersion in 1.0 M HCl in the presence of TBTBH.

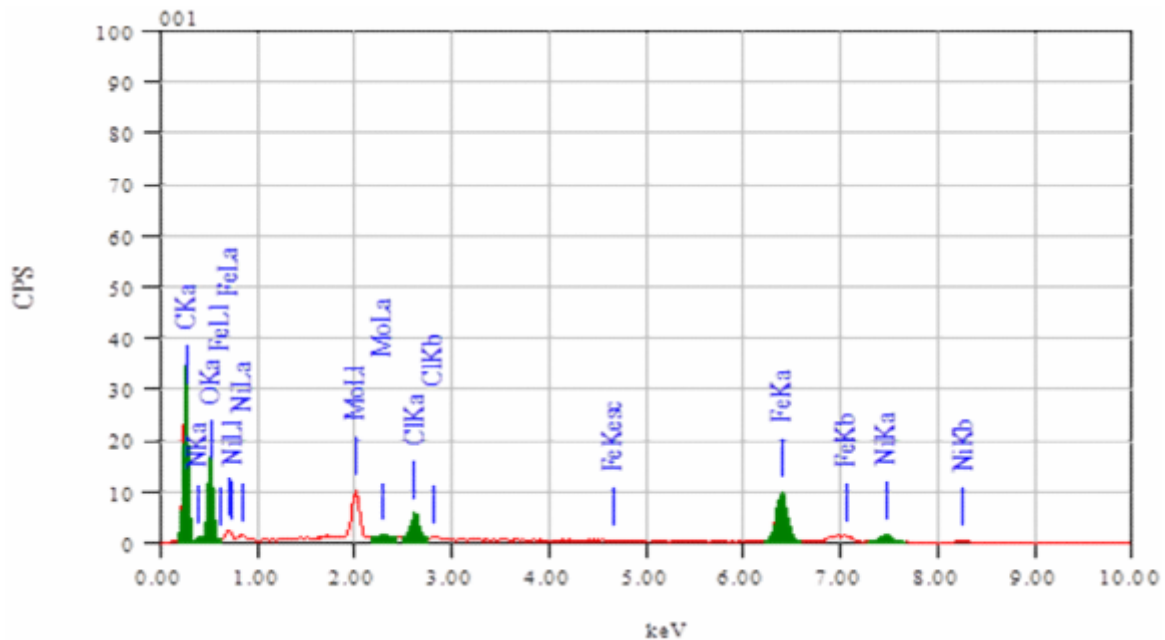


Fig. 3.59: EDX spectra of the welded maraging steel after immersion in 1.0 M HCl in the presence of TBTBH.

Table 3.59: Results of potentiodynamic polarization studies for the corrosion of welded maraging steel in 0.1 M hydrochloric acid containing different concentrations of TBTBH.

| Temperature (°C) | Conc. of inhibitor (mM) | $-E_{corr}$ (mV /SCE) | b_a (mV dec ⁻¹) | $-b_c$ (mV dec ⁻¹) | i_{corr} (mA cm ⁻²) | U_{corr} (mm y ⁻¹) | η (%) |
|------------------|-------------------------|-----------------------|-------------------------------|--------------------------------|-----------------------------------|----------------------------------|------------|
| 30 | Blank | 306 | 98 | 140 | 0.31 | 4.00 | |
| | 0.2 | 313 | 92 | 121 | 0.07 | 0.91 | 77.4 |
| | 0.4 | 317 | 91 | 118 | 0.05 | 0.65 | 83.8 |
| | 0.6 | 314 | 89 | 116 | 0.03 | 0.39 | 90.3 |
| | 0.8 | 321 | 89 | 115 | 0.02 | 0.26 | 93.5 |
| | 1.0 | 323 | 87 | 112 | 0.01 | 0.13 | 96.8 |
| | 35 | Blank | 310 | 101 | 146 | 0.36 | 4.64 |
| 0.2 | | 304 | 96 | 129 | 0.09 | 1.17 | 74.8 |
| 0.4 | | 298 | 94 | 127 | 0.07 | 0.91 | 80.5 |
| 0.6 | | 319 | 93 | 125 | 0.05 | 0.65 | 86.1 |
| 0.8 | | 327 | 92 | 124 | 0.04 | 0.52 | 88.9 |
| 1.0 | | 331 | 91 | 122 | 0.02 | 0.26 | 94.3 |
| 40 | | Blank | 312 | 103 | 147 | 0.46 | 5.93 |
| | 0.2 | 327 | 100 | 132 | 0.13 | 1.63 | 72.5 |
| | 0.4 | 332 | 98 | 129 | 0.10 | 1.34 | 77.4 |
| | 0.6 | 320 | 95 | 127 | 0.07 | 0.94 | 84.1 |
| | 0.8 | 307 | 93 | 124 | 0.06 | 0.78 | 87.1 |
| | 1.0 | 313 | 91 | 121 | 0.04 | 0.52 | 91.5 |
| | 45 | Blank | 315 | 108 | 156 | 0.67 | 8.64 |
| 0.2 | | 323 | 102 | 138 | 0.21 | 2.64 | 69.4 |
| 0.4 | | 319 | 98 | 135 | 0.16 | 2.10 | 75.7 |
| 0.6 | | 337 | 95 | 132 | 0.13 | 1.62 | 81.3 |
| 0.8 | | 341 | 94 | 130 | 0.11 | 1.43 | 83.4 |
| 1.0 | | 348 | 92 | 128 | 0.07 | 0.92 | 89.7 |
| 50 | | Blank | 313 | 113 | 161 | 0.83 | 10.70 |
| | 0.2 | 325 | 104 | 143 | 0.27 | 3.51 | 67.2 |
| | 0.4 | 332 | 102 | 140 | 0.25 | 3.17 | 70.4 |
| | 0.6 | 328 | 99 | 138 | 0.18 | 2.31 | 78.4 |
| | 0.8 | 319 | 97 | 136 | 0.16 | 2.06 | 80.7 |
| | 1.0 | 313 | 96 | 133 | 0.12 | 1.58 | 85.2 |

Table 3.60: Results of potentiodynamic polarization studies for the corrosion of welded maraging steel in 0.5 M hydrochloric acid containing different concentrations of TBTBH.

| Temperature (°C) | Conc. of inhibitor (mM) | $-E_{corr}$ (mV /SCE) | b_a (mV dec ⁻¹) | $-b_c$ (mV dec ⁻¹) | i_{corr} (mA cm ⁻²) | \mathcal{U}_{corr} (mm y ⁻¹) | η (%) |
|------------------|-------------------------|-----------------------|-------------------------------|--------------------------------|-----------------------------------|--|------------|
| 30 | Blank | 315 | 103 | 149 | 0.35 | 4.51 | |
| | 0.2 | 352 | 99 | 127 | 0.09 | 1.14 | 74.8 |
| | 0.4 | 347 | 97 | 124 | 0.07 | 0.89 | 80.3 |
| | 0.6 | 334 | 94 | 121 | 0.04 | 0.53 | 88.2 |
| | 0.8 | 338 | 92 | 119 | 0.03 | 0.45 | 90.1 |
| | 1.0 | 321 | 91 | 117 | 0.02 | 0.24 | 94.3 |
| | 35 | Blank | 323 | 105 | 152 | 0.48 | 6.19 |
| 0.2 | | 329 | 101 | 135 | 0.13 | 1.71 | 72.3 |
| 0.4 | | 338 | 98 | 131 | 0.10 | 1.29 | 79.1 |
| 0.6 | | 325 | 96 | 128 | 0.07 | 0.95 | 84.7 |
| 0.8 | | 318 | 95 | 125 | 0.06 | 0.77 | 87.5 |
| 1.0 | | 309 | 93 | 123 | 0.04 | 0.50 | 91.9 |
| 40 | | Blank | 330 | 112 | 158 | 0.60 | 7.73 |
| | 0.2 | 321 | 104 | 141 | 0.18 | 2.31 | 70.1 |
| | 0.4 | 334 | 102 | 138 | 0.15 | 1.95 | 74.8 |
| | 0.6 | 317 | 99 | 135 | 0.11 | 1.45 | 81.3 |
| | 0.8 | 308 | 98 | 133 | 0.10 | 1.28 | 83.4 |
| | 1.0 | 297 | 95 | 131 | 0.06 | 0.82 | 89.4 |
| | 45 | Blank | 328 | 116 | 165 | 0.77 | 9.93 |
| 0.2 | | 321 | 109 | 144 | 0.25 | 3.27 | 67.1 |
| 0.4 | | 316 | 107 | 141 | 0.21 | 2.75 | 72.3 |
| 0.6 | | 339 | 103 | 139 | 0.17 | 2.24 | 77.4 |
| 0.8 | | 318 | 102 | 137 | 0.16 | 2.00 | 79.8 |
| 1.0 | | 307 | 99 | 134 | 0.11 | 1.48 | 85.1 |
| 50 | | Blank | 324 | 118 | 173 | 1.03 | 13.28 |
| | 0.2 | 317 | 111 | 158 | 0.36 | 4.67 | 64.8 |
| | 0.4 | 311 | 108 | 154 | 0.33 | 4.22 | 68.2 |
| | 0.6 | 302 | 106 | 151 | 0.27 | 3.44 | 74.1 |
| | 0.8 | 321 | 103 | 149 | 0.23 | 2.95 | 77.8 |
| | 1.0 | 335 | 101 | 146 | 0.18 | 2.30 | 82.7 |

Table 3.61: Results of potentiodynamic polarization studies for the corrosion of welded maraging steel in 1.0 M hydrochloric acid containing different concentrations of TBTBH.

| Temperature (°C) | Conc. of inhibitor (mM) | $-E_{corr}$ (mV /SCE) | b_a (mV dec ⁻¹) | $-b_c$ (mV dec ⁻¹) | i_{corr} (mA cm ⁻²) | \mathcal{U}_{corr} (mm y ⁻¹) | η (%) |
|------------------|-------------------------|-----------------------|-------------------------------|--------------------------------|-----------------------------------|--|------------|
| 30 | Blank | 324 | 112 | 158 | 0.51 | 6.57 | |
| | 0.2 | 346 | 103 | 132 | 0.14 | 1.80 | 72.5 |
| | 0.4 | 352 | 101 | 129 | 0.11 | 1.42 | 78.4 |
| | 0.6 | 292 | 98 | 127 | 0.07 | 0.90 | 86.3 |
| | 0.8 | 293 | 96 | 124 | 0.06 | 0.77 | 88.2 |
| | 1.0 | 316 | 95 | 120 | 0.03 | 0.39 | 94.1 |
| 35 | Blank | 328 | 118 | 163 | 0.68 | 8.77 | |
| | 0.2 | 343 | 109 | 141 | 0.20 | 2.63 | 70.6 |
| | 0.4 | 339 | 107 | 137 | 0.16 | 2.10 | 76.5 |
| | 0.6 | 324 | 104 | 134 | 0.12 | 1.49 | 82.3 |
| | 0.8 | 308 | 101 | 132 | 0.11 | 1.40 | 83.8 |
| | 1.0 | 319 | 99 | 127 | 0.06 | 0.79 | 91.2 |
| 40 | Blank | 336 | 126 | 171 | 0.95 | 12.25 | |
| | 0.2 | 298 | 117 | 152 | 0.31 | 4.04 | 67.4 |
| | 0.4 | 307 | 115 | 149 | 0.27 | 3.43 | 71.6 |
| | 0.6 | 334 | 112 | 147 | 0.21 | 2.69 | 77.9 |
| | 0.8 | 341 | 109 | 145 | 0.19 | 2.45 | 80.0 |
| | 1.0 | 354 | 105 | 141 | 0.12 | 1.59 | 87.4 |
| 45 | Blank | 331 | 131 | 179 | 1.07 | 13.79 | |
| | 0.2 | 326 | 119 | 154 | 0.37 | 4.83 | 65.4 |
| | 0.4 | 337 | 116 | 151 | 0.33 | 4.28 | 69.2 |
| | 0.6 | 328 | 114 | 149 | 0.28 | 3.59 | 73.8 |
| | 0.8 | 343 | 111 | 147 | 0.26 | 3.31 | 75.7 |
| | 1.0 | 351 | 108 | 143 | 0.19 | 2.48 | 82.2 |
| 50 | Blank | 328 | 142 | 191 | 1.75 | 22.56 | |
| | 0.2 | 319 | 124 | 165 | 0.67 | 8.57 | 61.7 |
| | 0.4 | 335 | 121 | 162 | 0.58 | 7.44 | 66.9 |
| | 0.6 | 329 | 119 | 160 | 0.51 | 6.54 | 70.9 |
| | 0.8 | 347 | 116 | 157 | 0.46 | 5.87 | 73.7 |
| | 1.0 | 354 | 112 | 153 | 0.37 | 4.74 | 78.9 |

Table 3.62: Results of potentiodynamic polarization studies for the corrosion of welded maraging steel in 1.5 M hydrochloric acid containing different concentrations of TBTBH.

| Temperature (°C) | Conc. of inhibitor (mM) | $-E_{corr}$ (mV /SCE) | b_a (mV dec ⁻¹) | $-b_c$ (mV dec ⁻¹) | i_{corr} (mA cm ⁻²) | ν_{corr} (mm y ⁻¹) | η (%) |
|------------------|-------------------------|-----------------------|-------------------------------|--------------------------------|-----------------------------------|------------------------------------|------------|
| 30 | Blank | 316 | 109 | 163 | 0.57 | 7.35 | |
| | 0.2 | 341 | 101 | 138 | 0.16 | 2.12 | 71.2 |
| | 0.4 | 348 | 98 | 135 | 0.13 | 1.70 | 76.8 |
| | 0.6 | 332 | 96 | 131 | 0.09 | 1.20 | 83.7 |
| | 0.8 | 329 | 96 | 130 | 0.08 | 1.02 | 86.1 |
| | 1.0 | 330 | 93 | 127 | 0.04 | 0.48 | 93.4 |
| | 35 | Blank | 320 | 117 | 171 | 0.98 | 12.63 |
| 0.2 | | 357 | 112 | 144 | 0.31 | 4.00 | 68.3 |
| 0.4 | | 352 | 108 | 142 | 0.25 | 3.27 | 74.1 |
| 0.6 | | 341 | 105 | 139 | 0.20 | 2.54 | 79.9 |
| 0.8 | | 323 | 103 | 138 | 0.18 | 2.31 | 81.7 |
| 1.0 | | 314 | 100 | 132 | 0.10 | 1.25 | 90.1 |
| 40 | | Blank | 328 | 124 | 183 | 1.31 | 16.89 |
| | 0.2 | 348 | 114 | 161 | 0.45 | 5.86 | 65.3 |
| | 0.4 | 356 | 112 | 158 | 0.41 | 5.34 | 68.4 |
| | 0.6 | 341 | 109 | 154 | 0.33 | 4.26 | 74.8 |
| | 0.8 | 334 | 107 | 152 | 0.29 | 3.70 | 78.1 |
| | 1.0 | 321 | 105 | 149 | 0.21 | 2.67 | 84.2 |
| | 45 | Blank | 322 | 132 | 198 | 1.80 | 23.20 |
| 0.2 | | 358 | 119 | 170 | 0.65 | 8.38 | 63.9 |
| 0.4 | | 361 | 116 | 167 | 0.59 | 7.63 | 67.1 |
| 0.6 | | 343 | 114 | 163 | 0.50 | 6.47 | 72.1 |
| 0.8 | | 329 | 111 | 161 | 0.47 | 6.08 | 73.8 |
| 1.0 | | 317 | 107 | 156 | 0.37 | 4.80 | 79.3 |
| 50 | | Blank | 315 | 147 | 209 | 2.63 | 33.90 |
| | 0.2 | 308 | 123 | 182 | 1.06 | 13.63 | 59.8 |
| | 0.4 | 319 | 120 | 177 | 0.93 | 11.97 | 64.7 |
| | 0.6 | 327 | 117 | 174 | 0.86 | 11.05 | 67.4 |
| | 0.8 | 335 | 114 | 170 | 0.75 | 9.66 | 71.5 |
| | 1.0 | 326 | 112 | 167 | 0.63 | 8.10 | 76.1 |

Table 3.63: Results of potentiodynamic polarization studies for the corrosion of welded maraging steel in 2.0 M hydrochloric acid containing different concentrations of TBTBH.

| Temperature (°C) | Conc. of inhibitor (mM) | $-E_{corr}$ (mV /SCE) | b_a (mV dec ⁻¹) | $-b_c$ (mV dec ⁻¹) | i_{corr} (mA cm ⁻²) | ν_{corr} (mm y ⁻¹) | η (%) |
|------------------|-------------------------|-----------------------|-------------------------------|--------------------------------|-----------------------------------|------------------------------------|------------|
| 30 | Blank | 324 | 114 | 178 | 0.90 | 11.60 | |
| | 0.2 | 341 | 108 | 152 | 0.28 | 3.56 | 69.3 |
| | 0.4 | 348 | 105 | 149 | 0.23 | 2.98 | 74.3 |
| | 0.6 | 353 | 101 | 147 | 0.16 | 2.11 | 81.8 |
| | 0.8 | 336 | 99 | 146 | 0.14 | 1.75 | 84.9 |
| | 1.0 | 329 | 97 | 141 | 0.07 | 0.90 | 92.2 |
| 35 | Blank | 316 | 129 | 186 | 1.34 | 17.27 | |
| | 0.2 | 348 | 123 | 163 | 0.45 | 5.75 | 66.7 |
| | 0.4 | 337 | 120 | 159 | 0.38 | 4.87 | 71.8 |
| | 0.6 | 329 | 118 | 156 | 0.31 | 3.94 | 77.2 |
| | 0.8 | 335 | 115 | 153 | 0.28 | 3.56 | 79.4 |
| | 1.0 | 340 | 113 | 149 | 0.14 | 1.78 | 89.7 |
| 40 | Blank | 310 | 137 | 193 | 2.61 | 33.64 | |
| | 0.2 | 295 | 126 | 171 | 0.94 | 12.08 | 64.1 |
| | 0.4 | 312 | 122 | 168 | 0.88 | 11.34 | 66.3 |
| | 0.6 | 318 | 119 | 165 | 0.72 | 9.32 | 72.3 |
| | 0.8 | 321 | 115 | 161 | 0.66 | 8.51 | 74.7 |
| | 1.0 | 337 | 113 | 157 | 0.44 | 5.69 | 83.1 |
| 45 | Blank | 327 | 143 | 212 | 4.46 | 57.49 | |
| | 0.2 | 313 | 129 | 187 | 1.67 | 21.56 | 62.5 |
| | 0.4 | 307 | 127 | 183 | 1.57 | 20.24 | 64.8 |
| | 0.6 | 298 | 124 | 181 | 1.32 | 17.07 | 70.3 |
| | 0.8 | 334 | 121 | 177 | 1.26 | 16.21 | 71.8 |
| | 1.0 | 347 | 116 | 173 | 1.00 | 12.94 | 77.5 |
| 50 | Blank | 332 | 159 | 223 | 5.93 | 76.44 | |
| | 0.2 | 362 | 134 | 191 | 2.53 | 32.64 | 57.3 |
| | 0.4 | 371 | 131 | 188 | 2.21 | 28.44 | 62.8 |
| | 0.6 | 345 | 128 | 184 | 2.12 | 27.29 | 64.3 |
| | 0.8 | 352 | 124 | 181 | 1.80 | 23.16 | 69.7 |
| | 1.0 | 367 | 121 | 176 | 1.58 | 20.33 | 73.4 |

Table 3.64: EIS data for the corrosion of welded maraging steel in 0.1 M hydrochloric acid containing different concentrations of TBTBH.

| Temperature (°C) | Conc. of inhibitor (mM) | R_p (ohm. cm ²) | C_{dl} (mF cm ⁻²) | η (%) |
|------------------|-------------------------|-------------------------------|---------------------------------|------------|
| 30 | Blank | 80.6 | 0.061 | |
| | 0.2 | 348.9 | 0.048 | 76.9 |
| | 0.4 | 437.0 | 0.045 | 81.6 |
| | 0.6 | 726.1 | 0.041 | 88.9 |
| | 0.8 | 876.0 | 0.039 | 90.8 |
| | 1.0 | 1408.1 | 0.034 | 94.3 |
| | 35 | Blank | 71.8 | 0.069 |
| 0.2 | | 269.9 | 0.043 | 73.4 |
| 0.4 | | 355.4 | 0.040 | 79.8 |
| 0.6 | | 491.7 | 0.037 | 85.4 |
| 0.8 | | 635.4 | 0.033 | 88.7 |
| 1.0 | | 897.5 | 0.029 | 92.0 |
| 40 | | Blank | 56.4 | 0.135 |
| | 0.2 | 200.7 | 0.126 | 71.9 |
| | 0.4 | 250.6 | 0.121 | 77.5 |
| | 0.6 | 346.0 | 0.117 | 83.7 |
| | 0.8 | 417.7 | 0.112 | 86.5 |
| | 1.0 | 613.0 | 0.107 | 90.8 |
| | 45 | Blank | 41.3 | 0.183 |
| 0.2 | | 131.9 | 0.161 | 68.7 |
| 0.4 | | 164.5 | 0.157 | 74.9 |
| 0.6 | | 210.7 | 0.153 | 80.4 |
| 0.8 | | 241.5 | 0.148 | 82.9 |
| 1.0 | | 365.4 | 0.142 | 88.7 |
| 50 | | Blank | 34.5 | 0.224 |
| | 0.2 | 104.2 | 0.201 | 66.9 |
| | 0.4 | 113.1 | 0.194 | 69.5 |
| | 0.6 | 156.0 | 0.189 | 77.9 |
| | 0.8 | 170.7 | 0.182 | 79.8 |
| | 1.0 | 225.4 | 0.179 | 84.7 |

Table 3.65: EIS data for the corrosion of welded maraging steel in 0.5 M hydrochloric acid containing different concentrations of TBTBH.

| Temperature (°C) | Conc. of inhibitor (mM) | R_p (ohm. cm ²) | C_{dl} (mF cm ⁻²) | η (%) |
|------------------|-------------------------|-------------------------------|---------------------------------|------------|
| 30 | Blank | 73.8 | 0.071 | |
| | 0.2 | 286.0 | 0.058 | 74.2 |
| | 0.4 | 358.2 | 0.051 | 79.4 |
| | 0.6 | 585.7 | 0.046 | 87.4 |
| | 0.8 | 716.5 | 0.041 | 89.7 |
| | 1.0 | 934.1 | 0.034 | 92.1 |
| | 35 | Blank | 55.4 | 0.112 |
| 0.2 | | 196.4 | 0.103 | 71.8 |
| 0.4 | | 256.5 | 0.097 | 78.4 |
| 0.6 | | 341.9 | 0.089 | 83.8 |
| 0.8 | | 443.2 | 0.083 | 87.5 |
| 1.0 | | 644.2 | 0.077 | 91.4 |
| 40 | | Blank | 47.1 | 0.165 |
| | 0.2 | 159.1 | 0.141 | 70.4 |
| | 0.4 | 199.6 | 0.134 | 76.3 |
| | 0.6 | 255.9 | 0.128 | 81.6 |
| | 0.8 | 273.8 | 0.121 | 82.8 |
| | 1.0 | 444.3 | 0.114 | 89.4 |
| | 45 | Blank | 38.0 | 0.216 |
| 0.2 | | 113.0 | 0.174 | 66.3 |
| 0.4 | | 134.2 | 0.168 | 71.7 |
| 0.6 | | 164.5 | 0.161 | 76.9 |
| 0.8 | | 192.8 | 0.155 | 80.3 |
| 1.0 | | 240.5 | 0.149 | 84.2 |
| 50 | | Blank | 29.6 | 0.279 |
| | 0.2 | 82.6 | 0.231 | 64.2 |
| | 0.4 | 90.7 | 0.224 | 67.4 |
| | 0.6 | 110.4 | 0.217 | 73.2 |
| | 0.8 | 125.9 | 0.211 | 76.5 |
| | 1.0 | 163.5 | 0.204 | 81.9 |

Table 3.66: EIS data for the corrosion of welded maraging steel in 1.0 M hydrochloric acid containing different concentrations of TBTBH.

| Temperature (°C) | Conc. of inhibitor (mM) | R_p (ohm. cm ²) | C_{dl} (mF cm ⁻²) | η (%) |
|------------------|-------------------------|-------------------------------|---------------------------------|------------|
| 30 | Blank | 56.1 | 0.110 | |
| | 0.2 | 199.6 | 0.092 | 71.9 |
| | 0.4 | 253.8 | 0.087 | 77.8 |
| | 0.6 | 397.9 | 0.079 | 85.9 |
| | 0.8 | 475.4 | 0.071 | 88.2 |
| | 1.0 | 684.1 | 0.064 | 91.8 |
| | 35 | Blank | 43.2 | 0.203 |
| 0.2 | | 144.5 | 0.174 | 70.1 |
| 0.4 | | 178.4 | 0.168 | 75.8 |
| 0.6 | | 245.4 | 0.163 | 82.4 |
| 0.8 | | 252.6 | 0.157 | 82.9 |
| 1.0 | | 450.0 | 0.152 | 90.4 |
| 40 | | Blank | 32.9 | 0.276 |
| | 0.2 | 99.1 | 0.227 | 66.8 |
| | 0.4 | 130.0 | 0.219 | 74.7 |
| | 0.6 | 144.2 | 0.213 | 77.2 |
| | 0.8 | 167.9 | 0.208 | 80.4 |
| | 1.0 | 276.4 | 0.203 | 88.1 |
| | 45 | Blank | 30.6 | 0.308 |
| 0.2 | | 86.7 | 0.254 | 64.7 |
| 0.4 | | 96.8 | 0.247 | 68.4 |
| 0.6 | | 113.7 | 0.241 | 73.1 |
| 0.8 | | 128.0 | 0.238 | 76.1 |
| 1.0 | | 173.9 | 0.232 | 82.4 |
| 50 | | Blank | 20.2 | 0.346 |
| | 0.2 | 53.6 | 0.287 | 62.3 |
| | 0.4 | 59.2 | 0.281 | 65.9 |
| | 0.6 | 71.3 | 0.274 | 71.7 |
| | 0.8 | 77.9 | 0.269 | 74.1 |
| | 1.0 | 91.4 | 0.253 | 77.9 |

Table 3.67: EIS data for the corrosion of welded maraging steel in 1.5 M hydrochloric acid containing different concentrations of TBTBH.

| Temperature (°C) | Conc. of inhibitor (mM) | R_p (ohm. cm ²) | C_{dl} (mF cm ⁻²) | η (%) |
|------------------|-------------------------|-------------------------------|---------------------------------|------------|
| 30 | Blank | 49.2 | 0.166 | |
| | 0.2 | 166.2 | 0.132 | 70.4 |
| | 0.4 | 199.1 | 0.129 | 75.3 |
| | 0.6 | 286.0 | 0.124 | 82.8 |
| | 0.8 | 344.1 | 0.119 | 85.7 |
| | 1.0 | 529.0 | 0.114 | 90.6 |
| | 35 | Blank | 30.6 | 0.315 |
| 0.2 | | 95.3 | 0.244 | 67.9 |
| 0.4 | | 116.3 | 0.241 | 73.7 |
| 0.6 | | 143.6 | 0.238 | 78.7 |
| 0.8 | | 156.1 | 0.231 | 80.4 |
| 1.0 | | 297.0 | 0.224 | 89.7 |
| 40 | | Blank | 24.5 | 0.378 |
| | 0.2 | 69.6 | 0.283 | 64.8 |
| | 0.4 | 74.5 | 0.274 | 67.1 |
| | 0.6 | 91.4 | 0.267 | 73.2 |
| | 0.8 | 110.8 | 0.261 | 77.9 |
| | 1.0 | 194.4 | 0.253 | 87.4 |
| | 45 | Blank | 19.1 | 0.395 |
| 0.2 | | 51.9 | 0.294 | 63.2 |
| 0.4 | | 57.2 | 0.289 | 66.6 |
| 0.6 | | 69.9 | 0.282 | 72.7 |
| 0.8 | | 71.8 | 0.274 | 73.4 |
| 1.0 | | 90.5 | 0.269 | 78.9 |
| 50 | | Blank | 14.2 | 0.402 |
| | 0.2 | 34.4 | 0.311 | 58.7 |
| | 0.4 | 39.2 | 0.294 | 63.8 |
| | 0.6 | 44.5 | 0.288 | 68.1 |
| | 0.8 | 49.4 | 0.281 | 71.3 |
| | 1.0 | 58.6 | 0.273 | 75.8 |

Table 3.68: EIS data for the corrosion of welded maraging steel in 2.0 M hydrochloric acid containing different concentrations of TBTBH.

| Temperature (°C) | Conc. of inhibitor (mM) | R_p (ohm. cm ²) | C_{dl} (mF cm ⁻²) | η (%) |
|------------------|-------------------------|-------------------------------|---------------------------------|------------|
| 30 | Blank | 33.6 | 0.248 | |
| | 0.2 | 107.3 | 0.197 | 68.7 |
| | 0.4 | 128.2 | 0.189 | 73.8 |
| | 0.6 | 175.9 | 0.183 | 80.9 |
| | 0.8 | 212.6 | 0.176 | 84.2 |
| | 1.0 | 329.4 | 0.167 | 89.8 |
| | 35 | Blank | 24.5 | 0.362 |
| 0.2 | | 70.8 | 0.271 | 65.4 |
| 0.4 | | 85.6 | 0.263 | 71.4 |
| 0.6 | | 106.1 | 0.257 | 76.9 |
| 0.8 | | 115.5 | 0.248 | 78.8 |
| 1.0 | | 209.4 | 0.242 | 88.3 |
| 40 | | Blank | 13.3 | 0.399 |
| | 0.2 | 36.1 | 0.284 | 63.2 |
| | 0.4 | 39.0 | 0.279 | 65.9 |
| | 0.6 | 47.1 | 0.272 | 71.8 |
| | 0.8 | 51.5 | 0.264 | 74.2 |
| | 1.0 | 75.6 | 0.257 | 82.4 |
| | 45 | Blank | 8.3 | 0.418 |
| 0.2 | | 21.8 | 0.313 | 62.1 |
| 0.4 | | 23.2 | 0.302 | 64.3 |
| 0.6 | | 27.4 | 0.297 | 69.8 |
| 0.8 | | 28.0 | 0.283 | 70.4 |
| 1.0 | | 35.9 | 0.274 | 76.9 |
| 50 | | Blank | 6.8 | 0.439 |
| | 0.2 | 15.5 | 0.312 | 56.2 |
| | 0.4 | 17.7 | 0.303 | 61.6 |
| | 0.6 | 19.5 | 0.294 | 65.2 |
| | 0.8 | 21.4 | 0.287 | 68.3 |
| | 1.0 | 25.9 | 0.272 | 73.8 |

Table 3.69: Activation parameters for the corrosion of welded maraging steel in hydrochloric acid containing different concentrations of TBTBH.

| Molarity of HCl (M) | Conc. of inhibitor (mM) | E_a (kJ mol ⁻¹) | ΔH^\ddagger (kJ mol ⁻¹) | ΔS^\ddagger (J mol ⁻¹ K ⁻¹) |
|------------------------|----------------------------|----------------------------------|--|---|
| 0.1 | Blank | 42.28 | 39.62 | -103.29 |
| | 0.2 | 57.11 | 54.51 | -66.46 |
| | 0.4 | 63.31 | 60.71 | -48.42 |
| | 0.6 | 71.34 | 68.74 | -25.81 |
| | 0.8 | 75.67 | 73.07 | -13.34 |
| | 1.0 | 76.58 | 75.98 | -6.52 |
| 0.5 | Blank | 42.97 | 39.37 | -102.37 |
| | 0.2 | 56.45 | 53.35 | -66.21 |
| | 0.4 | 62.94 | 60.53 | -47.09 |
| | 0.6 | 74.89 | 72.28 | -11.42 |
| | 0.8 | 76.81 | 74.21 | -6.73 |
| | 1.0 | 78.58 | 77.98 | -4.32 |
| 1.0 | Blank | 47.51 | 44.97 | -81.34 |
| | 0.2 | 60.57 | 57.93 | -49.00 |
| | 0.4 | 65.49 | 62.89 | -34.70 |
| | 0.6 | 74.89 | 72.28 | -11.42 |
| | 0.8 | 77.81 | 76.21 | -3.43 |
| | 1.0 | 79.58 | 78.98 | -2.12 |
| 1.5 | Blank | 59.37 | 56.78 | -40.52 |
| | 0.2 | 58.57 | 59.93 | -51.00 |
| | 0.4 | 63.49 | 61.89 | -44.70 |
| | 0.6 | 71.89 | 72.28 | -21.42 |
| | 0.8 | 74.81 | 75.21 | -16.73 |
| | 1.0 | 76.58 | 74.98 | -14.32 |
| 2.0 | Blank | 80.98 | 78.36 | -33.72 |
| | 0.2 | 53.07 | 53.91 | -49.00 |
| | 0.4 | 55.39 | 54.86 | -34.70 |
| | 0.6 | 64.17 | 62.54 | -11.42 |
| | 0.8 | 66.82 | 65.30 | -6.73 |
| | 1.0 | 71.53 | 69.08 | -4.32 |

Table 3.70: Maximum inhibition efficiency attained in different concentrations of hydrochloric acid at different temperatures for TBTBH.

| Temperature (°C) | Welded Maraging Steel | | | |
|---------------------|--|-----------------------------------|---|------------|
| | Hydrochloric acid concentration (M) | Concentration of TBTBH (mM) | η (%) | |
| | | | Potentiodynamic polarization method | EIS method |
| 30 | 0.1 | 1.0 | 96.8 | 94.3 |
| | 0.5 | | 94.3 | 92.1 |
| | 1.0 | | 94.1 | 91.8 |
| | 1.5 | | 93.4 | 90.6 |
| | 2.0 | | 92.2 | 89.8 |
| 35 | 0.1 | 1.0 | 94.3 | 92.0 |
| | 0.5 | | 91.9 | 91.4 |
| | 1.0 | | 91.2 | 90.4 |
| | 1.5 | | 90.1 | 89.7 |
| | 2.0 | | 89.7 | 88.3 |
| 40 | 0.1 | 1.0 | 91.5 | 90.8 |
| | 0.5 | | 89.4 | 89.4 |
| | 1.0 | | 87.4 | 88.1 |
| | 1.5 | | 84.2 | 87.4 |
| | 2.0 | | 83.1 | 82.4 |
| 45 | 0.1 | 1.0 | 89.7 | 88.7 |
| | 0.5 | | 85.1 | 84.2 |
| | 1.0 | | 82.2 | 82.4 |
| | 1.5 | | 79.3 | 78.9 |
| | 2.0 | | 77.5 | 76.9 |
| 50 | 0.1 | 1.0 | 85.2 | 84.7 |
| | 0.5 | | 82.7 | 81.9 |
| | 1.0 | | 78.9 | 77.9 |
| | 1.5 | | 76.1 | 75.8 |
| | 2.0 | | 73.4 | 73.8 |

Table 3.71: Thermodynamic parameters for the adsorption of TBTBH on welded maraging steel surface in hydrochloric acid at different temperatures.

| Molarity of HCl (M) | Temperature (° C) | $-\Delta G^{\circ}_{ads}$ (kJ mol ⁻¹) | ΔH°_{ads} (kJ mol ⁻¹) | ΔS°_{ads} (J mol ⁻¹ K ⁻¹) |
|------------------------|----------------------|--|---|--|
| 0.1 | 30 | 34.04 | -24.87 | -63.61 |
| | 35 | 33.89 | | |
| | 40 | 33.64 | | |
| | 45 | 33.50 | | |
| | 50 | 33.35 | | |
| 0.5 | 30 | 34.48 | -25.93 | -61.80 |
| | 35 | 34.20 | | |
| | 40 | 34.09 | | |
| | 45 | 33.97 | | |
| | 50 | 33.68 | | |
| 1.0 | 30 | 33.35 | -24.29 | -91.84 |
| | 35 | 33.23 | | |
| | 40 | 33.16 | | |
| | 45 | 32.84 | | |
| | 50 | 32.71 | | |
| 1.5 | 30 | 33.14 | -21.33 | -84.79 |
| | 35 | 33.01 | | |
| | 40 | 32.94 | | |
| | 45 | 32.81 | | |
| | 50 | 32.69 | | |
| 2.0 | 30 | 32.88 | -19.26 | -93.38 |
| | 35 | 32.65 | | |
| | 40 | 32.76 | | |
| | 45 | 32.47 | | |
| | 50 | 32.23 | | |

3.8 3,4,5-TRIMETHOXY-BENZOICACID(3,4,5-TRIMETHOXY-BENZYLIDENE) HYDRAZIDE (TBTBH) AS INHIBITOR FOR THE CORROSION OF WELDED MARAGING STEEL IN SULPHURIC ACID MEDIUM

3.8.1 Potentiodynamic polarization measurements

The potentiodynamic polarization plots for the corrosion of welded maraging steel in 1.0 M sulphuric acid in the presence of different concentrations of TBTBH, at 30 °C are shown in Fig. 3.60. Similar results were obtained at other temperatures and also in the other four concentrations of sulphuric acid. The potentiodynamic polarization parameters such as corrosion potential (E_{corr}), corrosion current density (i_{corr}), anodic and cathodic Tafel slopes (b_a , b_c) calculated from Tafel plots in the presence of different concentrations of TBTBH at different temperatures are summarized in Tables 3.72 to 3.76.

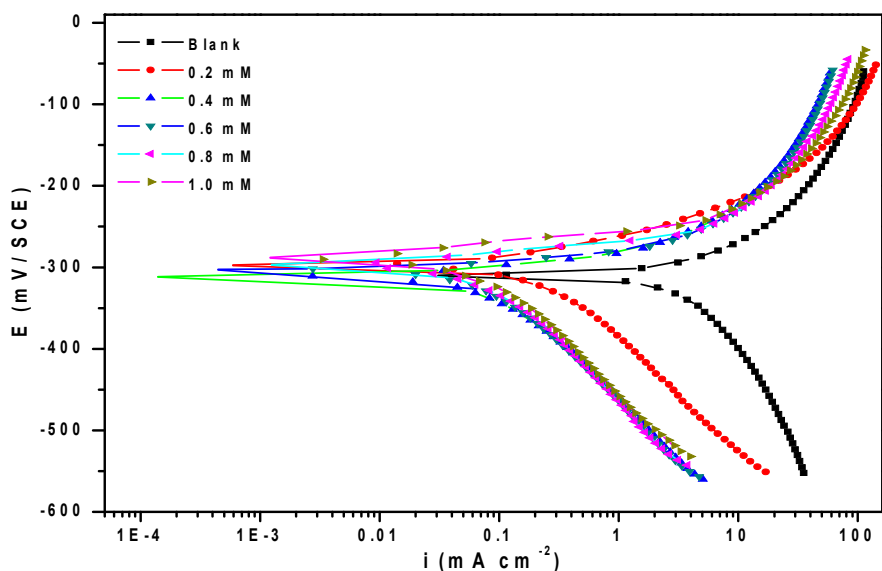


Fig. 3.60: Potentiodynamic polarization curves for the corrosion of welded maraging steel in 1.0 M H₂SO₄ containing different concentrations of TBTBH at 30 °C.

The presence of inhibitor brings down the corrosion rate considerably. Polarization curves are shifted to a lower current density region indicating a decrease in corrosion rate (Li et al. 2007). Inhibition efficiency increases with the increase in TBTBH

concentration. The presence of inhibitor does not cause any significant shift or a trend for the shift in the E_{corr} value, which implies that the inhibitor, TBTBH, acts as a mixed type inhibitor, affecting both anodic and cathodic reactions.

3.8.2 Electrochemical impedance spectroscopy (EIS) studies

Nyquist plots for the corrosion of welded maraging steel in 1.0 M sulphuric acid solution in the presence of different concentrations of TBTBH at 30 °C are shown in Fig. 3.61. Similar plots were obtained in other concentrations of sulphuric acid and also at other temperatures. The experimental results of EIS measurements obtained for the corrosion of welded maraging steel in 1.0 M sulphuric acid are summarized in Tables 3.77 to 3.81. The curves obtained are similar to the ones obtained in the presence of BTPO in sulphuric acid. The equivalent circuit given in Fig. 3.29 is used to fit the experimental data for the corrosion of welded maraging steel in sulphuric acid in the presence of TBTBH. The charge transfer resistance (R_{ct}) increases and double layer capacitance decreases with the increase in the concentration of TBTBH, indicating an increase in the inhibition efficiency. TBTBH inhibits the corrosion primarily through its adsorption and subsequent formation of a barrier film on the metal surface (El Hosary et al. 1972, Sanaa et al. 2008). The results obtained from impedance studies are in good agreement with the results of potentiodynamic polarization studies.

The Bode plots of phase angle and amplitude for the corrosion of the alloy in the presence of TBTBH in 1.0 M sulphuric acid are shown in Fig. 3.62 (a) and Fig. 3.62 (b), respectively. Phase angle increases with increase in concentrations of TBTBH in sulphuric acid medium. The difference between the HF and LF for the inhibited system in the Bode plot increases with the increase in the concentration of TBTBH. The increase in phase angle with the increase in TBTBH concentration suggests decrease in the corrosion rate. An increase in TBTBH concentration leads to an increase in the impedance ($|Z|$) value.

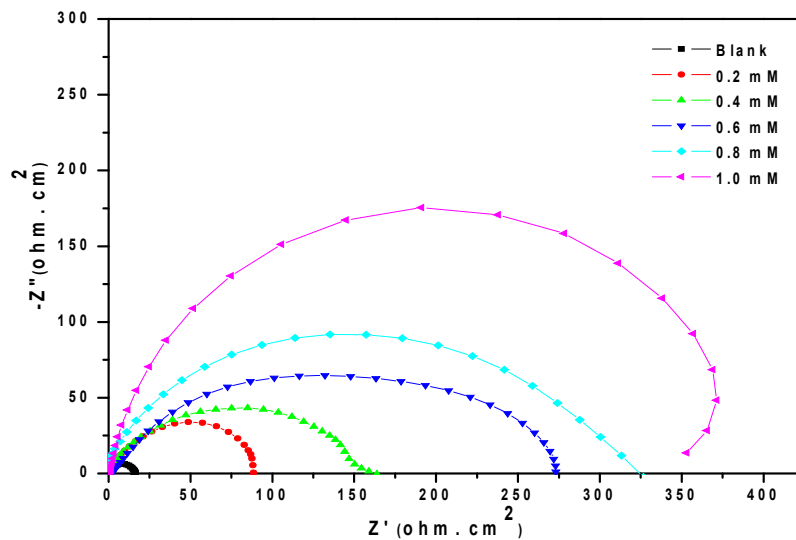


Fig. 3.61: Nyquist plots for the corrosion of welded maraging steel in 1.0 M H_2SO_4 containing different concentrations of TBTBH at 30 °C.

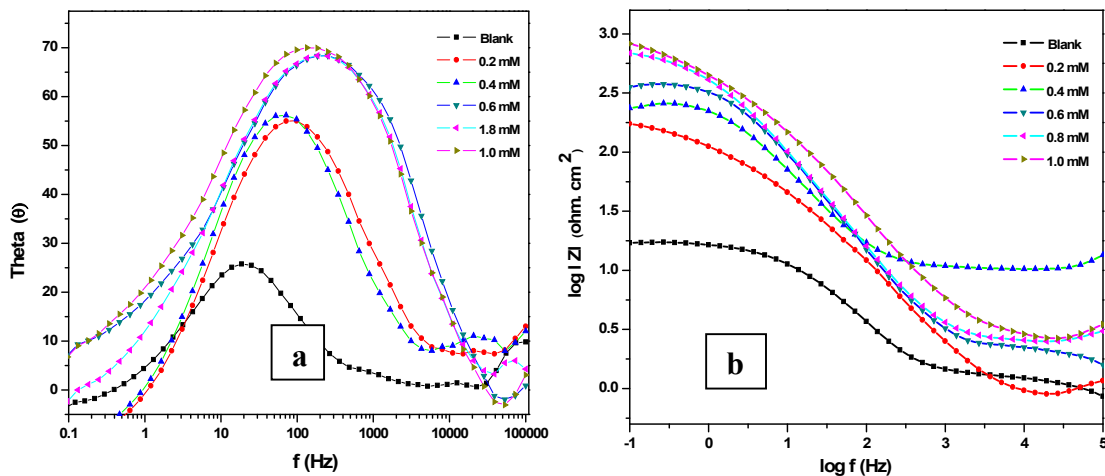


Fig. 3.62: Bode (a) phase angle plots and (b) amplitude plots for the corrosion of welded maraging steel in 1.0 M H_2SO_4 containing different concentrations of TBTBH at 30 °C.

3.8.3 Effect of temperature

The potentiodynamic polarization and EIS results pertaining to different temperatures in different concentrations of sulphuric acid in the presence of TBTBH,

have been listed in the Tables 3.72 to 3.81. The decrease in inhibition efficiency with the increase in temperature indicates desorption of the inhibitor molecules from the metal surface on increasing the temperature (Poornima et al. 2011). This fact is also suggestive of physisorption of the inhibitor molecules on the metal surface. The Arrhenius plots for the corrosion of welded maraging steel in the presence of different concentrations of TBTBH in 1.0 M H₂SO₄ acid are shown in Fig. 3.63. The plots of $\ln(v_{\text{corr}}/T)$ versus $1/T$ in 1.0 M H₂SO₄ acid in the presence of different concentrations of TBTBH are shown in Fig. 3.64.

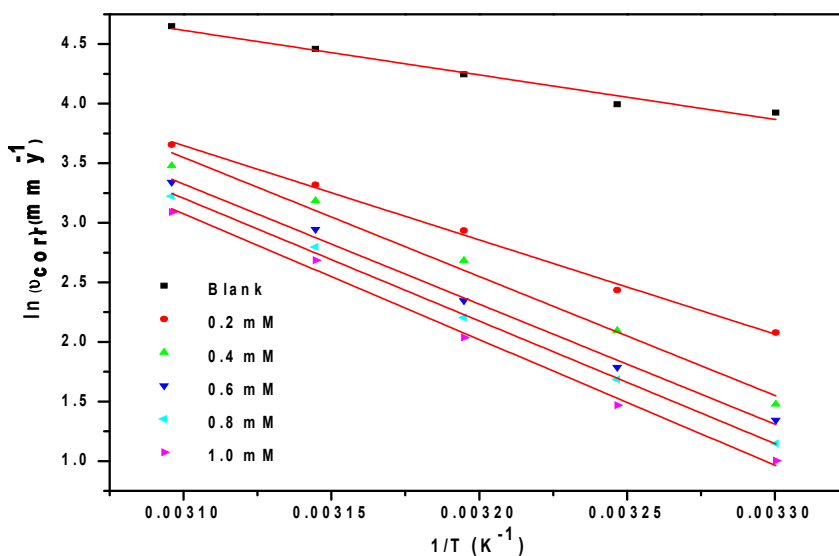


Fig. 3.63: Arrhenius plots for the corrosion of welded maraging steel in 1.0 M H₂SO₄ containing different concentrations of TBTBH.

The calculated values of E_a , ΔH^\ddagger and ΔS^\ddagger are given in Table 3.82. The proportionate increase in the activation energy on the addition of TBTBH can be attributed to the adsorption of TBTBH providing a barrier on the alloy surface (Avci et al. 2008). The values of entropy of activation indicates that the activated complex in the rate determining step represents an association rather than dissociation, resulting in a decrease in randomness on going from the reactants to the activated complex.

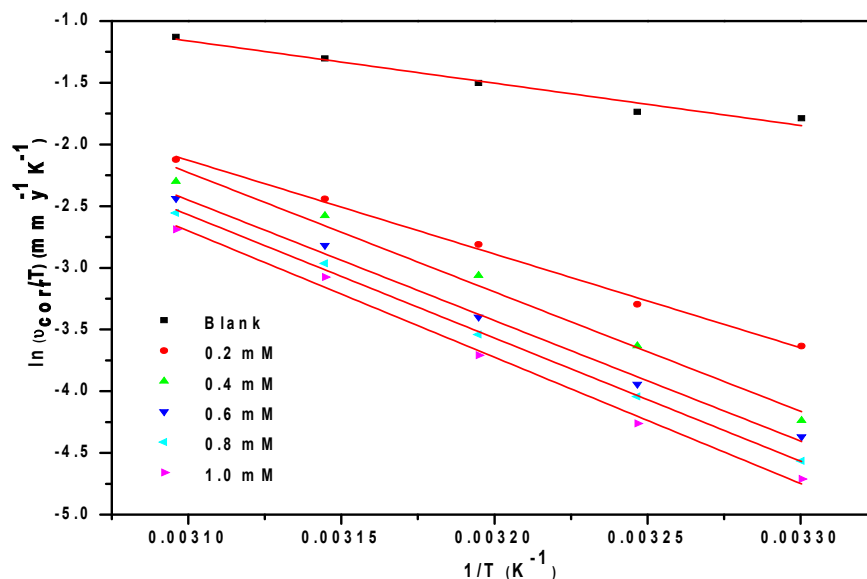


Fig. 3.64: Plots of $\ln(v_{corr}/T)$ versus $1/T$ for the corrosion of welded maraging steel in 1.0 M H_2SO_4 containing different concentrations of TBTBH.

3.8.4 Effect of acid concentration

Table 3.83 summarizes the maximum inhibition efficiencies exhibited by TBTBH in the H_2SO_4 solution of different concentrations. It is evident from both polarization and EIS experimental results that, for a particular concentration of inhibitor, the inhibition efficiency decreases with the increase in sulphuric acid concentration on the welded maraging steel. The highest inhibition efficiency is observed in sulphuric acid of 0.1 M concentration.

3.8.5 Adsorption isotherm

The adsorption of TBTBH on the surface of welded maraging steel was found to obey Langmuir adsorption isotherm. The Langmuir adsorption isotherms for the adsorption of TBTBH on welded maraging steel in 1.0 M H_2SO_4 are shown in Fig. 3.65. The thermodynamic data obtained for the adsorption of TBTBH on welded maraging steel are tabulated in Table 3.84. The linear regression coefficients are close to unity and the slopes of the straight lines are nearly unity, suggesting that the adsorption of TBTBH

obeys Langmuir's adsorption isotherm with negligible interaction between the adsorbed molecules. The exothermic ΔH^0_{ads} values of less than $-41.86 \text{ kJ mol}^{-1}$ predict the physisorption of TBTBH on the alloy surfaces (Ashish Kumar et al. 2010). The ΔG^0_{ads} values predict both physisorption and chemisorption of TBTBH. Therefore it can be concluded that the adsorption of TBTBH on the welded maraging steel is predominantly through physisorption. These facts are also supported by the variation of inhibition efficiencies with temperature on the alloy surface.

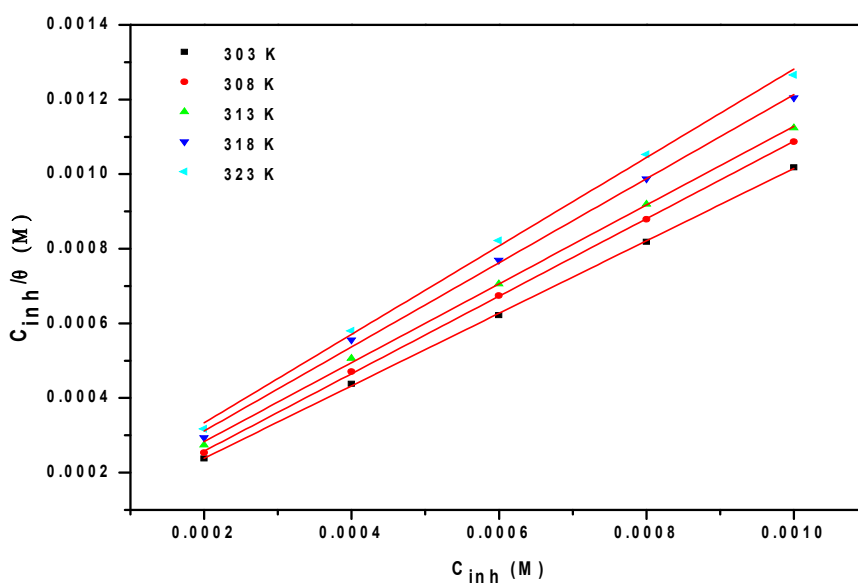


Fig. 3.65: Langmuir adsorption isotherms for the adsorption of TBTBH on welded maraging steel in 1.0 M H_2SO_4 at different temperatures.

3.8.6 Mechanism of corrosion inhibition

The corrosion inhibition mechanism of TBTBH in sulphuric acid solution can be explained in the same lines as that of TBTBH in the section 3.7.6. The inhibitor TBTBH protects the alloy surface through predominant physisorption mode in which the positive charge centers of TBTBH gets adsorbed on the alloy surface through electrostatic attraction and also to some extent through chemisorption mode of adsorption with a predominant physisorption.

3.8.7 SEM/EDX studies

Fig. 3.66 represents SEM image of welded maraging steel after the corrosion tests in a medium of sulphuric acid containing 1.0 mM of TBTBH. The image clearly shows a smooth surface due to the adsorbed layer of inhibitor molecules on the alloy surface, thus protecting the metal from corrosion.

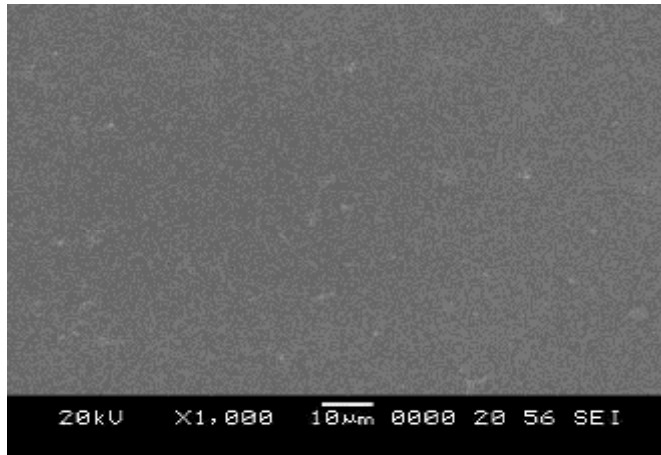


Fig.3.66: SEM image of the welded maraging steel after immersion in 1.0 M H₂SO₄ in the presence of TBTBH.

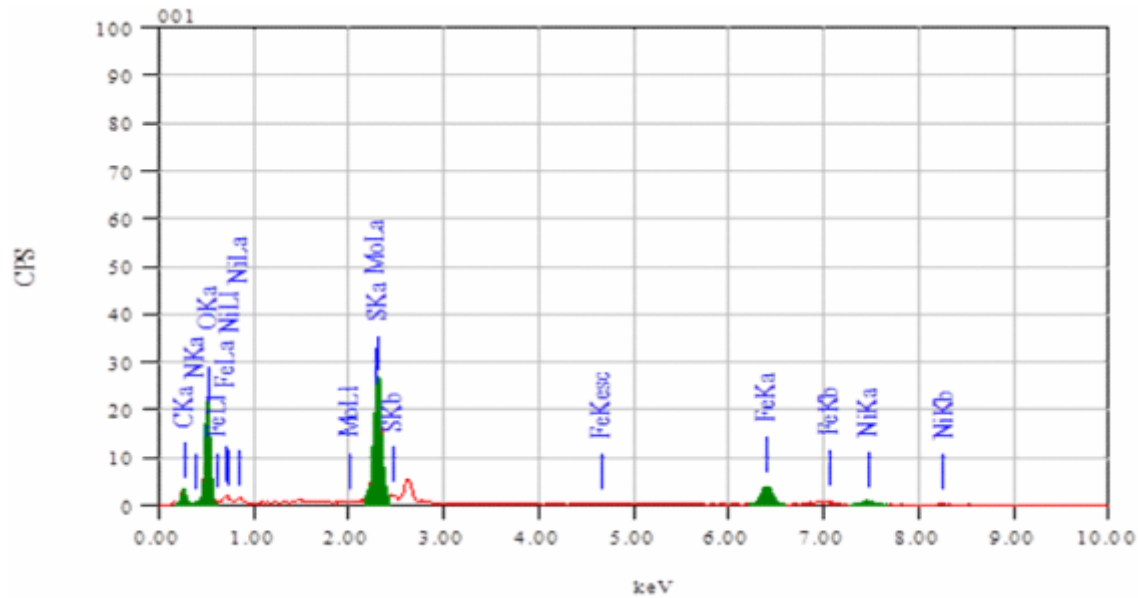


Fig. 3.67: EDX spectra of the welded maraging steel after immersion in 1.0 M H₂SO₄ in the presence of TBTBH.

The EDX spectra for the selected areas on the SEM images of Fig. 3.66 is shown in Fig. 3.67. The atomic percentage of the elements found in the EDX spectra for inhibited metal surface was 2.75% Fe, 0.76% Ni, 0.26% Mo, 51.60% O, 12.82% N, 24.90% C and 6.82% S and indicated the formation of inhibitor film on the area. The elemental compositions mentioned above were mean values of different regions.

Table 3.72: Results of potentiodynamic polarization studies for the corrosion of welded maraging steel in 0.1 M sulphuric acid containing different concentrations of TBTBH.

| Temperature (°C) | Conc. of inhibitor (mM) | $-E_{corr}$ (mV /SCE) | b_a (mV dec ⁻¹) | $-b_c$ (mV dec ⁻¹) | i_{corr} (mA cm ⁻²) | U_{corr} (mm y ⁻¹) | η (%) |
|------------------|-------------------------|-----------------------|-------------------------------|--------------------------------|-----------------------------------|----------------------------------|------------|
| 30 | Blank | 356 | 162 | 113 | 1.98 | 25.52 | |
| | 0.2 | 337 | 124 | 108 | 0.33 | 4.24 | 83.4 |
| | 0.4 | 324 | 121 | 105 | 0.18 | 2.37 | 90.7 |
| | 0.6 | 329 | 116 | 101 | 0.10 | 1.32 | 91.8 |
| | 0.8 | 322 | 113 | 97 | 0.09 | 1.12 | 92.6 |
| | 1.0 | 342 | 104 | 92 | 0.07 | 0.94 | 94.1 |
| | 35 | Blank | 353 | 171 | 124 | 2.41 | 31.07 |
| 0.2 | | 328 | 137 | 119 | 0.48 | 6.15 | 80.2 |
| 0.4 | | 361 | 129 | 115 | 0.36 | 4.62 | 85.1 |
| 0.6 | | 337 | 124 | 112 | 0.24 | 3.10 | 90.0 |
| 0.8 | | 341 | 119 | 109 | 0.21 | 2.70 | 91.3 |
| 1.0 | | 320 | 117 | 104 | 0.17 | 2.23 | 92.8 |
| 40 | | Blank | 347 | 183 | 131 | 2.93 | 37.77 |
| | 0.2 | 334 | 148 | 124 | 0.79 | 10.12 | 73.2 |
| | 0.4 | 341 | 141 | 121 | 0.71 | 9.17 | 75.7 |
| | 0.6 | 327 | 134 | 118 | 0.49 | 6.26 | 83.4 |
| | 0.8 | 332 | 129 | 114 | 0.42 | 5.40 | 85.7 |
| | 1.0 | 316 | 123 | 110 | 0.34 | 4.38 | 88.4 |
| | 45 | Blank | 345 | 197 | 142 | 3.47 | 44.73 |
| 0.2 | | 351 | 154 | 131 | 1.01 | 21.78 | 70.9 |
| 0.4 | | 338 | 148 | 127 | 0.93 | 20.03 | 73.2 |
| 0.6 | | 327 | 143 | 123 | 0.86 | 15.29 | 75.3 |
| 0.8 | | 334 | 131 | 118 | 0.73 | 13.37 | 78.9 |
| 1.0 | | 329 | 126 | 114 | 0.52 | 11.89 | 85.0 |
| 50 | | Blank | 342 | 214 | 154 | 6.14 | 79.15 |
| | 0.2 | 348 | 183 | 143 | 2.02 | 54.84 | 68.3 |
| | 0.4 | 351 | 178 | 137 | 1.85 | 47.96 | 71.1 |
| | 0.6 | 329 | 165 | 134 | 1.63 | 39.81 | 73.4 |
| | 0.8 | 298 | 157 | 129 | 1.42 | 33.87 | 76.2 |
| | 1.0 | 332 | 149 | 123 | 1.19 | 30.62 | 80.6 |

Table 3.73: Results of potentiodynamic polarization studies for the corrosion of welded maraging steel in 0.5 M sulphuric acid containing different concentrations of TBTBH.

| Temperature (°C) | Conc. of inhibitor (mM) | $-E_{corr}$ (mV /SCE) | b_a (mV dec ⁻¹) | $-b_c$ (mV dec ⁻¹) | i_{corr} (mA cm ⁻²) | ν_{corr} (mm y ⁻¹) | η (%) |
|------------------|-------------------------|-----------------------|-------------------------------|--------------------------------|-----------------------------------|------------------------------------|------------|
| 30 | Blank | 322 | 172 | 115 | 2.47 | 31.84 | |
| | 0.2 | 317 | 129 | 113 | 0.42 | 5.47 | 82.8 |
| | 0.4 | 324 | 126 | 108 | 0.24 | 3.05 | 90.4 |
| | 0.6 | 327 | 119 | 105 | 0.14 | 1.81 | 91.3 |
| | 0.8 | 314 | 117 | 102 | 0.12 | 1.49 | 92.3 |
| | 1.0 | 332 | 112 | 97 | 0.09 | 1.24 | 92.9 |
| 35 | Blank | 321 | 191 | 132 | 2.68 | 34.55 | |
| | 0.2 | 316 | 142 | 124 | 0.59 | 7.56 | 78.1 |
| | 0.4 | 311 | 138 | 121 | 0.42 | 5.42 | 84.3 |
| | 0.6 | 308 | 134 | 116 | 0.29 | 3.76 | 89.1 |
| | 0.8 | 324 | 129 | 112 | 0.25 | 3.17 | 90.8 |
| | 1.0 | 334 | 124 | 107 | 0.21 | 2.76 | 92.0 |
| 40 | Blank | 318 | 207 | 144 | 4.71 | 60.71 | |
| | 0.2 | 294 | 154 | 129 | 1.48 | 19.12 | 68.5 |
| | 0.4 | 310 | 149 | 124 | 1.26 | 16.27 | 73.2 |
| | 0.6 | 327 | 142 | 121 | 0.89 | 11.41 | 81.2 |
| | 0.8 | 334 | 131 | 117 | 0.76 | 9.83 | 83.8 |
| | 1.0 | 341 | 127 | 114 | 0.64 | 8.32 | 86.3 |
| 45 | Blank | 314 | 224 | 158 | 5.38 | 69.35 | |
| | 0.2 | 308 | 163 | 135 | 2.79 | 35.92 | 48.2 |
| | 0.4 | 297 | 157 | 132 | 2.51 | 32.31 | 53.4 |
| | 0.6 | 310 | 149 | 127 | 1.95 | 25.17 | 63.7 |
| | 0.8 | 312 | 142 | 122 | 1.65 | 21.29 | 69.3 |
| | 1.0 | 329 | 137 | 117 | 1.46 | 18.93 | 72.7 |
| 50 | Blank | 312 | 232 | 163 | 6.94 | 89.45 | |
| | 0.2 | 298 | 192 | 149 | 5.04 | 64.94 | 27.4 |
| | 0.4 | 304 | 184 | 141 | 4.32 | 55.64 | 37.8 |
| | 0.6 | 318 | 173 | 137 | 3.64 | 46.96 | 47.5 |
| | 0.8 | 309 | 164 | 133 | 3.20 | 41.32 | 53.8 |
| | 1.0 | 321 | 157 | 128 | 2.89 | 37.21 | 58.4 |

Table 3.74: Results of potentiodynamic polarization studies for the corrosion of welded maraging steel in 1.0 M sulphuric acid containing different concentrations of TBTBH.

| Temperature (°C) | Conc. of inhibitor (mM) | $-E_{corr}$ (mV /SCE) | b_a (mV dec ⁻¹) | $-b_c$ (mV dec ⁻¹) | i_{corr} (mA cm ⁻²) | U_{corr} (mm y ⁻¹) | η (%) |
|------------------|-------------------------|-----------------------|-------------------------------|--------------------------------|-----------------------------------|----------------------------------|------------|
| 30 | Blank | 315 | 187 | 132 | 3.93 | 50.65 | |
| | 0.2 | 292 | 134 | 127 | 0.71 | 9.15 | 81.9 |
| | 0.4 | 314 | 129 | 124 | 0.39 | 5.03 | 89.1 |
| | 0.6 | 309 | 126 | 123 | 0.23 | 2.96 | 90.1 |
| | 0.8 | 295 | 124 | 119 | 0.19 | 2.45 | 91.2 |
| | 1.0 | 288 | 123 | 117 | 0.16 | 2.06 | 91.9 |
| | 35 | Blank | 313 | 198 | 147 | 4.21 | 54.12 |
| 0.2 | | 317 | 176 | 131 | 0.88 | 11.40 | 77.5 |
| 0.4 | | 298 | 174 | 129 | 0.63 | 8.14 | 83.9 |
| 0.6 | | 312 | 169 | 124 | 0.46 | 5.97 | 88.2 |
| 0.8 | | 307 | 164 | 122 | 0.38 | 4.88 | 90.4 |
| 1.0 | | 309 | 159 | 119 | 0.34 | 4.34 | 91.4 |
| 40 | | Blank | 310 | 212 | 163 | 5.41 | 69.72 |
| | 0.2 | 312 | 191 | 147 | 1.46 | 18.83 | 62.8 |
| | 0.4 | 308 | 187 | 141 | 1.14 | 14.64 | 71.1 |
| | 0.6 | 298 | 184 | 137 | 0.81 | 10.46 | 79.4 |
| | 0.8 | 307 | 182 | 132 | 0.70 | 9.07 | 82.1 |
| | 1.0 | 319 | 178 | 129 | 0.59 | 7.67 | 84.9 |
| | 45 | Blank | 312 | 243 | 178 | 6.70 | 86.36 |
| 0.2 | | 315 | 216 | 153 | 2.14 | 27.64 | 45.4 |
| 0.4 | | 319 | 213 | 148 | 1.88 | 24.18 | 52.3 |
| 0.6 | | 304 | 209 | 145 | 1.47 | 19.00 | 62.5 |
| 0.8 | | 307 | 204 | 141 | 1.28 | 16.41 | 67.6 |
| 1.0 | | 297 | 201 | 139 | 1.14 | 14.68 | 71.0 |
| 50 | | Blank | 320 | 269 | 192 | 8.11 | 104.54 |
| | 0.2 | 316 | 237 | 158 | 3.00 | 38.68 | 23.6 |
| | 0.4 | 313 | 232 | 153 | 2.51 | 32.41 | 36.0 |
| | 0.6 | 324 | 229 | 151 | 2.19 | 28.23 | 44.3 |
| | 0.8 | 317 | 224 | 149 | 1.95 | 25.09 | 50.5 |
| | 1.0 | 308 | 221 | 145 | 1.70 | 21.95 | 56.7 |

Table 3.75: Results of potentiodynamic polarization studies for the corrosion of welded maraging steel in 1.5 M sulphuric acid containing different concentrations of TBTBH.

| Temperature (°C) | Conc. of inhibitor (mM) | $-E_{corr}$ (mV /SCE) | b_a (mV dec ⁻¹) | $-b_c$ (mV dec ⁻¹) | i_{corr} (mA cm ⁻²) | ν_{corr} (mm y ⁻¹) | η (%) |
|------------------|-------------------------|-----------------------|-------------------------------|--------------------------------|-----------------------------------|------------------------------------|------------|
| 30 | Blank | 313 | 240 | 146 | 4.28 | 55.17 | |
| | 0.2 | 292 | 158 | 137 | 0.84 | 10.86 | 80.3 |
| | 0.4 | 297 | 147 | 129 | 0.45 | 5.84 | 89.4 |
| | 0.6 | 304 | 134 | 127 | 0.27 | 3.47 | 89.7 |
| | 0.8 | 303 | 131 | 121 | 0.24 | 3.14 | 90.3 |
| | 1.0 | 316 | 127 | 119 | 0.21 | 2.70 | 91.1 |
| | 35 | Blank | 308 | 242 | 151 | 5.31 | 68.45 |
| 0.2 | | 304 | 187 | 143 | 1.23 | 15.87 | 76.8 |
| 0.4 | | 301 | 179 | 136 | 0.95 | 12.25 | 82.1 |
| 0.6 | | 295 | 174 | 132 | 0.66 | 8.48 | 87.6 |
| 0.8 | | 312 | 168 | 128 | 0.56 | 7.18 | 89.5 |
| 1.0 | | 317 | 163 | 123 | 0.49 | 6.36 | 90.7 |
| 40 | | Blank | 300 | 248 | 156 | 6.48 | 83.53 |
| | 0.2 | 307 | 204 | 151 | 2.57 | 33.07 | 60.4 |
| | 0.4 | 304 | 194 | 147 | 2.00 | 25.72 | 69.2 |
| | 0.6 | 298 | 191 | 142 | 1.48 | 19.04 | 77.2 |
| | 0.8 | 314 | 188 | 138 | 1.23 | 15.87 | 81.0 |
| | 1.0 | 324 | 183 | 132 | 1.14 | 14.70 | 82.4 |
| | 45 | Blank | 301 | 290 | 197 | 7.54 | 97.19 |
| 0.2 | | 304 | 234 | 169 | 4.30 | 55.39 | 43.0 |
| 0.4 | | 317 | 227 | 158 | 3.79 | 48.88 | 49.7 |
| 0.6 | | 292 | 218 | 152 | 2.88 | 37.12 | 61.8 |
| 0.8 | | 309 | 207 | 148 | 2.54 | 32.75 | 66.3 |
| 1.0 | | 312 | 204 | 143 | 2.32 | 29.93 | 69.2 |
| 50 | | Blank | 295 | 349 | 242 | 8.64 | 111.37 |
| | 0.2 | 298 | 269 | 183 | 6.73 | 86.75 | 22.1 |
| | 0.4 | 303 | 257 | 174 | 5.68 | 73.28 | 34.2 |
| | 0.6 | 305 | 243 | 169 | 5.01 | 64.59 | 42.0 |
| | 0.8 | 309 | 237 | 162 | 4.47 | 57.58 | 48.3 |
| | 1.0 | 314 | 230 | 153 | 4.12 | 53.12 | 52.3 |

Table 3.76: Results of potentiodynamic polarization studies for the corrosion of welded maraging steel in 2.0 M sulphuric acid containing different concentrations of TBTBH.

| Temperature (°C) | Conc. of inhibitor (mM) | $-E_{corr}$ (mV /SCE) | b_a (mV dec ⁻¹) | $-b_c$ (mV dec ⁻¹) | i_{corr} (mA cm ⁻²) | U_{corr} (mm y ⁻¹) | η (%) |
|------------------|-------------------------|-----------------------|-------------------------------|--------------------------------|-----------------------------------|----------------------------------|------------|
| 30 | Blank | 315 | 312 | 154 | 4.97 | 64.06 | |
| | 0.2 | 312 | 173 | 141 | 1.01 | 13.00 | 79.7 |
| | 0.4 | 321 | 161 | 134 | 0.58 | 7.43 | 86.4 |
| | 0.6 | 327 | 157 | 131 | 0.35 | 4.54 | 87.9 |
| | 0.8 | 309 | 154 | 126 | 0.33 | 4.22 | 88.4 |
| | 1.0 | 298 | 149 | 121 | 0.29 | 3.71 | 89.2 |
| | 35 | Blank | 313 | 283 | 208 | 6.12 | 78.89 |
| 0.2 | | 317 | 194 | 157 | 1.46 | 18.85 | 76.1 |
| 0.4 | | 323 | 184 | 143 | 1.14 | 14.67 | 81.4 |
| 0.6 | | 306 | 182 | 134 | 0.87 | 11.20 | 85.8 |
| 0.8 | | 328 | 174 | 129 | 0.72 | 9.22 | 88.3 |
| 1.0 | | 314 | 171 | 124 | 0.67 | 8.59 | 89.1 |
| 40 | | Blank | 310 | 261 | 225 | 7.32 | 94.36 |
| | 0.2 | 294 | 208 | 163 | 2.99 | 38.59 | 59.1 |
| | 0.4 | 291 | 199 | 154 | 2.31 | 29.81 | 68.4 |
| | 0.6 | 304 | 194 | 149 | 1.77 | 22.83 | 75.8 |
| | 0.8 | 307 | 191 | 142 | 1.49 | 19.15 | 79.7 |
| | 1.0 | 313 | 187 | 137 | 1.39 | 17.92 | 81.0 |
| | 45 | Blank | 312 | 282 | 231 | 8.23 | 106.09 |
| 0.2 | | 317 | 241 | 178 | 4.83 | 62.27 | 41.3 |
| 0.4 | | 314 | 239 | 167 | 4.34 | 56.01 | 47.2 |
| 0.6 | | 292 | 224 | 164 | 3.20 | 41.26 | 61.1 |
| 0.8 | | 306 | 218 | 159 | 2.85 | 36.70 | 65.4 |
| 1.0 | | 319 | 215 | 152 | 2.69 | 34.69 | 67.3 |
| 50 | | Blank | 320 | 329 | 204 | 9.02 | 116.27 |
| | 0.2 | 327 | 278 | 189 | 7.09 | 91.50 | 21.3 |
| | 0.4 | 308 | 263 | 185 | 6.07 | 78.24 | 32.7 |
| | 0.6 | 301 | 247 | 173 | 5.45 | 70.22 | 39.6 |
| | 0.8 | 318 | 242 | 168 | 4.79 | 61.73 | 46.9 |
| | 1.0 | 323 | 238 | 165 | 4.43 | 57.20 | 50.8 |

Table 3.77: EIS data for the corrosion of welded maraging steel in 0.1 M sulphuric acid containing different concentrations of TBTBH.

| Temperature (°C) | Conc. of inhibitor (mM) | R_p (ohm. cm ²) | C_{dl} (mF cm ⁻²) | η (%) |
|------------------|-------------------------|-------------------------------|---------------------------------|------------|
| 30 | Blank | 20.1 | 0.324 | |
| | 0.2 | 117.5 | 0.212 | 82.9 |
| | 0.4 | 181.1 | 0.189 | 88.9 |
| | 0.6 | 295.5 | 0.161 | 90.2 |
| | 0.8 | 358.9 | 0.134 | 91.4 |
| | 1.0 | 410.2 | 0.115 | 92.8 |
| 35 | Blank | 17.4 | 0.469 | |
| | 0.2 | 84.0 | 0.384 | 79.3 |
| | 0.4 | 110.8 | 0.352 | 84.3 |
| | 0.6 | 156.7 | 0.313 | 88.9 |
| | 0.8 | 187.0 | 0.272 | 90.7 |
| | 1.0 | 200.1 | 0.267 | 91.3 |
| 40 | Blank | 14.1 | 0.531 | |
| | 0.2 | 51.6 | 0.454 | 72.7 |
| | 0.4 | 53.8 | 0.438 | 73.8 |
| | 0.6 | 78.7 | 0.409 | 82.1 |
| | 0.8 | 89.8 | 0.396 | 84.3 |
| | 1.0 | 110.1 | 0.364 | 87.2 |
| 45 | Blank | 12.3 | 0.668 | |
| | 0.2 | 41.2 | 0.591 | 70.2 |
| | 0.4 | 46.1 | 0.552 | 73.2 |
| | 0.6 | 55.1 | 0.534 | 77.6 |
| | 0.8 | 63.0 | 0.501 | 80.4 |
| | 1.0 | 79.8 | 0.481 | 85.1 |
| 50 | Blank | 10.2 | 0.830 | |
| | 0.2 | 31.1 | 0.791 | 67.1 |
| | 0.4 | 36.0 | 0.774 | 71.7 |
| | 0.6 | 39.2 | 0.742 | 73.8 |
| | 0.8 | 45.1 | 0.711 | 77.3 |
| | 1.0 | 57.0 | 0.681 | 82.1 |

Table 3.78: EIS data for the corrosion of welded maraging steel in 0.5 M sulphuric acid containing different concentrations of TBTBH.

| Temperature (°C) | Conc. of inhibitor (mM) | R_p (ohm. cm ²) | C_{dl} (mF cm ⁻²) | η (%) |
|------------------|-------------------------|-------------------------------|---------------------------------|------------|
| 30 | Blank | 18.7 | 0.633 | |
| | 0.2 | 102.1 | 0.471 | 81.7 |
| | 0.4 | 159.8 | 0.442 | 88.3 |
| | 0.6 | 271.0 | 0.394 | 89.1 |
| | 0.8 | 306.5 | 0.365 | 90.9 |
| | 1.0 | 322.4 | 0.329 | 92.2 |
| 35 | Blank | 15.4 | 0.682 | |
| | 0.2 | 70.3 | 0.544 | 78.1 |
| | 0.4 | 94.4 | 0.515 | 83.7 |
| | 0.6 | 132.7 | 0.486 | 88.4 |
| | 0.8 | 155.5 | 0.468 | 90.1 |
| | 1.0 | 169.2 | 0.457 | 90.9 |
| 40 | Blank | 11.4 | 0.727 | |
| | 0.2 | 34.9 | 0.664 | 67.4 |
| | 0.4 | 42.5 | 0.631 | 73.2 |
| | 0.6 | 59.6 | 0.601 | 80.9 |
| | 0.8 | 67.8 | 0.585 | 83.2 |
| | 1.0 | 83.2 | 0.561 | 86.3 |
| 45 | Blank | 10.5 | 0.831 | |
| | 0.2 | 20.1 | 0.712 | 47.9 |
| | 0.4 | 22.4 | 0.694 | 53.2 |
| | 0.6 | 28.9 | 0.686 | 63.7 |
| | 0.8 | 33.9 | 0.667 | 69.1 |
| | 1.0 | 37.3 | 0.634 | 71.9 |
| 50 | Blank | 7.9 | 0.965 | |
| | 0.2 | 11.0 | 0.911 | 28.4 |
| | 0.4 | 12.7 | 0.892 | 38.1 |
| | 0.6 | 15.3 | 0.864 | 48.4 |
| | 0.8 | 16.8 | 0.843 | 53.2 |
| | 1.0 | 18.7 | 0.834 | 57.9 |

Table 3.79: EIS data for the corrosion of welded maraging steel in 1.0 M sulphuric acid containing different concentrations of TBTBH.

| Temperature (°C) | Conc. Of inhibitor (mM) | R_p (ohm. cm ²) | C_{dl} (mF cm ⁻²) | η (%) |
|------------------|-------------------------|-------------------------------|---------------------------------|------------|
| 30 | Blank | 16.1 | 0.641 | |
| | 0.2 | 81.7 | 0.572 | 80.3 |
| | 0.4 | 151.8 | 0.521 | 88.4 |
| | 0.6 | 236.7 | 0.464 | 89.2 |
| | 0.8 | 303.7 | 0.423 | 90.7 |
| | 1.0 | 315.6 | 0.397 | 91.9 |
| 35 | Blank | 13.5 | 0.714 | |
| | 0.2 | 58.1 | 0.624 | 76.8 |
| | 0.4 | 76.7 | 0.582 | 82.4 |
| | 0.6 | 106.2 | 0.557 | 87.3 |
| | 0.8 | 128.5 | 0.539 | 89.5 |
| | 1.0 | 139.1 | 0.514 | 90.3 |
| 40 | Blank | 10.4 | 0.670 | |
| | 0.2 | 27.1 | 0.621 | 61.7 |
| | 0.4 | 34.5 | 0.592 | 69.9 |
| | 0.6 | 48.8 | 0.583 | 78.7 |
| | 0.8 | 56.8 | 0.559 | 81.7 |
| | 1.0 | 66.2 | 0.554 | 84.3 |
| 45 | Blank | 8.6 | 0.873 | |
| | 0.2 | 15.2 | 0.811 | 43.5 |
| | 0.4 | 18.0 | 0.792 | 52.3 |
| | 0.6 | 23.1 | 0.764 | 62.8 |
| | 0.8 | 26.3 | 0.748 | 67.4 |
| | 1.0 | 29.4 | 0.734 | 70.8 |
| 50 | Blank | 7.3 | 1.123 | |
| | 0.2 | 9.6 | 1.014 | 24.7 |
| | 0.4 | 11.4 | 0.982 | 36.1 |
| | 0.6 | 13.3 | 0.954 | 45.5 |
| | 0.8 | 14.9 | 0.945 | 51.3 |
| | 1.0 | 17.0 | 0.926 | 57.1 |

Table 3.80: EIS data for the corrosion of welded maraging steel in 1.5 M sulphuric acid containing different concentrations of TBTBH.

| Temperature (°C) | Conc. Of inhibitor (mM) | R_p (ohm. cm ²) | C_{dl} (mF cm ⁻²) | η (%) |
|------------------|-------------------------|-------------------------------|---------------------------------|------------|
| 30 | Blank | 15.9 | 0.958 | |
| | 0.2 | 78.7 | 0.912 | 79.8 |
| | 0.4 | 143.2 | 0.885 | 88.9 |
| | 0.6 | 220.8 | 0.847 | 89.8 |
| | 0.8 | 230.4 | 0.826 | 90.1 |
| | 1.0 | 300.0 | 0.784 | 90.7 |
| 35 | Blank | 11.6 | 0.982 | |
| | 0.2 | 48.9 | 0.944 | 76.3 |
| | 0.4 | 64.8 | 0.917 | 82.1 |
| | 0.6 | 88.5 | 0.896 | 86.9 |
| | 0.8 | 104.5 | 0.871 | 88.9 |
| | 1.0 | 113.7 | 0.864 | 89.8 |
| 40 | Blank | 9.4 | 1.070 | |
| | 0.2 | 23.3 | 1.012 | 59.8 |
| | 0.4 | 30.0 | 0.977 | 68.7 |
| | 0.6 | 39.6 | 0.945 | 76.3 |
| | 0.8 | 47.9 | 0.916 | 80.4 |
| | 1.0 | 51.8 | 0.891 | 81.9 |
| 45 | Blank | 8.1 | 1.281 | |
| | 0.2 | 14.3 | 1.214 | 43.7 |
| | 0.4 | 16.0 | 1.188 | 49.4 |
| | 0.6 | 20.9 | 1.161 | 61.3 |
| | 0.8 | 23.6 | 1.157 | 65.8 |
| | 1.0 | 25.8 | 1.145 | 68.7 |
| 50 | Blank | 6.9 | 1.318 | |
| | 0.2 | 9.0 | 1.281 | 23.9 |
| | 0.4 | 10.5 | 1.267 | 34.8 |
| | 0.6 | 12.1 | 1.259 | 42.8 |
| | 0.8 | 13.5 | 1.254 | 49.1 |
| | 1.0 | 14.6 | 1.245 | 52.7 |

Table 3.81: EIS data for the corrosion of welded maraging steel in 2.0 M sulphuric acid containing different concentrations of TBTBH.

| Temperature (°C) | Conc. Of inhibitor (mM) | R_p (ohm. cm ²) | C_{dl} (mF cm ⁻²) | η (%) |
|------------------|-------------------------|-------------------------------|---------------------------------|------------|
| 30 | Blank | 13.9 | 1.093 | |
| | 0.2 | 64.0 | 0.992 | 78.3 |
| | 0.4 | 118.8 | 0.964 | 84.3 |
| | 0.6 | 167.4 | 0.924 | 86.7 |
| | 0.8 | 182.8 | 0.917 | 87.4 |
| | 1.0 | 224.1 | 0.899 | 89.8 |
| 35 | Blank | 10.8 | 1.241 | |
| | 0.2 | 44.6 | 1.154 | 75.8 |
| | 0.4 | 57.7 | 1.127 | 81.3 |
| | 0.6 | 72.9 | 1.085 | 85.2 |
| | 0.8 | 85.7 | 1.042 | 87.4 |
| | 1.0 | 95.5 | 1.027 | 88.7 |
| 40 | Blank | 9.2 | 1.324 | |
| | 0.2 | 22.6 | 1.278 | 59.3 |
| | 0.4 | 28.2 | 1.257 | 67.4 |
| | 0.6 | 36.9 | 1.225 | 75.1 |
| | 0.8 | 42.2 | 1.204 | 78.2 |
| | 1.0 | 46.9 | 1.171 | 80.4 |
| 45 | Blank | 7.4 | 1.369 | |
| | 0.2 | 12.7 | 1.314 | 42.1 |
| | 0.4 | 13.9 | 1.282 | 46.9 |
| | 0.6 | 19.3 | 1.257 | 61.7 |
| | 0.8 | 21.0 | 1.231 | 64.9 |
| | 1.0 | 22.9 | 1.225 | 67.8 |
| 50 | Blank | 6.5 | 1.508 | |
| | 0.2 | 8.3 | 1.474 | 22.1 |
| | 0.4 | 9.8 | 1.451 | 33.7 |
| | 0.6 | 11.0 | 1.427 | 41.0 |
| | 0.8 | 11.9 | 1.416 | 45.7 |
| | 1.0 | 13.1 | 1.384 | 50.4 |

Table 3.82: Activation parameters for the corrosion of welded maraging steel in sulphuric acid containing different concentrations of TBTBH.

| Molarity of H ₂ SO ₄ (M) | Conc. of inhibitor (mM) | E_a (kJ mol ⁻¹) | ΔH^\ddagger (kJ mol ⁻¹) | ΔS^\ddagger (J mol ⁻¹ K ⁻¹) |
|--|-------------------------|-------------------------------|---|--|
| 0.1 | Blank | 42.58 | 39.98 | -86.83 |
| | 0.2 | 45.18 | 44.71 | -74.43 |
| | 0.4 | 63.31 | 60.71 | -48.42 |
| | 0.6 | 71.34 | 68.74 | -25.81 |
| | 0.8 | 75.67 | 73.07 | -13.34 |
| | 1.0 | 76.58 | 75.98 | -6.52 |
| 0.5 | Blank | 44.97 | 42.37 | -77.02 |
| | 0.2 | 56.45 | 53.35 | -66.21 |
| | 0.4 | 62.94 | 60.53 | -47.09 |
| | 0.6 | 74.89 | 72.28 | -11.42 |
| | 0.8 | 76.81 | 74.21 | -6.73 |
| | 1.0 | 78.58 | 77.98 | -4.32 |
| 1.0 | Blank | 32.07 | 29.46 | -115.68 |
| | 0.2 | 60.57 | 57.93 | -49.00 |
| | 0.4 | 65.49 | 62.89 | -34.70 |
| | 0.6 | 74.89 | 72.28 | -21.42 |
| | 0.8 | 77.81 | 76.21 | -13.43 |
| | 1.0 | 79.58 | 78.98 | -2.12 |
| 1.5 | Blank | 30.55 | 29.12 | -120.54 |
| | 0.2 | 58.57 | 59.93 | -51.00 |
| | 0.4 | 63.49 | 61.89 | -44.70 |
| | 0.6 | 71.89 | 72.28 | -21.42 |
| | 0.8 | 74.81 | 75.21 | -16.73 |
| | 1.0 | 76.58 | 74.98 | -14.32 |
| 2.0 | Blank | 28.24 | 26.21 | -122.45 |
| | 0.2 | 53.07 | 53.91 | -49.00 |
| | 0.4 | 55.39 | 54.86 | -34.70 |
| | 0.6 | 64.17 | 62.54 | -11.42 |
| | 0.8 | 66.82 | 65.30 | -6.73 |
| | 1.0 | 71.53 | 69.08 | -4.32 |

Table 3.83: Maximum inhibition efficiency attained in different concentrations of sulphuric acid at different temperatures for TBTBH.

| Temperature (°C) | Welded Maraging Steel | | | |
|---------------------|-------------------------------------|-----------------------------------|---|------------|
| | Sulphuric acid concentration (M) | Concentration of TBTBH (mM) | η (%) | |
| | | | Potentiodynamic polarization method | EIS method |
| 30 | 0.1 | 1.0 | 96.3 | 95.1 |
| | 0.5 | | 96.1 | 94.2 |
| | 1.0 | | 95.9 | 94.9 |
| | 1.5 | | 95.1 | 94.7 |
| | 2.0 | | 94.2 | 93.8 |
| 35 | 0.1 | 1.0 | 92.8 | 91.3 |
| | 0.5 | | 92.0 | 90.9 |
| | 1.0 | | 91.4 | 90.3 |
| | 1.5 | | 90.7 | 89.8 |
| | 2.0 | | 89.1 | 88.7 |
| 40 | 0.1 | 1.0 | 88.4 | 87.2 |
| | 0.5 | | 86.3 | 86.3 |
| | 1.0 | | 84.9 | 84.3 |
| | 1.5 | | 82.4 | 81.9 |
| | 2.0 | | 81.0 | 80.4 |
| 45 | 0.1 | 1.0 | 73.4 | 72.4 |
| | 0.5 | | 72.7 | 71.9 |
| | 1.0 | | 71.0 | 70.8 |
| | 1.5 | | 69.2 | 68.7 |
| | 2.0 | | 67.3 | 67.8 |
| 50 | 0.1 | 1.0 | 61.3 | 60.4 |
| | 0.5 | | 58.4 | 57.9 |
| | 1.0 | | 56.7 | 57.1 |
| | 1.5 | | 52.3 | 52.7 |
| | 2.0 | | 50.8 | 50.4 |

Table 3.84: Thermodynamic parameters for the adsorption of TBTBH on welded maraging steel surface in sulphuric acid at different temperatures.

| Molarity of H ₂ SO ₄ (M) | Temperature (° C) | $-\Delta G^{\circ}_{ads}$ (kJ mol ⁻¹) | ΔH°_{ads} (kJ mol ⁻¹) | ΔS°_{ads} (J mol ⁻¹ K ⁻¹) |
|--|-------------------|---|--|---|
| 0.1 | 30 | 31.92 | -38.33 | -26.52 |
| | 35 | 30.81 | | |
| | 40 | 30.72 | | |
| | 45 | 30.58 | | |
| | 50 | 30.42 | | |
| 0.5 | 30 | 35.53 | -32.92 | -23.34 |
| | 35 | 35.45 | | |
| | 40 | 34.53 | | |
| | 45 | 32.78 | | |
| | 50 | 31.03 | | |
| 1.0 | 30 | 35.36 | -31.28 | -22.82 |
| | 35 | 35.27 | | |
| | 40 | 35.24 | | |
| | 45 | 35.16 | | |
| | 50 | 35.02 | | |
| 1.5 | 30 | 35.30 | -34.4 | -25.24 |
| | 35 | 35.24 | | |
| | 40 | 33.83 | | |
| | 45 | 33.34 | | |
| | 50 | 33.17 | | |
| 2.0 | 30 | 35.28 | -36.24 | -26.48 |
| | 35 | 35.35 | | |
| | 40 | 33.79 | | |
| | 45 | 32.15 | | |
| | 50 | 30.26 | | |

3.9 2-(5-CHLORO-1H-BENZOIMIDAZOL-2-YL) PHENOL (CBP) AS INHIBITOR FOR THE CORROSION OF WELDED MARAGING STEEL IN HYDROCHLORIC ACID MEDIUM

3.9.1 Potentiodynamic polarization measurements

Polarization curves for the corrosion of maraging steel in 1.0 M HCl solution in the presence of different concentrations of CBP are shown in Fig. 3.68. Similar results were obtained at other temperatures and in other concentrations of hydrochloric acid. The potentiodynamic polarization parameters are summarized in Tables 3.85 to 3.89.

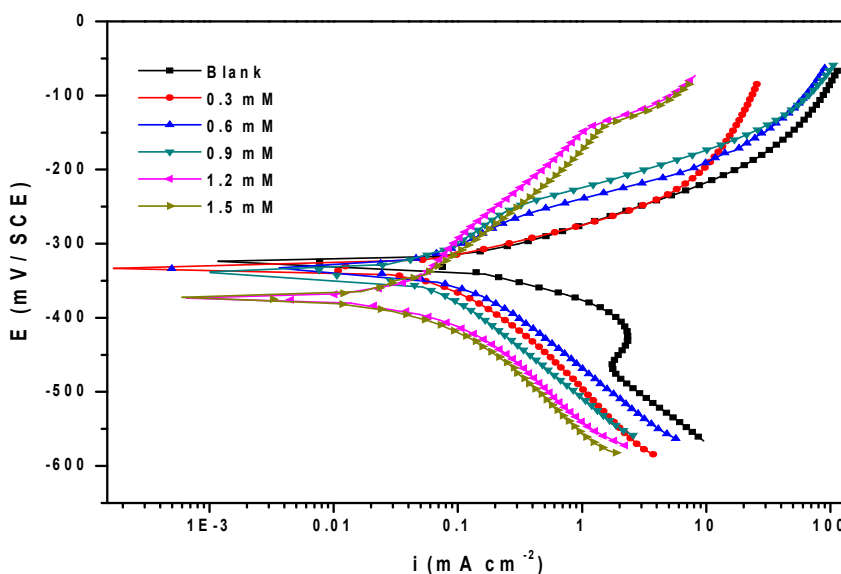


Fig. 3.68: Potentiodynamic polarization curves for the corrosion of welded maraging steel in 1.0 M hydrochloric acid containing different concentrations of CBP at 30 °C.

It could be observed that both the anodic and cathodic reactions were suppressed with the addition of CBP. The E_{corr} values show a small shift on the more negative side, indicating that CBP acts as a mixed inhibitor with predominant cathodic action.

3.9.2 Electrochemical impedance spectroscopy (EIS) studies

Nyquist plots for the corrosion of welded maraging steel in 1.0 M HCl solution in the presence of different concentrations of CBP are given in Fig. 3.69. Similar plots were

obtained in other concentrations of the acid and also at other temperatures. The impedance parameters are presented in Tables 3.90 to 3.94.

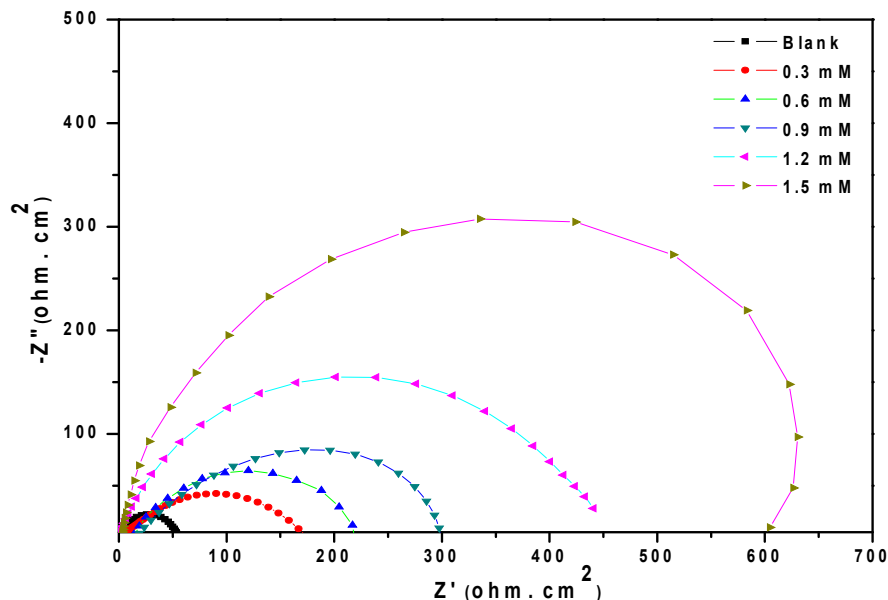


Fig. 3.69: Nyquist plots for the corrosion of welded maraging steel in 1.0 M hydrochloric acid containing different concentrations of CBP at 30 °C.

It is clear from Fig. 3.69 that the shapes of the impedance plots for the corrosion of welded maraging steel in the presence of inhibitor are not substantially different from those of the uninhibited one. The plots are similar to those obtained in the presence of BTPO as discussed in the section 3.3.2. The equivalent circuit given in Fig. 3.17 is used to fit the experimental data for the corrosion of welded maraging steel in hydrochloric acid in the presence of CBP. As can be seen from the Tables, R_{ct} value increases and C_{dl} value decreases with the increase in the concentration of CBP which suggest the decrease in the corrosion rate.

The Bode plots of phase angle and amplitude for the corrosion of the alloy in the presence of different concentrations of CBP is shown in Fig. 3.70 (a) and Fig. 3.70 (b), respectively. Phase angle increases with the increase in the concentrations of CBP in hydrochloric acid. This might be attributed to the decrease in the capacitive behavior on the metal surface due to the decrease in the dissolution rate of the metal.

An increase in CBP concentration leads to an increase in the impedance ($|Z|$) value.

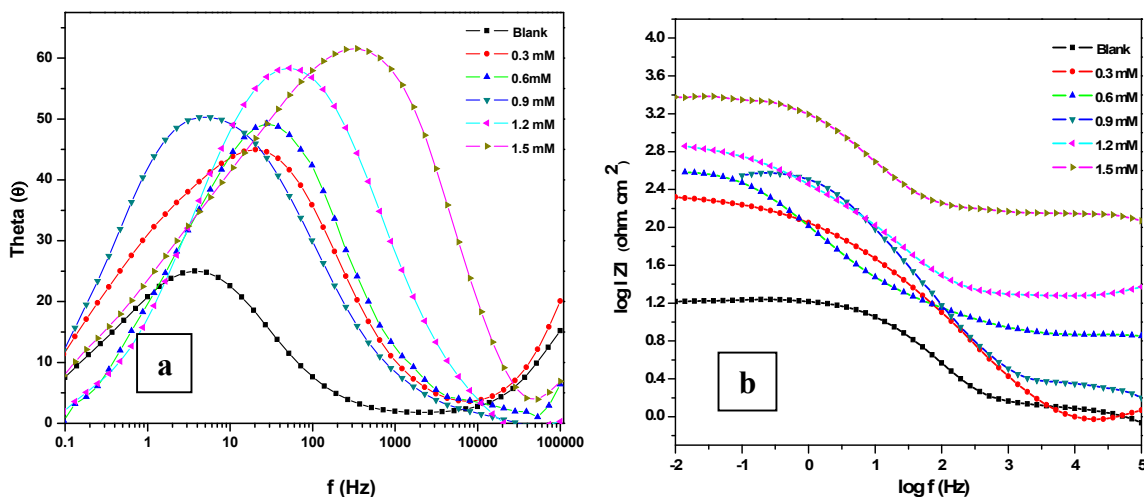


Fig. 3.70: (a) Bode (a) Phase angle plots and (b) Amplitude plots for the corrosion of welded maraging steel in 1.0 M HCl containing different concentrations of CBP at 30 °C.

3.9.3 Effect of temperature

The potentiodynamic polarization and EIS results pertaining to different temperatures in different concentrations of hydrochloric acid have already been listed in Tables 3.85 to 3.94. The effect of temperature on corrosion inhibition behaviour of CBP is similar to that of BTPO on welded maraging steel as discussed in the section 3.3.3. The decrease in the inhibition efficiency of CBP with the increase in temperature on welded maraging steel surface may be attributed to the physisorption of CBP. The Arrhenius plots for the corrosion of welded maraging steel in 1.0 M hydrochloric acid in the presence of different concentrations of CBP are shown in Fig. 3.71. The plots of $\ln(v_{\text{corr}}/T)$ versus $(1/T)$ are shown in Fig. 3.72. The calculated values of activation parameters are given in Table 3.95. The observations are similar to the ones obtained in the presence of BTPO and PNPT.

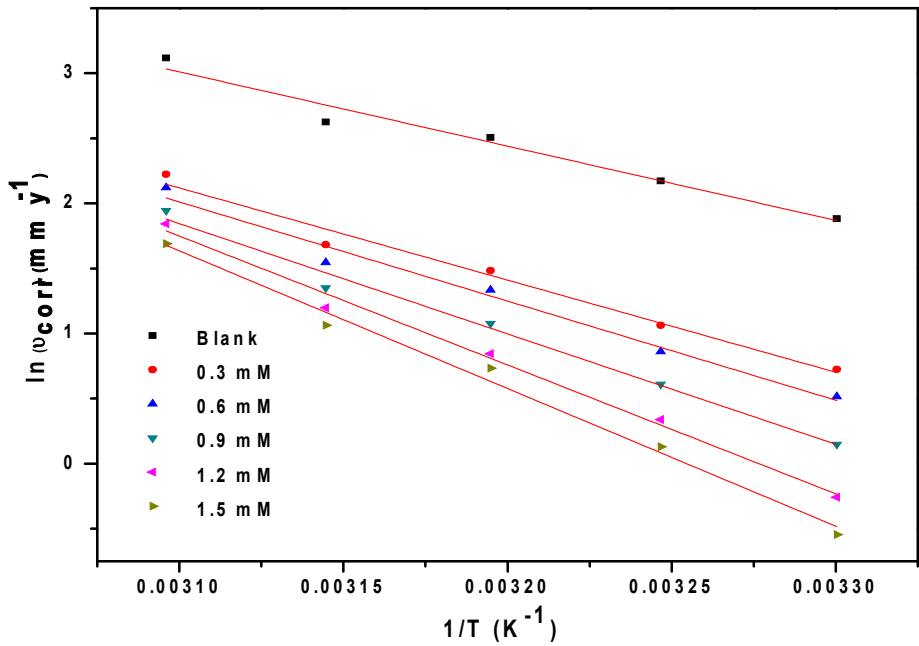


Fig. 3.71: Arrhenius Plots for the corrosion of welded maraging steel in 1.0 M hydrochloric acid containing different concentrations of CBP.

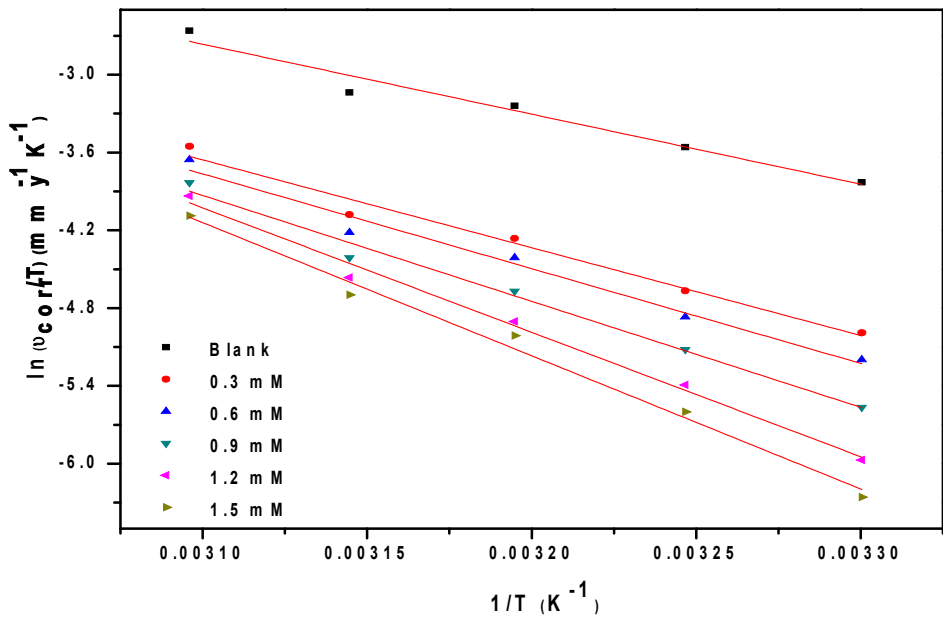


Fig. 3.72: Plots of $\ln(v_{corr}/T)$ versus $1/T$ for the corrosion of welded maraging steel in 1.0 M hydrochloric acid containing different concentrations of CBP.

The increase in the E_a values with the increase in CBP concentration indicates the increase in energy barrier for the corrosion reaction as discussed in earlier sections. The entropy of activation in the absence and presence of CBP is large and negative for the corrosion of the alloy. This implies that the activated complex in the rate determining step represents an association rather than dissociation step, indicating that a decrease in disordering takes place on going from reactants to activated complex (Gomma and Wahdan 1995, Marsh 1988). The entropies of activation are higher for welded maraging steel in inhibited solutions than that in the uninhibited solutions.

3.9.4 Effect of hydrochloric acid concentration

Table 3.96 summarises the maximum inhibition efficiencies exhibited by CBP in the HCl solution of different concentrations. It is evident from both polarization and EIS experimental results that, for a particular concentration of inhibitor, the inhibition efficiency decreases with the increase in hydrochloric acid concentration on the welded maraging steel. The highest inhibition efficiency is observed in hydrochloric acid of 0.1 M concentration.

3.9.5 Adsorption isotherm

The adsorption of CBP on the surfaces of welded maraging steel was found to obey Langmuir adsorption isotherm. The Langmuir adsorption isotherms for the adsorption of CBP on welded maraging steel in 1.0 M hydrochloric acid are shown in Fig. 3.73. The thermodynamic parameters for the adsorption of CBP on welded maraging steel are tabulated in Tables 3.97. The values of ΔG_{ads}^0 and ΔH_{ads}^0 indicate both physisorption and chemisorption of CBP on welded maraging steel with predominant physisorption. The ΔS_{ads}^0 value values indicate decrease in randomness on going from the reactants to the metal adsorbed species.

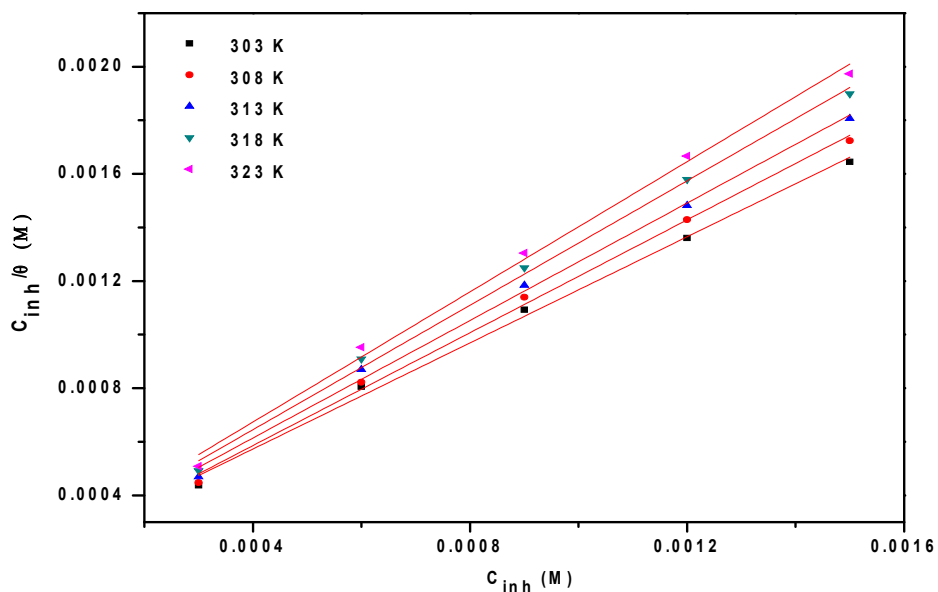


Fig. 3.73: Langmuir adsorption isotherms for the adsorption of CBP on welded maraging steel in 1.0 M HCl at different temperatures.

3.9.6 Mechanism of corrosion inhibition

The mechanism of corrosion inhibition of welded maraging steel in the presence of CBP is similar to that of BTPO as discussed under section 3.3.6. The adsorption of CBP molecules on the alloy surface can be attributed to the presence of nitrogen, oxygen and delocalized benzene ring. The inhibition mechanism of CBP in hydrochloric acid solution can be explained in the similar lines of BTPO as explained in the section 3.3.6.

3.9.7 SEM/EDX studies

Fig. 3.74 shows the SEM image of the sample after immersion in 1.0 M hydrochloric acid in the presence of CBP. It can be seen that the alloy surface in the presence of inhibitor is relatively smooth without much visible corrosion attack. Thus, it can be concluded that CBP protects the alloy from corrosion by forming a uniform film on the alloy surface. The EDX spectra of the corroded surface of the alloy in the presence of CBP is shown in Fig. 3.75. The atomic percentages of the

elements found in the EDX profile for inhibited metal surface was 17.40% Fe, 4.26% Ni, 0.64% Mo, 39.03% O, 21.17% C, 8.64% Cl and 8.86% N and indicated the formation of inhibitor film on the surface of alloy.

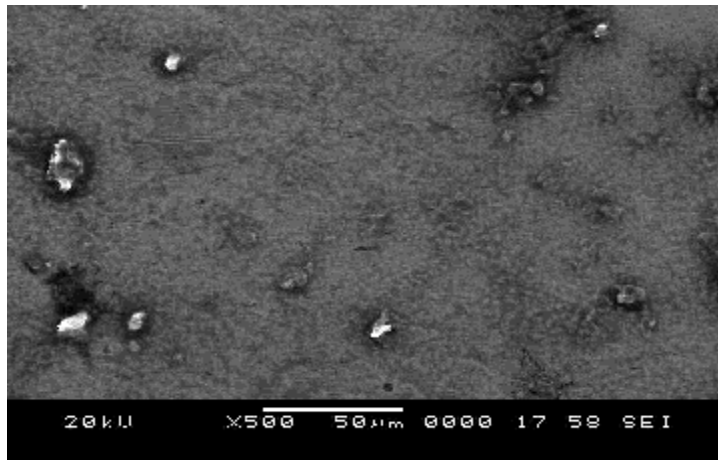


Fig. 3.74: SEM image of the welded maraging steel after immersion in 1.0 M HCl in the presence of CBP.

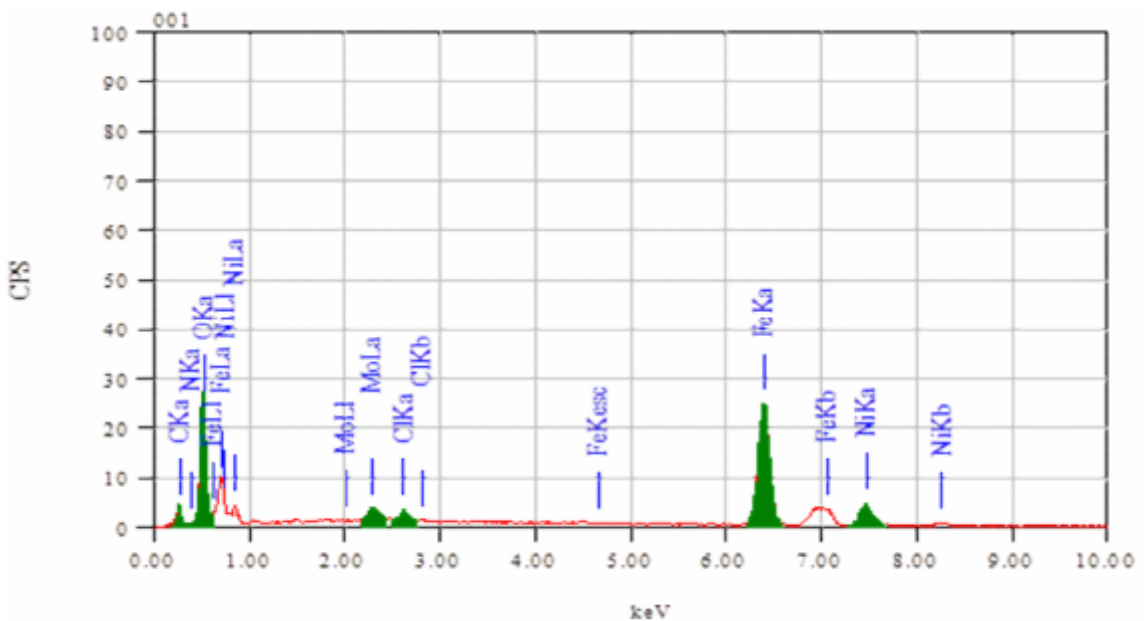


Fig. 3.75: EDX spectra of the welded maraging steel after immersion in 1.0 M HCl in the presence of CBP.

Table 3.85: Results of potentiodynamic polarization studies for the corrosion of welded maraging steel in 0.1 M hydrochloric acid containing different concentrations of CBP.

| Temperature (°C) | Conc. of inhibitor (mM) | $-E_{corr}$ (mV /SCE) | b_a (mV dec ⁻¹) | $-b_c$ (mV dec ⁻¹) | i_{corr} (mA cm ⁻²) | ν_{corr} (mm y ⁻¹) | η (%) |
|------------------|-------------------------|-----------------------|-------------------------------|--------------------------------|-----------------------------------|------------------------------------|------------|
| 30 | Blank | 306 | 98 | 140 | 0.31 | 4.00 | |
| | 0.3 | 324 | 89 | 121 | 0.09 | 1.11 | 72.3 |
| | 0.6 | 321 | 86 | 118 | 0.07 | 0.90 | 77.6 |
| | 0.9 | 336 | 85 | 114 | 0.05 | 0.60 | 84.9 |
| | 1.2 | 341 | 83 | 110 | 0.03 | 0.37 | 90.7 |
| | 1.5 | 352 | 80 | 107 | 0.02 | 0.25 | 93.8 |
| | 35 | Blank | 310 | 101 | 146 | 0.36 | 4.64 |
| 0.3 | | 317 | 92 | 121 | 0.11 | 1.36 | 70.8 |
| 0.6 | | 323 | 89 | 118 | 0.09 | 1.20 | 74.2 |
| 0.9 | | 334 | 85 | 116 | 0.06 | 0.75 | 83.8 |
| 1.2 | | 337 | 82 | 113 | 0.05 | 0.65 | 85.9 |
| 1.5 | | 345 | 81 | 109 | 0.04 | 0.50 | 89.3 |
| 40 | | Blank | 312 | 103 | 147 | 0.46 | 5.93 |
| | 0.3 | 317 | 101 | 124 | 0.14 | 1.81 | 69.4 |
| | 0.6 | 321 | 97 | 121 | 0.13 | 1.61 | 72.8 |
| | 0.9 | 332 | 94 | 118 | 0.09 | 1.14 | 80.8 |
| | 1.2 | 343 | 92 | 115 | 0.08 | 0.98 | 83.4 |
| | 1.5 | 356 | 91 | 113 | 0.06 | 0.72 | 87.7 |
| | 45 | Blank | 315 | 108 | 156 | 0.67 | 8.64 |
| 0.3 | | 308 | 103 | 131 | 0.24 | 3.03 | 64.9 |
| 0.6 | | 314 | 101 | 127 | 0.21 | 2.74 | 68.3 |
| 0.9 | | 325 | 97 | 124 | 0.15 | 1.89 | 78.1 |
| 1.2 | | 323 | 95 | 122 | 0.12 | 1.56 | 81.9 |
| 1.5 | | 341 | 93 | 118 | 0.10 | 1.28 | 85.2 |
| 50 | | Blank | 313 | 113 | 161 | 0.83 | 10.70 |
| | 0.3 | 318 | 104 | 140 | 0.31 | 1.03 | 62.3 |
| | 0.6 | 321 | 102 | 134 | 0.29 | 3.77 | 64.8 |
| | 0.9 | 306 | 99 | 131 | 0.22 | 2.87 | 73.2 |
| | 1.2 | 319 | 97 | 128 | 0.19 | 2.42 | 77.4 |
| | 1.5 | 330 | 94 | 124 | 0.14 | 1.83 | 82.9 |

Table 3.86: Results of potentiodynamic polarization studies for the corrosion of welded maraging steel in 0.5 M hydrochloric acid containing different concentrations of CBP.

| Temperature (°C) | Conc. of inhibitor (mM) | $-E_{corr}$ (mV /SCE) | b_a (mV dec ⁻¹) | $-b_c$ (mV dec ⁻¹) | i_{corr} (mA cm ⁻²) | \mathcal{U}_{corr} (mm y ⁻¹) | η (%) |
|------------------|-------------------------|-----------------------|-------------------------------|--------------------------------|-----------------------------------|--|------------|
| 30 | Blank | 315 | 103 | 149 | 0.35 | 4.51 | |
| | 0.3 | 326 | 101 | 121 | 0.09 | 1.31 | 70.9 |
| | 0.6 | 332 | 97 | 116 | 0.07 | 1.07 | 76.2 |
| | 0.9 | 336 | 95 | 113 | 0.05 | 0.76 | 83.2 |
| | 1.2 | 337 | 93 | 112 | 0.03 | 0.48 | 89.4 |
| | 1.5 | 339 | 90 | 110 | 0.02 | 0.35 | 92.3 |
| | 35 | Blank | 323 | 105 | 152 | 0.48 | 6.19 |
| 0.3 | | 339 | 102 | 131 | 0.11 | 1.93 | 68.8 |
| 0.6 | | 342 | 98 | 128 | 0.09 | 1.65 | 73.4 |
| 0.9 | | 345 | 94 | 124 | 0.06 | 1.20 | 80.6 |
| 1.2 | | 347 | 92 | 121 | 0.05 | 0.94 | 84.8 |
| 1.5 | | 337 | 91 | 118 | 0.04 | 0.72 | 88.4 |
| 40 | | Blank | 330 | 112 | 158 | 0.60 | 7.73 |
| | 0.3 | 337 | 107 | 134 | 0.14 | 2.49 | 67.8 |
| | 0.6 | 335 | 104 | 129 | 0.13 | 2.20 | 71.6 |
| | 0.9 | 341 | 98 | 127 | 0.09 | 1.68 | 78.3 |
| | 1.2 | 342 | 95 | 125 | 0.08 | 1.42 | 81.7 |
| | 1.5 | 345 | 92 | 121 | 0.06 | 1.14 | 85.3 |
| | 45 | Blank | 328 | 116 | 165 | 0.77 | 9.93 |
| 0.3 | | 341 | 108 | 141 | 0.24 | 3.69 | 62.8 |
| 0.6 | | 345 | 105 | 137 | 0.21 | 3.27 | 67.1 |
| 0.9 | | 351 | 103 | 134 | 0.15 | 2.46 | 75.2 |
| 1.2 | | 357 | 99 | 131 | 0.12 | 2.15 | 78.3 |
| 1.5 | | 360 | 96 | 129 | 0.10 | 1.85 | 81.4 |
| 50 | | Blank | 324 | 118 | 173 | 1.03 | 13.28 |
| | 0.3 | 348 | 111 | 148 | 0.31 | 5.26 | 60.4 |
| | 0.6 | 355 | 106 | 147 | 0.29 | 4.82 | 63.7 |
| | 0.9 | 357 | 103 | 144 | 0.22 | 3.76 | 71.7 |
| | 1.2 | 364 | 101 | 141 | 0.19 | 3.53 | 73.4 |
| | 1.5 | 369 | 97 | 137 | 0.14 | 2.76 | 79.2 |

Table 3.87: Results of potentiodynamic polarization studies for the corrosion of welded maraging steel in 1.0 M hydrochloric acid containing different concentrations of CBP.

| Temperature (°C) | Conc. of inhibitor (mM) | $-E_{corr}$ (mV /SCE) | b_a (mV dec ⁻¹) | $-b_c$ (mV dec ⁻¹) | i_{corr} (mA cm ⁻²) | ν_{corr} (mm y ⁻¹) | η (%) |
|------------------|-------------------------|-----------------------|-------------------------------|--------------------------------|-----------------------------------|------------------------------------|------------|
| 30 | Blank | 324 | 112 | 158 | 0.51 | 6.57 | |
| | 0.3 | 336 | 103 | 137 | 0.16 | 2.06 | 68.6 |
| | 0.6 | 337 | 101 | 132 | 0.13 | 1.68 | 74.5 |
| | 0.9 | 342 | 98 | 128 | 0.09 | 1.16 | 82.4 |
| | 1.2 | 373 | 96 | 124 | 0.06 | 0.77 | 88.2 |
| | 1.5 | 372 | 93 | 121 | 0.05 | 0.58 | 91.2 |
| | 35 | Blank | 328 | 118 | 163 | 0.68 | 8.77 |
| 0.3 | | 339 | 109 | 142 | 0.22 | 2.89 | 67.1 |
| 0.6 | | 341 | 107 | 139 | 0.18 | 2.37 | 72.9 |
| 0.9 | | 334 | 103 | 134 | 0.14 | 1.84 | 79.0 |
| 1.2 | | 349 | 100 | 131 | 0.11 | 1.40 | 84.1 |
| 1.5 | | 354 | 97 | 129 | 0.09 | 1.14 | 87.0 |
| 40 | | Blank | 336 | 126 | 171 | 0.95 | 12.25 |
| | 0.3 | 343 | 114 | 154 | 0.34 | 4.41 | 64.0 |
| | 0.6 | 344 | 112 | 151 | 0.29 | 3.80 | 68.9 |
| | 0.9 | 350 | 108 | 147 | 0.23 | 2.94 | 76.0 |
| | 1.2 | 352 | 105 | 143 | 0.18 | 2.33 | 80.9 |
| | 1.5 | 361 | 103 | 141 | 0.16 | 2.08 | 83.0 |
| | 45 | Blank | 331 | 131 | 179 | 1.07 | 13.79 |
| 0.3 | | 339 | 118 | 151 | 0.42 | 5.38 | 60.9 |
| 0.6 | | 343 | 115 | 147 | 0.36 | 4.69 | 65.9 |
| 0.9 | | 347 | 113 | 144 | 0.30 | 3.86 | 72.0 |
| 1.2 | | 356 | 110 | 142 | 0.26 | 3.31 | 76.0 |
| 1.5 | | 359 | 107 | 139 | 0.22 | 2.90 | 78.9 |
| 50 | | Blank | 328 | 142 | 191 | 1.75 | 22.56 |
| | 0.3 | 343 | 124 | 162 | 0.72 | 9.25 | 59.0 |
| | 0.6 | 349 | 121 | 159 | 0.65 | 8.35 | 62.9 |
| | 0.9 | 351 | 116 | 157 | 0.54 | 6.99 | 69.0 |
| | 1.2 | 356 | 114 | 154 | 0.49 | 6.32 | 71.9 |
| | 1.5 | 362 | 111 | 149 | 0.42 | 5.41 | 76.0 |

Table 3.88: Results of potentiodynamic polarization studies for the corrosion of welded maraging steel in 1.5 M hydrochloric acid containing different concentrations of CBP.

| Temperature (°C) | Conc. of inhibitor (mM) | $-E_{corr}$ (mV /SCE) | b_a (mV dec ⁻¹) | $-b_c$ (mV dec ⁻¹) | i_{corr} (mA cm ⁻²) | \mathcal{U}_{corr} (mm y ⁻¹) | η (%) |
|------------------|-------------------------|-----------------------|-------------------------------|--------------------------------|-----------------------------------|--|------------|
| 30 | Blank | 316 | 109 | 163 | 0.57 | 7.35 | |
| | 0.3 | 343 | 101 | 137 | 0.20 | 2.55 | 65.3 |
| | 0.6 | 345 | 98 | 132 | 0.15 | 1.97 | 73.2 |
| | 0.9 | 347 | 96 | 129 | 0.12 | 1.49 | 79.7 |
| | 1.2 | 354 | 95 | 125 | 0.09 | 1.19 | 83.8 |
| | 1.5 | 353 | 94 | 121 | 0.08 | 1.00 | 86.4 |
| 35 | Blank | 320 | 117 | 171 | 0.98 | 12.63 | |
| | 0.3 | 343 | 113 | 152 | 0.35 | 4.52 | 64.2 |
| | 0.6 | 346 | 110 | 149 | 0.29 | 3.75 | 70.3 |
| | 0.9 | 349 | 107 | 145 | 0.22 | 2.80 | 77.8 |
| | 1.2 | 356 | 103 | 142 | 0.17 | 2.24 | 82.3 |
| | 1.5 | 361 | 99 | 138 | 0.15 | 1.88 | 85.1 |
| 40 | Blank | 328 | 124 | 183 | 1.31 | 16.89 | |
| | 0.3 | 341 | 113 | 157 | 0.48 | 6.15 | 63.6 |
| | 0.6 | 343 | 109 | 154 | 0.43 | 5.52 | 67.3 |
| | 0.9 | 349 | 105 | 151 | 0.33 | 4.26 | 74.8 |
| | 1.2 | 351 | 103 | 147 | 0.28 | 3.56 | 78.9 |
| | 1.5 | 365 | 101 | 142 | 0.24 | 3.11 | 81.6 |
| 45 | Blank | 322 | 132 | 198 | 1.80 | 23.20 | |
| | 0.3 | 341 | 123 | 164 | 0.72 | 9.26 | 60.1 |
| | 0.6 | 346 | 116 | 161 | 0.66 | 8.54 | 63.2 |
| | 0.9 | 348 | 113 | 157 | 0.55 | 7.03 | 69.7 |
| | 1.2 | 357 | 108 | 153 | 0.49 | 6.31 | 72.8 |
| | 1.5 | 361 | 103 | 148 | 0.43 | 5.50 | 76.3 |
| 50 | Blank | 315 | 147 | 209 | 2.63 | 33.90 | |
| | 0.3 | 338 | 127 | 182 | 1.12 | 14.48 | 57.3 |
| | 0.6 | 343 | 124 | 178 | 1.05 | 13.49 | 60.2 |
| | 0.9 | 349 | 121 | 174 | 0.86 | 11.12 | 67.2 |
| | 1.2 | 352 | 119 | 171 | 0.80 | 10.37 | 69.4 |
| | 1.5 | 343 | 115 | 167 | 0.71 | 9.12 | 73.1 |

Table 3.89: Results of potentiodynamic polarization studies for the corrosion of welded maraging steel in 2.0 M hydrochloric acid containing different concentrations of CBP.

| Temperature (°C) | Conc. of inhibitor (mM) | $-E_{corr}$ (mV /SCE) | b_a (mV dec ⁻¹) | $-b_c$ (mV dec ⁻¹) | i_{corr} (mA cm ⁻²) | ν_{corr} (mm y ⁻¹) | η (%) |
|------------------|-------------------------|-----------------------|-------------------------------|--------------------------------|-----------------------------------|------------------------------------|------------|
| 30 | Blank | 324 | 114 | 178 | 0.90 | 11.60 | |
| | 0.3 | 353 | 110 | 161 | 0.32 | 4.08 | 64.8 |
| | 0.6 | 358 | 106 | 157 | 0.28 | 3.56 | 69.3 |
| | 0.9 | 345 | 105 | 149 | 0.23 | 2.99 | 74.2 |
| | 1.2 | 352 | 101 | 140 | 0.18 | 2.29 | 80.3 |
| | 1.5 | 365 | 99 | 133 | 0.16 | 2.01 | 82.7 |
| | 35 | Blank | 316 | 129 | 186 | 1.34 | 17.27 |
| 0.3 | | 359 | 119 | 173 | 0.49 | 6.32 | 63.4 |
| 0.6 | | 354 | 114 | 161 | 0.43 | 5.49 | 68.2 |
| 0.9 | | 363 | 108 | 153 | 0.36 | 4.65 | 73.1 |
| 1.2 | | 360 | 105 | 141 | 0.28 | 3.56 | 79.4 |
| 1.5 | | 348 | 98 | 132 | 0.25 | 3.18 | 81.6 |
| 40 | | Blank | 310 | 137 | 193 | 2.61 | 33.64 |
| | 0.3 | 363 | 130 | 181 | 0.97 | 12.55 | 62.7 |
| | 0.6 | 365 | 123 | 175 | 0.90 | 11.64 | 65.4 |
| | 0.9 | 359 | 117 | 172 | 0.71 | 9.18 | 72.7 |
| | 1.2 | 361 | 113 | 160 | 0.60 | 7.67 | 77.2 |
| | 1.5 | 368 | 108 | 145 | 0.53 | 6.80 | 79.8 |
| | 45 | Blank | 327 | 143 | 212 | 4.46 | 57.49 |
| 0.3 | | 362 | 136 | 192 | 1.82 | 23.40 | 59.3 |
| 0.6 | | 367 | 132 | 181 | 1.73 | 22.36 | 61.1 |
| 0.9 | | 369 | 126 | 172 | 1.65 | 21.21 | 63.1 |
| 1.2 | | 373 | 124 | 163 | 1.55 | 19.95 | 65.3 |
| 1.5 | | 370 | 115 | 162 | 1.35 | 17.42 | 69.7 |
| 50 | | Blank | 332 | 159 | 223 | 5.93 | 76.44 |
| | 0.3 | 344 | 141 | 214 | 2.72 | 35.01 | 54.2 |
| | 0.6 | 349 | 137 | 204 | 2.47 | 31.88 | 58.3 |
| | 0.9 | 348 | 130 | 192 | 2.20 | 28.36 | 62.9 |
| | 1.2 | 365 | 123 | 188 | 2.06 | 26.60 | 65.2 |
| | 1.5 | 369 | 119 | 170 | 1.73 | 22.24 | 70.9 |

Table 3.90: EIS data for the corrosion of welded maraging steel in 0.1 M hydrochloric acid containing different concentrations of CBP.

| Temperature (°C) | Conc. of inhibitor (mM) | R_p (ohm. cm ²) | C_{dl} (mF cm ⁻²) | η (%) |
|------------------|-------------------------|-------------------------------|---------------------------------|------------|
| 30 | Blank | 80.6 | 0.061 | |
| | 0.3 | 284.8 | 0.053 | 71.7 |
| | 0.6 | 348.9 | 0.051 | 76.9 |
| | 0.9 | 510.1 | 0.049 | 84.2 |
| | 1.2 | 1168.1 | 0.046 | 93.1 |
| | 1.5 | 1414.0 | 0.041 | 94.3 |
| | 35 | Blank | 71.8 | 0.069 |
| 0.3 | | 241.8 | 0.061 | 70.3 |
| 0.6 | | 273.0 | 0.057 | 73.7 |
| 0.9 | | 424.9 | 0.053 | 83.1 |
| 1.2 | | 481.9 | 0.051 | 85.1 |
| 1.5 | | 635.4 | 0.046 | 88.7 |
| 40 | | Blank | 56.4 | 0.135 |
| | 0.3 | 180.2 | 0.131 | 68.7 |
| | 0.6 | 203.6 | 0.127 | 72.3 |
| | 0.9 | 286.3 | 0.125 | 80.3 |
| | 1.2 | 327.9 | 0.121 | 82.8 |
| | 1.5 | 440.6 | 0.114 | 87.2 |
| | 45 | Blank | 41.3 | 0.183 |
| 0.3 | | 116.3 | 0.172 | 64.5 |
| 0.6 | | 128.7 | 0.171 | 67.9 |
| 0.9 | | 182.7 | 0.169 | 77.4 |
| 1.2 | | 215.1 | 0.165 | 80.8 |
| 1.5 | | 269.9 | 0.157 | 84.7 |
| 50 | | Blank | 34.5 | 0.224 |
| | 0.3 | 89.4 | 0.210 | 61.4 |
| | 0.6 | 95.6 | 0.207 | 63.9 |
| | 0.9 | 125.9 | 0.203 | 72.6 |
| | 1.2 | 148.7 | 0.201 | 76.8 |
| | 1.5 | 179.7 | 0.198 | 80.7 |

Table 3.91: EIS data for the corrosion of welded maraging steel in 0.5 M hydrochloric acid containing different concentrations of CBP.

| Temperature (°C) | Conc. of inhibitor (mM) | R_p (ohm. cm ²) | C_{dl} (mF cm ⁻²) | η (%) |
|------------------|-------------------------|-------------------------------|---------------------------------|------------|
| 30 | Blank | 73.8 | 0.071 | |
| | 0.3 | 249.3 | 0.069 | 70.4 |
| | 0.6 | 298.8 | 0.064 | 75.3 |
| | 0.9 | 431.6 | 0.059 | 82.9 |
| | 1.2 | 889.2 | 0.057 | 91.7 |
| | 1.5 | 1025.0 | 0.052 | 92.8 |
| | 35 | Blank | 55.4 | 0.112 |
| 0.3 | | 172.6 | 0.107 | 67.9 |
| 0.6 | | 202.2 | 0.104 | 72.6 |
| 0.9 | | 279.8 | 0.101 | 80.2 |
| 1.2 | | 355.1 | 0.097 | 84.4 |
| 1.5 | | 457.9 | 0.094 | 87.9 |
| 40 | | Blank | 47.1 | 0.165 |
| | 0.3 | 144.0 | 0.161 | 67.3 |
| | 0.6 | 161.9 | 0.157 | 70.9 |
| | 0.9 | 213.1 | 0.154 | 77.9 |
| | 1.2 | 253.2 | 0.152 | 81.4 |
| | 1.5 | 316.1 | 0.147 | 85.1 |
| | 45 | Blank | 38.0 | 0.216 |
| 0.3 | | 101.1 | 0.212 | 62.4 |
| 0.6 | | 113.4 | 0.207 | 66.5 |
| 0.9 | | 150.2 | 0.203 | 74.7 |
| 1.2 | | 168.1 | 0.195 | 77.4 |
| 1.5 | | 199.0 | 0.191 | 80.9 |
| 50 | | Blank | 29.6 | 0.279 |
| | 0.3 | 73.4 | 0.273 | 59.7 |
| | 0.6 | 79.6 | 0.269 | 62.8 |
| | 0.9 | 101.7 | 0.266 | 70.9 |
| | 1.2 | 109.2 | 0.263 | 72.9 |
| | 1.5 | 137.0 | 0.258 | 78.4 |

Table 3.92: EIS data for the corrosion of welded maraging steel in 1.0 M hydrochloric acid containing different concentrations of CBP.

| Temperature (°C) | Conc. of inhibitor (mM) | R_p (ohm. cm ²) | C_{dl} (mF cm ⁻²) | η (%) |
|------------------|-------------------------|-------------------------------|---------------------------------|------------|
| 30 | Blank | 56.1 | 0.110 | |
| | 0.3 | 176.4 | 0.104 | 68.2 |
| | 0.6 | 217.4 | 0.101 | 74.1 |
| | 0.9 | 313.4 | 0.095 | 82.1 |
| | 1.2 | 623.3 | 0.093 | 91.0 |
| | 1.5 | 684.1 | 0.091 | 91.8 |
| | 35 | Blank | 43.2 | 0.203 |
| 0.3 | | 130.1 | 0.191 | 66.8 |
| 0.6 | | 154.8 | 0.190 | 72.1 |
| 0.9 | | 198.2 | 0.187 | 78.2 |
| 1.2 | | 266.7 | 0.185 | 83.8 |
| 1.5 | | 317.6 | 0.181 | 86.4 |
| 40 | | Blank | 32.9 | 0.276 |
| | 0.3 | 90.6 | 0.263 | 63.7 |
| | 0.6 | 103.8 | 0.261 | 68.3 |
| | 0.9 | 133.7 | 0.253 | 75.4 |
| | 1.2 | 167.0 | 0.251 | 80.3 |
| | 1.5 | 186.9 | 0.242 | 82.4 |
| | 45 | Blank | 30.6 | 0.308 |
| 0.3 | | 76.7 | 0.300 | 60.1 |
| 0.6 | | 88.4 | 0.292 | 65.4 |
| 0.9 | | 107.7 | 0.285 | 71.6 |
| 1.2 | | 122.9 | 0.278 | 75.1 |
| 1.5 | | 137.8 | 0.270 | 77.8 |
| 50 | | Blank | 20.2 | 0.346 |
| | 0.3 | 48.2 | 0.339 | 58.1 |
| | 0.6 | 53.0 | 0.335 | 61.9 |
| | 0.9 | 63.7 | 0.332 | 68.3 |
| | 1.2 | 69.2 | 0.328 | 70.8 |
| | 1.5 | 83.1 | 0.324 | 75.7 |

Table 3.93: EIS data for the corrosion of welded maraging steel in 1.5 M hydrochloric acid containing different concentrations of CBP.

| Temperature (°C) | Conc. of inhibitor (mM) | R_p (ohm. cm ²) | C_{dl} (mF cm ⁻²) | η (%) |
|------------------|-------------------------|-------------------------------|---------------------------------|------------|
| 30 | Blank | 49.2 | 0.166 | |
| | 0.3 | 140.1 | 0.157 | 64.9 |
| | 0.6 | 180.0 | 0.154 | 72.7 |
| | 0.9 | 238.8 | 0.151 | 79.4 |
| | 1.2 | 359.1 | 0.149 | 86.3 |
| | 1.5 | 381.4 | 0.147 | 87.1 |
| | 35 | Blank | 30.6 | 0.315 |
| 0.3 | | 84.8 | 0.310 | 63.9 |
| 0.6 | | 101.7 | 0.307 | 69.8 |
| 0.9 | | 129.6 | 0.305 | 76.4 |
| 1.2 | | 168.1 | 0.301 | 81.8 |
| 1.5 | | 200.0 | 0.298 | 84.7 |
| 40 | | Blank | 24.5 | 0.378 |
| | 0.3 | 66.0 | 0.372 | 62.9 |
| | 0.6 | 74.1 | 0.370 | 66.8 |
| | 0.9 | 94.6 | 0.367 | 74.1 |
| | 1.2 | 112.9 | 0.364 | 78.3 |
| | 1.5 | 131.0 | 0.361 | 81.3 |
| | 45 | Blank | 19.1 | 0.395 |
| 0.3 | | 47.5 | 0.392 | 59.8 |
| 0.6 | | 51.6 | 0.385 | 62.9 |
| 0.9 | | 61.4 | 0.381 | 68.9 |
| 1.2 | | 68.0 | 0.379 | 72.0 |
| 1.5 | | 79.3 | 0.374 | 75.8 |
| 50 | | Blank | 14.2 | 0.402 |
| | 0.3 | 32.6 | 0.390 | 56.5 |
| | 0.6 | 35.3 | 0.387 | 59.8 |
| | 0.9 | 42.8 | 0.384 | 66.8 |
| | 1.2 | 45.7 | 0.382 | 68.7 |
| | 1.5 | 50.5 | 0.372 | 71.9 |

Table 3.94: EIS data for the corrosion of welded maraging steel in 2.0 M hydrochloric acid containing different concentrations of CBP.

| Temperature (°C) | Conc. of inhibitor (mM) | R_p (ohm. cm ²) | C_{dl} (mF cm ⁻²) | η (%) |
|------------------|-------------------------|-------------------------------|---------------------------------|------------|
| 30 | Blank | 33.6 | 0.248 | |
| | 0.3 | 91.3 | 0.240 | 63.2 |
| | 0.6 | 106.7 | 0.234 | 68.5 |
| | 0.9 | 127.3 | 0.232 | 73.6 |
| | 1.2 | 212.7 | 0.226 | 84.2 |
| | 1.5 | 238.3 | 0.218 | 85.9 |
| | 35 | Blank | 24.5 | 0.362 |
| 0.3 | | 65.7 | 0.352 | 62.7 |
| 0.6 | | 76.8 | 0.350 | 68.1 |
| 0.9 | | 89.4 | 0.347 | 72.6 |
| 1.2 | | 115.0 | 0.342 | 78.7 |
| 1.5 | | 128.3 | 0.336 | 80.9 |
| 40 | | Blank | 13.3 | 0.399 |
| | 0.3 | 34.8 | 0.391 | 61.8 |
| | 0.6 | 37.8 | 0.387 | 64.7 |
| | 0.9 | 46.8 | 0.385 | 71.6 |
| | 1.2 | 58.1 | 0.383 | 77.1 |
| | 1.5 | 64.6 | 0.380 | 79.4 |
| | 45 | Blank | 8.3 | 0.418 |
| 0.3 | | 20.3 | 0.412 | 59.1 |
| 0.6 | | 21.1 | 0.407 | 60.7 |
| 0.9 | | 22.2 | 0.405 | 62.6 |
| 1.2 | | 23.6 | 0.403 | 64.9 |
| 1.5 | | 26.5 | 0.392 | 68.7 |
| 50 | | Blank | 6.8 | 0.439 |
| | 0.3 | 14.7 | 0.431 | 53.7 |
| | 0.6 | 16.0 | 0.427 | 57.6 |
| | 0.9 | 17.8 | 0.424 | 61.7 |
| | 1.2 | 18.8 | 0.423 | 63.8 |
| | 1.5 | 22.5 | 0.416 | 69.9 |

Table 3.95: Activation parameters for the corrosion of welded maraging steel in hydrochloric acid containing different concentrations of CBP.

| Molarity of HCl (M) | Conc. of inhibitor (mM) | E_a (kJ mol ⁻¹) | ΔH^\ddagger (kJ mol ⁻¹) | ΔS^\ddagger (J mol ⁻¹ K ⁻¹) |
|---------------------|-------------------------|-------------------------------|---|--|
| 0.1 | Blank | 42.28 | 39.62 | -103.29 |
| | 0.3 | 52.68 | 50.09 | -79.52 |
| | 0.6 | 59.97 | 57.37 | -57.15 |
| | 0.9 | 65.84 | 63.24 | -41.52 |
| | 1.2 | 75.41 | 72.81 | -32.84 |
| | 1.5 | 80.15 | 77.59 | -28.41 |
| 0.5 | Blank | 42.97 | 39.37 | -102.37 |
| | 0.3 | 55.76 | 53.16 | -67.45 |
| | 0.6 | 60.10 | 57.50 | -54.73 |
| | 0.9 | 63.71 | 61.11 | -45.59 |
| | 1.2 | 78.48 | 75.88 | -30.19 |
| | 1.5 | 82.71 | 80.13 | -21.36 |
| 1.0 | Blank | 47.51 | 44.97 | -81.34 |
| | 0.3 | 58.88 | 56.28 | -53.49 |
| | 0.6 | 63.34 | 60.74 | -40.61 |
| | 0.9 | 70.49 | 67.90 | -29.82 |
| | 1.2 | 82.35 | 79.95 | -26.18 |
| | 1.5 | 87.96 | 85.36 | -22.64 |
| 1.5 | Blank | 59.37 | 56.78 | -40.52 |
| | 0.3 | 68.22 | 65.62 | -30.32 |
| | 0.6 | 76.08 | 73.48 | -23.62 |
| | 0.9 | 80.45 | 77.85 | -15.51 |
| | 1.2 | 87.34 | 84.74 | -10.22 |
| | 1.5 | 89.44 | 86.84 | -2.70 |
| 2.0 | Blank | 80.98 | 78.36 | -33.72 |
| | 0.3 | 71.23 | 70.68 | -28.91 |
| | 0.6 | 74.25 | 75.65 | -26.56 |
| | 0.9 | 83.93 | 81.33 | -21.12 |
| | 1.2 | 87.63 | 85.27 | -14.15 |
| | 1.5 | 88.95 | 87.35 | -10.46 |

Table 3.96: Maximum inhibition efficiency attained in different concentrations of hydrochloric acid at different temperatures for CBP.

| Temperature (°C) | Welded Maraging Steel | | | |
|---------------------|--|---------------------------------|---|------------|
| | Hydrochloric acid concentration (M) | Concentration of CBP (mM) | η (%) | |
| | | | Potentiodynamic polarization method | EIS method |
| 30 | 0.1 | 1.5 | 93.8 | 94.3 |
| | 0.5 | | 92.3 | 92.8 |
| | 1.0 | | 91.2 | 91.8 |
| | 1.5 | | 86.4 | 87.1 |
| | 2.0 | | 82.7 | 85.9 |
| 35 | 0.1 | 1.5 | 89.3 | 88.7 |
| | 0.5 | | 88.4 | 87.9 |
| | 1.0 | | 87.0 | 86.4 |
| | 1.5 | | 85.1 | 84.7 |
| | 2.0 | | 81.6 | 80.9 |
| 40 | 0.1 | 1.5 | 87.7 | 87.2 |
| | 0.5 | | 85.3 | 85.1 |
| | 1.0 | | 83.0 | 82.4 |
| | 1.5 | | 81.6 | 81.3 |
| | 2.0 | | 79.8 | 79.4 |
| 45 | 0.1 | 1.5 | 85.2 | 84.7 |
| | 0.5 | | 81.4 | 80.9 |
| | 1.0 | | 78.9 | 77.8 |
| | 1.5 | | 76.3 | 75.8 |
| | 2.0 | | 69.7 | 68.7 |
| 50 | 0.1 | 1.5 | 82.9 | 80.7 |
| | 0.5 | | 79.2 | 78.4 |
| | 1.0 | | 76.0 | 75.7 |
| | 1.5 | | 73.1 | 71.9 |
| | 2.0 | | 70.9 | 69.9 |

Table 3.97: Thermodynamic parameters for the adsorption of CBP on welded maraging steel surface in hydrochloric acid at different temperatures.

| Molarity of HCl (M) | Temperature (° C) | $-\Delta G^{\circ}_{ads}$ (kJ mol ⁻¹) | ΔH°_{ads} (kJ mol ⁻¹) | ΔS°_{ads} (J mol ⁻¹ K ⁻¹) |
|---------------------|-------------------|---|--|---|
| 0.1 | 30 | 32.16 | -14.24 | -60.05 |
| | 35 | 31.89 | | |
| | 40 | 31.52 | | |
| | 45 | 31.39 | | |
| | 50 | 31.16 | | |
| 0.5 | 30 | 32.27 | -7.99 | -79.03 |
| | 35 | 32.16 | | |
| | 40 | 32.02 | | |
| | 45 | 31.87 | | |
| | 50 | 31.68 | | |
| 1.0 | 30 | 31.88 | -3.45 | -94.21 |
| | 35 | 31.60 | | |
| | 40 | 31.53 | | |
| | 45 | 31.41 | | |
| | 50 | 31.33 | | |
| 1.5 | 30 | 31.65 | -4.67 | -90.19 |
| | 35 | 31.35 | | |
| | 40 | 31.24 | | |
| | 45 | 30.84 | | |
| | 50 | 30.78 | | |
| 2.0 | 30 | 31.47 | -2.93 | -96.07 |
| | 35 | 31.39 | | |
| | 40 | 31.23 | | |
| | 45 | 30.95 | | |
| | 50 | 30.89 | | |

3.10 2-(5-CHLORO-1H-BENZOIMIDAZOL-2-YL) PHENOL (CBP) AS INHIBITOR FOR THE CORROSION OF WELDED MARAGING STEEL IN SULPHURIC ACID MEDIUM

3.10.1 Potentiodynamic polarization measurements

The potentiodynamic polarization plots for the corrosion of welded maraging steel in 1.0 M sulphuric acid in the presence of different concentrations of CBP, at 30 °C are shown in Fig. 3.76. Similar results were obtained at other temperatures and also in the other four concentrations of sulphuric acid. The potentiodynamic polarization parameters such as corrosion potential (E_{corr}), corrosion current density (i_{corr}), anodic and cathodic Tafel slopes (b_a , b_c), calculated from Tafel plots in the presence of different concentrations of CBP at different temperatures are summarized in Tables 3.98 to 3.102.

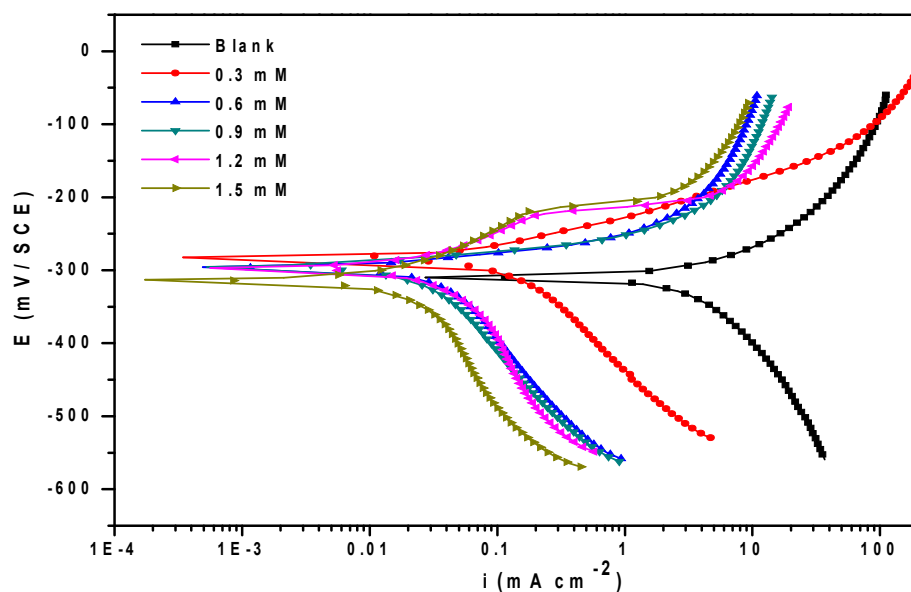


Fig. 3.76: Potentiodynamic polarization curves for the corrosion of welded maraging steel in 1.0 M H_2SO_4 containing different concentrations of CBP at 30 °C.

The presence of inhibitor brings down the corrosion rate considerably. Polarization curves are shifted to a lower current density region indicating a decrease in corrosion rate (Li et al. 2007). Inhibition efficiency increases with the increase in CBP

concentration. In the presence of inhibitor, the E_{corr} value, shift slightly without any definite trend implying that the inhibitor, CBP, acts as a mixed type inhibitor, affecting both anodic and cathodic reactions.

3.10.2 Electrochemical impedance spectroscopy (EIS) studies

Nyquist plots for the corrosion of welded maraging steel in 1.0 M sulphuric acid solution in the presence of different concentrations of CBP are shown in Fig. 3.77. Similar plots were obtained in other concentrations of sulphuric acid and also at other temperatures. The experimental results of EIS measurements obtained for the corrosion of welded maraging steel in 1.0 M sulphuric acid in the presence of CBP are summarized in Tables 3.103 to 3.107. The charge transfer resistance (R_{ct}) increases and double layer capacitance decreases with the increase in the concentration of CBP, indicating an increase in the inhibition efficiency. The results obtained from impedance studies are in good agreement with the results of potentiodynamic polarization studies.

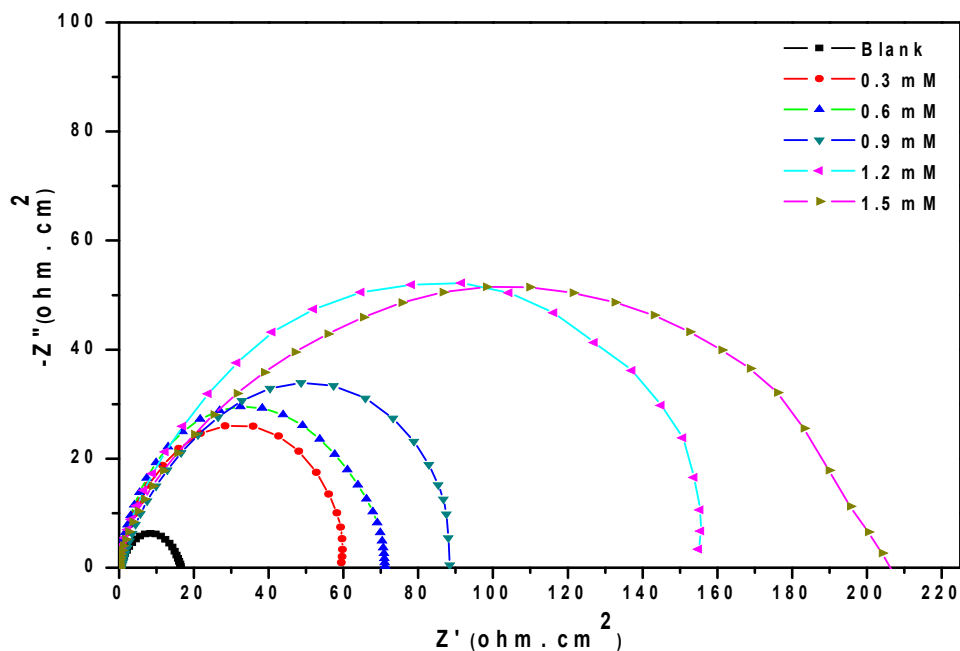


Fig. 3.77: Nyquist plots for the corrosion of welded maraging steel in 1.0 M H_2SO_4 containing different concentrations of CBP at 30 °C.

The Bode plots of phase angle and amplitude for the corrosion of the alloy in the presence of CBP in 1.0 M sulphuric acid are shown in Fig. 3.78 (a) and Fig. 3.78 (b), respectively. Phase angle increases with increase in concentrations of CBP in the sulphuric acid medium. The difference between the HF and LF for the inhibited system in the Bode plot increases with increase in the concentration of CBP. The increase in phase angle with the increase in CBP concentration suggests the decrease in the corrosion rate. An increase in CBP concentration leads to an increase in the impedance ($|Z|$) value.

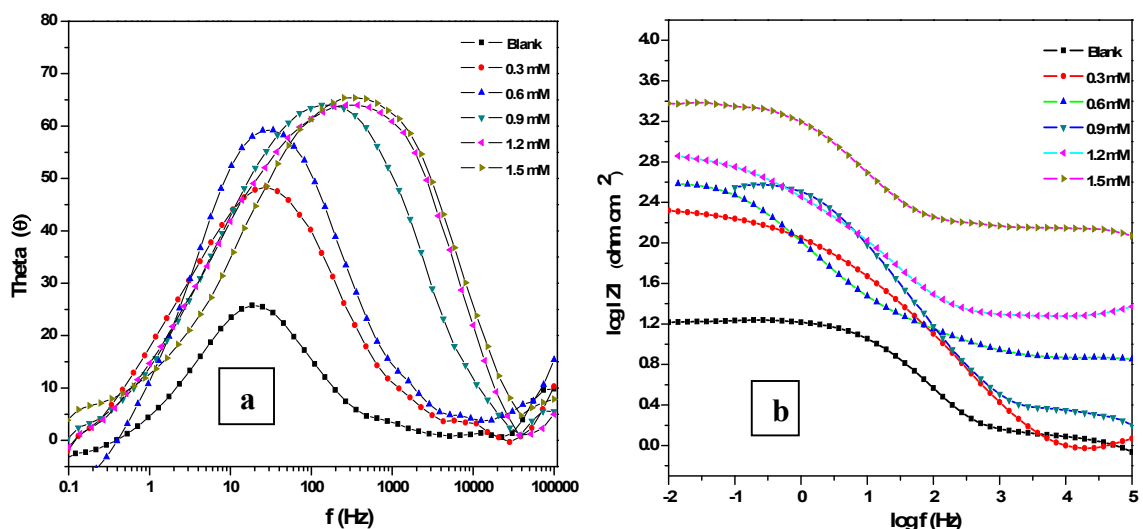


Fig. 3.78: Bode (a) phase angle plots and (b) amplitude plots for the corrosion of welded maraging steel in 1.0 M H₂SO₄ containing different concentrations of CBP at 30 °C.

3.10.3 Effect of temperature

The potentiodynamic polarization and EIS results pertaining to different temperatures in different concentrations of sulphuric acid in the presence of CBP have been listed in the Tables 3.98 to 3.107. The decrease in inhibition efficiency with the increase in temperature indicates desorption of the inhibitor molecules from the metal surface on increasing the temperature (Poornima et al. 2011). This fact is also suggestive of physisorption of the inhibitor molecules on the metal surface.

The Arrhenius plots for the corrosion of welded maraging steel in the presence of different concentrations of CBP in 1.0 M H₂SO₄ acid are shown in Fig. 3.79.

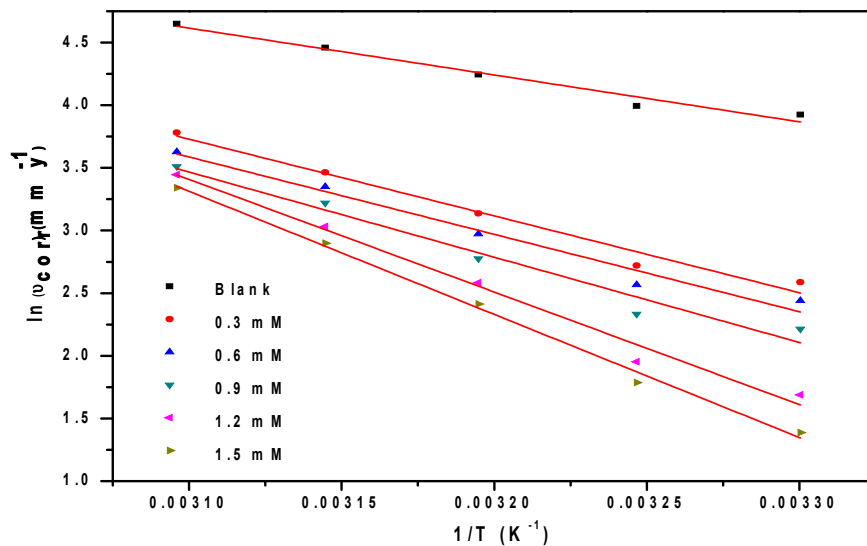


Fig. 3.79: Arrhenius plots for the corrosion of welded maraging steel in 1.0 M H₂SO₄ containing different concentrations of CBP.

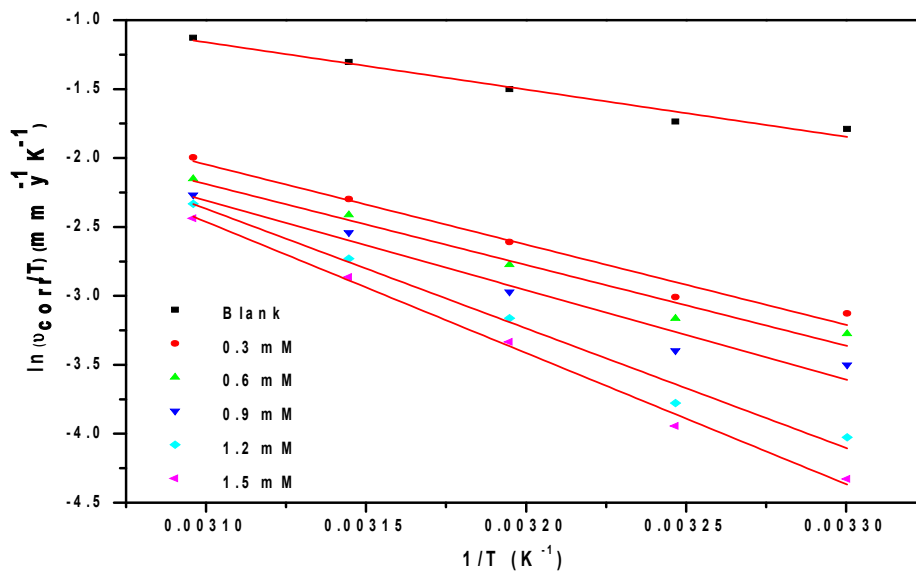


Fig. 3.80: Plots of $\ln(v_{corr}/T)$ versus $1/T$ for the corrosion of welded maraging steel in 1.0 M H₂SO₄ containing different concentrations of CBP.

The plots of $\ln(v_{\text{corr}}/T)$ versus $1/T$ for the corrosion of the alloy in 1.0 M H_2SO_4 acid in the presence of different concentrations of CBP are shown in Fig. 3.80. The calculated values of E_a , ΔH^\ddagger and ΔS^\ddagger are given in Table 3.108. The proportionate increase in the activation energy on the addition of CBP can be attributed to the increased adsorption of CBP providing a barrier on the alloy surface (Avci et al. 2008). The values of entropy of activation indicates that the activated complex in the rate determining step represents an association rather than dissociation, resulting in a decrease in randomness on going from the reactants to the activated complex.

3.10.4 Effect of acid concentration

Table 3.109 summarizes the maximum inhibition efficiencies exhibited by CBP in the H_2SO_4 solution of different concentrations. It is evident from both the polarization and EIS experimental results that, for a particular concentration of inhibitor, the inhibition efficiency decreases with the increase in sulphuric acid concentration on the welded maraging steel. The highest inhibition efficiency is observed in sulphuric acid of 0.1 M concentration.

3.10.5 Adsorption isotherm

The adsorption of CBP on the surface of welded maraging steel was found to obey Langmuir adsorption isotherm. The Langmuir adsorption isotherms for the adsorption of CBP on welded maraging steel in 1.0 M H_2SO_4 are shown in Fig. 3.81. The thermodynamic data obtained for the adsorption of CBP on welded maraging steel are tabulated in Table 3.110. The linear regression coefficients are close to unity and the slopes of the straight lines are nearly unity, suggesting that the adsorption of CBP obeys Langmuir's adsorption isotherm with negligible interaction between the adsorbed molecules. The exothermic ΔH_{ads}^0 values of less than $-41.86 \text{ kJ mol}^{-1}$ predict physisorption of CBP on the alloy surfaces (Ashish Kumar et al. 2010). The ΔG_{ads}^0 values predict both physisorption and chemisorption of CBP. Therefore it can be concluded that the adsorption of CBP on the welded maraging steel is predominantly

through physisorption. These facts are also supported by the decrease in inhibition efficiencies with the increase temperature.

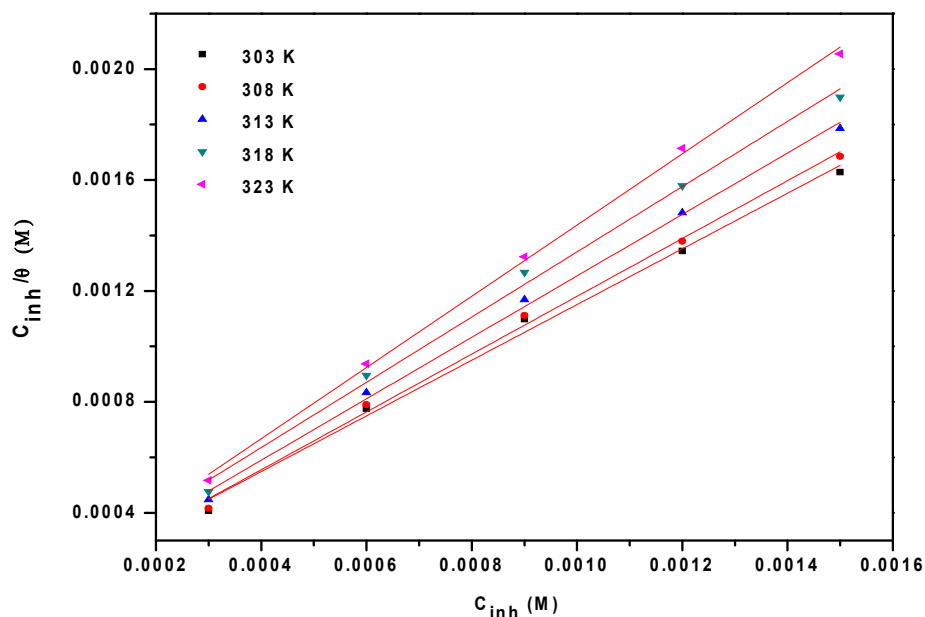


Fig. 3.81: Langmuir adsorption isotherms for the adsorption of CBP on welded maraging steel in 1.0 M H₂SO₄ at different temperatures.

3.10.6 Mechanism of corrosion inhibition

The corrosion inhibition mechanism of CBP in sulphuric acid solution can be explained in the same lines as that of CBP in the section 3.9.6. The inhibitor CBP protects the alloy surface through predominant physisorption mode in which the positive charge centers of CBP gets adsorbed on the alloy surface through electrostatic attraction and also to some extent through chemisorption mode involving neutral CBP molecules.

3.10.7 SEM/EDX studies

Fig. 3.82 represents the SEM image of welded maraging steel after the corrosion tests in a medium of sulphuric acid containing 1.0 mM of CBP. The image clearly shows a smooth surface due to the adsorbed layer of inhibitor molecules on the alloy surface, thus protecting the metal from corrosion. EDX investigations were carried out in order to identify the composition of the species formed on the metal surface in 1.0 M sulphuric

acid in the absence and presence of CBP. The EDX spectra of the alloy surface after corrosion test in the presence of CBP is shown in Fig. 3.83.

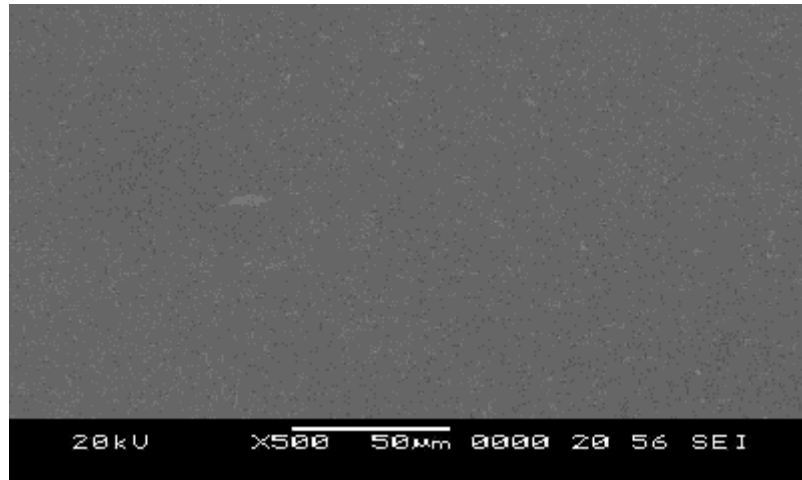


Fig.3.82: SEM image of the welded maraging steel after immersion in 1.0 M H₂SO₄ in the presence of CBP.

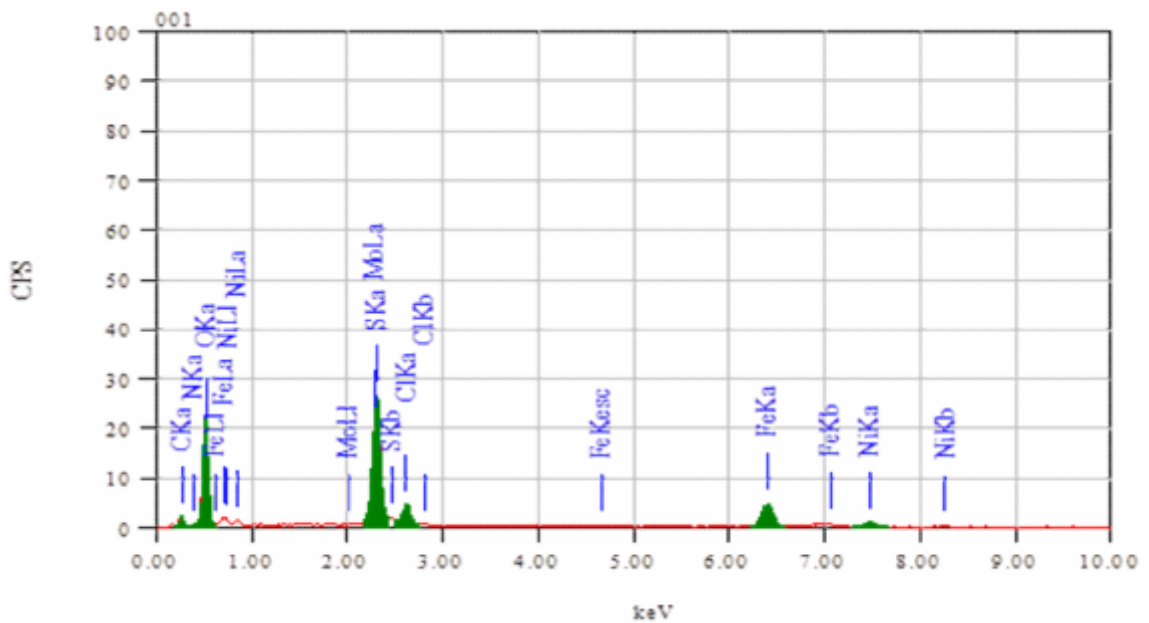


Fig. 3.83: EDX spectra of the welded maraging steel after immersion in 1.0 M H₂SO₄ in the presence of CBP.

The atomic percentage of the elements found in the EDX profile for inhibited metal surface was 3.60% Fe, 0.84% Ni, 54.00% O, 11.12% N, 21.01% C, 1.43% Cl and 7.99% S and indicated the formation of inhibitor film on the area. The elemental compositions mentioned above were mean values of different regions.

Table 3.98: Results of potentiodynamic polarization studies for the corrosion of welded maraging steel in 0.1 M sulphuric acid containing different concentrations of CBP.

| Temperature (°C) | Conc. of inhibitor (mM) | $-E_{corr}$ (mV /SCE) | b_a (mV dec ⁻¹) | $-b_c$ (mV dec ⁻¹) | i_{corr} (mA cm ⁻²) | U_{corr} (mm y ⁻¹) | η (%) |
|------------------|-------------------------|-----------------------|-------------------------------|--------------------------------|-----------------------------------|----------------------------------|------------|
| 30 | Blank | 356 | 162 | 113 | 1.98 | 25.52 | |
| | 0.3 | 327 | 123 | 102 | 0.45 | 5.82 | 77.2 |
| | 0.6 | 318 | 117 | 98 | 0.41 | 5.31 | 79.1 |
| | 0.9 | 306 | 113 | 95 | 0.31 | 4.01 | 84.3 |
| | 1.2 | 312 | 110 | 91 | 0.19 | 2.45 | 90.4 |
| | 1.5 | 304 | 108 | 87 | 0.12 | 1.58 | 93.8 |
| 35 | Blank | 353 | 171 | 124 | 2.41 | 31.07 | |
| | 0.3 | 339 | 145 | 112 | 0.57 | 7.33 | 76.4 |
| | 0.6 | 331 | 141 | 107 | 0.53 | 6.77 | 78.2 |
| | 0.9 | 324 | 138 | 103 | 0.40 | 5.09 | 83.6 |
| | 1.2 | 319 | 132 | 99 | 0.27 | 3.51 | 88.7 |
| | 1.5 | 310 | 129 | 92 | 0.19 | 2.45 | 92.1 |
| 40 | Blank | 347 | 183 | 131 | 2.93 | 37.77 | |
| | 0.3 | 332 | 162 | 117 | 0.72 | 9.33 | 75.3 |
| | 0.6 | 317 | 157 | 115 | 0.68 | 8.72 | 76.9 |
| | 0.9 | 308 | 153 | 109 | 0.54 | 7.03 | 81.4 |
| | 1.2 | 324 | 149 | 102 | 0.40 | 5.17 | 86.3 |
| | 1.5 | 341 | 144 | 97 | 0.28 | 3.63 | 90.4 |
| 45 | Blank | 345 | 197 | 142 | 3.47 | 44.73 | |
| | 0.3 | 351 | 171 | 128 | 0.91 | 11.76 | 73.7 |
| | 0.6 | 316 | 165 | 124 | 0.87 | 11.27 | 74.8 |
| | 0.9 | 328 | 162 | 119 | 0.75 | 9.71 | 78.3 |
| | 1.2 | 334 | 157 | 116 | 0.53 | 6.84 | 84.7 |
| | 1.5 | 326 | 153 | 112 | 0.41 | 5.23 | 88.3 |
| 50 | Blank | 342 | 214 | 154 | 6.14 | 79.15 | |
| | 0.3 | 325 | 183 | 132 | 2.14 | 27.54 | 65.2 |
| | 0.6 | 337 | 179 | 127 | 2.01 | 25.88 | 67.3 |
| | 0.9 | 318 | 172 | 123 | 1.76 | 22.71 | 71.3 |
| | 1.2 | 323 | 170 | 121 | 1.73 | 22.24 | 71.9 |
| | 1.5 | 319 | 166 | 116 | 1.41 | 18.28 | 76.8 |

Table 3.99: Results of potentiodynamic polarization studies for the corrosion of welded maraging steel in 0.5 M sulphuric acid containing different concentrations of CBP.

| Temperature (°C) | Conc. of inhibitor (mM) | $-E_{corr}$ (mV /SCE) | b_a (mV dec ⁻¹) | $-b_c$ (mV dec ⁻¹) | i_{corr} (mA cm ⁻²) | ν_{corr} (mm y ⁻¹) | η (%) |
|------------------|-------------------------|-----------------------|-------------------------------|--------------------------------|-----------------------------------|------------------------------------|------------|
| 30 | Blank | 322 | 172 | 115 | 2.47 | 31.84 | |
| | 0.3 | 339 | 151 | 109 | 0.62 | 7.93 | 75.1 |
| | 0.6 | 334 | 148 | 106 | 0.53 | 6.84 | 78.5 |
| | 0.9 | 324 | 144 | 104 | 0.40 | 5.18 | 83.7 |
| | 1.2 | 317 | 138 | 101 | 0.25 | 3.21 | 89.9 |
| | 1.5 | 308 | 136 | 98 | 0.18 | 2.26 | 92.9 |
| 35 | Blank | 321 | 191 | 132 | 2.68 | 34.55 | |
| | 0.3 | 327 | 163 | 121 | 0.69 | 8.87 | 74.3 |
| | 0.6 | 332 | 160 | 119 | 0.61 | 7.88 | 77.2 |
| | 0.9 | 318 | 154 | 115 | 0.47 | 6.08 | 82.4 |
| | 1.2 | 322 | 151 | 113 | 0.35 | 4.46 | 87.1 |
| | 1.5 | 306 | 148 | 110 | 0.23 | 3.01 | 91.3 |
| 40 | Blank | 318 | 207 | 144 | 4.71 | 60.71 | |
| | 0.3 | 323 | 186 | 132 | 1.29 | 16.57 | 72.7 |
| | 0.6 | 331 | 181 | 128 | 1.21 | 15.60 | 74.3 |
| | 0.9 | 315 | 173 | 125 | 0.97 | 12.45 | 79.5 |
| | 1.2 | 310 | 169 | 123 | 0.79 | 10.20 | 83.2 |
| | 1.5 | 308 | 163 | 119 | 0.59 | 7.65 | 87.4 |
| 45 | Blank | 314 | 224 | 158 | 5.38 | 69.35 | |
| | 0.3 | 321 | 191 | 143 | 1.66 | 21.36 | 69.2 |
| | 0.6 | 330 | 186 | 138 | 1.54 | 19.90 | 71.3 |
| | 0.9 | 337 | 180 | 135 | 1.34 | 17.27 | 75.1 |
| | 1.2 | 329 | 176 | 131 | 1.11 | 14.36 | 79.3 |
| | 1.5 | 311 | 169 | 129 | 0.82 | 10.61 | 84.7 |
| 50 | Blank | 312 | 232 | 163 | 6.94 | 89.45 | |
| | 0.3 | 309 | 207 | 151 | 2.56 | 33.01 | 63.1 |
| | 0.6 | 314 | 201 | 148 | 2.41 | 31.13 | 65.2 |
| | 0.9 | 323 | 196 | 144 | 2.12 | 27.28 | 69.5 |
| | 1.2 | 328 | 194 | 141 | 2.03 | 26.12 | 70.8 |
| | 1.5 | 334 | 183 | 134 | 1.76 | 22.72 | 74.6 |

Table 3.100: Results of potentiodynamic polarization studies for the corrosion of welded maraging steel in 1.0 M sulphuric acid containing different concentrations of CBP.

| Temperature (°C) | Conc. of inhibitor (mM) | $-E_{corr}$ (mV /SCE) | b_a (mV dec ⁻¹) | $-b_c$ (mV dec ⁻¹) | i_{corr} (mA cm ⁻²) | ν_{corr} (mm y ⁻¹) | η (%) |
|------------------|-------------------------|-----------------------|-------------------------------|--------------------------------|-----------------------------------|------------------------------------|------------|
| 30 | Blank | 315 | 187 | 132 | 3.93 | 50.32 | |
| | 0.3 | 280 | 161 | 118 | 1.03 | 13.28 | 73.8 |
| | 0.6 | 293 | 154 | 116 | 0.89 | 11.47 | 77.4 |
| | 0.9 | 295 | 151 | 113 | 0.71 | 9.15 | 81.9 |
| | 1.2 | 298 | 144 | 109 | 0.42 | 5.41 | 89.3 |
| | 1.5 | 318 | 142 | 106 | 0.31 | 4.00 | 92.1 |
| | 35 | Blank | 313 | 198 | 147 | 4.21 | 54.12 |
| 0.3 | | 324 | 174 | 132 | 1.18 | 15.20 | 72.0 |
| 0.6 | | 338 | 171 | 128 | 1.01 | 13.02 | 76.0 |
| 0.9 | | 341 | 169 | 125 | 0.80 | 10.31 | 81.1 |
| 1.2 | | 339 | 163 | 121 | 0.55 | 7.05 | 86.9 |
| 1.5 | | 328 | 158 | 116 | 0.46 | 5.97 | 89.1 |
| 40 | | Blank | 310 | 212 | 163 | 5.41 | 69.72 |
| | 0.3 | 327 | 189 | 141 | 1.79 | 23.01 | 66.9 |
| | 0.6 | 334 | 185 | 137 | 1.51 | 19.53 | 72.1 |
| | 0.9 | 328 | 181 | 133 | 1.24 | 16.04 | 77.1 |
| | 1.2 | 345 | 176 | 129 | 1.03 | 13.25 | 81.0 |
| | 1.5 | 318 | 172 | 124 | 0.87 | 11.16 | 83.9 |
| | 45 | Blank | 312 | 243 | 178 | 6.70 | 86.36 |
| 0.3 | | 324 | 208 | 153 | 2.48 | 31.95 | 63.1 |
| 0.6 | | 308 | 203 | 149 | 2.21 | 28.50 | 67.0 |
| 0.9 | | 319 | 196 | 145 | 1.94 | 25.05 | 71.2 |
| 1.2 | | 327 | 191 | 141 | 1.61 | 20.73 | 75.0 |
| 1.5 | | 331 | 184 | 136 | 1.41 | 18.14 | 79.1 |
| 50 | | Blank | 320 | 269 | 192 | 8.11 | 104.54 |
| | 0.3 | 328 | 224 | 169 | 3.40 | 43.91 | 58.0 |
| | 0.6 | 319 | 216 | 166 | 2.92 | 37.63 | 64.1 |
| | 0.9 | 331 | 211 | 161 | 2.60 | 33.45 | 67.9 |
| | 1.2 | 334 | 207 | 158 | 2.43 | 31.36 | 70.0 |
| | 1.5 | 326 | 202 | 157 | 2.19 | 28.23 | 73.1 |

Table 3.101: Results of potentiodynamic polarization studies for the corrosion of welded maraging steel in 1.5 M sulphuric acid containing different concentrations of CBP.

| Temperature (°C) | Conc. of inhibitor (mM) | $-E_{corr}$ (mV /SCE) | b_a (mV dec ⁻¹) | $-b_c$ (mV dec ⁻¹) | i_{corr} (mA cm ⁻²) | U_{corr} (mm y ⁻¹) | η (%) |
|------------------|-------------------------|-----------------------|-------------------------------|--------------------------------|-----------------------------------|----------------------------------|------------|
| 30 | Blank | 313 | 240 | 146 | 4.28 | 55.17 | |
| | 0.3 | 328 | 201 | 123 | 1.19 | 15.34 | 72.2 |
| | 0.6 | 335 | 194 | 119 | 1.07 | 13.74 | 75.1 |
| | 0.9 | 329 | 189 | 116 | 0.95 | 12.25 | 77.8 |
| | 1.2 | 323 | 183 | 112 | 0.58 | 7.50 | 86.4 |
| | 1.5 | 317 | 179 | 107 | 0.40 | 5.13 | 90.7 |
| | 35 | Blank | 308 | 242 | 151 | 5.31 | 68.45 |
| 0.3 | | 317 | 208 | 139 | 1.60 | 20.67 | 69.8 |
| 0.6 | | 328 | 202 | 137 | 1.37 | 17.66 | 74.2 |
| 0.9 | | 339 | 196 | 133 | 1.26 | 16.22 | 76.3 |
| 1.2 | | 341 | 189 | 128 | 0.78 | 9.99 | 85.4 |
| 1.5 | | 325 | 184 | 126 | 0.60 | 7.73 | 88.7 |
| 40 | | Blank | 300 | 248 | 156 | 6.48 | 83.53 |
| | 0.3 | 327 | 211 | 144 | 2.24 | 28.90 | 65.4 |
| | 0.6 | 331 | 203 | 142 | 1.99 | 25.64 | 69.3 |
| | 0.9 | 338 | 197 | 139 | 1.78 | 22.97 | 72.5 |
| | 1.2 | 323 | 194 | 134 | 1.40 | 18.04 | 78.4 |
| | 1.5 | 314 | 191 | 132 | 1.22 | 15.70 | 81.2 |
| | 45 | Blank | 301 | 290 | 197 | 7.54 | 97.19 |
| 0.3 | | 329 | 229 | 165 | 2.88 | 37.13 | 61.8 |
| 0.6 | | 338 | 223 | 161 | 2.69 | 34.70 | 64.3 |
| 0.9 | | 325 | 218 | 156 | 2.48 | 31.98 | 67.1 |
| 1.2 | | 337 | 212 | 151 | 2.19 | 28.19 | 71.0 |
| 1.5 | | 341 | 207 | 147 | 1.79 | 23.03 | 76.3 |
| 50 | | Blank | 295 | 349 | 242 | 8.64 | 111.37 |
| | 0.3 | 299 | 245 | 198 | 3.78 | 48.67 | 56.3 |
| | 0.6 | 307 | 238 | 192 | 3.21 | 41.43 | 62.8 |
| | 0.9 | 328 | 234 | 189 | 2.96 | 38.20 | 65.7 |
| | 1.2 | 315 | 229 | 183 | 2.73 | 35.19 | 68.4 |
| | 1.5 | 309 | 226 | 178 | 2.52 | 32.52 | 70.8 |

Table 3.102: Results of potentiodynamic polarization studies for the corrosion of welded maraging steel in 2.0 M sulphuric acid containing different concentrations of CBP.

| Temperature (°C) | Conc. of inhibitor (mM) | $-E_{corr}$ (mV /SCE) | b_a (mV dec ⁻¹) | $-b_c$ (mV dec ⁻¹) | i_{corr} (mA cm ⁻²) | ν_{corr} (mm y ⁻¹) | η (%) |
|------------------|-------------------------|-----------------------|-------------------------------|--------------------------------|-----------------------------------|------------------------------------|------------|
| 30 | Blank | 315 | 312 | 154 | 4.97 | 64.06 | |
| | 0.3 | 329 | 223 | 138 | 1.48 | 19.03 | 70.3 |
| | 0.6 | 334 | 218 | 135 | 1.28 | 16.53 | 74.2 |
| | 0.9 | 325 | 212 | 131 | 1.17 | 15.12 | 76.4 |
| | 1.2 | 327 | 209 | 126 | 0.86 | 11.08 | 82.7 |
| | 1.5 | 318 | 201 | 122 | 0.68 | 8.78 | 86.3 |
| | 35 | Blank | 313 | 283 | 208 | 6.12 | 78.89 |
| 0.3 | | 309 | 231 | 151 | 2.00 | 25.72 | 67.4 |
| 0.6 | | 321 | 227 | 146 | 1.66 | 21.46 | 72.8 |
| 0.9 | | 328 | 221 | 143 | 1.59 | 20.43 | 74.1 |
| 1.2 | | 336 | 217 | 138 | 1.11 | 14.28 | 81.9 |
| 1.5 | | 333 | 212 | 132 | 0.97 | 12.54 | 84.1 |
| 40 | | Blank | 310 | 261 | 225 | 7.32 | 94.36 |
| | 0.3 | 307 | 242 | 159 | 2.57 | 33.12 | 64.9 |
| | 0.6 | 318 | 240 | 156 | 2.34 | 30.10 | 68.1 |
| | 0.9 | 323 | 237 | 151 | 2.14 | 27.55 | 70.8 |
| | 1.2 | 327 | 234 | 148 | 1.81 | 23.31 | 75.3 |
| | 1.5 | 324 | 229 | 145 | 1.41 | 18.12 | 80.8 |
| | 45 | Blank | 312 | 282 | 231 | 8.23 | 106.09 |
| 0.3 | | 317 | 257 | 162 | 3.27 | 42.12 | 60.3 |
| 0.6 | | 308 | 251 | 159 | 3.07 | 39.57 | 62.7 |
| 0.9 | | 326 | 246 | 154 | 2.86 | 37.02 | 65.1 |
| 1.2 | | 334 | 242 | 148 | 2.58 | 33.21 | 68.7 |
| 1.5 | | 339 | 237 | 141 | 2.05 | 26.42 | 75.1 |
| 50 | | Blank | 320 | 329 | 204 | 9.02 | 116.27 |
| | 0.3 | 325 | 271 | 171 | 3.73 | 48.02 | 58.7 |
| | 0.6 | 318 | 264 | 168 | 3.50 | 45.11 | 61.2 |
| | 0.9 | 327 | 259 | 167 | 3.27 | 42.09 | 63.8 |
| | 1.2 | 309 | 253 | 164 | 2.99 | 38.49 | 66.9 |
| | 1.5 | 321 | 248 | 161 | 2.77 | 35.69 | 69.3 |

Table 3.103: EIS data for the corrosion of welded maraging steel in 0.1 M sulphuric acid containing different concentrations of CBP.

| Temperature (°C) | Conc. of inhibitor (mM) | R_p (ohm. cm ²) | C_{dl} (mF cm ⁻²) | η (%) |
|------------------|-------------------------|-------------------------------|---------------------------------|------------|
| 30 | Blank | 20.1 | 0.324 | |
| | 0.3 | 87.0 | 0.247 | 76.9 |
| | 0.6 | 93.1 | 0.212 | 78.4 |
| | 0.9 | 123.3 | 0.184 | 83.7 |
| | 1.2 | 184.4 | 0.166 | 89.1 |
| | 1.5 | 261.0 | 0.154 | 92.3 |
| 35 | Blank | 17.4 | 0.469 | |
| | 0.3 | 70.4 | 0.392 | 75.3 |
| | 0.6 | 78.7 | 0.361 | 77.9 |
| | 0.9 | 100.6 | 0.345 | 82.6 |
| | 1.2 | 137.0 | 0.317 | 87.3 |
| | 1.5 | 191.2 | 0.288 | 90.9 |
| 40 | Blank | 14.1 | 0.531 | |
| | 0.3 | 54.7 | 0.495 | 74.2 |
| | 0.6 | 58.0 | 0.427 | 75.7 |
| | 0.9 | 69.8 | 0.399 | 79.8 |
| | 1.2 | 92.2 | 0.374 | 84.7 |
| | 1.5 | 130.6 | 0.348 | 89.2 |
| 45 | Blank | 12.3 | 0.668 | |
| | 0.3 | 45.2 | 0.515 | 72.8 |
| | 0.6 | 46.8 | 0.484 | 73.7 |
| | 0.9 | 53.7 | 0.468 | 77.1 |
| | 1.2 | 74.5 | 0.447 | 83.5 |
| | 1.5 | 95.3 | 0.414 | 87.1 |
| 50 | Blank | 10.2 | 0.830 | |
| | 0.3 | 29.0 | 0.691 | 64.8 |
| | 0.6 | 30.2 | 0.664 | 66.2 |
| | 0.9 | 35.1 | 0.645 | 70.9 |
| | 1.2 | 36.2 | 0.604 | 71.8 |
| | 1.5 | 41.3 | 0.587 | 75.3 |

Table 3.104: EIS data for the corrosion of welded maraging steel in 0.5 M sulphuric acid containing different concentrations of CBP.

| Temperature (°C) | Conc. of inhibitor (mM) | R_p (ohm. cm ²) | C_{dl} (mF cm ⁻²) | η (%) |
|------------------|-------------------------|-------------------------------|---------------------------------|------------|
| 30 | Blank | 18.7 | 0.633 | |
| | 0.3 | 73.0 | 0.524 | 74.4 |
| | 0.6 | 82.4 | 0.487 | 77.3 |
| | 0.9 | 103.3 | 0.468 | 81.9 |
| | 1.2 | 158.5 | 0.417 | 88.2 |
| | 1.5 | 228.0 | 0.385 | 91.8 |
| 35 | Blank | 15.4 | 0.682 | |
| | 0.3 | 57.5 | 0.574 | 73.2 |
| | 0.6 | 67.0 | 0.557 | 77.0 |
| | 0.9 | 84.6 | 0.526 | 81.8 |
| | 1.2 | 112.4 | 0.498 | 86.3 |
| | 1.5 | 151.0 | 0.461 | 89.8 |
| 40 | Blank | 11.4 | 0.727 | |
| | 0.3 | 40.4 | 0.614 | 71.8 |
| | 0.6 | 42.5 | 0.587 | 73.2 |
| | 0.9 | 53.5 | 0.546 | 78.7 |
| | 1.2 | 64.8 | 0.518 | 82.4 |
| | 1.5 | 84.4 | 0.481 | 86.5 |
| 45 | Blank | 10.5 | 0.831 | |
| | 0.3 | 32.9 | 0.692 | 68.1 |
| | 0.6 | 35.5 | 0.668 | 70.4 |
| | 0.9 | 40.7 | 0.629 | 74.2 |
| | 1.2 | 47.5 | 0.584 | 77.9 |
| | 1.5 | 60.7 | 0.551 | 82.7 |
| 50 | Blank | 7.9 | 0.965 | |
| | 0.3 | 21.2 | 0.751 | 62.8 |
| | 0.6 | 22.1 | 0.697 | 64.3 |
| | 0.9 | 24.8 | 0.649 | 68.1 |
| | 1.2 | 26.2 | 0.624 | 69.9 |
| | 1.5 | 29.7 | 0.596 | 73.4 |

Table 3.105: EIS data for the corrosion of welded maraging steel in 1.0 M sulphuric acid containing different concentrations of CBP.

| Temperature (°C) | Conc. of inhibitor (mM) | R_p (ohm. cm ²) | C_{dl} (mF cm ⁻²) | η (%) |
|------------------|-------------------------|-------------------------------|---------------------------------|------------|
| 30 | Blank | 16.1 | 0.641 | |
| | 0.3 | 59.0 | 0.573 | 72.7 |
| | 0.6 | 70.9 | 0.540 | 77.3 |
| | 0.9 | 83.4 | 0.503 | 80.7 |
| | 1.2 | 128.8 | 0.462 | 87.5 |
| | 1.5 | 180.9 | 0.411 | 91.1 |
| 35 | Blank | 13.5 | 0.714 | |
| | 0.3 | 47.2 | 0.582 | 71.4 |
| | 0.6 | 54.2 | 0.567 | 75.1 |
| | 0.9 | 65.2 | 0.529 | 79.3 |
| | 1.2 | 91.1 | 0.484 | 85.2 |
| | 1.5 | 115.4 | 0.435 | 88.3 |
| 40 | Blank | 10.4 | 0.670 | |
| | 0.3 | 30.1 | 0.621 | 65.4 |
| | 0.6 | 36.1 | 0.597 | 71.2 |
| | 0.9 | 42.3 | 0.569 | 75.4 |
| | 1.2 | 52.8 | 0.525 | 80.3 |
| | 1.5 | 56.7 | 0.501 | 81.7 |
| 45 | Blank | 8.6 | 0.873 | |
| | 0.3 | 22.9 | 0.781 | 62.4 |
| | 0.6 | 25.7 | 0.768 | 66.5 |
| | 0.9 | 28.8 | 0.737 | 70.1 |
| | 1.2 | 33.2 | 0.716 | 74.1 |
| | 1.5 | 39.6 | 0.684 | 78.3 |
| 50 | Blank | 7.3 | 1.123 | |
| | 0.3 | 17.0 | 0.974 | 57.1 |
| | 0.6 | 19.6 | 0.925 | 62.8 |
| | 0.9 | 21.8 | 0.877 | 66.5 |
| | 1.2 | 23.6 | 0.839 | 69.1 |
| | 1.5 | 26.4 | 0.781 | 72.4 |

Table 3.106: EIS data for the corrosion of welded maraging steel in 1.5 M sulphuric acid containing different concentrations of CBP.

| Temperature (°C) | Conc. of inhibitor (mM) | R_p (ohm. cm ²) | C_{dl} (mF cm ⁻²) | η (%) |
|------------------|-------------------------|-------------------------------|---------------------------------|------------|
| 30 | Blank | 15.9 | 0.958 | |
| | 0.3 | 56.4 | 0.814 | 71.8 |
| | 0.6 | 60.5 | 0.786 | 73.7 |
| | 0.9 | 67.4 | 0.754 | 76.4 |
| | 1.2 | 104.6 | 0.713 | 84.8 |
| | 1.5 | 145.9 | 0.684 | 89.1 |
| 35 | Blank | 11.6 | 0.982 | |
| | 0.3 | 37.1 | 0.891 | 68.7 |
| | 0.6 | 43.3 | 0.877 | 73.2 |
| | 0.9 | 47.9 | 0.845 | 75.8 |
| | 1.2 | 71.2 | 0.809 | 83.7 |
| | 1.5 | 89.9 | 0.781 | 87.1 |
| 40 | Blank | 9.4 | 1.070 | |
| | 0.3 | 26.3 | 0.962 | 64.2 |
| | 0.6 | 30.0 | 0.927 | 68.7 |
| | 0.9 | 32.4 | 0.894 | 71.0 |
| | 1.2 | 42.5 | 0.813 | 77.9 |
| | 1.5 | 47.2 | 0.798 | 80.1 |
| 45 | Blank | 8.1 | 1.281 | |
| | 0.3 | 20.6 | 1.112 | 60.7 |
| | 0.6 | 22.7 | 1.047 | 64.3 |
| | 0.9 | 25.5 | 0.998 | 68.2 |
| | 1.2 | 26.9 | 0.954 | 69.9 |
| | 1.5 | 31.4 | 0.923 | 74.2 |
| 50 | Blank | 6.9 | 1.318 | |
| | 0.3 | 15.6 | 1.212 | 55.7 |
| | 0.6 | 17.9 | 1.144 | 61.4 |
| | 0.9 | 19.3 | 1.108 | 64.2 |
| | 1.2 | 21.1 | 1.046 | 67.3 |
| | 1.5 | 22.4 | 1.024 | 69.2 |

Table 3.107: EIS data for the corrosion of welded maraging steel in 2.0 M sulphuric acid containing different concentrations of CBP.

| Temperature (°C) | Conc. of inhibitor (mM) | R_p (ohm. cm ²) | C_{dl} (mF cm ⁻²) | η (%) |
|------------------|-------------------------|-------------------------------|---------------------------------|------------|
| 30 | Blank | 13.9 | 1.093 | |
| | 0.3 | 46.0 | 0.947 | 69.8 |
| | 0.6 | 51.7 | 0.914 | 73.1 |
| | 0.9 | 56.5 | 0.878 | 75.4 |
| | 1.2 | 76.0 | 0.832 | 81.7 |
| | 1.5 | 88.5 | 0.810 | 84.3 |
| 35 | Blank | 10.8 | 1.241 | |
| | 0.3 | 32.0 | 1.075 | 66.2 |
| | 0.6 | 36.6 | 1.027 | 70.5 |
| | 0.9 | 39.7 | 0.963 | 72.8 |
| | 1.2 | 54.5 | 0.938 | 80.2 |
| | 1.5 | 62.8 | 0.871 | 82.8 |
| 40 | Blank | 9.2 | 1.324 | |
| | 0.3 | 25.3 | 1.175 | 63.7 |
| | 0.6 | 28.3 | 1.098 | 67.5 |
| | 0.9 | 30.0 | 1.049 | 69.3 |
| | 1.2 | 34.3 | 1.010 | 73.2 |
| | 1.5 | 43.6 | 0.974 | 78.9 |
| 45 | Blank | 7.4 | 1.369 | |
| | 0.3 | 18.4 | 1.262 | 59.8 |
| | 0.6 | 19.1 | 1.218 | 61.3 |
| | 0.9 | 20.7 | 1.176 | 64.2 |
| | 1.2 | 22.5 | 1.121 | 67.1 |
| | 1.5 | 28.1 | 1.070 | 73.7 |
| 50 | Blank | 6.5 | 1.508 | |
| | 0.3 | 15.2 | 1.322 | 57.1 |
| | 0.6 | 16.5 | 1.277 | 60.7 |
| | 0.9 | 17.2 | 1.236 | 62.3 |
| | 1.2 | 18.8 | 1.191 | 65.4 |
| | 1.5 | 20.1 | 1.158 | 67.6 |

Table 3.108: Activation parameters for the corrosion of welded maraging steel in sulphuric acid containing different concentrations of CBP.

| Molarity of H ₂ SO ₄ (M) | Conc. of inhibitor (mM) | E_a (kJ mol ⁻¹) | ΔH^\ddagger (kJ mol ⁻¹) | ΔS^\ddagger (J mol ⁻¹ K ⁻¹) |
|--|-------------------------|-------------------------------|---|--|
| 0.1 | Blank | 42.58 | 39.98 | -86.83 |
| | 0.3 | 57.95 | 55.35 | -48.84 |
| | 0.6 | 59.53 | 56.93 | -44.35 |
| | 0.9 | 68.08 | 64.02 | -23.48 |
| | 1.2 | 67.01 | 79.64 | 23.91 |
| | 1.5 | 91.60 | 88.97 | 31.09 |
| 0.5 | Blank | 44.97 | 42.37 | -77.02 |
| | 0.3 | 60.63 | 58.03 | -37.19 |
| | 0.6 | 64.34 | 61.74 | -26.14 |
| | 0.9 | 80.91 | 68.39 | -6.60 |
| | 1.2 | 84.76 | 84.63 | 43.28 |
| | 1.5 | 95.51 | 92.91 | 67.31 |
| 1.0 | Blank | 32.07 | 29.46 | -115.68 |
| | 0.3 | 50.94 | 48.34 | -64.79 |
| | 0.6 | 51.33 | 48.73 | -64.72 |
| | 0.9 | 56.53 | 53.94 | -49.58 |
| | 1.2 | 74.70 | 72.10 | 6.20 |
| | 1.5 | 81.68 | 79.68 | 27.07 |
| 1.5 | Blank | 30.55 | 29.12 | -120.54 |
| | 0.3 | 47.13 | 44.54 | -75.35 |
| | 0.6 | 46.96 | 44.36 | -76.94 |
| | 0.9 | 48.11 | 45.51 | -74.03 |
| | 1.2 | 65.73 | 64.65 | -15.25 |
| | 1.5 | 77.97 | 75.37 | 17.25 |
| 2.0 | Blank | 28.24 | 26.21 | -122.45 |
| | 0.3 | 38.24 | 35.64 | -102.71 |
| | 0.6 | 42.71 | 40.11 | -89.24 |
| | 0.9 | 43.08 | 40.48 | -88.74 |
| | 1.2 | 52.13 | 51.74 | -54.41 |
| | 1.5 | 57.79 | 55.19 | -44.76 |

Table 3.109: Maximum inhibition efficiency attained in different concentrations of sulphuric acid at different temperatures for CBP.

| Temperature (°C) | Welded Maraging Steel | | | |
|---------------------|--|---------------------------------|---|------------|
| | Hydrochloric acid concentration (M) | Concentration of CBP (mM) | η (%) | |
| | | | Potentiodynamic polarization method | EIS method |
| 30 | 0.1 | 1.5 | 93.4 | 92.3 |
| | 0.5 | | 92.9 | 91.8 |
| | 1.0 | | 92.1 | 91.1 |
| | 1.5 | | 90.7 | 89.1 |
| | 2.0 | | 86.3 | 84.3 |
| 35 | 0.1 | 1.5 | 92.1 | 90.9 |
| | 0.5 | | 91.3 | 89.8 |
| | 1.0 | | 89.1 | 88.3 |
| | 1.5 | | 88.7 | 87.1 |
| | 2.0 | | 84.1 | 82.8 |
| 40 | 0.1 | 1.5 | 90.4 | 89.2 |
| | 0.5 | | 87.4 | 86.5 |
| | 1.0 | | 83.9 | 81.7 |
| | 1.5 | | 81.2 | 80.1 |
| | 2.0 | | 80.8 | 78.9 |
| 45 | 0.1 | 1.5 | 88.3 | 87.1 |
| | 0.5 | | 84.7 | 82.7 |
| | 1.0 | | 79.1 | 78.3 |
| | 1.5 | | 76.3 | 74.2 |
| | 2.0 | | 75.1 | 73.7 |
| 50 | 0.1 | 1.5 | 76.8 | 75.3 |
| | 0.5 | | 74.6 | 73.4 |
| | 1.0 | | 73.1 | 72.4 |
| | 1.5 | | 70.8 | 69.2 |
| | 2.0 | | 69.3 | 67.6 |

Table 3.110: Thermodynamic parameters for the adsorption of CBP on welded maraging steel surface in sulphuric acid at different temperatures.

| Molarity of H ₂ SO ₄ (M) | Temperature (° C) | $-\Delta G^{\circ}_{ads}$ (kJ mol ⁻¹) | ΔH°_{ads} (kJ mol ⁻¹) | ΔS°_{ads} (J mol ⁻¹ K ⁻¹) |
|--|-------------------|---|--|---|
| 0.1 | 30 | 32.63 | -24.39 | -115.6 |
| | 35 | 32.47 | | |
| | 40 | 32.29 | | |
| | 45 | 32.17 | | |
| | 50 | 32.09 | | |
| 0.5 | 30 | 32.52 | -27.53 | -112.4 |
| | 35 | 32.10 | | |
| | 40 | 31.94 | | |
| | 45 | 31.75 | | |
| | 50 | 31.68 | | |
| 1.0 | 30 | 32.35 | -22.76 | -117.60 |
| | 35 | 32.24 | | |
| | 40 | 32.13 | | |
| | 45 | 32.05 | | |
| | 50 | 31.86 | | |
| 1.5 | 30 | 32.09 | -24.51 | -110.80 |
| | 35 | 32.02 | | |
| | 40 | 31.86 | | |
| | 45 | 31.70 | | |
| | 50 | 31.51 | | |
| 2.0 | 30 | 31.96 | -19.10 | -136.78 |
| | 35 | 31.81 | | |
| | 40 | 31.75 | | |
| | 45 | 31.42 | | |
| | 50 | 30.89 | | |

3.11 2-(4-METHOXY-PHENYL)-BENZO[d]IMIDAZO[2,1-b]THIAZOLE (MPBIT) AS INHIBITOR FOR THE CORROSION OF WELDED MARAGING STEEL IN HYDROCHLORIC ACID MEDIUM

3.11.1 Potentiodynamic polarization measurements

Polarization curves for the corrosion of maraging steel in 1.0 M HCl solution in the presence of different concentrations of MPBIT are shown in Fig. 3.84. Similar results were obtained at other temperatures and in other concentrations of hydrochloric acid also. The potentiodynamic polarization parameters are summarized in Tables 3.111 to 3.115.

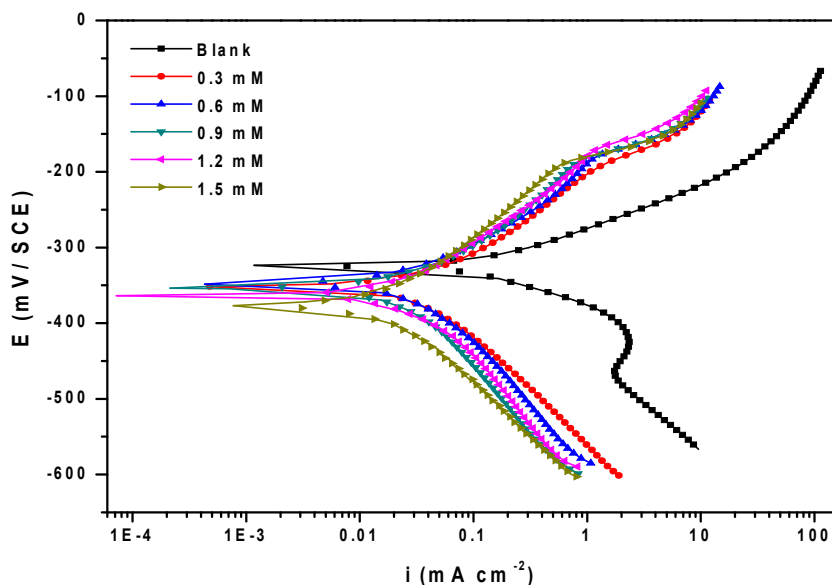


Fig. 3.84: Potentiodynamic polarization curves for the corrosion of welded maraging steel in 1.0 M hydrochloric acid containing different concentrations of MPBIT at 30 °C.

It could be observed that both the anodic and cathodic reactions were suppressed with the addition of inhibitor, which suggested that the inhibitor can serve as a mixed type of inhibitor. The addition of MPBIT shift the E_{corr} values slightly to the more negative potential indicating the mixed inhibition action by MPBIT with predominant cathodic action.

3.11.2 Electrochemical impedance spectroscopy (EIS) studies

Nyquist plots for the corrosion of welded maraging steel in 1.0 M HCl solution in the presence of different concentrations of MPBIT are given in Fig. 3.85. Similar plots were obtained in other concentrations of the acid and also at other temperatures. The impedance parameters are presented in Tables 3.116 to 3.120.

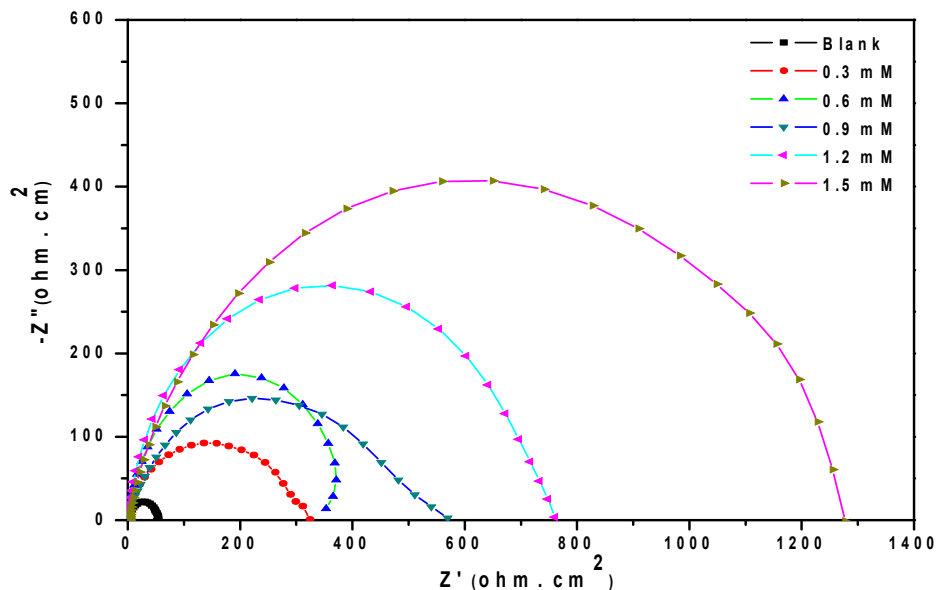


Fig. 3.85: Nyquist plots for the corrosion of welded maraging steel in 1.0 M hydrochloric acid containing different concentrations of MPBIT at 30 °C.

It is clear from Fig. 3.85 that the shapes of the impedance plots for the corrosion of welded maraging steel in the presence of inhibitor are not substantially different from those of the uninhibited one. The plots are similar to those obtained in the presence of BTPO as discussed in the section 3.3.2. The equivalent circuit given in Fig. 3.17 is used to fit the experimental data for the corrosion of welded maraging steel in hydrochloric acid in the presence of MPBIT. As can be seen from the Tables, R_{ct} value increases and C_{dl} value decreases with the increase in the concentration of MPBIT which suggests decrease in corrosion rate.

The Bode plots of phase angle and amplitude for the corrosion of the alloy in the presence of different concentrations of MPBIT is shown in Fig. 3.86 (a) and

Fig. 3.86 (b), respectively. Phase angle and also impedance ($|Z|$) increases with the increase in the concentrations of MPBIT in hydrochloric acid.

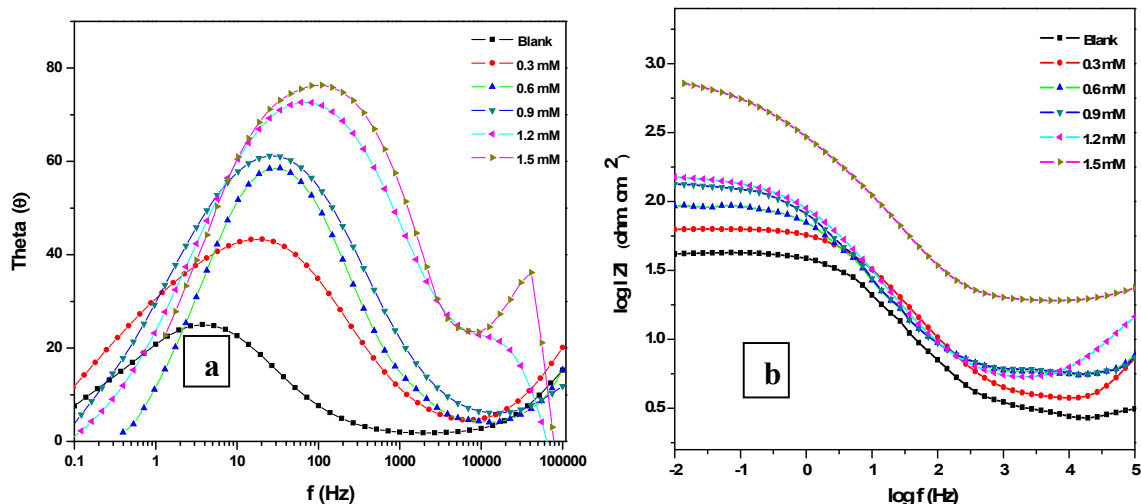


Fig. 3.86: Bode (a) phase angle plots and (b) amplitude plots for the corrosion of welded maraging steel in 1.0 M HCl containing different concentrations of MPBIT at 30 °C.

3.11.3 Effect of temperature

The potentiodynamic polarization and EIS results pertaining to different temperatures in different concentrations of hydrochloric acid in the presence of MPBIT have already been listed in Tables 3.111 to 3.120. The effect of temperature on corrosion inhibition behaviour of MPBIT is similar to that of BTPO on welded maraging steel as discussed in the section 3.3.3. The decrease in the inhibition efficiency of MPBIT with the increase in temperature on welded maraging steel surface may be attributed to the physisorption of MPBIT. The Arrhenius plots for the corrosion of welded maraging steel in 1.0 M hydrochloric acid in the presence of different concentrations of MPBIT are shown in Fig. 3.87. The plots of $\ln(v_{\text{corr}}/T)$ versus $(1/T)$ for welded maraging steel are shown in Fig. 3.88. The calculated values of activation parameters are given in Table 3.121. The observations are similar to the ones obtained in the presence of BTPO and PNPT.

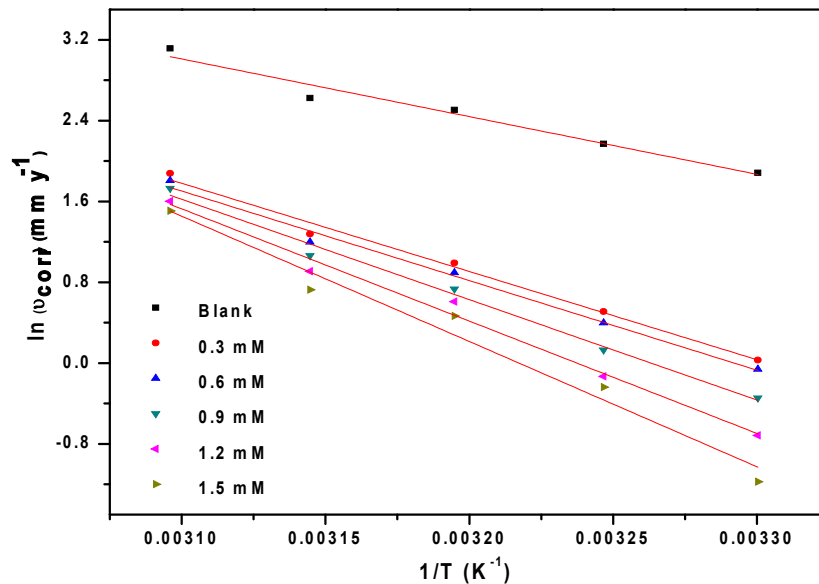


Fig. 3.87: Arrhenius plots for the corrosion of welded maraging steel in 1.0 M hydrochloric acid containing different concentrations of MPBIT.

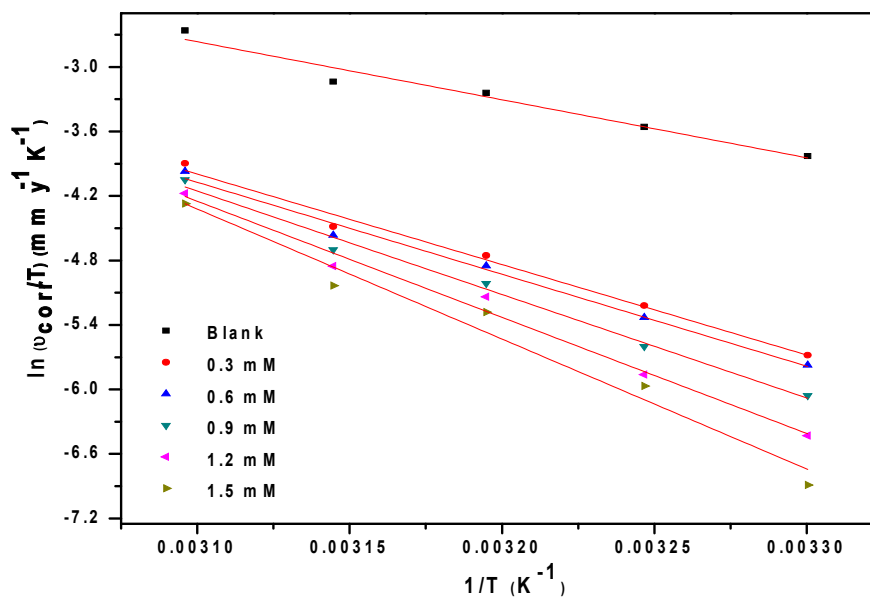


Fig. 3.88: Plots of $\ln(v_{corr}/T)$ versus $1/T$ for the corrosion of welded maraging steel in 1.0 M hydrochloric acid containing different concentrations of MPBIT.

The increase in the E_a values with the increase in MPBIT concentration indicates the increase in energy barrier for the corrosion reaction as discussed in earlier sections. The entropy of activation in the absence and presence of MPBIT is large and negative for the corrosion of alloy. This implies that the activated complex in the rate determining step represents an association rather than dissociation step, indicating that a decrease in disordering takes place on going from reactants to activated complex (Gomma and Wahdan 1995, Marsh 1988). The entropies of activation are higher for welded maraging steel in inhibited solutions than that in the uninhibited solutions.

3.11.4 Effect of acid concentration

Table 3.122 summarises the maximum inhibition efficiencies exhibited by MPBIT in the HCl solution of different concentrations. It is evident from both polarization and EIS experimental results that, for a particular concentration of inhibitor, the inhibition efficiency decreases with the increase in hydrochloric acid concentration on the welded maraging steel. The highest inhibition efficiency is observed in hydrochloric acid of 0.1 M concentration.

3.11.5 Adsorption isotherm

The adsorption of MPBIT on the surfaces of welded maraging steel was found to obey Langmuir adsorption isotherm. The Langmuir adsorption isotherms for the adsorption of MPBIT on welded maraging steel in 1.0 M hydrochloric acid are shown in Fig. 3.89. The thermodynamic parameters for the adsorption of MPBIT on welded maraging steel are tabulated in Tables 3.123. The values of ΔG_{ads}^0 and ΔH_{ads}^0 indicate both physisorption and chemisorption of MPBIT on welded maraging steel with predominant physisorption. The ΔS_{ads}^0 value values indicate a decrease in randomness on going from the reactants to the metal adsorbed species.

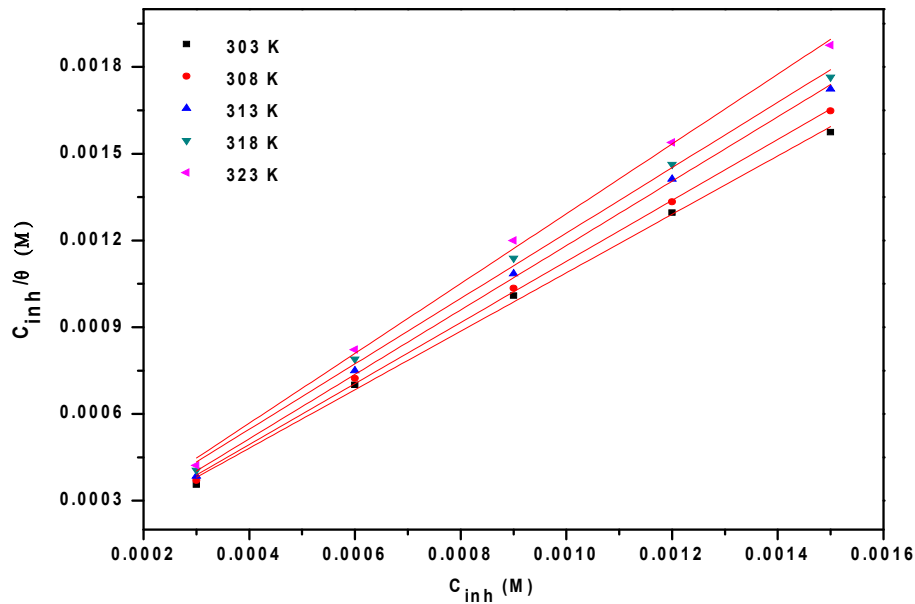


Fig. 3.89: Langmuir adsorption isotherms for the adsorption of MPBIT on welded maraging steel in 1.0 M HCl at different temperatures.

3.11.6 Mechanism of corrosion inhibition

The inhibition action of MPBIT can be attributed to its adsorption on the alloy surface through nitrogen, sulphur, oxygen and delocalized π electrons of the benzene rings. The positive centres on the MPBIT can electrostatically interact with the alloy surface adsorbed with the negatively charged chloride ions and the negative charge centres of MPBIT can electrostatically interact with the positive alloy surface free from adsorbed chloride ions. Chemisorption of MPBIT is possible on the neutral unadsorbed metal surface by the interaction of π electrons cloud of MPBIT.

3.11.7 SEM/EDX studies

Fig. 3.90 shows the SEM image of the sample after immersion in 1.0 M hydrochloric acid in the presence of MPBIT. It can be seen that the alloy surface in the presence of MPBIT is smooth without any visible corrosion attack. Thus, it can be concluded that MPBIT protects the alloy from corrosion by forming a uniform film on the alloy surface.

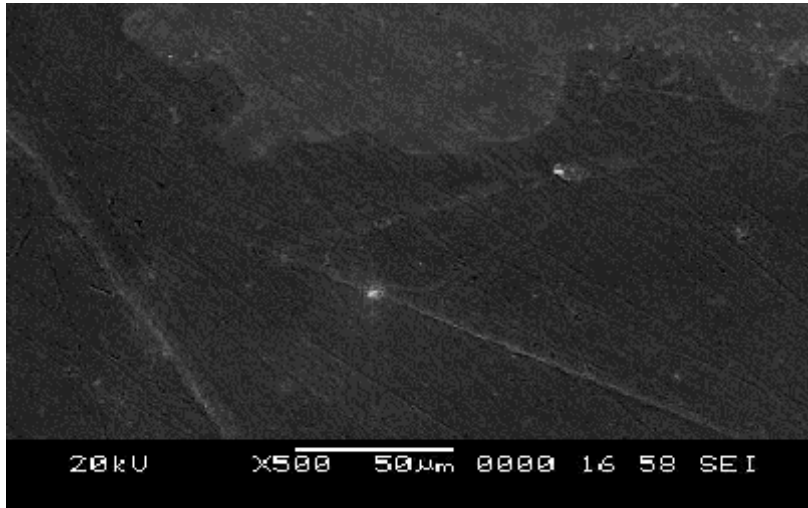


Fig. 3.90: SEM image of the welded maraging steel after immersion in 1.0 M HCl in the presence of MPBIT.

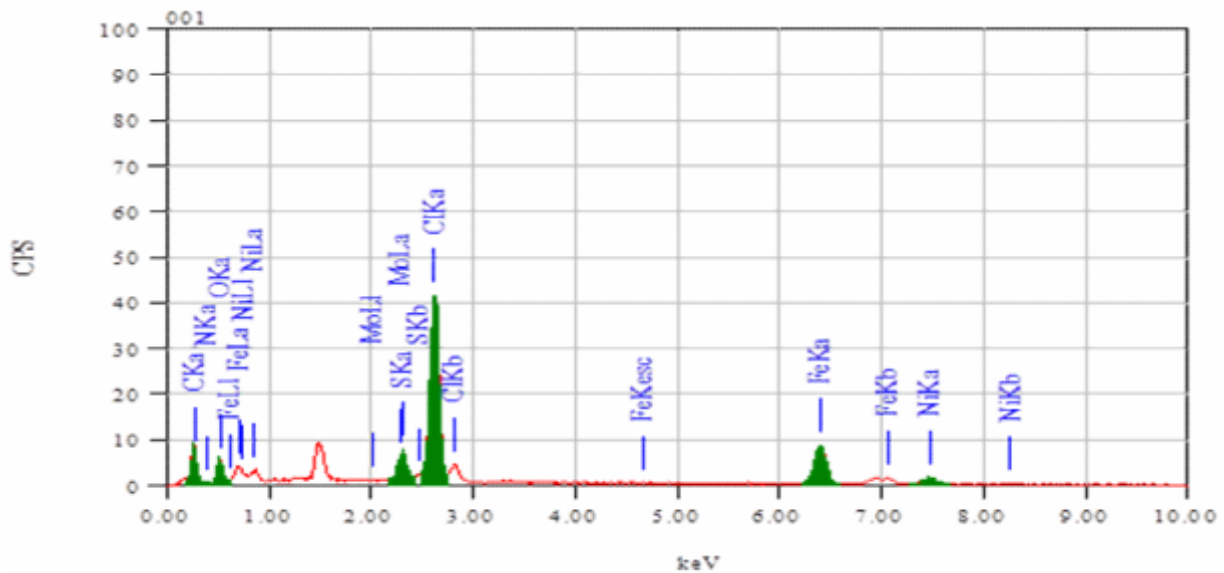


Fig. 3.91: EDX spectra of the welded maraging steel after immersion in 1.0 M HCl in the presence of MPBIT.

The EDX spectra of the corroded surface of the alloy in the presence of MPBIT is shown in Fig. 3.91. The atomic percentages of the elements found in the EDX spectra for inhibited metal surface was 2.61% Fe, 0.58% Ni, 0.10% Mo,

24.86% O, 41.88% C, 0.51% Cl and 29.45% N and indicated the formation of inhibitor film on the surface of alloy.

Table 3.111: Results of potentiodynamic polarization studies for the corrosion of welded maraging steel in 0.1 M hydrochloric acid containing different concentrations of MPBIT.

| Temperature (°C) | Conc. of inhibitor (mM) | $-E_{corr}$ (mV /SCE) | b_a (mV dec ⁻¹) | $-b_c$ (mV dec ⁻¹) | i_{corr} (mA cm ⁻²) | ν_{corr} (mm y ⁻¹) | η (%) |
|------------------|-------------------------|-----------------------|-------------------------------|--------------------------------|-----------------------------------|------------------------------------|------------|
| 30 | Blank | 306 | 98 | 140 | 0.31 | 4.00 | |
| | 0.3 | 313 | 87 | 120 | 0.06 | 0.52 | 80.6 |
| | 0.6 | 324 | 84 | 117 | 0.05 | 0.43 | 83.9 |
| | 0.9 | 331 | 82 | 116 | 0.04 | 0.39 | 87.1 |
| | 1.2 | 329 | 81 | 114 | 0.03 | 0.26 | 90.3 |
| | 1.5 | 340 | 79 | 111 | 0.01 | 0.16 | 96.1 |
| | 35 | Blank | 310 | 101 | 146 | 0.36 | 4.64 |
| 0.3 | | 317 | 95 | 123 | 0.08 | 0.64 | 77.8 |
| 0.6 | | 328 | 92 | 121 | 0.07 | 0.73 | 80.5 |
| 0.9 | | 342 | 91 | 118 | 0.05 | 0.59 | 86.1 |
| 1.2 | | 334 | 88 | 115 | 0.04 | 0.54 | 88.4 |
| 1.5 | | 351 | 86 | 112 | 0.03 | 0.34 | 92.7 |
| 40 | | Blank | 312 | 103 | 147 | 0.46 | 5.93 |
| | 0.3 | 324 | 99 | 127 | 0.11 | 1.43 | 75.9 |
| | 0.6 | 332 | 97 | 125 | 0.10 | 1.35 | 77.3 |
| | 0.9 | 337 | 95 | 123 | 0.08 | 1.06 | 82.2 |
| | 1.2 | 341 | 93 | 116 | 0.07 | 0.95 | 83.9 |
| | 1.5 | 345 | 91 | 114 | 0.04 | 0.55 | 90.8 |
| | 45 | Blank | 315 | 108 | 156 | 0.67 | 8.64 |
| 0.3 | | 320 | 101 | 132 | 0.20 | 2.57 | 70.2 |
| 0.6 | | 331 | 97 | 130 | 0.18 | 2.35 | 72.8 |
| 0.9 | | 324 | 95 | 128 | 0.13 | 1.70 | 80.3 |
| 1.2 | | 341 | 93 | 125 | 0.12 | 1.55 | 82.1 |
| 1.5 | | 347 | 91 | 123 | 0.08 | 1.09 | 87.4 |
| 50 | | Blank | 313 | 113 | 161 | 0.83 | 10.70 |
| | 0.3 | 328 | 105 | 140 | 0.29 | 3.71 | 65.3 |
| | 0.6 | 334 | 102 | 136 | 0.26 | 3.30 | 69.2 |
| | 0.9 | 321 | 100 | 129 | 0.21 | 2.77 | 74.1 |
| | 1.2 | 326 | 97 | 126 | 0.17 | 2.23 | 79.2 |
| | 1.5 | 332 | 95 | 124 | 0.15 | 1.89 | 82.3 |

Table 3.112: Results of potentiodynamic polarization studies for the corrosion of welded maraging steel in 0.5 M hydrochloric acid containing different concentrations of MPBIT.

| Temperature (°C) | Conc. of inhibitor (mM) | $-E_{corr}$ (mV /SCE) | b_a (mV dec ⁻¹) | $-b_c$ (mV dec ⁻¹) | i_{corr} (mA cm ⁻²) | \mathcal{U}_{corr} (mm y ⁻¹) | η (%) |
|------------------|-------------------------|-----------------------|-------------------------------|--------------------------------|-----------------------------------|--|------------|
| 30 | Blank | 315 | 103 | 149 | 0.35 | 4.51 | |
| | 0.3 | 329 | 96 | 123 | 0.05 | 0.62 | 86.2 |
| | 0.6 | 332 | 94 | 120 | 0.05 | 0.58 | 87.1 |
| | 0.9 | 342 | 92 | 117 | 0.04 | 0.46 | 89.7 |
| | 1.2 | 351 | 90 | 115 | 0.02 | 0.32 | 92.9 |
| | 1.5 | 362 | 87 | 113 | 0.02 | 0.19 | 95.7 |
| 35 | Blank | 323 | 105 | 152 | 0.48 | 6.19 | |
| | 0.3 | 341 | 99 | 131 | 0.08 | 1.01 | 83.7 |
| | 0.6 | 337 | 96 | 127 | 0.08 | 1.00 | 83.9 |
| | 0.9 | 348 | 94 | 124 | 0.07 | 0.95 | 84.7 |
| | 1.2 | 354 | 92 | 121 | 0.06 | 0.82 | 86.8 |
| | 1.5 | 357 | 91 | 119 | 0.04 | 0.54 | 91.2 |
| 40 | Blank | 330 | 112 | 158 | 0.60 | 7.73 | |
| | 0.3 | 328 | 101 | 137 | 0.18 | 2.26 | 70.8 |
| | 0.6 | 335 | 98 | 134 | 0.16 | 2.03 | 73.8 |
| | 0.9 | 341 | 96 | 131 | 0.12 | 1.52 | 80.3 |
| | 1.2 | 347 | 95 | 129 | 0.11 | 1.41 | 81.9 |
| | 1.5 | 358 | 92 | 127 | 0.07 | 0.86 | 89.0 |
| 45 | Blank | 328 | 116 | 165 | 0.77 | 9.93 | |
| | 0.3 | 334 | 106 | 140 | 0.25 | 3.25 | 67.3 |
| | 0.6 | 331 | 104 | 137 | 0.22 | 2.89 | 70.9 |
| | 0.9 | 327 | 100 | 134 | 0.17 | 2.20 | 77.8 |
| | 1.2 | 323 | 99 | 133 | 0.16 | 2.05 | 79.3 |
| | 1.5 | 332 | 96 | 130 | 0.12 | 1.56 | 84.4 |
| 50 | Blank | 324 | 118 | 173 | 1.03 | 13.28 | |
| | 0.3 | 319 | 108 | 154 | 0.37 | 4.81 | 63.8 |
| | 0.6 | 332 | 104 | 150 | 0.33 | 4.21 | 68.3 |
| | 0.9 | 341 | 103 | 147 | 0.28 | 3.64 | 72.6 |
| | 1.2 | 352 | 101 | 145 | 0.24 | 3.13 | 76.4 |
| | 1.5 | 364 | 98 | 142 | 0.20 | 2.62 | 80.2 |

Table 3.113: Results of potentiodynamic polarization studies for the corrosion of welded maraging steel in 1.0 M hydrochloric acid containing different concentrations of MPBIT.

| Temperature (°C) | Conc. of inhibitor (mM) | $-E_{corr}$ (mV /SCE) | b_a (mV dec ⁻¹) | $-b_c$ (mV dec ⁻¹) | i_{corr} (mA cm ⁻²) | \mathcal{U}_{corr} (mm y ⁻¹) | η (%) |
|------------------|-------------------------|-----------------------|-------------------------------|--------------------------------|-----------------------------------|--|------------|
| 30 | Blank | 324 | 112 | 158 | 0.51 | 6.57 | |
| | 0.3 | 353 | 98 | 132 | 0.08 | 1.03 | 84.3 |
| | 0.6 | 351 | 96 | 127 | 0.07 | 0.94 | 85.7 |
| | 0.9 | 354 | 93 | 123 | 0.06 | 0.71 | 89.2 |
| | 1.2 | 364 | 91 | 120 | 0.04 | 0.49 | 92.5 |
| | 1.5 | 378 | 88 | 117 | 0.02 | 0.31 | 95.3 |
| 35 | Blank | 328 | 118 | 163 | 0.68 | 8.77 | |
| | 0.3 | 349 | 104 | 137 | 0.13 | 1.67 | 80.9 |
| | 0.6 | 357 | 102 | 134 | 0.12 | 1.49 | 83.0 |
| | 0.9 | 361 | 98 | 129 | 0.09 | 1.14 | 83.9 |
| | 1.2 | 364 | 95 | 126 | 0.07 | 0.88 | 89.9 |
| | 1.5 | 376 | 92 | 124 | 0.06 | 0.79 | 90.8 |
| 40 | Blank | 336 | 126 | 171 | 0.95 | 12.25 | |
| | 0.3 | 354 | 109 | 149 | 0.21 | 2.69 | 67.0 |
| | 0.6 | 360 | 107 | 146 | 0.19 | 2.45 | 72.0 |
| | 0.9 | 357 | 103 | 142 | 0.16 | 2.08 | 78.1 |
| | 1.2 | 367 | 101 | 139 | 0.14 | 1.84 | 80.2 |
| | 1.5 | 381 | 98 | 135 | 0.12 | 1.59 | 87.1 |
| 45 | Blank | 331 | 131 | 179 | 1.07 | 13.79 | |
| | 0.3 | 342 | 113 | 146 | 0.28 | 3.59 | 64.9 |
| | 0.6 | 357 | 110 | 142 | 0.26 | 3.31 | 68.8 |
| | 0.9 | 368 | 108 | 140 | 0.22 | 2.90 | 73.9 |
| | 1.2 | 374 | 105 | 138 | 0.19 | 2.48 | 75.8 |
| | 1.5 | 371 | 102 | 134 | 0.16 | 2.07 | 82.0 |
| 50 | Blank | 328 | 142 | 191 | 1.75 | 22.56 | |
| | 0.3 | 357 | 119 | 157 | 0.51 | 6.54 | 62.1 |
| | 0.6 | 364 | 116 | 154 | 0.47 | 6.09 | 67.0 |
| | 0.9 | 371 | 111 | 153 | 0.44 | 5.64 | 71.2 |
| | 1.2 | 375 | 109 | 150 | 0.39 | 4.96 | 73.9 |
| | 1.5 | 381 | 105 | 144 | 0.35 | 4.51 | 78.8 |

Table 3.114: Results of potentiodynamic polarization studies for the corrosion of welded maraging steel in 1.5 M hydrochloric acid containing different concentrations of MPBIT.

| Temperature (°C) | Conc. of inhibitor (mM) | $-E_{corr}$ (mV /SCE) | b_a (mV dec ⁻¹) | $-b_c$ (mV dec ⁻¹) | i_{corr} (mA cm ⁻²) | \mathcal{U}_{corr} (mm y ⁻¹) | η (%) |
|------------------|-------------------------|-----------------------|-------------------------------|--------------------------------|-----------------------------------|--|------------|
| 30 | Blank | 316 | 109 | 163 | 0.57 | 7.35 | |
| | 0.3 | 345 | 102 | 132 | 0.12 | 1.54 | 79.1 |
| | 0.6 | 351 | 93 | 127 | 0.10 | 1.30 | 82.3 |
| | 0.9 | 364 | 91 | 124 | 0.09 | 1.13 | 84.6 |
| | 1.2 | 368 | 90 | 120 | 0.07 | 0.89 | 87.9 |
| | 1.5 | 371 | 87 | 116 | 0.04 | 0.57 | 92.3 |
| | 35 | Blank | 320 | 117 | 171 | 0.98 | 12.63 |
| 0.3 | | 337 | 108 | 147 | 0.24 | 3.06 | 75.8 |
| 0.6 | | 341 | 105 | 144 | 0.26 | 3.37 | 73.3 |
| 0.9 | | 349 | 102 | 140 | 0.19 | 2.40 | 81.0 |
| 1.2 | | 354 | 98 | 138 | 0.16 | 2.12 | 83.2 |
| 1.5 | | 369 | 94 | 133 | 0.11 | 1.43 | 88.7 |
| 40 | | Blank | 328 | 124 | 183 | 1.31 | 16.89 |
| | 0.3 | 337 | 108 | 152 | 0.45 | 5.86 | 65.3 |
| | 0.6 | 343 | 104 | 150 | 0.40 | 5.10 | 69.8 |
| | 0.9 | 349 | 100 | 146 | 0.31 | 3.95 | 76.6 |
| | 1.2 | 354 | 98 | 142 | 0.28 | 3.66 | 78.3 |
| | 1.5 | 367 | 96 | 138 | 0.20 | 2.55 | 84.9 |
| | 45 | Blank | 322 | 132 | 198 | 1.80 | 23.20 |
| 0.3 | | 338 | 118 | 160 | 0.67 | 8.63 | 62.8 |
| 0.6 | | 345 | 111 | 156 | 0.62 | 8.05 | 65.3 |
| 0.9 | | 352 | 108 | 153 | 0.51 | 6.59 | 71.6 |
| 1.2 | | 367 | 106 | 149 | 0.48 | 6.22 | 73.2 |
| 1.5 | | 372 | 101 | 144 | 0.35 | 4.57 | 80.3 |
| 50 | | Blank | 315 | 147 | 209 | 2.63 | 33.90 |
| | 0.3 | 327 | 125 | 178 | 1.03 | 13.29 | 60.8 |
| | 0.6 | 334 | 119 | 173 | 0.93 | 11.93 | 64.8 |
| | 0.9 | 342 | 116 | 170 | 0.82 | 10.54 | 68.9 |
| | 1.2 | 351 | 114 | 167 | 0.76 | 9.76 | 71.2 |
| | 1.5 | 360 | 110 | 163 | 0.71 | 9.12 | 73.1 |

Table 3.115: Results of potentiodynamic polarization studies for the corrosion of welded maraging steel in 2.0 M hydrochloric acid containing different concentrations of MPBIT.

| Temperature (°C) | Conc. of inhibitor (mM) | $-E_{corr}$ (mV /SCE) | b_a (mV dec ⁻¹) | $-b_c$ (mV dec ⁻¹) | i_{corr} (mA cm ⁻²) | ν_{corr} (mm y ⁻¹) | η (%) |
|------------------|-------------------------|-----------------------|-------------------------------|--------------------------------|-----------------------------------|------------------------------------|------------|
| 30 | Blank | 324 | 114 | 178 | 0.90 | 11.60 | |
| | 0.3 | 329 | 105 | 157 | 0.24 | 3.04 | 73.8 |
| | 0.6 | 334 | 101 | 153 | 0.21 | 2.74 | 76.4 |
| | 0.9 | 345 | 98 | 144 | 0.17 | 2.15 | 81.5 |
| | 1.2 | 352 | 94 | 135 | 0.13 | 1.66 | 85.7 |
| | 1.5 | 361 | 90 | 128 | 0.10 | 1.24 | 89.3 |
| | 35 | Blank | 316 | 129 | 186 | 1.34 | 17.27 |
| 0.3 | | 347 | 119 | 168 | 0.26 | 5.16 | 70.1 |
| 0.6 | | 354 | 114 | 156 | 0.24 | 4.97 | 71.2 |
| 0.9 | | 361 | 108 | 148 | 0.19 | 3.73 | 78.4 |
| 1.2 | | 367 | 105 | 136 | 0.16 | 3.20 | 81.5 |
| 1.5 | | 372 | 98 | 127 | 0.11 | 2.23 | 87.1 |
| 40 | | Blank | 310 | 137 | 193 | 2.61 | 33.64 |
| | 0.3 | 326 | 130 | 174 | 0.45 | 12.15 | 63.9 |
| | 0.6 | 341 | 123 | 170 | 0.40 | 11.00 | 67.3 |
| | 0.9 | 358 | 117 | 167 | 0.31 | 9.02 | 73.2 |
| | 1.2 | 364 | 113 | 155 | 0.28 | 7.84 | 76.7 |
| | 1.5 | 372 | 108 | 140 | 0.20 | 6.32 | 81.2 |
| | 45 | Blank | 327 | 143 | 212 | 4.46 | 57.49 |
| 0.3 | | 345 | 136 | 187 | 0.67 | 22.25 | 61.3 |
| 0.6 | | 329 | 132 | 176 | 0.62 | 21.04 | 63.4 |
| 0.9 | | 336 | 126 | 167 | 0.51 | 17.65 | 69.3 |
| 1.2 | | 341 | 124 | 158 | 0.48 | 16.50 | 71.3 |
| 1.5 | | 357 | 115 | 153 | 0.35 | 13.68 | 76.2 |
| 50 | | Blank | 332 | 159 | 223 | 5.93 | 76.44 |
| | 0.3 | 347 | 141 | 192 | 1.03 | 31.19 | 59.2 |
| | 0.6 | 358 | 137 | 187 | 0.93 | 28.97 | 62.1 |
| | 0.9 | 374 | 130 | 183 | 0.82 | 27.29 | 64.3 |
| | 1.2 | 363 | 123 | 180 | 0.76 | 25.76 | 66.3 |
| | 1.5 | 378 | 119 | 176 | 0.71 | 23.62 | 69.1 |

Table 3.116: EIS data for the corrosion of welded maraging steel in 0.1 M hydrochloric acid containing different concentrations of MPBIT.

| Temperature (°C) | Conc. of inhibitor (mM) | R_p (ohm. cm ²) | C_{dl} (mF cm ⁻²) | η (%) |
|------------------|-------------------------|-------------------------------|---------------------------------|------------|
| 30 | Blank | 80.6 | 0.061 | |
| | 0.3 | 480.6 | 0.048 | 83.3 |
| | 0.6 | 613.3 | 0.046 | 86.9 |
| | 0.9 | 653.9 | 0.043 | 87.8 |
| | 1.2 | 1040.0 | 0.040 | 92.3 |
| | 1.5 | 1921.7 | 0.036 | 95.8 |
| | 35 | Blank | 71.8 | 0.069 |
| 0.3 | | 410.3 | 0.051 | 82.4 |
| 0.6 | | 469.2 | 0.048 | 84.7 |
| 0.9 | | 548.1 | 0.045 | 86.9 |
| 1.2 | | 619.0 | 0.043 | 88.4 |
| 1.5 | | 983.6 | 0.040 | 92.4 |
| 40 | | Blank | 56.4 | 0.135 |
| | 0.3 | 238.0 | 0.127 | 76.3 |
| | 0.6 | 261.1 | 0.124 | 78.4 |
| | 0.9 | 309.9 | 0.121 | 81.8 |
| | 1.2 | 354.7 | 0.118 | 84.1 |
| | 1.5 | 648.3 | 0.112 | 91.3 |
| | 45 | Blank | 41.3 | 0.183 |
| 0.3 | | 151.3 | 0.167 | 72.7 |
| 0.6 | | 159.5 | 0.163 | 74.1 |
| 0.9 | | 219.7 | 0.159 | 81.2 |
| 1.2 | | 233.3 | 0.155 | 82.3 |
| 1.5 | | 315.2 | 0.150 | 86.9 |
| 50 | | Blank | 34.5 | 0.224 |
| | 0.3 | 104.2 | 0.204 | 66.9 |
| | 0.6 | 114.1 | 0.201 | 69.8 |
| | 0.9 | 139.0 | 0.197 | 75.2 |
| | 1.2 | 165.9 | 0.193 | 79.2 |
| | 1.5 | 213.0 | 0.189 | 83.8 |

Table 3.117: EIS data for the corrosion of welded maraging steel in 0.5 M hydrochloric acid containing different concentrations of MPBIT.

| Temperature (°C) | Conc. of inhibitor (mM) | R_p (ohm. cm ²) | C_{dl} (mF cm ⁻²) | η (%) |
|------------------|-------------------------|-------------------------------|---------------------------------|------------|
| 30 | Blank | 73.8 | 0.071 | |
| | 0.3 | 405.5 | 0.069 | 81.9 |
| | 0.6 | 488.7 | 0.064 | 85.1 |
| | 0.9 | 576.2 | 0.059 | 87.3 |
| | 1.2 | 678.4 | 0.057 | 88.5 |
| | 1.5 | 1039.2 | 0.052 | 92.9 |
| | 35 | Blank | 55.4 | 0.112 |
| 0.3 | | 299.5 | 0.107 | 81.5 |
| 0.6 | | 333.7 | 0.104 | 83.4 |
| 0.9 | | 362.1 | 0.101 | 84.7 |
| 1.2 | | 419.7 | 0.097 | 86.8 |
| 1.5 | | 629.5 | 0.094 | 91.2 |
| 40 | | Blank | 47.1 | 0.165 |
| | 0.3 | 166.4 | 0.161 | 71.7 |
| | 0.6 | 181.9 | 0.157 | 74.1 |
| | 0.9 | 246.6 | 0.154 | 80.9 |
| | 1.2 | 289.0 | 0.152 | 83.7 |
| | 1.5 | 432.1 | 0.147 | 89.2 |
| | 45 | Blank | 38.0 | 0.216 |
| 0.3 | | 123.4 | 0.212 | 69.2 |
| 0.6 | | 139.2 | 0.207 | 72.7 |
| 0.9 | | 169.6 | 0.203 | 77.6 |
| 1.2 | | 197.9 | 0.195 | 80.8 |
| 1.5 | | 255.0 | 0.191 | 85.1 |
| 50 | | Blank | 29.6 | 0.279 |
| | 0.3 | 82.5 | 0.273 | 64.1 |
| | 0.6 | 93.1 | 0.269 | 68.2 |
| | 0.9 | 105.0 | 0.266 | 71.8 |
| | 1.2 | 121.3 | 0.263 | 75.6 |
| | 1.5 | 159.1 | 0.258 | 81.4 |

Table 3.118: EIS data for the corrosion of welded maraging steel in 1.0 M hydrochloric acid containing different concentrations of MPBIT.

| Temperature (°C) | Conc. of inhibitor (mM) | R_p (ohm. cm ²) | C_{dl} (mF cm ⁻²) | η (%) |
|------------------|-------------------------|-------------------------------|---------------------------------|------------|
| 30 | Blank | 56.1 | 0.110 | |
| | 0.3 | 268.8 | 0.104 | 79.1 |
| | 0.6 | 310.3 | 0.101 | 81.9 |
| | 0.9 | 389.5 | 0.095 | 85.5 |
| | 1.2 | 504.6 | 0.093 | 88.7 |
| | 1.5 | 709.3 | 0.091 | 92.1 |
| | 35 | Blank | 43.2 | 0.203 |
| 0.3 | | 226.2 | 0.191 | 80.9 |
| 0.6 | | 241.3 | 0.190 | 82.1 |
| 0.9 | | 268.3 | 0.187 | 83.9 |
| 1.2 | | 271.7 | 0.185 | 84.1 |
| 1.5 | | 396.3 | 0.181 | 89.1 |
| 40 | | Blank | 32.9 | 0.276 |
| | 0.3 | 106.8 | 0.263 | 69.2 |
| | 0.6 | 119.6 | 0.261 | 72.5 |
| | 0.9 | 158.9 | 0.253 | 79.3 |
| | 1.2 | 180.8 | 0.251 | 81.8 |
| | 1.5 | 265.3 | 0.242 | 87.6 |
| | 45 | Blank | 30.6 | 0.308 |
| 0.3 | | 91.1 | 0.300 | 66.4 |
| 0.6 | | 99.0 | 0.292 | 69.1 |
| 0.9 | | 118.1 | 0.285 | 74.1 |
| 1.2 | | 138.5 | 0.278 | 77.9 |
| 1.5 | | 168.1 | 0.270 | 81.8 |
| 50 | | Blank | 20.2 | 0.346 |
| | 0.3 | 55.2 | 0.339 | 63.4 |
| | 0.6 | 57.9 | 0.335 | 65.1 |
| | 0.9 | 70.1 | 0.332 | 71.2 |
| | 1.2 | 75.4 | 0.328 | 73.2 |
| | 1.5 | 95.7 | 0.324 | 78.9 |

Table 3.119: EIS data for the corrosion of welded maraging steel in 1.5 M hydrochloric acid containing different concentrations of MPBIT.

| Temperature (°C) | Conc. of inhibitor (mM) | R_p (ohm. cm ²) | C_{dl} (mF cm ⁻²) | η (%) |
|------------------|-------------------------|-------------------------------|---------------------------------|------------|
| 30 | Blank | 49.2 | 0.166 | |
| | 0.3 | 228.8 | 0.157 | 78.5 |
| | 0.6 | 270.3 | 0.154 | 81.8 |
| | 0.9 | 319.5 | 0.151 | 84.6 |
| | 1.2 | 406.6 | 0.149 | 87.9 |
| | 1.5 | 609.0 | 0.147 | 91.8 |
| | 35 | Blank | 30.6 | 0.315 |
| 0.3 | | 135.4 | 0.310 | 77.4 |
| 0.6 | | 118.6 | 0.307 | 74.2 |
| 0.9 | | 161.1 | 0.305 | 81.0 |
| 1.2 | | 166.3 | 0.301 | 81.6 |
| 1.5 | | 257.1 | 0.298 | 88.1 |
| 40 | | Blank | 24.5 | 0.378 |
| | 0.3 | 71.8 | 0.372 | 65.9 |
| | 0.6 | 84.2 | 0.370 | 70.9 |
| | 0.9 | 108.4 | 0.367 | 77.4 |
| | 1.2 | 117.2 | 0.364 | 79.1 |
| | 1.5 | 154.1 | 0.361 | 84.1 |
| | 45 | Blank | 19.1 | 0.395 |
| 0.3 | | 52.5 | 0.392 | 63.6 |
| 0.6 | | 54.3 | 0.385 | 64.8 |
| 0.9 | | 67.7 | 0.381 | 71.8 |
| 1.2 | | 77.0 | 0.379 | 75.2 |
| 1.5 | | 96.0 | 0.374 | 80.1 |
| 50 | | Blank | 14.2 | 0.402 |
| | 0.3 | 37.1 | 0.390 | 61.7 |
| | 0.6 | 38.5 | 0.387 | 63.1 |
| | 0.9 | 45.7 | 0.384 | 68.9 |
| | 1.2 | 49.3 | 0.382 | 71.2 |
| | 1.5 | 51.3 | 0.372 | 72.3 |

Table 3.120: EIS data for the corrosion of welded maraging steel in 2.0 M hydrochloric acid containing different concentrations of MPBIT.

| Temperature (°C) | Conc. of inhibitor (mM) | R_p (ohm. cm ²) | C_{dl} (mF cm ⁻²) | η (%) |
|------------------|-------------------------|-------------------------------|---------------------------------|------------|
| 30 | Blank | 33.6 | 0.248 | |
| | 0.3 | 129.7 | 0.240 | 74.1 |
| | 0.6 | 136.6 | 0.234 | 75.4 |
| | 0.9 | 178.7 | 0.232 | 81.2 |
| | 1.2 | 225.5 | 0.226 | 85.1 |
| | 1.5 | 252.6 | 0.218 | 86.7 |
| | 35 | Blank | 24.5 | 0.362 |
| 0.3 | | 87.2 | 0.352 | 71.9 |
| 0.6 | | 90.1 | 0.350 | 72.8 |
| 0.9 | | 113.4 | 0.347 | 78.4 |
| 1.2 | | 132.3 | 0.342 | 81.5 |
| 1.5 | | 164.4 | 0.336 | 85.1 |
| 40 | | Blank | 13.3 | 0.399 |
| | 0.3 | 37.8 | 0.391 | 64.8 |
| | 0.6 | 43.2 | 0.387 | 69.2 |
| | 0.9 | 48.9 | 0.385 | 72.8 |
| | 1.2 | 54.1 | 0.383 | 75.4 |
| | 1.5 | 67.9 | 0.380 | 80.4 |
| | 45 | Blank | 8.3 | 0.418 |
| 0.3 | | 21.7 | 0.412 | 61.8 |
| 0.6 | | 22.3 | 0.407 | 62.7 |
| 0.9 | | 26.6 | 0.405 | 68.8 |
| 1.2 | | 31.2 | 0.403 | 73.4 |
| 1.5 | | 36.9 | 0.392 | 77.5 |
| 50 | | Blank | 6.8 | 0.439 |
| | 0.3 | 17.1 | 0.431 | 60.3 |
| | 0.6 | 18.1 | 0.427 | 62.4 |
| | 0.9 | 19.0 | 0.424 | 64.3 |
| | 1.2 | 20.2 | 0.423 | 66.3 |
| | 1.5 | 21.7 | 0.416 | 68.7 |

Table 3.121: Activation parameters for the corrosion of welded maraging steel in hydrochloric acid containing different concentrations of MPBIT.

| Molarity of HCl (M) | Conc. of inhibitor (mM) | E_a (kJ mol ⁻¹) | ΔH^\ddagger (kJ mol ⁻¹) | ΔS^\ddagger (J mol ⁻¹ K ⁻¹) |
|---------------------|-------------------------|-------------------------------|---|--|
| 0.1 | Blank | 42.28 | 39.62 | -103.29 |
| | 0.3 | 86.23 | 83.92 | -59.41 |
| | 0.6 | 85.41 | 82.85 | -41.50 |
| | 0.9 | 81.00 | 78.40 | -35.54 |
| | 1.2 | 87.29 | 84.69 | -24.08 |
| | 1.5 | 99.46 | 96.75 | -19.33 |
| 0.5 | Blank | 42.97 | 39.37 | -102.37 |
| | 0.3 | 85.79 | 83.25 | -45.90 |
| | 0.6 | 81.95 | 79.35 | -32.69 |
| | 0.9 | 81.12 | 78.52 | -28.45 |
| | 1.2 | 89.43 | 86.83 | -23.69 |
| | 1.5 | 102.89 | 100.29 | -11.54 |
| 1.0 | Blank | 47.51 | 44.97 | -81.34 |
| | 0.3 | 72.59 | 69.99 | -33.83 |
| | 0.6 | 73.71 | 71.13 | -30.92 |
| | 0.9 | 82.63 | 80.03 | -25.93 |
| | 1.2 | 92.41 | 89.81 | -15.44 |
| | 1.5 | 103.14 | 100.54 | -8.20 |
| 1.5 | Blank | 59.37 | 56.78 | -40.52 |
| | 0.3 | 87.20 | 84.60 | -28.46 |
| | 0.6 | 86.58 | 83.98 | -25.80 |
| | 0.9 | 89.24 | 86.64 | -22.62 |
| | 1.2 | 95.66 | 93.06 | -15.16 |
| | 1.5 | 109.24 | 106.64 | -10.98 |
| 2.0 | Blank | 80.98 | 78.36 | -33.72 |
| | 0.3 | 99.70 | 97.10 | -25.69 |
| | 0.6 | 100.39 | 97.79 | -24.27 |
| | 0.9 | 111.12 | 108.52 | -19.27 |
| | 1.2 | 115.46 | 113.46 | -10.57 |
| | 1.5 | 125.49 | 122.89 | -5.23 |

Table 3.122: Maximum inhibition efficiency attained in different concentrations of hydrochloric acid at different temperatures for MPBIT.

| Temperature (°C) | Welded Maraging Steel | | | |
|---------------------|--|-----------------------------------|---|------------|
| | Hydrochloric acid concentration (M) | Concentration of MPBIT (mM) | η (%) | |
| | | | Potentiodynamic polarization method | EIS method |
| 30 | 0.1 | 1.5 | 96.1 | 95.8 |
| | 0.5 | | 95.7 | 95.5 |
| | 1.0 | | 95.3 | 95.1 |
| | 1.5 | | 92.3 | 92.3 |
| | 2.0 | | 89.3 | 86.7 |
| 35 | 0.1 | 1.5 | 92.7 | 92.4 |
| | 0.5 | | 91.2 | 91.2 |
| | 1.0 | | 90.8 | 89.1 |
| | 1.5 | | 88.7 | 88.1 |
| | 2.0 | | 87.1 | 85.1 |
| 40 | 0.1 | 1.5 | 90.8 | 91.3 |
| | 0.5 | | 89.0 | 89.1 |
| | 1.0 | | 87.1 | 87.6 |
| | 1.5 | | 84.9 | 84.1 |
| | 2.0 | | 81.2 | 80.4 |
| 45 | 0.1 | 1.5 | 87.4 | 86.9 |
| | 0.5 | | 84.4 | 85.1 |
| | 1.0 | | 82.0 | 81.8 |
| | 1.5 | | 80.3 | 80.1 |
| | 2.0 | | 76.2 | 77.5 |
| 50 | 0.1 | 1.5 | 82.3 | 83.8 |
| | 0.5 | | 80.2 | 81.4 |
| | 1.0 | | 78.8 | 78.9 |
| | 1.5 | | 73.1 | 72.3 |
| | 2.0 | | 69.1 | 68.7 |

Table 3.123: Thermodynamic parameters for the adsorption of MPBIT on welded maraging steel surface in hydrochloric acid at different temperatures.

| Molarity of HCl (M) | Temperature (° C) | $-\Delta G^{\circ}_{ads}$ (kJ mol ⁻¹) | ΔH°_{ads} (kJ mol ⁻¹) | ΔS°_{ads} (J mol ⁻¹ K ⁻¹) |
|---------------------|-------------------|---|--|---|
| 0.1 | 30 | 34.67 | -26.09 | -47.12 |
| | 35 | 34.24 | | |
| | 40 | 33.95 | | |
| | 45 | 33.63 | | |
| | 50 | 33.20 | | |
| 0.5 | 30 | 34.32 | -28.93 | -43.01 |
| | 35 | 34.15 | | |
| | 40 | 33.92 | | |
| | 45 | 33.61 | | |
| | 50 | 33.27 | | |
| 1.0 | 30 | 33.97 | -31.05 | -38.07 |
| | 35 | 33.71 | | |
| | 40 | 33.40 | | |
| | 45 | 33.11 | | |
| | 50 | 32.95 | | |
| 1.5 | 30 | 33.47 | -34.14 | -35.22 |
| | 35 | 33.25 | | |
| | 40 | 33.00 | | |
| | 45 | 32.89 | | |
| | 50 | 32.62 | | |
| 2.0 | 30 | 32.72 | -38.26 | -31.61 |
| | 35 | 32.61 | | |
| | 40 | 32.37 | | |
| | 45 | 32.09 | | |
| | 50 | 31.83 | | |

3.12 2-(4-METHOXY-PHENYL)-BENZO[d]IMIDAZO[2,1-B]THIAZOLE (MPBIT) AS INHIBITOR FOR THE CORROSION OF WELDED MARAGING STEEL IN SULPHURIC ACID MEDIUM

3.12.1 Potentiodynamic polarization measurements

The potentiodynamic polarization plots for the corrosion of welded maraging steel in 1.0 M sulphuric acid in the presence of different concentrations of MPBIT, at 30 °C are shown in Fig. 3.92. Similar results were obtained at other temperatures and also in the other four concentrations of sulphuric acid. The potentiodynamic polarization parameters for the corrosion of alloy in sulphuric acid solution of different concentrations, in the presence of different concentrations of MPBIT at different temperatures are summarized in Tables 3.124 to 3.128.

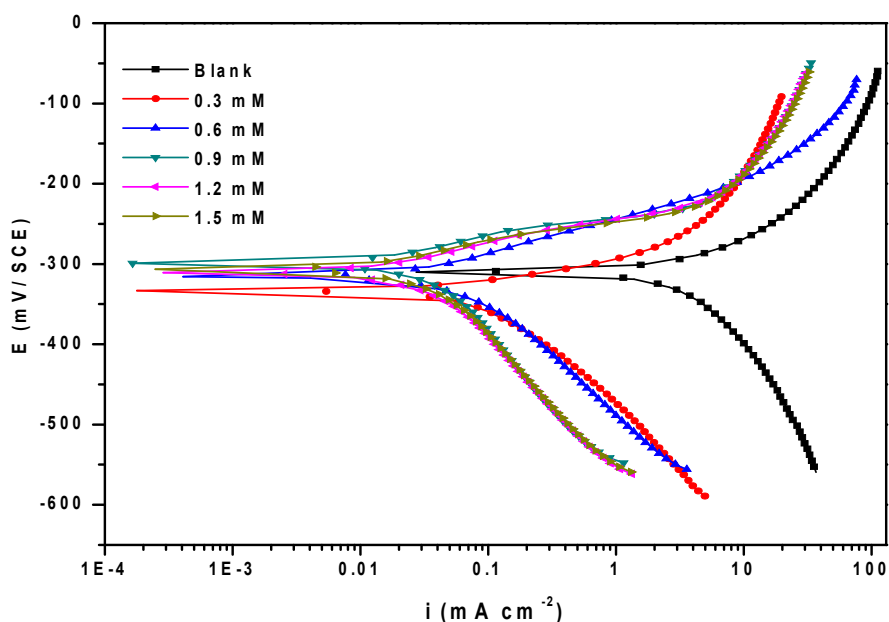


Fig. 3.92: Potentiodynamic polarization curves for the corrosion of welded maraging steel in 1.0 M H₂SO₄ containing different concentrations of MPBIT at 30 °C.

The presence of inhibitor brings down the corrosion rate considerably. Polarization curves are shifted to a lower current density region indicating a decrease in corrosion rate (Li et al. 2007). Inhibition efficiency increases with the increase in MPBIT concentration. The presence of inhibitor, does not cause significant shift in the E_{corr} value

and also there is no definite trend for the shift in E_{corr} value, which implies that the inhibitor, MPBIT, acts as a mixed type inhibitor, affecting both anodic and cathodic reactions.

3.12.2 Electrochemical impedance spectroscopy (EIS) studies

Nyquist plots for the corrosion of welded maraging steel in 1.0 M sulphuric acid solution in the presence of different concentrations of MPBIT are shown in Fig. 3.93. Similar plots were obtained in other concentrations of sulphuric acid and also at other temperatures. The experimental results of EIS measurements obtained for the corrosion of welded maraging steel in 1.0 M sulphuric acid are summarized in Tables 3.129 to 3.133. The charge transfer resistance (R_{ct}) increases and double layer capacitance (C_{dl}) decreases with the increase in the concentration of MPBIT, indicating an increase in the inhibition efficiency. The results obtained from impedance studies are in good agreement with potentiodynamic polarization studies.

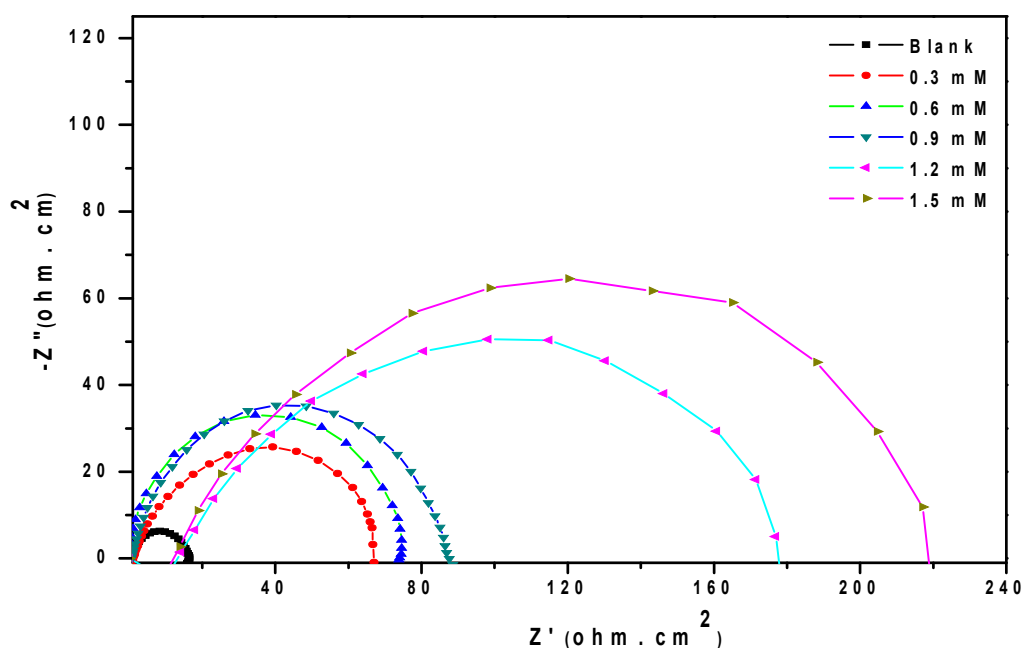


Fig. 3.93: Nyquist plots for the corrosion of welded maraging steel in 1.0 M H₂SO₄ containing different concentrations of MPBIT at 30 °C.

The Bode plots for phase angle and amplitude for the corrosion of the alloy in the presence of MPBIT in 1.0 M sulphuric acid are shown in Fig. 3.94 (a) and Fig. 3.94 (b), respectively. Phase angle increases with increase in concentrations of MPBIT in sulphuric acid medium. The difference between the HF and LF for the inhibited system in the Bode plot increases with increase in the concentration of MPBIT. The increase in phase angle and impedance ($|Z|$) with the increase in MPBIT concentration suggests decrease in corrosion rate.

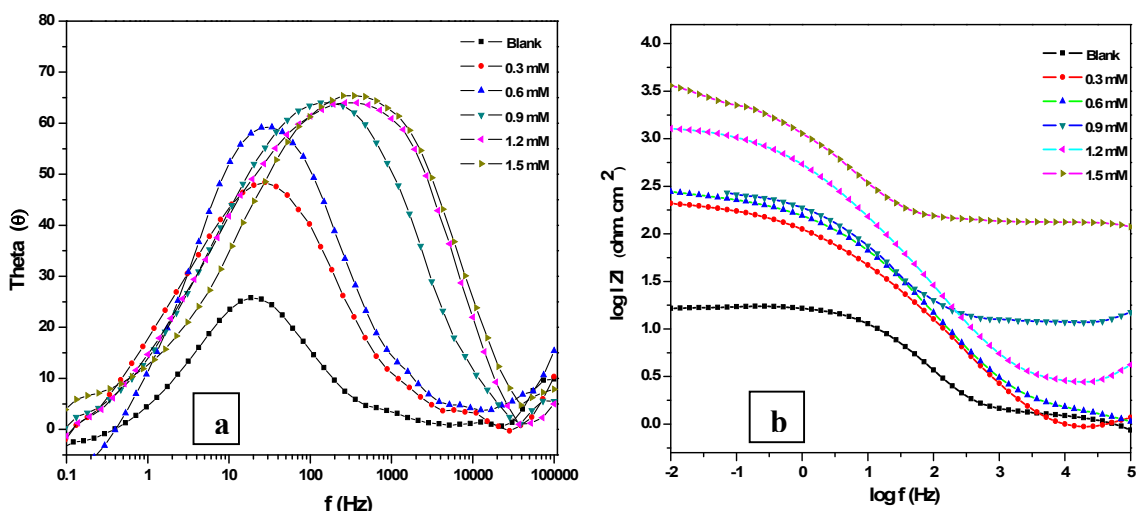


Fig. 3.94: Bode (a) phase angle plots and (b) amplitude plots for the corrosion of welded maraging steel in 1.0 M H₂SO₄ containing different concentrations of MPBIT at 30 °C.

3.12.3 Effect of temperature

The Potentiodynamic polarization and EIS results pertaining to different temperatures in different concentrations of sulphuric acid have been listed in the Tables 3.125 to 3.134. The decrease in inhibition efficiency with the increase in temperature indicates desorption of the inhibitor molecules from the metal surface on increasing the temperature (Poornima et al. 2011). This fact is also suggestive of physisorption of the inhibitor molecules on the metal surface.

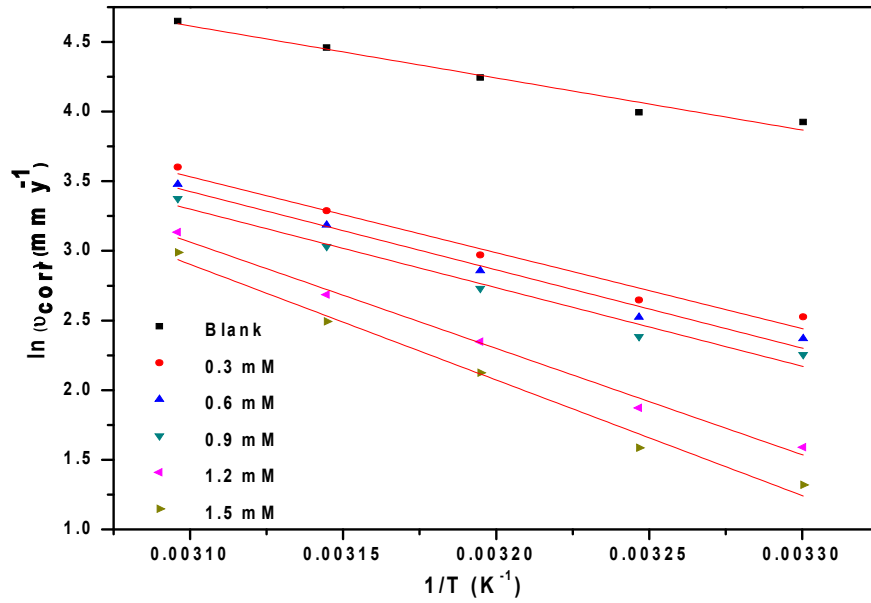


Fig. 3.95: Arrhenius plots for the corrosion of welded maraging steel in 1.0 M H_2SO_4 containing different concentrations of MPBIT.

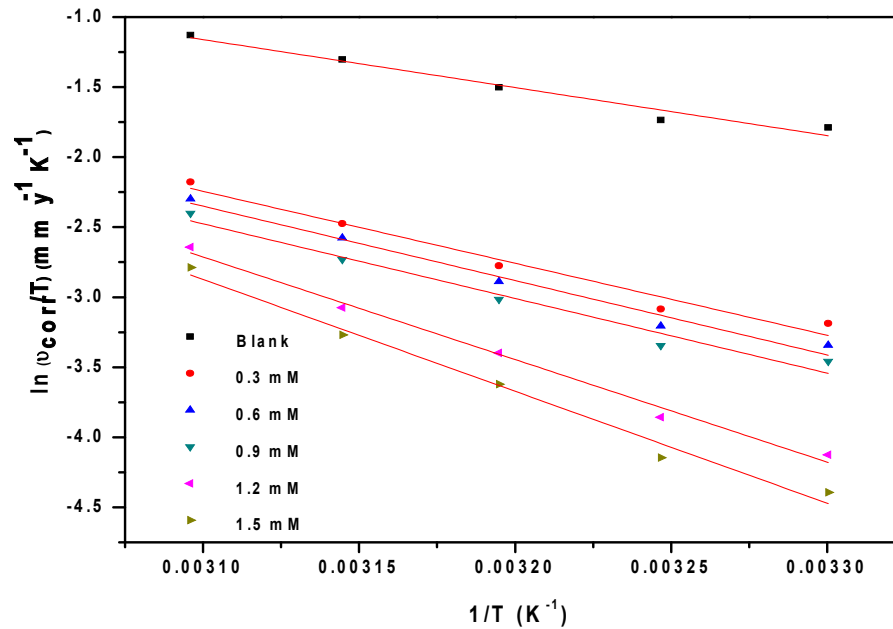


Fig. 3.96: Plots of $\ln(v_{corr}/T)$ versus $1/T$ for the corrosion of welded maraging steel in 1.0 M H_2SO_4 containing different concentrations of MPBIT.

The Arrhenius plots for the corrosion of welded maraging steel in the presence of different concentrations of MPBIT in 1.0 M H₂SO₄ acid are shown in Fig. 3.95. The plots of $\ln(v_{\text{corr}}/T)$ versus $1/T$ in 1.0 M H₂SO₄ acid in the absence and presence of various concentrations of MPBIT are shown in Fig. 3.96. The calculated values of E_a , ΔH^\ddagger and ΔS^\ddagger are given in Table 3.134. The proportionate increase in the activation energy on the addition of MPBIT can be attributed to the increased adsorption of MPBIT providing a barrier on the alloy surface (Avcı et al. 2008). The values of entropy of activation indicates that the activated complex in the rate determining step represents an association rather than dissociation, resulting in a decrease in randomness on going from the reactants to the activated complex.

3.12.4 Effect of acid concentration

Table 3.135 summarizes the maximum inhibition efficiencies exhibited by MPBIT in the H₂SO₄ solution of different concentrations. It is evident from both polarization and EIS experimental results that, for a particular concentration of inhibitor, the inhibition efficiency decreases with the increase in sulphuric acid concentration on the welded maraging steel. The highest inhibition efficiency is observed in sulphuric acid of 0.1 M concentration.

3.12.5 Adsorption isotherm

The adsorption of MPBIT on the surface of welded maraging steel was found to obey Langmuir adsorption isotherm. The Langmuir adsorption isotherms for the adsorption of MPBIT on welded maraging steel in 1.0 M H₂SO₄ are shown in Fig. 3.97. The thermodynamic data obtained for the adsorption of MPBIT on welded maraging steel are tabulated in Table 3.136. The linear regression coefficients are close to unity and the slopes of the straight lines are nearly unity, suggesting that the adsorption of MPBIT obeys Langmuir's adsorption isotherm with negligible interaction between the adsorbed molecules. The exothermic ΔH_{ads}^0 values of less negative than -41.86 kJ mol⁻¹ predict physisorption of MPBIT on the alloy surfaces (Ashish Kumar et al. 2010). The ΔG_{ads}^0 values predict both physisorption and chemisorption of MPBIT. Therefore it can be

concluded that the adsorption of MPBIT on the welded maraging steel is predominantly through physisorption. These facts are also supported by the decrease in inhibition efficiencies with the increase in temperature.

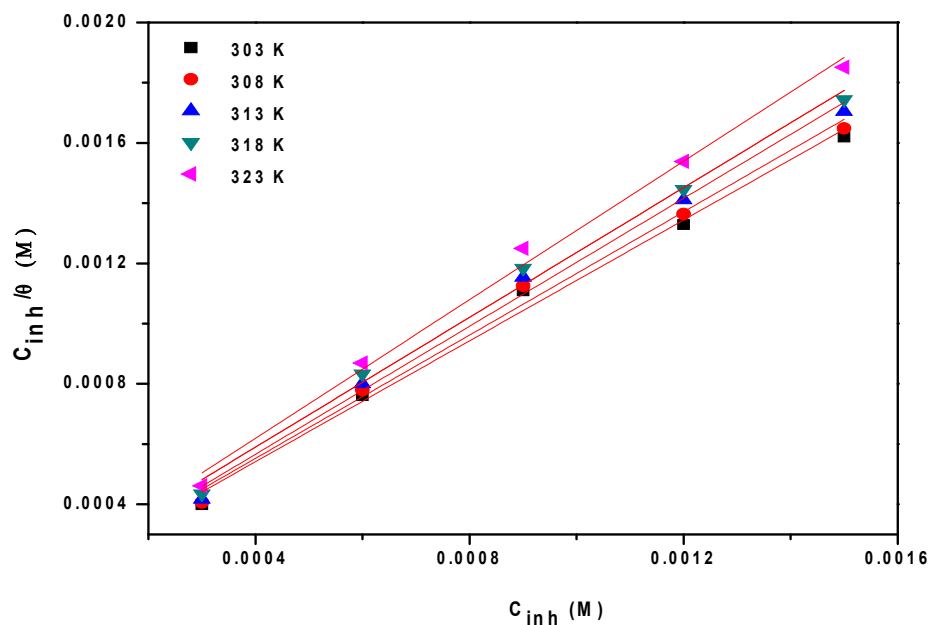


Fig. 3.97: Langmuir adsorption isotherms for the adsorption of MPBIT on welded maraging steel in 1.0 M H₂SO₄ at different temperatures.

3.12.6 Mechanism of corrosion inhibition

The corrosion inhibition mechanism of MPBIT in sulphuric acid solution can be explained similar to the one in hydrochloric acid as explained in section 3.11.6. The inhibitor MPBIT protects the alloy surface through predominant physisorption mode in which the positive charge centers of MPBIT gets adsorbed on the alloy surface through electrostatic attraction and also to some extent through chemisorption mode.

3.12.7 SEM/EDX studies

Fig. 3.98 represents the SEM image of welded maraging steel after the corrosion tests in a medium of sulphuric acid containing 1.5 mM of MPBIT. The image clearly shows a smooth surface due to the adsorbed layer of inhibitor molecules on the alloy

surface, thus protecting the metal from corrosion. The EDX spectra for the selected areas on the SEM image is shown in Fig. 3.99.

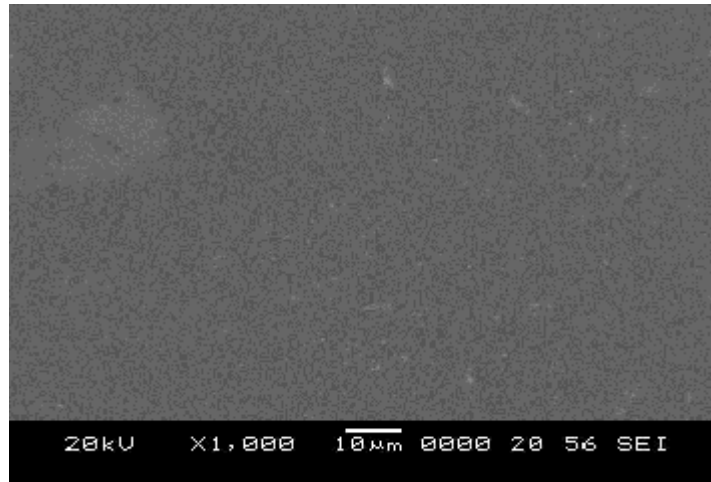


Fig.3.98: SEM image of the welded maraging steel after immersion in 1.0 M H₂SO₄ in the presence of MPBIT.

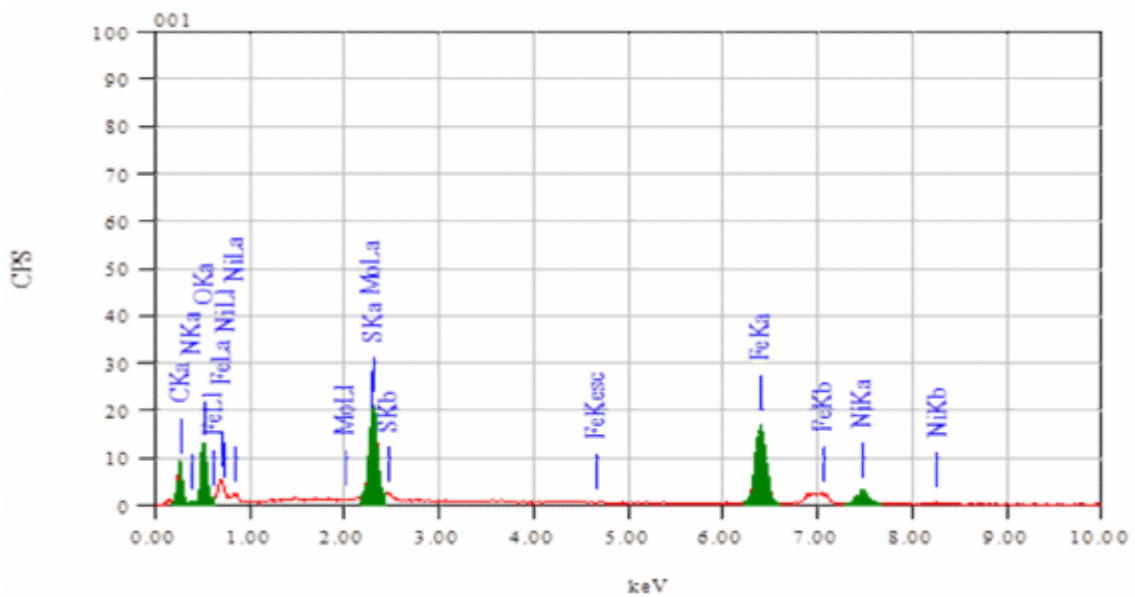


Fig. 3.99: EDX analysis of the welded maraging steel after immersion in 1.0 M H₂SO₄ in the presence of MPBIT.

The atomic percentage of the elements found in the EDX profile for inhibited metal surface was 8.15% Fe, 1.89% Ni, 0.47% Mo, 28.07% O, 17.28% N, 40.33% C and

3.81% S and indicated the formation of inhibitor film on the surface of the alloy. The elemental compositions mentioned above were mean values of different regions.

Table 3.124: Results of potentiodynamic polarization studies for the corrosion of welded maraging steel in 0.1 M sulphuric acid containing different concentrations of MPBIT.

| Temperature (°C) | Conc. of inhibitor (mM) | $-E_{corr}$ (mV /SCE) | b_a (mV dec ⁻¹) | $-b_c$ (mV dec ⁻¹) | i_{corr} (mA cm ⁻²) | ν_{corr} (mm y ⁻¹) | η (%) |
|------------------|-------------------------|-----------------------|-------------------------------|--------------------------------|-----------------------------------|------------------------------------|------------|
| 30 | Blank | 356 | 162 | 113 | 1.98 | 25.52 | |
| | 0.2 | 343 | 113 | 95 | 0.37 | 4.80 | 81.2 |
| | 0.4 | 339 | 108 | 92 | 0.30 | 3.91 | 84.7 |
| | 0.6 | 348 | 102 | 88 | 0.24 | 3.11 | 87.8 |
| | 0.8 | 351 | 99 | 85 | 0.17 | 2.19 | 91.4 |
| | 1.0 | 342 | 92 | 83 | 0.12 | 1.58 | 93.8 |
| | 35 | Blank | 353 | 171 | 124 | 2.41 | 31.07 |
| 0.2 | | 337 | 135 | 108 | 0.52 | 6.71 | 78.4 |
| 0.4 | | 341 | 132 | 104 | 0.45 | 5.75 | 81.5 |
| 0.6 | | 328 | 127 | 101 | 0.35 | 4.47 | 85.6 |
| 0.8 | | 324 | 124 | 97 | 0.23 | 3.01 | 90.3 |
| 1.0 | | 319 | 120 | 95 | 0.19 | 2.42 | 92.2 |
| 40 | | Blank | 347 | 183 | 131 | 2.93 | 37.77 |
| | 0.2 | 332 | 148 | 117 | 0.70 | 8.99 | 76.2 |
| | 0.4 | 321 | 142 | 113 | 0.57 | 7.36 | 80.5 |
| | 0.6 | 314 | 139 | 108 | 0.48 | 6.16 | 83.7 |
| | 0.8 | 334 | 134 | 104 | 0.34 | 4.38 | 88.4 |
| | 1.0 | 329 | 128 | 101 | 0.29 | 3.74 | 90.1 |
| | 45 | Blank | 345 | 197 | 142 | 3.47 | 44.73 |
| 0.2 | | 332 | 163 | 123 | 0.89 | 11.50 | 74.3 |
| 0.4 | | 351 | 158 | 120 | 0.75 | 9.62 | 78.5 |
| 0.6 | | 357 | 154 | 116 | 0.65 | 8.36 | 81.3 |
| 0.8 | | 361 | 150 | 113 | 0.50 | 6.44 | 85.6 |
| 1.0 | | 364 | 147 | 111 | 0.41 | 5.28 | 88.2 |
| 50 | | Blank | 342 | 214 | 154 | 6.14 | 79.15 |
| | 0.2 | 358 | 191 | 139 | 1.76 | 22.71 | 71.3 |
| | 0.4 | 339 | 184 | 132 | 1.68 | 21.61 | 72.7 |
| | 0.6 | 351 | 181 | 127 | 1.41 | 18.20 | 77.0 |
| | 0.8 | 347 | 176 | 124 | 1.09 | 14.09 | 82.2 |
| | 1.0 | 342 | 173 | 121 | 0.90 | 11.56 | 85.4 |

Table 3.125: Results of potentiodynamic polarization studies for the corrosion of welded maraging steel in 0.5 M sulphuric acid containing different concentrations of MPBIT.

| Temperature (°C) | Conc. of inhibitor (mM) | $-E_{corr}$ (mV /SCE) | b_a (mV dec ⁻¹) | $-b_c$ (mV dec ⁻¹) | i_{corr} (mA cm ⁻²) | ν_{corr} (mm y ⁻¹) | η (%) |
|------------------|-------------------------|-----------------------|-------------------------------|--------------------------------|-----------------------------------|------------------------------------|------------|
| 30 | Blank | 322 | 172 | 115 | 2.47 | 31.84 | |
| | 0.2 | 337 | 157 | 103 | 0.53 | 6.85 | 78.5 |
| | 0.4 | 328 | 151 | 97 | 0.46 | 5.92 | 81.4 |
| | 0.6 | 332 | 148 | 95 | 0.38 | 4.94 | 84.5 |
| | 0.8 | 341 | 144 | 91 | 0.23 | 2.96 | 90.7 |
| | 1.0 | 354 | 141 | 89 | 0.17 | 2.17 | 93.2 |
| | 35 | Blank | 321 | 191 | 132 | 2.68 | 34.55 |
| 0.2 | | 334 | 168 | 119 | 0.62 | 8.01 | 76.8 |
| 0.4 | | 327 | 165 | 112 | 0.55 | 7.15 | 79.3 |
| 0.6 | | 319 | 159 | 107 | 0.44 | 5.63 | 83.7 |
| 0.8 | | 312 | 154 | 103 | 0.31 | 3.97 | 88.5 |
| 1.0 | | 316 | 151 | 98 | 0.22 | 2.83 | 91.8 |
| 40 | | Blank | 318 | 207 | 144 | 4.71 | 60.71 |
| | 0.2 | 341 | 181 | 121 | 1.14 | 14.75 | 75.7 |
| | 0.4 | 337 | 176 | 117 | 1.06 | 13.66 | 77.5 |
| | 0.6 | 339 | 172 | 114 | 0.89 | 11.54 | 81.0 |
| | 0.8 | 343 | 169 | 112 | 0.62 | 8.01 | 86.8 |
| | 1.0 | 347 | 164 | 109 | 0.52 | 6.68 | 89.0 |
| | 45 | Blank | 314 | 224 | 158 | 5.38 | 69.35 |
| 0.2 | | 328 | 193 | 137 | 1.55 | 19.97 | 71.2 |
| 0.4 | | 334 | 189 | 132 | 1.32 | 17.06 | 75.4 |
| 0.6 | | 340 | 185 | 128 | 1.16 | 14.91 | 78.5 |
| 0.8 | | 349 | 182 | 126 | 0.88 | 11.30 | 83.7 |
| 1.0 | | 352 | 178 | 123 | 0.67 | 8.67 | 87.5 |
| 50 | | Blank | 312 | 232 | 163 | 6.94 | 89.45 |
| | 0.2 | 326 | 201 | 142 | 2.21 | 28.45 | 68.2 |
| | 0.4 | 338 | 195 | 139 | 2.05 | 26.39 | 70.5 |
| | 0.6 | 346 | 192 | 135 | 1.71 | 22.10 | 75.3 |
| | 0.8 | 319 | 187 | 131 | 1.46 | 18.79 | 79.0 |
| | 1.0 | 323 | 183 | 128 | 1.15 | 14.85 | 83.4 |

Table 3.126: Results of potentiodynamic polarization studies for the corrosion of welded maraging steel in 1.0 M sulphuric acid containing different concentrations of MPBIT.

| Temperature (°C) | Conc. of inhibitor (mM) | $-E_{corr}$ (mV /SCE) | b_a (mV dec ⁻¹) | $-b_c$ (mV dec ⁻¹) | i_{corr} (mA cm ⁻²) | ν_{corr} (mm y ⁻¹) | η (%) |
|------------------|-------------------------|-----------------------|-------------------------------|--------------------------------|-----------------------------------|------------------------------------|------------|
| 30 | Blank | 315 | 187 | 132 | 3.93 | 50.32 | |
| | 0.2 | 332 | 146 | 117 | 0.97 | 12.50 | 75.3 |
| | 0.4 | 317 | 141 | 113 | 0.83 | 10.70 | 78.9 |
| | 0.6 | 298 | 137 | 108 | 0.74 | 9.54 | 81.2 |
| | 0.8 | 313 | 131 | 104 | 0.38 | 4.90 | 90.3 |
| | 1.0 | 309 | 129 | 101 | 0.29 | 3.74 | 92.6 |
| 35 | Blank | 313 | 198 | 147 | 4.21 | 54.12 | |
| | 0.2 | 341 | 157 | 122 | 1.09 | 14.11 | 74.1 |
| | 0.4 | 328 | 151 | 118 | 0.97 | 12.48 | 76.9 |
| | 0.6 | 309 | 148 | 114 | 0.84 | 10.85 | 80.0 |
| | 0.8 | 312 | 141 | 109 | 0.51 | 6.51 | 87.9 |
| | 1.0 | 321 | 136 | 103 | 0.38 | 4.88 | 91.0 |
| 40 | Blank | 310 | 212 | 163 | 5.41 | 69.72 | |
| | 0.2 | 321 | 174 | 139 | 1.51 | 19.53 | 72.1 |
| | 0.4 | 319 | 169 | 135 | 1.35 | 17.43 | 75.0 |
| | 0.6 | 327 | 162 | 132 | 1.19 | 15.34 | 78.0 |
| | 0.8 | 334 | 154 | 128 | 0.81 | 10.46 | 85.1 |
| | 1.0 | 325 | 148 | 124 | 0.65 | 8.37 | 87.9 |
| 45 | Blank | 312 | 243 | 178 | 6.70 | 86.36 | |
| | 0.2 | 297 | 191 | 151 | 2.08 | 26.77 | 68.9 |
| | 0.4 | 318 | 186 | 146 | 1.88 | 24.18 | 71.8 |
| | 0.6 | 324 | 183 | 141 | 1.61 | 20.73 | 75.9 |
| | 0.8 | 331 | 177 | 139 | 1.14 | 14.68 | 82.8 |
| | 1.0 | 339 | 173 | 136 | 0.94 | 12.09 | 85.7 |
| 50 | Blank | 320 | 269 | 192 | 8.11 | 104.54 | |
| | 0.2 | 327 | 204 | 164 | 2.84 | 36.59 | 64.9 |
| | 0.4 | 332 | 197 | 159 | 2.51 | 32.41 | 69.1 |
| | 0.6 | 348 | 191 | 153 | 2.27 | 29.27 | 72.0 |
| | 0.8 | 353 | 186 | 148 | 1.78 | 23.00 | 78.1 |
| | 1.0 | 364 | 181 | 144 | 1.54 | 19.86 | 81.0 |

Table 3.127: Results of potentiodynamic polarization studies for the corrosion of welded maraging steel in 1.5 M sulphuric acid containing different concentrations of MPBIT.

| Temperature (°C) | Conc. of inhibitor (mM) | $-E_{corr}$ (mV /SCE) | b_a (mV dec ⁻¹) | $-b_c$ (mV dec ⁻¹) | i_{corr} (mA cm ⁻²) | v_{corr} (mm y ⁻¹) | η (%) |
|------------------|-------------------------|-----------------------|-------------------------------|--------------------------------|-----------------------------------|----------------------------------|------------|
| 30 | Blank | 313 | 240 | 146 | 4.28 | 55.17 | |
| | 0.2 | 325 | 197 | 129 | 1.17 | 15.06 | 72.7 |
| | 0.4 | 338 | 192 | 125 | 1.01 | 13.08 | 76.3 |
| | 0.6 | 342 | 188 | 121 | 0.88 | 11.31 | 79.5 |
| | 0.8 | 354 | 184 | 117 | 0.51 | 6.57 | 88.1 |
| | 1.0 | 362 | 179 | 115 | 0.38 | 4.85 | 91.2 |
| | 35 | Blank | 308 | 242 | 151 | 5.31 | 68.45 |
| 0.2 | | 319 | 208 | 136 | 1.51 | 19.51 | 71.5 |
| 0.4 | | 304 | 203 | 132 | 1.31 | 16.91 | 75.3 |
| 0.6 | | 335 | 197 | 129 | 1.18 | 15.20 | 77.8 |
| 0.8 | | 347 | 193 | 127 | 0.83 | 10.68 | 84.4 |
| 1.0 | | 351 | 188 | 122 | 0.57 | 7.32 | 89.3 |
| 40 | | Blank | 300 | 248 | 156 | 6.48 | 83.53 |
| | 0.2 | 327 | 212 | 141 | 1.92 | 24.72 | 70.4 |
| | 0.4 | 336 | 207 | 137 | 1.76 | 22.71 | 72.8 |
| | 0.6 | 342 | 203 | 132 | 1.56 | 20.05 | 76.0 |
| | 0.8 | 348 | 199 | 129 | 1.17 | 14.95 | 82.1 |
| | 1.0 | 355 | 195 | 124 | 0.89 | 11.44 | 86.3 |
| | 45 | Blank | 301 | 290 | 197 | 7.54 | 97.19 |
| 0.2 | | 328 | 231 | 156 | 2.53 | 32.56 | 66.5 |
| 0.4 | | 317 | 225 | 151 | 2.22 | 28.67 | 70.5 |
| 0.6 | | 331 | 221 | 146 | 1.98 | 25.56 | 73.7 |
| 0.8 | | 346 | 217 | 142 | 1.39 | 17.98 | 81.5 |
| 1.0 | | 353 | 214 | 137 | 1.25 | 16.13 | 83.4 |
| 50 | | Blank | 295 | 349 | 242 | 8.64 | 111.37 |
| | 0.2 | 307 | 251 | 171 | 3.27 | 42.10 | 62.2 |
| | 0.4 | 326 | 247 | 168 | 2.84 | 36.64 | 67.1 |
| | 0.6 | 347 | 241 | 164 | 2.62 | 33.75 | 69.7 |
| | 0.8 | 352 | 234 | 159 | 2.22 | 28.62 | 74.3 |
| | 1.0 | 355 | 228 | 153 | 2.06 | 26.59 | 77.2 |

Table 3.128: Results of potentiodynamic polarization studies for the corrosion of welded maraging steel in 2.0 M sulphuric acid containing different concentrations of MPBIT.

| Temperature (°C) | Conc. of inhibitor (mM) | $-E_{corr}$ (mV /SCE) | b_a (mV dec ⁻¹) | $-b_c$ (mV dec ⁻¹) | i_{corr} (mA cm ⁻²) | U_{corr} (mm y ⁻¹) | η (%) |
|------------------|-------------------------|-----------------------|-------------------------------|--------------------------------|-----------------------------------|----------------------------------|------------|
| 30 | Blank | 315 | 312 | 154 | 4.97 | 64.06 | |
| | 0.2 | 351 | 237 | 138 | 1.47 | 18.96 | 70.4 |
| | 0.4 | 356 | 228 | 133 | 1.33 | 17.17 | 73.2 |
| | 0.6 | 348 | 225 | 129 | 1.15 | 14.86 | 76.8 |
| | 0.8 | 334 | 217 | 124 | 0.68 | 8.71 | 86.4 |
| | 1.0 | 339 | 214 | 119 | 0.51 | 6.60 | 89.7 |
| | 35 | Blank | 313 | 283 | 208 | 6.12 | 78.89 |
| 0.2 | | 348 | 242 | 152 | 1.93 | 24.93 | 68.4 |
| 0.4 | | 337 | 238 | 148 | 1.63 | 21.06 | 73.3 |
| 0.6 | | 318 | 233 | 141 | 1.58 | 20.35 | 74.2 |
| 0.8 | | 329 | 229 | 137 | 1.03 | 13.33 | 83.1 |
| 1.0 | | 335 | 226 | 133 | 0.81 | 10.41 | 86.8 |
| 40 | | Blank | 310 | 261 | 225 | 7.32 | 94.36 |
| | 0.2 | 327 | 249 | 171 | 2.34 | 30.19 | 68.0 |
| | 0.4 | 332 | 244 | 166 | 2.19 | 28.21 | 70.1 |
| | 0.6 | 329 | 241 | 162 | 2.00 | 25.76 | 72.7 |
| | 0.8 | 345 | 236 | 157 | 1.51 | 19.34 | 79.5 |
| | 1.0 | 351 | 232 | 153 | 1.15 | 14.81 | 84.3 |
| | 45 | Blank | 312 | 282 | 231 | 8.23 | 106.09 |
| 0.2 | | 318 | 253 | 182 | 2.94 | 37.87 | 64.3 |
| 0.4 | | 316 | 247 | 175 | 2.70 | 34.80 | 67.2 |
| 0.6 | | 325 | 243 | 169 | 2.46 | 31.72 | 70.1 |
| 0.8 | | 337 | 239 | 164 | 1.86 | 23.98 | 77.4 |
| 1.0 | | 342 | 236 | 160 | 1.42 | 18.25 | 82.8 |
| 50 | | Blank | 320 | 329 | 204 | 9.02 | 116.27 |
| | 0.2 | 327 | 274 | 185 | 3.64 | 46.86 | 59.7 |
| | 0.4 | 319 | 268 | 182 | 3.25 | 41.84 | 64.0 |
| | 0.6 | 334 | 265 | 178 | 3.14 | 40.46 | 65.2 |
| | 0.8 | 341 | 259 | 171 | 2.58 | 33.25 | 73.0 |
| | 1.0 | 349 | 257 | 169 | 2.44 | 31.29 | 71.4 |

Table 3.129: EIS data for the corrosion of welded maraging steel in 0.1 M sulphuric acid containing different concentrations of MPBIT.

| Temperature (°C) | Conc. of inhibitor (mM) | R_p (ohm. cm ²) | C_{dl} (mF cm ⁻²) | η (%) |
|------------------|-------------------------|-------------------------------|---------------------------------|------------|
| 30 | Blank | 20.1 | 0.324 | |
| | 0.2 | 103.1 | 0.241 | 80.5 |
| | 0.4 | 125.6 | 0.222 | 84.0 |
| | 0.6 | 155.8 | 0.217 | 87.2 |
| | 0.8 | 216.1 | 0.181 | 90.6 |
| | 1.0 | 291.3 | 0.168 | 93.1 |
| 35 | Blank | 17.4 | 0.469 | |
| | 0.2 | 78.7 | 0.354 | 77.8 |
| | 0.4 | 91.6 | 0.334 | 81.0 |
| | 0.6 | 116.8 | 0.317 | 85.1 |
| | 0.8 | 170.6 | 0.289 | 89.8 |
| | 1.0 | 209.6 | 0.251 | 91.7 |
| 40 | Blank | 14.1 | 0.531 | |
| | 0.2 | 58.3 | 0.472 | 75.8 |
| | 0.4 | 70.9 | 0.437 | 80.1 |
| | 0.6 | 84.4 | 0.420 | 83.3 |
| | 0.8 | 117.5 | 0.397 | 88.0 |
| | 1.0 | 136.9 | 0.371 | 89.7 |
| 45 | Blank | 12.3 | 0.668 | |
| | 0.2 | 47.1 | 0.532 | 73.9 |
| | 0.4 | 56.2 | 0.514 | 78.1 |
| | 0.6 | 64.4 | 0.495 | 80.9 |
| | 0.8 | 83.1 | 0.468 | 85.2 |
| | 1.0 | 100.8 | 0.449 | 87.8 |
| 50 | Blank | 10.2 | 0.830 | |
| | 0.2 | 35.1 | 0.717 | 70.9 |
| | 0.4 | 36.8 | 0.684 | 72.3 |
| | 0.6 | 43.6 | 0.663 | 76.6 |
| | 0.8 | 56.0 | 0.631 | 81.8 |
| | 1.0 | 68.0 | 0.604 | 85.0 |

Table 3.130: EIS data for the corrosion of welded maraging steel in 0.5 M sulphuric acid containing different concentrations of MPBIT.

| Temperature (°C) | Conc. of inhibitor (mM) | R_p (ohm. cm ²) | C_{dl} (mF cm ⁻²) | η (%) |
|------------------|-------------------------|-------------------------------|---------------------------------|------------|
| 30 | Blank | 18.7 | 0.633 | |
| | 0.2 | 85.8 | 0.481 | 78.2 |
| | 0.4 | 98.9 | 0.464 | 81.1 |
| | 0.6 | 118.4 | 0.429 | 84.2 |
| | 0.8 | 194.8 | 0.415 | 90.4 |
| | 1.0 | 263.4 | 0.402 | 92.9 |
| 35 | Blank | 15.4 | 0.682 | |
| | 0.2 | 65.0 | 0.531 | 76.3 |
| | 0.4 | 72.6 | 0.517 | 78.8 |
| | 0.6 | 91.7 | 0.499 | 83.2 |
| | 0.8 | 128.3 | 0.474 | 88.0 |
| | 1.0 | 177.0 | 0.437 | 91.3 |
| 40 | Blank | 11.4 | 0.727 | |
| | 0.2 | 45.8 | 0.591 | 75.1 |
| | 0.4 | 49.4 | 0.563 | 76.9 |
| | 0.6 | 58.2 | 0.524 | 80.4 |
| | 0.8 | 82.6 | 0.488 | 86.2 |
| | 1.0 | 98.3 | 0.454 | 88.4 |
| 45 | Blank | 10.5 | 0.831 | |
| | 0.2 | 36.2 | 0.732 | 71.0 |
| | 0.4 | 42.3 | 0.708 | 75.2 |
| | 0.6 | 48.4 | 0.689 | 78.3 |
| | 0.8 | 63.6 | 0.654 | 83.5 |
| | 1.0 | 82.7 | 0.627 | 87.3 |
| 50 | Blank | 7.9 | 0.965 | |
| | 0.2 | 22.1 | 0.802 | 64.2 |
| | 0.4 | 25.0 | 0.754 | 68.4 |
| | 0.6 | 28.0 | 0.739 | 71.8 |
| | 0.8 | 35.1 | 0.712 | 77.4 |
| | 1.0 | 40.5 | 0.693 | 80.5 |

Table 3.131: EIS data for the corrosion of welded maraging steel in 1.0 M sulphuric acid containing different concentrations of MPBIT.

| Temperature (°C) | Conc. of inhibitor (mM) | R_p (ohm. cm ²) | C_{dl} (mF cm ⁻²) | η (%) |
|------------------|-------------------------|-------------------------------|---------------------------------|------------|
| 30 | Blank | 16.1 | 0.641 | |
| | 0.2 | 64.7 | 0.552 | 75.1 |
| | 0.4 | 75.6 | 0.527 | 78.7 |
| | 0.6 | 84.7 | 0.495 | 81.0 |
| | 0.8 | 162.6 | 0.474 | 90.1 |
| | 1.0 | 211.8 | 0.439 | 92.4 |
| 35 | Blank | 13.5 | 0.714 | |
| | 0.2 | 51.9 | 0.552 | 74.0 |
| | 0.4 | 58.2 | 0.547 | 76.8 |
| | 0.6 | 68.9 | 0.520 | 80.4 |
| | 0.8 | 110.7 | 0.479 | 87.8 |
| | 1.0 | 148.4 | 0.454 | 90.9 |
| 40 | Blank | 10.4 | 0.670 | |
| | 0.2 | 36.4 | 0.604 | 71.4 |
| | 0.4 | 40.8 | 0.578 | 74.5 |
| | 0.6 | 45.8 | 0.551 | 77.3 |
| | 0.8 | 66.7 | 0.536 | 84.4 |
| | 1.0 | 81.3 | 0.514 | 87.2 |
| 45 | Blank | 8.6 | 0.873 | |
| | 0.2 | 26.9 | 0.711 | 68.0 |
| | 0.4 | 29.6 | 0.687 | 70.9 |
| | 0.6 | 34.4 | 0.669 | 75.0 |
| | 0.8 | 47.5 | 0.621 | 81.9 |
| | 1.0 | 56.6 | 0.607 | 84.8 |
| 50 | Blank | 7.3 | 1.123 | |
| | 0.2 | 20.8 | 1.004 | 64.9 |
| | 0.4 | 23.6 | 0.979 | 69.1 |
| | 0.6 | 26.5 | 0.937 | 72.5 |
| | 0.8 | 33.3 | 0.906 | 78.1 |
| | 1.0 | 38.8 | 0.881 | 81.2 |

Table 3.132: EIS data for the corrosion of welded maraging steel in 1.5 M sulphuric acid containing different concentrations of MPBIT.

| Temperature (°C) | Conc. of inhibitor (mM) | R_p (ohm. cm ²) | C_{dl} (mF cm ⁻²) | η (%) |
|------------------|-------------------------|-------------------------------|---------------------------------|------------|
| 30 | Blank | 15.9 | 0.958 | |
| | 0.2 | 56.6 | 0.864 | 71.9 |
| | 0.4 | 64.9 | 0.826 | 75.5 |
| | 0.6 | 74.6 | 0.791 | 78.7 |
| | 0.8 | 125.2 | 0.759 | 87.3 |
| | 1.0 | 165.6 | 0.727 | 90.4 |
| 35 | Blank | 11.6 | 0.982 | |
| | 0.2 | 40.0 | 0.907 | 71.0 |
| | 0.4 | 46.0 | 0.869 | 74.8 |
| | 0.6 | 51.1 | 0.834 | 77.3 |
| | 0.8 | 72.0 | 0.817 | 83.9 |
| | 1.0 | 103.6 | 0.781 | 88.8 |
| 40 | Blank | 9.4 | 1.070 | |
| | 0.2 | 31.1 | 0.924 | 69.8 |
| | 0.4 | 33.8 | 0.906 | 72.2 |
| | 0.6 | 38.2 | 0.867 | 75.4 |
| | 0.8 | 50.8 | 0.831 | 81.5 |
| | 1.0 | 65.7 | 0.794 | 85.7 |
| 45 | Blank | 8.1 | 1.281 | |
| | 0.2 | 23.5 | 1.156 | 65.5 |
| | 0.4 | 26.6 | 1.114 | 69.5 |
| | 0.6 | 29.7 | 1.078 | 72.7 |
| | 0.8 | 41.5 | 1.029 | 80.5 |
| | 1.0 | 46.0 | 0.961 | 82.4 |
| 50 | Blank | 6.9 | 1.318 | |
| | 0.2 | 17.7 | 1.192 | 61.0 |
| | 0.4 | 20.2 | 1.167 | 65.9 |
| | 0.6 | 21.9 | 1.139 | 68.5 |
| | 0.8 | 27.5 | 1.114 | 74.9 |
| | 1.0 | 25.7 | 1.043 | 73.1 |

Table 3.133: EIS data for the corrosion of welded maraging steel in 2.0 M sulphuric acid containing different concentrations of MPBIT.

| Temperature (°C) | Conc. of inhibitor (mM) | R_p (ohm. cm ²) | C_{dl} (mF cm ⁻²) | η (%) |
|------------------|-------------------------|-------------------------------|---------------------------------|------------|
| 30 | Blank | 13.9 | 1.093 | |
| | 0.2 | 45.7 | 0.932 | 69.6 |
| | 0.4 | 50.4 | 0.917 | 72.4 |
| | 0.6 | 57.9 | 0.649 | 76.0 |
| | 0.8 | 96.5 | 0.614 | 85.6 |
| | 1.0 | 125.2 | 0.581 | 88.9 |
| 35 | Blank | 10.8 | 1.241 | |
| | 0.2 | 32.7 | 1.072 | 67.0 |
| | 0.4 | 38.4 | 1.027 | 71.9 |
| | 0.6 | 39.7 | 0.986 | 72.8 |
| | 0.8 | 59.0 | 0.951 | 81.7 |
| | 1.0 | 74.0 | 0.932 | 85.4 |
| 40 | Blank | 9.2 | 1.324 | |
| | 0.2 | 27.8 | 1.141 | 66.9 |
| | 0.4 | 29.7 | 1.109 | 69.0 |
| | 0.6 | 32.4 | 1.074 | 71.6 |
| | 0.8 | 42.6 | 1.026 | 78.4 |
| | 1.0 | 54.8 | 0.961 | 83.2 |
| 45 | Blank | 7.4 | 1.369 | |
| | 0.2 | 20.1 | 1.224 | 63.1 |
| | 0.4 | 21.8 | 1.148 | 66.0 |
| | 0.6 | 23.8 | 1.132 | 68.9 |
| | 0.8 | 31.1 | 1.047 | 76.2 |
| | 1.0 | 40.2 | 1.021 | 81.6 |
| 50 | Blank | 6.5 | 1.508 | |
| | 0.2 | 15.6 | 1.242 | 58.4 |
| | 0.4 | 17.4 | 1.227 | 62.7 |
| | 0.6 | 18.0 | 1.189 | 63.9 |
| | 0.8 | 23.0 | 1.144 | 70.1 |
| | 1.0 | 21.7 | 1.117 | 71.7 |

Table 3.134: Activation parameters for the corrosion of welded maraging steel in sulphuric acid containing different concentrations of MPBIT.

| Molarity of H ₂ SO ₄ (M) | Conc. of inhibitor (mM) | E_a (kJ mol ⁻¹) | ΔH^\ddagger (kJ mol ⁻¹) | ΔS^\ddagger (J mol ⁻¹ K ⁻¹) |
|--|-------------------------|-------------------------------|---|--|
| 0.1 | Blank | 42.58 | 39.98 | -86.83 |
| | 0.3 | 59.17 | 56.58 | -45.84 |
| | 0.6 | 63.78 | 61.18 | -32.37 |
| | 0.9 | 60.53 | 64.87 | -22.23 |
| | 1.2 | 51.31 | 70.11 | -8.18 |
| | 1.5 | 77.29 | 74.69 | -4.62 |
| 0.5 | Blank | 44.97 | 42.37 | -77.02 |
| | 0.3 | 61.17 | 58.57 | -36.45 |
| | 0.6 | 63.37 | 60.76 | -30.29 |
| | 0.9 | 72.93 | 61.98 | -27.97 |
| | 1.2 | 70.13 | 74.54 | -19.36 |
| | 1.5 | 80.81 | 78.21 | -8.92 |
| 1.0 | Blank | 32.07 | 29.46 | -115.68 |
| | 0.3 | 45.31 | 42.71 | -83.84 |
| | 0.6 | 46.75 | 44.15 | -80.26 |
| | 0.9 | 46.91 | 44.30 | -80.85 |
| | 1.2 | 63.48 | 60.78 | -31.38 |
| | 1.5 | 69.02 | 66.42 | -15.58 |
| 1.5 | Blank | 30.55 | 29.12 | -120.54 |
| | 0.3 | 41.78 | 39.18 | -93.32 |
| | 0.6 | 42.13 | 39.53 | -93.23 |
| | 0.9 | 44.05 | 41.45 | -88.08 |
| | 1.2 | 57.60 | 53.81 | -51.41 |
| | 1.5 | 68.21 | 65.61 | -23.58 |
| 2.0 | Blank | 28.24 | 26.21 | -122.45 |
| | 0.3 | 36.27 | 33.67 | -109.36 |
| | 0.6 | 37.19 | 34.59 | -107.37 |
| | 0.9 | 39.86 | 37.26 | -99.47 |
| | 1.2 | 51.34 | 50.64 | -59.56 |
| | 1.5 | 59.77 | 57.17 | -38.53 |

Table 3.135: Maximum inhibition efficiency attained in different concentrations of sulphuric acid at different temperatures for MPBIT.

| Temperature (°C) | Welded Maraging Steel | | | |
|---------------------|-------------------------------------|-----------------------------------|---|------------|
| | Sulphuric acid concentration (M) | Concentration of MPBIT (mM) | η (%) | |
| | | | Potentiodynamic polarization method | EIS method |
| 30 | 0.1 | 1.5 | 93.8 | 93.1 |
| | 0.5 | | 93.2 | 92.9 |
| | 1.0 | | 92.6 | 92.4 |
| | 1.5 | | 91.2 | 90.4 |
| | 2.0 | | 89.7 | 88.9 |
| 35 | 0.1 | 1.5 | 92.2 | 91.7 |
| | 0.5 | | 91.8 | 91.3 |
| | 1.0 | | 91.0 | 90.9 |
| | 1.5 | | 89.3 | 88.8 |
| | 2.0 | | 86.8 | 85.4 |
| 40 | 0.1 | 1.5 | 90.1 | 89.7 |
| | 0.5 | | 89.0 | 88.4 |
| | 1.0 | | 87.9 | 87.2 |
| | 1.5 | | 86.3 | 85.7 |
| | 2.0 | | 84.3 | 83.2 |
| 45 | 0.1 | 1.5 | 88.2 | 87.8 |
| | 0.5 | | 87.5 | 87.3 |
| | 1.0 | | 85.7 | 84.8 |
| | 1.5 | | 83.4 | 82.4 |
| | 2.0 | | 82.8 | 81.6 |
| 50 | 0.1 | 1.5 | 85.4 | 85.0 |
| | 0.5 | | 83.4 | 80.5 |
| | 1.0 | | 81.0 | 81.2 |
| | 1.5 | | 76.1 | 73.1 |
| | 2.0 | | 73.0 | 71.7 |

Table 3.136: Thermodynamic parameters for the adsorption of MPBIT on welded maraging steel surface in sulphuric acid at different temperatures.

| Molarity of H ₂ SO ₄ (M) | Temperature (° C) | $-\Delta G^{\circ}_{ads}$ (kJ mol ⁻¹) | ΔH°_{ads} (kJ mol ⁻¹) | ΔS°_{ads} (J mol ⁻¹ K ⁻¹) |
|--|-------------------|---|--|---|
| 0.1 | 30 | 33.79 | -17.40 | -57.21 |
| | 35 | 33.55 | | |
| | 40 | 33.39 | | |
| | 45 | 33.21 | | |
| | 50 | 33.02 | | |
| 0.5 | 30 | 33.05 | -21.07 | -42.80 |
| | 35 | 32.47 | | |
| | 40 | 32.28 | | |
| | 45 | 32.17 | | |
| | 50 | 31.82 | | |
| 1.0 | 30 | 32.47 | -23.41 | -37.32 |
| | 35 | 32.25 | | |
| | 40 | 31.92 | | |
| | 45 | 31.74 | | |
| | 50 | 31.84 | | |
| 1.5 | 30 | 32.21 | -25.53 | -34.08 |
| | 35 | 32.18 | | |
| | 40 | 31.89 | | |
| | 45 | 31.66 | | |
| | 50 | 31.40 | | |
| 2.0 | 30 | 31.88 | -24.63 | -33.52 |
| | 35 | 31.56 | | |
| | 40 | 31.42 | | |
| | 45 | 31.18 | | |
| | 50 | 31.03 | | |

3.13 COMPARISON OF INHIBITION EFFICIENCIES OF THE FIVE INHIBITORS

A comparison of inhibition efficiencies of BTPO, PNPT, TBTBH, CBP and MPBIT for the corrosion of welded maraging steel in 0.1 M hydrochloric acid and sulphuric acid at different temperatures are summarized in Tables 3.137 and 3.138, respectively. The inhibition efficiencies of the five inhibitors vary in the following order in hydrochloric acid medium is TBTBH > BTPO > PNPT > MPBIT > CBP, whereas the order in sulphuric acid medium is BTPO > TBTBH > PNPT > MPBIT > CBP.

The inhibitor molecules BTPO and TBTBH are structurally very similar except that in BTPO one of the oxygen atom is in the oxadiazole ring whereas in TBTBH it is ketonic. Further these two molecules have six terminal methoxy groups, whose electron donating nature increases the electron density in the aromatic rings. Therefore, they can be better adsorbed on the alloy surface, compared to the other three inhibitors.

The decrease in inhibition efficiency is also observed to be in accordance with the decreasing bulkiness of the inhibitor molecules. When the molecule is bigger, it can spread on the alloy surface when adsorbed through the anchoring sites of the molecules thereby providing an umbrella effect on the alloy surface.

Table 3.137: Comparison of inhibition efficiencies of BTPO, PNPT, TBTBH, CBP and MPBIT for the corrosion of welded maraging steel in 0.1 M hydrochloric acid medium at different temperatures, obtained by Tafel polarisation and EIS techniques.

| Temperature | Inhibitor | Concentration of inhibitor | η (%) | |
|-------------|-----------|----------------------------|--------------|------------|
| | | | Tafel method | EIS method |
| 30 °C | TBTBH | 1.0 mM | 96.8 | 94.3 |
| | BTPO | | 93.6 | 94.1 |
| | PNPT | | 90.3 | 89.1 |
| | MPBIT | | 87.1 | 87.8 |
| | CBP | | 84.9 | 84.2 |
| 35 °C | TBTBH | 1.0 mM | 94.3 | 92.0 |
| | BTPO | | 91.7 | 91.4 |
| | PNPT | | 88.8 | 88.4 |
| | MPBIT | | 86.1 | 86.9 |
| | CBP | | 83.8 | 83.1 |
| 40 °C | TBTBH | 1.0 mM | 91.5 | 90.8 |
| | BTPO | | 91.3 | 89.7 |
| | PNPT | | 84.5 | 83.4 |
| | MPBIT | | 82.2 | 81.8 |
| | CBP | | 80.8 | 80.3 |
| 45 °C | TBTBH | 1.0 mM | 89.7 | 88.7 |
| | BTPO | | 89.6 | 89.1 |
| | PNPT | | 82.7 | 81.7 |
| | MPBIT | | 80.3 | 81.2 |
| | CBP | | 78.1 | 77.4 |
| 50 °C | TBTBH | 1.0 mM | 85.2 | 84.7 |
| | BTPO | | 86.7 | 86.9 |
| | PNPT | | 79.5 | 78.7 |
| | MPBIT | | 74.1 | 75.2 |
| | CBP | | 73.2 | 72.6 |

Table 3.138: Comparison of inhibition efficiencies of BTPO, PNPT, TBTBH, CBP and MPBIT for the corrosion of welded maraging steel in 0.1 M sulphuric acid medium at different temperatures, obtained by Tafel polarisation and EIS techniques.

| Temperature | Inhibitor | Concentration of inhibitor | η (%) | |
|-------------|-----------|----------------------------|--------------|------------|
| | | | Tafel method | EIS method |
| 30 °C | BTPO | 1.0 mM | 94.8 | 93.2 |
| | TBTBH | | 94.1 | 92.8 |
| | PNPT | | 93.5 | 92.4 |
| | MPBIT | | 87.8 | 87.2 |
| | CBP | | 84.3 | 83.7 |
| 35 °C | BTPO | 1.0 mM | 92.9 | 91.0 |
| | TBTBH | | 92.8 | 91.3 |
| | PNPT | | 90.0 | 91.4 |
| | MPBIT | | 85.6 | 85.1 |
| | CBP | | 83.6 | 82.6 |
| 40 °C | BTPO | 1.0 mM | 89.3 | 88.7 |
| | TBTBH | | 88.4 | 87.2 |
| | PNPT | | 87.0 | 88.1 |
| | MPBIT | | 83.7 | 83.3 |
| | CBP | | 81.4 | 79.8 |
| 45 °C | BTPO | 1.0 mM | 85.2 | 85.4 |
| | TBTBH | | 85.0 | 85.1 |
| | PNPT | | 84.4 | 84.7 |
| | MPBIT | | 81.3 | 80.9 |
| | CBP | | 78.3 | 77.1 |
| 50 °C | BTPO | 1.0 mM | 82.5 | 81.5 |
| | TBTBH | | 80.6 | 82.1 |
| | PNPT | | 80.5 | 79.3 |
| | MPBIT | | 77.0 | 76.6 |
| | CBP | | 71.3 | 70.9 |

CHAPTER 4

SUMMARY AND CONCLUSIONS

4.1 SUMMARY

The corrosion behaviour of 18% Ni M 250 grade maraging steel under welded condition in hydrochloric acid and sulphuric acid was studied by potentiodynamic polarisation and EIS techniques. The effects of acid concentration and temperature on the corrosion rate were investigated. The inhibition effect of five inhibitors, namely, PNPT, BTPO, MPBIT, TBTBH and CBP on the corrosion of maraging steel was studied in the two acid media of hydrochloric acid and sulphuric acid of different concentrations and at different temperatures. The effects of acid concentrations, temperature and inhibitor concentrations on the inhibition efficiency were investigated in detail. The activation parameters for the corrosion of the alloy in the absence and presence of the inhibitors were calculated and analysed. The thermodynamic parameters like free energy of adsorption (ΔG_{ads}^0), enthalpy of adsorption (ΔH_{ads}^0) and entropy of adsorption (ΔS_{ads}^0) have been calculated and analysed to determine the type and adsorption of inhibitor molecules on the alloy surface. The probable mechanism for the adsorption of the inhibitor molecules were proposed. SEM and EDX analysis were carried out to study the surface morphology of the fresh surface of the alloy as well as the corroded alloy surface in the absence and presence of inhibitors.

4.2 CONCLUSIONS

Based on the results of the present investigation, the following conclusions are drawn:

1. The corrosion rates of welded maraging steel in both hydrochloric acid sulphuric acid medium is substantial.
2. The potentiodynamic polarization and impedance studies showed that the corrosion rate of the alloy increases with the increase in the concentration of the acids and the solution temperature.
3. The inhibitors, BTPO, PNPT, CBP, MPBIT and TBTBH act as mixed type of inhibitors.
4. The inhibitors, BTPO, PNPT, CBP, MPBIT and TBTBH affect both the anodic dissolution of welded maraging steel and cathodic hydrogen evolution reactions.

5. The inhibition efficiencies of all the five inhibitors decrease with the increase in temperature and concentrations of the acid in both the acid media.
6. The adsorption of all the five inhibitors on the surface of welded maraging steel obey Langmuir adsorption isotherm with negligible interaction between the adsorbed molecules in all the media.
7. The adsorption of all the five inhibitors is through both physisorption and chemisorption, with predominant physical adsorption on the welded maraging steel in both the media.
8. The inhibition efficiencies of the five inhibitors vary in the following order in hydrochloric acid medium is $TBTBH > BTPO > PNPT > MPBIT > CBP$, whereas the order in sulphuric acid medium is $BTPO > TBTBH > PNPT > MPBIT > CBP$.

4.3 SCOPE FOR FUTURE WORK

The following extensions are recommended to the work presented in this thesis,

- Above study can be extended to other structurally related inhibitors to understand the effect of structure of inhibitor on corrosion inhibition.
- Study of corrosion behaviour and inhibition of welded maraging steel in presence of green inhibitors.
- Comparative study of corrosion behaviour of 18 % Ni M250 grade maraging steel with other grades of maraging steel.

REFERENCES

Abd El Rehim, S. S., Hassan, H. H. and Amin, M. A. (2003). “The corrosion inhibition study of sodium dodecyl benzene sulphonate to aluminium and its alloys in 1.0 M HCl solution.” *Mater. Chem. Phys.*, 78, 337–348.

Abd Ei-Rehim, S. S., Ibrahim, M. A. M. and Khaled, K. F. (1999). “4-Aminoantipyrine as an inhibitor of mild steel corrosion in HCl solution.” *J. Appl. Electrochem.*, 29, 593-599.

Adams, C. M., Jr. and Travis, R. E. (1994). “Welding of 18% Ni-Co-Mo Maraging Alloys.” *Research Suppl., Weld. Jnl.*, 43, 193-197.

Amin, A. M., Khaled, K. F., Mohsen, Q. and Arida, H. A. (2010). “A study of the inhibition of iron corrosion in HCl solutions by some amino acids.” *Corros. Sci.*, 52, 1684 -1695.

Amin, M. A., Abd El-Rehim, S. S., El-Sherbini, E. E. F. and Bayyomi, R. S. (2007). “The inhibition of low carbon steel corrosion in hydrochloric acid solutions by succinic acid: Part I. Weight Loss, Polarization, EIS, PZC, EDX and SEM Studies.” *Electrochim. Acta*, 52, 3588 -3600.

Amy Forsgren (2006). “*Corrosion control through organic coatings.*” CRC Press LLC, Taylor & Francis.

Ashassi-Sorkhabi, H and Nabavi-Amri, S. A. (2000). “Corrosion inhibition of carbon steel in petroleum /water mixtures by N-containing compounds.” *Acta. Chimica. Slov.*, 47, 507-517.

Ashish Kumar, S. and Quraishi, M. A. (2010). “Effect of cefazolin on the corrosion of mild steel in HCl solution.” *Corros. Sci.*, 52, 152–160.

Ateya, B. G., El-Khair, M. B. A. and Abdel-Hamed, I. A. (1976). “Thiosemicarbazide as an Inhibitor for the Acid Corrosion of Iron.” *Corros. Sci.*, 16, 163–169.

Atta, N. F., Fekry, A. M. and Hassaneen, H. M. (2011). “Corrosion inhibition, hydrogen evolution and antibacterial properties of newly synthesized organic inhibitors on 316L stainless steel alloy in acid medium.” *Int. J. Hydrogen Energy.*, 36, 6462-6471.

Avadhani, G. S. (2001). "Hot deformation mechanisms and microstructural evolution during upset forging of γ -Fe, Fe-5Ni, Fe-5Co and Fe-5Mo alloys and maraging steel." *Doctoral dissertation*, Indian Institute of science, Bangalore.

Avci, G. (2008). "Corrosion inhibition of indole-3-acetic acid on mild steel in 0.5 M HCl." *Colloids Surf., A*, 317, 730 -736.

Banerjee, S. N. (1985). "*An introduction to science of corrosion and its inhibition.*" Oxonian press, New Delhi.

Barouni, K., Bazzi, L., Salghi, R., Mihit, M., Hammouti, B., Albourine, A. and El Issami, S. (2008). "Some amino acids as corrosion inhibitors for copper in nitric acid solution." *Mater. Lett.*, 62, 3325-3327.

Bellanger, G. (1994). "Effect of carbonate in slightly alkaline medium on the corrosion of maraging steel." *J. Nucl. Mater.*, 217, 187- 192.

Bellanger, G. and Rameau, J. J. (1996). "Effect of slightly acid pH with or without chloride in radioactive water on the corrosion of maraging steel." *J. Nucl. Mater.*, 228, 24 -29.

Benali, O., Larabi, L. and Harek, Y. (2009). "Adsorption and inhibitive corrosion properties of thiourea derivatives on cold rolled steel in 1 M HClO₄ solutions." *J. Appl. Electrochem.*, 39, 769-778.

Bentiss, F., Lebrini, M. and Lagrenee, M. (2005). "Thermodynamic characterization of metal dissolution and inhibitor process in mild steel/2,5-bis(n-Thienyl)-1,3,4-thiadiazoles/Hydrochloric Acid System." *Corros. Sci.*, 47, 2915-2931.

Blomgren, E. and Bckris, J. O. M. (1959). "The adsorption of aromatic amines at the interface: mercury-aqueous acid solution." *J. Phys. Chem.*, 63, 1475 -1486.

Bouklah, M., Hammouti, B., Aounti, A. and Benhadda, T. (2004). "Thiophene derivatives as effective inhibitors for the corrosion of steel in 0.5 M H₂SO₄." *Prog. Org. Coat.*, 49, 227 -235.

Bouklah, M., Hammouti, B., Benkaddour, M. and Benhadda, T. (2005). "Thiophene derivatives as effective inhibitors for the corrosion of steel in 0.5 M H₂SO₄." *J. Appl. Electrochem.*, 35, 1095-1101.

Britto, M. M., Almeida, T. M. G., Leitão, A., Donnici, C. L., Lopes, M. T. P. and Montanari, C. A., (2006). "Synthesis of Mesoionic 4-(para-substituted Phenyl-5-2,4-dichlorophenyl)-1,3,4-thiadiazolium-2-aminides by direct cyclization via acylation of thiosemicarbazides." *An International Journal for Rapid Communication of Synthetic Organic Chemistry*, 36, 3359-3369.

Burstein, G. and Wright, G. (1976). "The anodic dissolution of nickel- ii. Bromide and iodide electrolytes." *Electrochim. Acta*, 21, 311- 314.

Coban, G., Zencir, S., Zupko, I., Rethy, B., Gunes, H.S., Topcu, Z. (2009). "Synthesis and biological activity evaluation of 1H-benzimidazoles via mammalian DNA topoisomerase I and cytostaticity assays." *Eur. J. Med. Chem.*, 44, 2280-2285.

Dautovich, D. P. (1976). "Corrosion resistance of maraging steels." *Corrosion*, vol. 1, Shreir, L. L, (Ed.) second ed., Newnes–Butterworths, London, 3, 69.

Davis, J. R. and Davis Associates (2000). "Corrosion understanding the basics." ASM international, Ohio.

Dean, S. W. and Copson, H. R. (1965). "Stress corrosion behaviour of managing nickel steels in natural environments." *Corrosion*, 21, 95-103.

Deepika, R. (2003). "Processing and Properties of Environmentally-friendly corrosion resistant hybrid nanocomposite coatings for Aluminum alloy AA2024." University of Cincinnati.

Dehri, I. and Erbil, M. (2000). "The effect of relative humidity on the atmospheric corrosion of defective organic coating materials: an EIS study with a new approach." *Corros. Sci.*, 42, 969-978.

Dehri, I. and Ozcan, M. (2006)., "The inhibitive effect of 6-amino-m-cresol and its Schiff base on the corrosion of mild steel in 0.5 M HCl medium." *Mater. Chem. Phys.*, 98, 316-323.

Ehteshamzadeh, M., Jafari, A.H., Naderi, E. and Hosseini, M.G. (2009). "Effect of carbon steel microstructure and molecular structure of two new schiff base compounds on inhibition performance in 1 N HCl solution by EIS." *Mater. Chem. Phys.*, 113, 986–993.

Einar Bardal (2003). "Corrosion and Protection." Springer-Verlag London Limited, United States of America.

Ekpe, U. J., Ibok, U. J., Ita, B. I., Offiong, O. E. and Ebenso, E. E. (1995). "Inhibitory action of methyl and phenylthiosemicarbazone derivatives on the corrosion of mild steel in hydrochloric acid." *Mater. Chem. Phys.*, 40, 87-93.

El Azhar, M., Mernari, B., Traisnel, M., Bentiss, F. and Lagrenee, M. (2001). "Corrosion inhibition of mild steel by the new class of inhibitors [2,5-bis(n-pyridyl)-1,3,4-thiadiazoles] in acidic media." *Corros. Sci.*, 43, 2229-2238.

El Hosary, A. A., Saleh, R. M. and Shams El Din, A.M. (1972). "Corrosion inhibition by naturally occurring substances -I. The effect of hibiscus subdariffa (karkade) extract on the dissolution of Al and Zn." *Corros. Sci.*, 12, 897-904.

Elewady, G.Y. (2008). "Pyrimidine derivatives as corrosion inhibitors for carbon-steel in 2 M hydrochloric acid solution." *Int. J. Electrochem. Sci.*, 3, 1149 - 1161.

EL-Sayed, A. (1997). "Phenothiazine as inhibitor of the corrosion of cadmium in acidic solutions." *J. Appl. Electrochem.*, 27,193-200.

Fekry, A. M. and Ameer, M. A. (2010). "Corrosion inhibition of mild steel in acidic media using newly synthesized heterocyclic organic molecules." *Int. J. Hydrogen Energy*, 35, 7641 - 7651.

Fekry, A. M. and Ameer, M. A. (2011). "Electrochemical investigation on the corrosion and hydrogen evolution rate of mild steel in sulphuric acid solution." *Int. J. Hydrogen Energy*, 36, 11207 -11215.

Ferreira, E. S., Giacomelli, C., Giacomelli, F. C. and Spinelli, A. (2004). "Evaluation of the Inhibitor Effect of - Ascorbic Acid on the Corrosion of Mild Steel." *Mater. Chem. Phys.*, 83, 129-134.

Fontana, M. G. (1987). "*Corrosion engineering*." Third edition, McGraw-Hill, Singapor.

Fouda, A. S., Heakal, F. E. and Radwan, M. S. (2009). "Role of some thiadiazole derivatives as inhibitors for the corrosion of C-steel in 1.0 M H₂SO₄." *J. Appl. Electrochem.*, 39, 391-402.

Fuchs, G. R. (2006). "The adsorption, CMC determination and corrosion inhibition of some N-aalkyl quaternary ammonium salts on carbon steel surface in 2 M H₂SO₄." *Colloids Surf. A.*, 280, 130-138.

- Gadag, R.V. and Shetty, A. N. (1994). “*Engineering chemistry.*” United Publishers.
- Gao, J., Weng, Y., Salitanat, Feng, Li and Yue, H. (2009). “Corrosion Inhibition of α , β -unsaturated Carbonyl Compounds on Steel in Acid Medium.” *Pet. Sci.*, 6, 201-207.
- Geetha, M. P., Nayak, J. and Shetty, A. N. (2011). “Corrosion inhibition of 6061Al-15 vol.pct.SiC(p) composite and its base alloy in a mixture of sulphuric acid and hydrochloric acid by 4-(N,N-dimethylamino) benzaldehyde thiosemicarbazone.” *Mater. Chem. Phys.*, 125, 628-640.
- Grum, J. and Slabe, J. M. (2006). “Effect of laser-remelting of surface cracks on microstructure and residual stresses in 12Ni maraging steel.” *Appl. Surf. Sci.*, 252, 4486–4492.
- Hackerman, N., Snavelly, E.S., J.S. and Payne, J.r. (1966). “Effects of anions on corrosion inhibition by organic compounds.” *J. Electrochem. Soc.*, 113, 677-686.
- Hosseini, N. S., Teimouri, J., Tahmasebifar, A., Shirazib, H. and Ahmadabadi, M. N. (2009). “A new concept in further alloying of Fe-Ni-Mn maraging steels.” *Scr. Mater.*, 60, 528–531.
- Hosseini, M., Mertens S.F.L. and Arshadi M.R. (2003). “Synergism and antagonism in mild steel corrosion inhibition by sodium dodecyl benzenesulphonate and hexamethylenetetramine.” *Corros. Sci.*, 45, 1473-1482.
- Javaherdashti, R. (2007). “*Microbiologically Influenced Corrosion.*” Springer-Verlag London Limited.
- Kelly, L. T. and Howard, H. W. (1932). “Phenacyl and p-bromophenacyl esters of monosubstituted benzoic acids.” *J. Am. Chem. Soc.*, 54, 4383-4385.
- Khaled, K. F. and Hackerman, N. (2003). “Investigation of the inhibitive effect of ortho-substituted anilines on corrosion of iron in 1 M HCl solutions.” *Electrochim. Acta.*, 48, 2715- 2723.
- Khaled, K. F., Babic-Samardzija, K. and Hackerman, N. (2004). “Piperidines as corrosion inhibitors for iron in HCl.” *J. Appl. Electrochem.*, 34, 697-704.
- Klobcar, D., Tusek, J., Taljat, B., Kosec, L. and Pleterski, M. (2008). “Aging of maraging steel welds during aluminum alloy die casting.” *Mater. Sci.*, 44, 515–522.

- Kriaa, A., Hamdi, N., Jbali, K. and Tzinmann, M. (2009). "Corrosion of iron in highly acidic hydro-organic solutions." *Corros. Sci.*, 51, 668–676.
- Kirk, W. W., Covert, R. A. and May, T. P. (1968). "Corrosion behavior of high strength steels in marine environment." *Met. Eng. Quart.*, 8, 31-38.
- Kumbhare, R. M., Kumar, K. V., Ramaiah, M. J., Dadmal, T., Pushpavalli, S.N.C.V.L., Mukhopadhyay, D., Divya, B., Devi, T.A., Pal-Bhadra, M., Kosurkar, U. (2011). "Synthesis and biological evaluation of novel Mannich bases of 2-aryl midazo[2,1-b]benzothiazoles as potential anti-cancer agents." *Eur. J. Med. Chem.*, 46, 4258-4266.
- Larabi, L., Harek, Y., Benali, O. and Ghalem, S. (2005). "Hydrazide derivatives as corrosion inhibitors for mild steel in 1M HCl." *Prog. Org. Coat.*, 54, 256-262.
- Lee, Y. J., Kung, M. C., Lee, K. I. and Chou, C.P. (2007). "Effect of lath microstructure on the mechanical properties of flow-formed C-250 maraging steels." *Mater. Sci. Eng., A.*, 454 - 455 602–607.
- Li, W. H., He, Q., Pei, C.L. and Hou, B.R. (2007). "Experimental and Theoretical Investigation of the Adsorption Behavior of New Triazole Derivatives as Inhibitors for Mild Steel Corrosion in Acid Media." *Electrochim. Acta*, 52, 6386-6394.
- Li, W. H., He, Q., Pei, C. L., Hou and B. R., H. (2008). "Some new triazole derivatives as inhibitors for mild steel corrosion in acidic medium." *J. Appl. Electrochem.*, 38, 289–295.
- Maayta, A. K. and Al-Rawashdeh N. A. F. (2004). "Inhibition of acidic corrosion of pure aluminum by some organic compounds." *Corros. Sci.*, 46, 1129-1140.
- Machnikova, E., Kenton Whitmire, H. and Hackerman, N. (2008). "Corrosion inhibition of carbon steel in hydrochloric acid by furan derivatives." *Electrochim. Acta.*, 53, 6024-6032.
- Mazzone, G., Bonina, F., Puglisi, G., Panico, A. M. and Reina, R. A. (1984). "2,5-diaryl-substituted 1,3,4-oxadiazoles: synthesis and preliminary pharmacological investigation." *Farmaco-Ed. Sci.*, 39, 414-420.
- Menapace, C., Lonardelli, I. and Molinari, A. (2010). "Phase transformation in a nanostructured M300 maraging steel obtained by SPS of mechanically alloyed powders." *J. Therm. Anal. Calorim.*, 101, 815-822.

- Mohammed Amin, A., Khaled, K. F., Mohsen, Q., and Arida, H. A. (2010). "A study of the inhibition of iron corrosion in HCl solutions by some amino acids." *Corros. Sci.*, 52, 1684-1695.
- Morad, M. S. (2007). "Effect of sulfur-containing amino acids on the corrosion of mild steel in sulfide-polluted sulfuric acid solutions." *J. Appl. Electrochem.*, 37, 1191–1200.
- Morad, M. S. and Kamal El-Dean, A.M. (2006). "2,2'-Dithiobis (3-cyano-4,6-dimethylpyridine): a new class of acid corrosion inhibitors for mild steel." *Corros. Sci.*, 48, 3398–3412.
- Morad, M., Morvan, J. and Pagetti, J. (1995). "Proceedings of the Eighth European Symposium on Corrosion Inhibitors (8SEIC)." Sez V, Suppl. N. 10, Ann. Univ. Ferrara, NS, 159.
- Nayak, J. (2004). "Corrosion behavior of maraging steels in aqueous media." *Ph.D Research thesis*, NITK Surathkal.
- Nestor, P. (2004). "Electrochemistry and Corrosion science." Kluwer Academic Publishers, Boston.
- Obot. I. B., Obi-Egbedi, N. O., Odozi, N. W. (2010). "Acenaphtho [1,2-b] quinoxaline as a novel corrosion inhibitor for mild steel in 0.5 M H₂SO₄." *Corros. Sci.*, 52, 923-926.
- Oguzie, E. E., Njoku, V.O., Enenebeak, C.K., Akalezi, C.O. and Obi, C. (2008). "Effect of hexamethylpararosaniline chloride (crystal violet) on mild steel corrosion in acidic media." *Corros Sci.*, 50, 3480-3486.
- Ohue, Y. and Matsumoto, K. (2007). "Sliding–rolling contact fatigue and wear of maraging steel roller with ion-nitriding and fine particle shot-peening." *Wear*, 263, 782-789.
- Ousslim, A., Bekkouch, K., Hammouti B., Elidrissi, A. and Aouniti, A. (2009). "Piperazine derivatives as inhibitors of the corrosion of mild steel in 3.9 M HCl." *J. Appl. Electrochem.*, 39, 1075–1079.
- Ozcan, M., Dehri, I. and Erbil, M. (2004). "Organic sulphur-containing compounds as corrosion inhibitors for mild steel in acidic media: correlation between inhibition efficiency and chemical structure." *Appl. Surf. Sci.*, 236, 155-164.

Philip, A. S. (2007). “*Corrosion Engineering Handbook.*” 2nd edition, Taylors and Francis Group, CRC Press, United States of America.

Pierre, R. R. (2008). “*Corrosion Engineering Principles and Practice.*” McGraw Hill, New Delhi.

Poornima, T. Nayak, J. and Shetty, A. N. (2010). “Studies on corrosion of annealed and aged 18 Ni 250 grade maraging steel in sulphuric acid medium.” *Port. Electrochim. Acta*, 28, 173-188.

Poornima, T. Nayak, J. and Shetty, A.N. (2011). “Effect of 4-(N, N-diethylamino)benzaldehyde thiosemicarbazone on the corrosion of aged 18 Ni 250 grade maraging steel in phosphoric acid solution.” *Corros. Sci.*, 53, 3688 - 3696.

Poornima, T., Nayak, J. and Shetty, A. N. (2010). “Corrosion of aged and annealed 18 Ni 250 grade maraging steel in phosphoric acid medium.” *Int. J. Electrochem. Sci.*, 5, 56 – 71.

Poornima, T., Nayak, J. and Shetty, A. N. (2011). “3, 4-Dimethoxy benzaldehyde thiosemicarbazone as corrosion inhibitor for aged 18 Ni 250 grade maraging steel in 0.5 M sulfuric acid.” *J. Appl. Electrochem.*, 41, 223-233.

Popova, A., Christov, M., Raicheva, S. and Sokolova, E. (2004). “Adsorption and inhibitive properties of benzimidazole derivatives in acid mild steel corrosion.” *Corros. Sci.*, 46, 1333–1350.

Prabhu, R. A., Shanbhag, A. V. and Venkatesha, T. V. (2007). “Influence of tramadol [2-[(dimethylamino) methyl]-1-(3- methoxyphenyl) cyclohexanol hydrate] on corrosion inhibition of mild steel in acidic media.” *J. Appl. Electrochem.*, 37, 491- 497.

Prabhu, R. A., Venkatesha, T. V., Shanbhag, A. V., Kulkarni, G. M. and Kalkhambkar, R. G. (2008). “Inhibition effects of some Schiff’s bases on the corrosion of mild steel in hydrochloric acid solution.” *Corros. Sci.*, 50, 3356–3362.

Quraishi, M. A. and Sardar, R. (2003). “Hector bases - a new class of heterocyclic corrosion inhibitors for mild steel in acid solutions.” *J. Appl. Electrochem.*, 33, 1163–1168.

Quraishi, M. A. and Jamal, D. (2002). “Inhibition of mild steel corrosion in the presence of fatty acid triazoles.” *J. Appl. Electrochem.*, 32, 425-430.

- Rao, N. M., Mohan, M. K. and Uma Maheswara Reddy, P. (2009). "Environmentally assisted cracking of 18%Ni maraging steel." *Corros. Sci.*, 51, 1645 - 1650.
- Revie, R. W. and Uhlig, H. H. (2008). "*Corrosion and Corrosion control.*" John Wiley & Sons, Inc. New Jersey.
- Revie, R. W. (2000). "*Uhlig's corrosion handbook.*" Second edition, Wiley-interscience publication, New York.
- Rezek, J., Klein, I. E. and Yhalom, J. (1997). "Structure and corrosion resistance of oxides grown on maraging steel in steam at elevated temperatures." *Appl. Surf. Sci.*, 108 159 - 165.
- Rezek, J., Klein, I. E. and Yhalom, J. (1997). "Electrochemical properties of protective Coatings on maraging steel." *Corros. Sci.*, 39, 385-392.
- Ronald, S., Michael, S., Silvia, Z. and Harald, L. (2010). "Effect of Cu on the evolution of precipitation in a Fe-Cr-Ni-Al-Ti maraging steel." *Acta. Mater.*, 58, 3733-3741.
- Sahin, M., Bilgic, S. and Yilmaz, H. (2002). "The inhibition effects of some cyclic nitrogen compounds on the corrosion of the steel in NaCl mediums." *Appl. Surf. Sci.*, 195, 1-7.
- Sanaa, T. A. (2008). "Inhibition Action of Thiosemicabazone and some of it is r-substituted compounds on the corrosion of iron-base metallic glass alloy in 0.5 M H₂SO₄ at 30 °C." *Mater. Res. Bull.*, 43, 510-521.
- Sanatkumar, B. S., Nayak, J. and Shetty, A. N. (2012). "Investigation of adsorption and corrosion inhibitive effect of 1(2E)-1-(4 amino phenyl)-3(2-thienyl) prop-2-en-1-one on corrosion of weld aged maraging steel in 0.5 M sulphuric acid media". *J. Electrochem Soc. India*, 60, 153-161.
- Sanatkumar, B. S., Nayak, J. and Shetty, A. N. (2012). "The corrosion inhibition of maraging steel under weld aged condition by 1(2E)-1-(4 - aminophenyl)-3-(2-thienyl) prop-2-en-1-one in 1.5 M hydrochloric acid medium". *J. Coat. Technol. Res.*, 9, 483-493.
- Sanatkumar, B. S., Nayak, J. and Shetty, A. N. (2012). "Influence of 2-(4chlorophenyl)-2-oxoethyl benzoate on the hydrogen evolution and corrosion inhibition of 18 Ni 250grade weld aged maraging steel in 1.0 M sulphuric acid medium". *Int. J. Hydrogen Energy*, 37, 9431 - 9442.

Sastri, V. S., Edward Ghali and Mimoun Elboujdaini (2007). “*Corrosion prevention and protection practical solutions.*” John Wiley & Sons Ltd, England.

Satpati, A. K. and Ravindran, P. V. (2008). “Electrochemical study of the inhibition of corrosion of stainless steel by 1,2,3-benzotriazole in acidic media.” *Mater. Chem. Phys.*, 109, 352-359.

Schmitt, G. (1984). “Application of inhibitors for acid media.” Report Prepared for the European Federation of Corrosion Working Party on Inhibitors, *Br. Corros. J.*, 19, 165-176.

Selim, I. Z., Khedr, A. A. and El-Shobki, K. M. (1996). “Efficiency of chalcone compounds inhibitors for acid corrosion of Al and Al-3.5 Mg Alloy.” *J. Mater. Sci. Technol.*, 12, 267-272.

Solmaz, R. Kardas, G. Culha, M., Yazıcı, B. and Erbil, M. (2008). “Investigation of adsorption and inhibitive effect of 2-mercaptotriazole on corrosion of mild steel in hydrochloric acid media.” *Electrochim. Acta*, 53, 5941-5952.

Stansbury, E. E. and Buchanan, R. A. (2000). “*Fundamentals of Electrochemical Corrosion.*” ASM International, Materials Park, Ohio.

Stiller, K., Danoix, F. and Bostel, A. (1996). “Investigation of precipitation in a new maraging stainless steel.” *Appl. Surf. Sci.*, 94/95, 326-333.

Tao, Z., Zhang, S., Li, W. and Hou, B. (2010) “Adsorption and corrosion inhibition behavior of mild steel by one derivative of benzoic-triazole in acidic solution.” *Ind. Eng. Chem. Res.*, 49, 2593-2599.

Touhamia, F., Aounitia, A., Abeda, Y., Hammoutia, B., Kertitb, S., Ramdanic, A. and Elkacemid, K. (2000). “Corrosion inhibition of armco iron in 1.0 M HCl media by new bipyrazolic derivatives.” *Corros. Sci.*, 42: 929-940.

Venkatasubramanian, S. (2009). “*Measurement of carbon dioxide corrosion on carbon steel using electrochemical frequency modulation.*” University of Saskatchewan, Canada.

Wang, H., Liu, R. B. and Xin, J. (2004). “Inhibiting effects of some mercapto-triazole derivatives on the corrosion of mild steel in 1.0 M HCl medium.” *Corros. Sci.*, 46, 2455-2466.

Wang, W., Yan, W., Duan, Q., Shan, Y., Zhang, Z. and Yang, K. (2010). "Study on fatigue property of a new 2.8 GPa grade maraging steel." *Mater. Sci. Eng., A*, 527, 3057–3063.

Wang, X., Yang, H. and Wang, F. (2010). "A cationic gemini-surfactant as effective inhibitor for mild steel in HCl solutions." *Corros. Sci.*, 52, 1268-1276.

Xianghong Li, Shuduan Deng, Hui Fu. (2009). "Synergistic inhibition effect of red tetrazolium and uracil on the corrosion of cold rolled steel in H₃PO₄ solution: Weight loss, electrochemical and AFM approaches." *Mater. Chem. Phys.*, 115, 815–824.

Yagan, A. Pekmez, N. O. and Yıldız, A. (2008). "Electrochemical synthesis of poly (N-methylaniline) on an iron electrode and its corrosion performance." *Electrochim. Acta*, 53, 5242-5251.

Yan, Y., Li, W., Cai, L. and Hou, B. (2008). "Electrochemical and quantum chemical study of purines as corrosion inhibitors for mild steel in 1.0 M HCl solution." *Electrochim. Acta*, 53, 5953-5960.

Zaki, A. (2006). "*Principles of corrosion engineering and corrosion control.*" Edition: illustrated, Published by Butterworth-Heinemann.

LIST OF PUBLICATIONS

a) In Journals

1. Pradeep Kumar and A. Nityananda Shetty. (2013). "Electrochemical investigation on the corrosion of 18%Ni M250 grade maraging steel under welded condition in sulfuric acid medium". *Surf. Eng. Appl. Electrochem.* 49, 3, 76–83.
2. Pradeep Kumar and A. Nityananda Shetty. (2013). "Corrosion behaviour of 18% Ni M250 grade maraging steel under welded condition in hydrochloric acid medium." *Port. Electrochim. Acta.* 31, 1, 21-32.
3. Pradeep Kumar and A. Nityananda Shetty. (2014). "Corrosion inhibition effect of 2,5-Bis-(3,4,5-trimethoxy phenyl)-[1,3,4] oxadiazole (BTPO) on 18 Ni M250 grade welded maraging steel in 1.0 M sulphuric acid medium." *J. Mater. Environ. Sci.* 5, 3, 873-886.
4. Pradeep Kumar and A. Nityananda Shetty. (2013). "1-phenyl-4-(4-nitrophenyl) thiosemicarbazide as a corrosion inhibitor for 18 Ni 250 grade maraging steel under welded condition in 1.0 M sulfuric acid medium." *Arabian Journal of Electrochemistry.* (Communicated).
5. Pradeep Kumar and A. Nityananda Shetty. (2013). "Adsorption and Inhibitory Mechanism of 1-phenyl-4-(4-nitrophenyl) thiosemicarbazide on corrosion of 18 Ni 250 grade welded maraging steel in 1.0 M hydrochloric acid medium." *International Journal of Corrosion.* (Under revision).

b) Papers presented in conferences

1. Pradeep Kumar and A. Nityananda Shetty. (2012). "Corrosion inhibition, Adsorption behavior and Thermodynamic properties of 1-phenyl-4-(4-nitrophenyl) thiosemicarbazide on maraging steel under welded condition in 1.0 M sulphuric acid medium." *TCBEP- 2012*, December 10-12, SVU Tirupati.
2. Pradeep Kumar and A. Nityananda Shetty. (2013). "Influence of 2,5-Bis-(3,4,5-trimethoxy phenyl)-[1,3,4] oxadiazole on the corrosion inhibition of 18 Ni 250 grade welded maraging steel in 1.0 M sulphuric acid medium." *ICRAMST- 13*, January 17-19, NITK Surathkal.

BIO DATA

Mr. PRADEEP KUMAR

S/o: VISHWANATH SHETTY

Kadoor Padumane,

Padukadoor

Udupi-576234.

State: Karnataka

Phone: +91- 9481916559 (M)

E-mail: pradeep7182@gmail.com

Date of Birth: 24/08/1985

Academic Details

| Course | Institution | Year | Class |
|--|----------------------------------|-------------|--------------|
| Master of Science- Organic Chemistry | Mangalore University. | 2009 | I |
| Bachelor of Science- Physics, Chemistry, Mathematics | Milagres College, Kallianpur. | 2007 | I |
| Pre-University Course | National Junior College, Barkur. | 2003 | I |
| S.S.L.C | Sri Vani High School, Nadur. | 2001 | I |

Professional Experience

| Industry | | Position | Year |
|-----------------------|--|--------------------|-----------------------|
| | Apotex Pharmachem, Bangalore. | Research Associate | June 2009 - Dec 2010 |
| Pre-University | Government Pre University College, Shankaranarayana. | Lecturer | July 2013 - Till date |